CHARACTERISING THE EFFECTIVE MATERIAL SOFTENING IN ULTRASONIC FORMING OF METALS

Sa'ardin Abdul Aziz

A thesis for the degree of Doctor of Philosophy (PhD)

Submitted to the School of Engineering,
College of Science and Engineering,
University of Glasgow

June 2012

ABSTRACT

This thesis has presented experimental and finite element (FE) analyses of the static and ultrasonic forming of two metals; aluminium 1050 and magnesium AM50. Aluminium and magnesium are considered to be soft metals and can be easily shaped by any of the main industrial metalworking processes. Frequently aluminium and magnesium have been the subject of research studies. These two metals most commonly chosen in manufacturing industry because of their cost, mechanical properties and flexibility in processing. In this research, simple compression and forming tests were designed and the effects of superimposed ultrasonic excitation on workpiece and die, which is tuned to a longitudinal mode at 20.8 kHz, were studied via stress-strain measurements. Research through experiments and finite element simulations studies in the application of ultrasonic excitation has been carried out to gain quantitative understanding of the mechanisms of improvement in ultrasonic forming characteristics, such as a reduction in material flow stress and oscillatory stress. This research study has shown these mechanisms by applying ultrasonic vibration to the tool and die in the forming test and, similarly, effects were measured and predicted in the experimental and numerical analysis.

The development and application of high power ultrasonic techniques in forming processes required the use of specifically designed ultrasonic components to correctly transmit the energy from the transducer to the workpiece and die interface. The application along with the ultrasonic vibration amplitude required for the process, were considered in order to design the most suitable horn profile. In this study, a 20 kHz transducer was used to provide up to 10 μm of peak-to-peak vibration amplitude, depending on the generator setting. Therefore, the booster and horn were designed to provide a range of ultrasonic vibration amplitudes between 5 to 20 μm and also used as a tool and die in the study of ultrasonic metal forming. The horn was designed using finite element modelling (FEM), and modal frequencies and associated mode shapes were subsequently confirmed using experimental modal analysis (EMA). The ultrasonic system has been measured and calculated as having a longitudinal mode of vibration at 20.8 kHz and to provide an amplitude gain of four. In this study, a

generator uses mains electricity to generate a high frequency ultrasonic signal to drive the transducer, which is tuned to a specific frequency of 20 kHz. The booster and horn were designed to meet the criteria of transducer, which is to provide a longitudinal vibration at tuned frequency of 20 kHz. However, the profile of booster and horn have been measured and calculated as having a longitudinal mode of vibration at 20.8 kHz, which is considered close to the transducer tuned frequency.

The review of previous studies of superimposed ultrasonic excitation on upsetting showed that the most experimental characterisations of the volume effects mainly depended on an interpretation of measurements of the mean flow stress, and have neglected the oscillatory stress. In this study, the characteristics of oscillatory stress and the material behaviour in plastic deformation when superimposed ultrasonic excitation is applied on a static compression test under dry friction were considered. The effects on material properties of superimposed ultrasonic excitation on compression tests were illustrated in the stress-strain curve in Figure A-1. The effects were explained in terms of flow stress reduction, oscillatory stress, mean flow stress, maximum and minimum path of oscillatory stress in the stress-strain diagram. In Figure A1, the mechanism of flow stress reduction is related to acoustic softening, friction reduction and stress superposition which are labelled as (i) and (ii). The results showed that the static flow stress of compressive deformation was lowered by the ultrasonic vibration superimposed on the static load and this phenomenon has been referred to as the material softening mechanism which is influenced by volume and surface effects. The volume effect is defined as a reduction in flow stress of the material being formed and the surface effect is defined as a reduction in frictional conditions at the interface between the vibrating device and the workpiece. Finite element models were used to investigate numerically the volume and surface effects during ultrasonically assisted compression. The finite element models were developed using material model parameters which were identified from the experimental analysis. The influence of volume and surface effects were investigated separately in the FE model and it was shown that the volume effect dominated the effective material softening results during ultrasonic excitation.

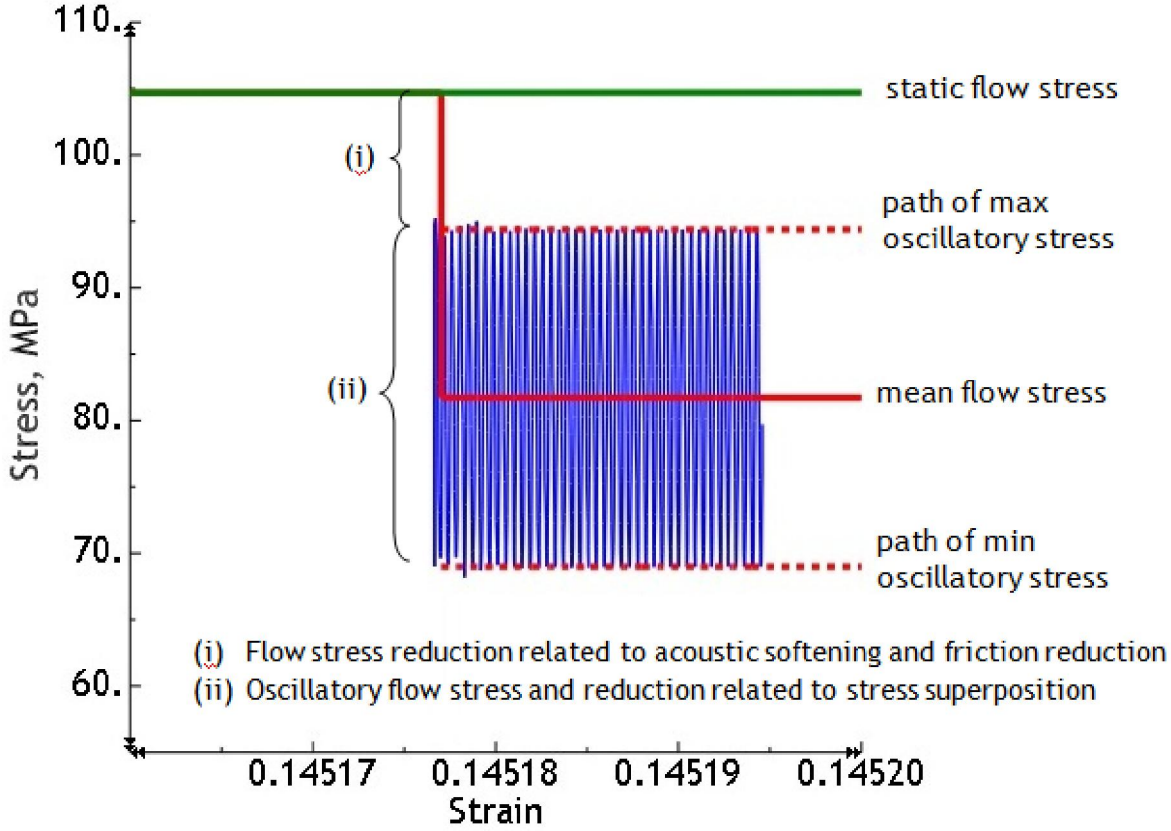

Figure A-1 The effects of material properties behaviour during experimental of superimposed ultrasonic excitation on compression test

The application of ultrasonic excitation on metals under plastic deformation conditions has been investigated previously. Most researchers have reported that superimposing ultrasonic excitation on metal working processes reduced the material flow stress. A further study of superimposed ultrasonic excitation on a static load during elastic deformation in metal working was not investigated, so it is not possible to determine the effect of ultrasonic excitation on the material. In this study, the investigation of oscillatory stress behaviour in the ultrasonic compression test of cylinder metal specimens during elastic deformation was carried out. In the stress-strain diagram, the ultrasonic vibration was shown to have lowered the static flow stress during elastic deformation under dry contact conditions and it was found that the reduction in static flow stress linearly increased with ultrasonic vibration amplitude. The stress reduction was influenced by volume and surface effects which occurred during the superimposed ultrasonic excitation. The results also showed that the maximum path of oscillatory stress exceeded the static flow stress, however, the mean flow stress is lower than the static flow stress at the onset of ultrasonic

excitation. To investigate the influence that volume and surface effects have on material softening during experimental compression tests, a series of FE models were developed. As mentioned previously, the FE models were developed using material model parameters which were identified from the experimental analysis in Figure A1, however, the mechanism of flow stress reduction which is related to acoustic softening and friction reduction which is labelled as (i) cannot be predicted in FE models. The FE models adopted the material softening effects in order to simulate realistic stress reduction compared with experimental results. The significant stress reduction in the FE analysis was obtained by adjusting the yield stress and contact conditions parameter. It was concluded that the surface effect dominated the stress reduction during metal upsetting test in elastic deformation.

The study continued to a simple forming test where samples of flat sheet metal were forced into a shaped die by a shaped plunger on a test machine. The results of this study illustrated how ultrasonically assisted metal forming resulted in a lowering of the static forming force during ultrasonic excitation of the die. As a result, the static forming force was seen to be reduced by ultrasonic excitation of the die and the path of the maximum oscillatory force was observed to be parallel to or below the path of the static forming force. Force reduction was measured in these experiments using a high power ultrasonic transducer and also by tuning the die and then the punch during the metal forming test. It was found that a good coupling between punch, specimen and die allowed ultrasonic energy to be effectively transferred into the materials during superimposed ultrasonic excitation in the static forming test.

This thesis has concluded that evaluation of the benefits of ultrasonic excitation not only relied on measurements of the mean flow stress alone but also on measurement of the oscillatory stress during superimposed ultrasonic excitation on forming tests. Findings on the effectiveness of ultrasonic excitation led the study to recognize that the lack of understanding of the effects of ultrasonic excitation on the forming process has resulted in difficulties in maximising the benefits and applications of this technology.

ACKNOWLEDGMENTS

I would like to give special recognition to the following colleagues, friends and family who have contributed their advice, criticisms, ideas and support towards the development of this studies. Most of this was highly constructive and truly much appreciated.

Professor Margaret Lucas, for her supervision, advice, guidance and encouragement throughout the research work. Her continuous support and encouragement both launched and sustained me in the study and the writing of this thesis. It was a privilege to work for a highly respected academician who is undoubtedly one of the leading names in high power ultrasonics, in the world.

The technical staffs, in particular Mr. Brian Robb and Mr. John Davidson, for their expertise, extensive help and assistance in the material lab, preparations of specimens, setting up the test-rig, and assistance throughout the studies.

The Government of Malaysia and the Universiti Teknologi Malaysia, for funding me throughout the studies.

The members of the Dynamics Group, for their helpful support and warmest friendship throughout my research.

Staffs at School of Engineering, University of Glasgow, for their assistance, help and accommodating my demanding needs on resources throughout my studies.

Finally, I am immensely indebted to my wife, Yusnani Nordin and my children, Nur Anis Batrisyia, Muhammad Aisy Darwisy and Muhammad Aisy Danish, for their support, patience, unflagging love, understanding and encouragement throughout my studies.

TABLE OF CONTENTS

LIST OF TABLES

LIST OF FIGURES

CHAPTER 1

INTRODUCTION

Ultrasonic metal forming involves the use of ultrasonic vibration in tools and dies. Simple ultrasonic metal forming tests are performed where samples of metal are placed between shaped tools and dies on a test machine. The tool and die are a part of a tuned ultrasonic system, and so ultrasonic excitation can be applied during the tests. The ultrasonic excitation system is shown in Fig. 1.1, below, and consists of a bolted Langevin piezoelectric transducer, a booster, and an ultrasonic horn, all tuned to their first longitudinal mode of vibration at 20.8 kHz. The forming tool and die in this study consist of the output end of the ultrasonic horn.

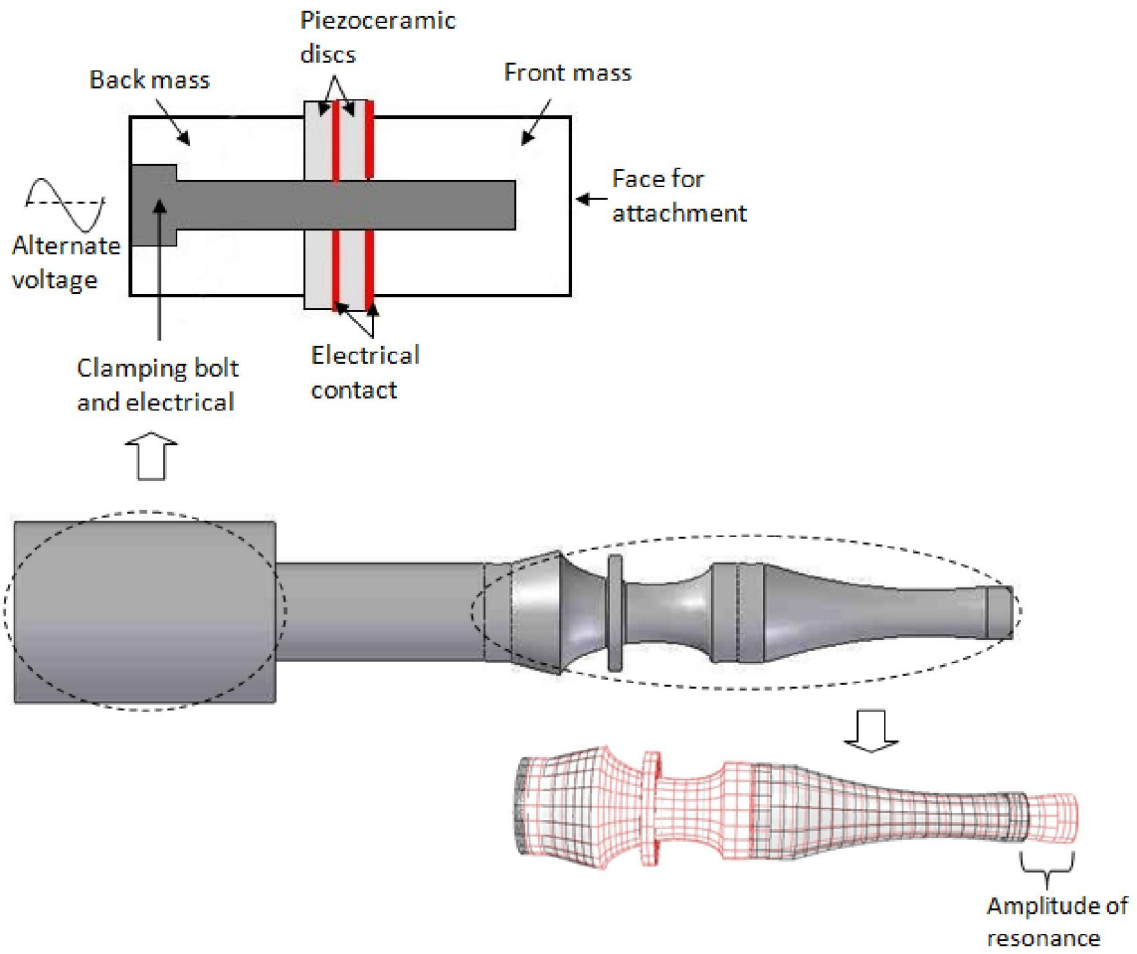

Figure 1-1 A tuned ultrasonic excitation system

This thesis presents experimental and finite element (FE) analyses of the static and ultrasonic forming of two metals namely aluminium and magnesium. In this research, simple compression and forming tests were designed and the effects of superimposing ultrasonic vibrations on the die, which is tuned to a longitudinal mode at 20.8 kHz, were studied via stress-strain and force-displacement measurements. Research through experiments and finite element simulations has been carried out to gain quantitative understanding of the mechanisms of improvement in ultrasonic forming characteristics such as a reduction in material flow stress, material forming force, oscillatory stress and oscillatory force.

When ultrasonic vibrations are superimposed on a metal forming on a metal forming process, many measurements have shown that metal specimens exhibit significant temporary material softening. This beneficial affect can be attributed to two main mechanisms such as volume effect and surface effect. Initially, it was proposed that the ultrasonic vibration preferentially absorbed at dislocation sites, enabling to proceed with reduction in forming forces, but there is little direct measurement evidence to support the claim. Later, it was suggested that the volume effect deals with the influence of oscillatory stress mechanism which is involved with very much reduced forces and the surface effect deals with the changed in the interface friction that involved a contact surface between the die and the specimen such a way as to reduce the forming force. In the last 50 years, a clear explanation of material softening mechanism during superimposed ultrasonic excitation has not been achieved, however a clear understanding from measurements is that the ultrasonic excitation results in the material softening even for low ultrasonic intensities, the softening effect is instantaneous, temperature and frequency have a negligible effect, no permanent change in material properties is detected for ultrasonic intensities lower than threshold value but resulted the permanent changes at high vibration amplitudes. Most recently, a study of significant effect during superimposed ultrasonic excitation on traditional forming process has growth up. An unclear explanations on the effects of high frequency vibration include stress superposition, acoustic softening and friction reduction due to the relative motion at the interface makes them difficult to understand. The explanation that was claimed from the

previous work have received doubt from the academic and industrial community due to lack of experimental and theoretical evidence.

In traditional method of metal-working process, vibration has been applied in various processes which include upsetting, wire drawing, tube drawing, extrusion, tensile, cutting and drilling. It is used in a wide range of applications that has historically been divided into two categories; low and high power applications. Low power applications are generated at low power intensities ranging from 0.1 to 0.5 W/cm^2 and the field of high power ultrasonic has been characterized between 20 kHz and 100 kHz and required at high power intensities ranging from 100 W to 10 kW. Previously, most ultrasonic applications were operated at frequencies from 15 to 80 kHz and 20 kHz is the most oscillation frequency of ultrasonic vibration was used during ultrasonic metal-forming. Pure aluminium and aluminium alloy are the most metal have been used in previous work as a specimen. The other commercial materials such as steel, copper, titanium and super alloy also have been chosen as specimen to study the beneficial effects of high-frequency vibration on the metals.

1.1 Research aims

The aim of this study is to investigate the characteristics of material softening during the application of ultrasonic excitation in the metal forming processes. Most the investigations in this study are carried out through experiments and finite element simulation methods, by applying ultrasonic oscillations to the tool and die in a compression test and to single sheet forming metals.

The investigation begins with the design and construction of a high gain ultrasonic excitation system that includes a Langevin piezoelectric transducer, an ultrasonic booster and a horn, which are all tuned to the first longitudinal mode of vibration at 20.8 kHz. All the ultrasonic components are connected together with rigs that can be fixed to the test machine.

The second part of the analysis aims to characterise the effects of flow stress and oscillatory stress on material behaviour in plastic deformation when ultrasonic excitation is superimposed on a static compression test under dry friction. Data resulting from the ultrasonic response can provide material flow characteristics in terms of stress-strain diagrams and oscillatory stress behaviour. The results of experimental analysis are used to define the material parameters for the FE models. In association with this, a series of finite element models is developed to examine the effects of changes in material flow stress parameters and coefficients of friction in simulated metal compression tests. A comparison of the stress-strain diagrams obtained from the experimental and numerical analyses is then conducted.

The third part of the study investigates the oscillatory response, in an ultrasonic compression test, of cylindrical metal specimens during elastic deformation by examining the maximum and mean flow of oscillatory stress. Finite element models are developed to investigate the effects of ultrasonic excitation during compression tests and to allow changes to the interfacial boundary conditions and material flow stress parameters. This part also investigates the effect of ultrasonic excitation on static compression loads in terms of the material softening mechanism during elastic deformation.

The fourth part of the research aims to study a simple forming test, where a flat sheet sample of metal is forced into shaped die by a shaped tool on a test machine. The result of this study can explain how ultrasonically assisted metal forming can result in a lowering of the mean forming force during ultrasonic excitation of the die. The investigation is continued to study the characteristics of oscillatory force during the ultrasonic forming. The objectives of this study are to experimentally measure the mean forming force and oscillatory force during superimposed ultrasonic excitation on metal forming process. Ultrasonic excitation during metal forming on a single sheet of materials is carried out.

1.2 Early history of sonic and ultrasonic applications

'Sonics' suggests a mechanical wave or an oscillation of pressure transmitted through a solid, liquid, or gas, composed of frequencies within the range of human hearing [1]. Sound wave propagation with the frequencies beyond the limit of human hearing is referred to as 'ultrasonic'. The history of ultrasonic wave propagation owes its origin to Paul Langevin, who in 1917 transmitted sound waves in sea water [2]. Langevin's work depended on another discovery, by Pierre and Jacques Curie, of the piezoelectric effect. They discovered that when a stress is applied to crystalline material, such as quartz, an electric charge is produced. They also found that, conversely, an electric charge applied to the material produces a change in the material's dimensions. Hence, an alternating voltage applied to the crystal can produce vibrations that generate sound waves in a surrounding medium. This system is known as piezoelectric transducer. The earliest form of an ultrasonic transducer was a whistle developed by Francis Galton in 1883 to investigate the threshold frequency of human hearing [3]. He produced a gas-driven transducer that generated sound of known frequencies and was able to determine that the normal limit of human hearing was around 18 kHz to 20 kHz.

Sound is transmitted through a medium by vibration of the molecules through which the wave is travelling. Sound wave propagation can be categorised into three types; audio, low and high ultrasonic and diagnostic ultrasound. The audio range falls between 16 Hz and 20 kHz, and this range is important because its frequencies can be detected by the human ear. The useful ultrasound range refers to the frequencies between 20 kHz and 2 MHz, for both low power and high power ultrasonics. This range is used in a wide range of applications such as manufacturing, sonochemistry and medicine [4-8]. Diagnostic ultrasound frequencies of 2 MHz to 10 MHz are mostly used in medical applications such as ultrasonography and elastography. One of the chief medical applications is obstetric sonography, which is commonly used during foetal examinations.

Low and high ultrasonics have been used to solve problems in such diverse areas as engineering, physics, chemistry, medicine, microscopy, underwater, ranging

and navigation. The first application of the ultrasonic frequencies was in the sonar detection of submarines during World War I [9]. Wood and Loomis established techniques for generating high acoustic powers to study the effects of high intensity sound [10]. The first practical application of ultrasound, outside sonar, was an ultrasonic flaw detection system which used the Wood and Loomis techniques [11, 12]. Later, during World War II, ultrasonic vibrations were applied in timing devices, anti-jamming devices, and moving target detecting systems which focus attention on the appearance of moving targets [13].

At the end of World War II considerable expertise had been developed in sending and receiving high frequency ultrasonic pulses to investigate many physical problems such as oscillatory magnetoacoustic phenomena in metals and the effect of dislocations and impurities on sound wave propagation and relaxation processes in gases, liquids and solids [14]. During post-war years, the introduction of the piezoelectric ceramics occurred, replacing quartz as a piezoelectric material. New applications in measurement and control were found in medicine, cleaning and machining.

1.3 Development of power ultrasonics

Following the Wood and Loomis work, the numbers and range of power ultrasonics studies increased steadily. At least 150 publications related to power ultrasonics can be identified in the period 1927 to 1939 [15]. The main studies covered emulsification and dispersion, the coagulating action, and chemical and biological effects. Investigations on power ultrasonic effects were carried out in gases, liquids, solids and living organisms. Between 1940 and 1955, major new development and research focused on transducer materials and ultrasonic generators [2]. Two important developments in high power ultrasonics also occurred, namely the production of the modern horn transducer and the concept of prestressed sandwich transducer [16, 17]. The horn transducer was described as a half wave-length rod to magnify the velocity of a resonant piezoelectric transducer, while the sandwich transducer was described as two different

materials bolted together in the transducer. In the sandwich transducer construction, a number of piezoelectric elements usually two or four are bolted between a pair of metal end masses. The piezo elements would be a pre-polarized lead zirconate titanate composition which exhibit high activity coupled with both low loss and ageing characteristics and suited to form the basis of efficient and rugged transducer.

Consider, the transducer is driven with an alternating voltage and the structure dimension changes in sympathy with the applied voltage at a tuned frequency corresponding to resonant length, however, the power handling capacity would be lower since the elements have poor thermal capacity and low tensile strength. Therefore, to reduce the inherent weaknesses a number of thin elements are clamped between two acoustically low loss metal end masses such as titanium or aluminium. The overall length of transducer would be designed to half-wave in order to obtain the required frequency of operation. Early implementations of power ultrasonic devices have included cleaning, plastic welding, metal welding, soldering and machining [18].

1.3.1 Cleaning

Ultrasonic cleaning is one of the oldest industrial application of power ultrasonics. The main advantage of ultrasonic cleaning is in brushless scrubbing due to the cavitations effect. Ultrasonic cleaning work best on relatively hard materials such as metals, glasses, ceramics and plastics, and cleaning equipment normally operates in the range of 20 kHz to 50 kHz. Cavitation occurs when high frequency alternating pressure in a liquid forms microscopic voids which grow to a certain size then collapse, causing very high instantaneous temperatures and pressures. This implosion of cavitational bubbles loosens dirt and grease stuck to the workpiece [19].

1.3.2 Plastic welding

Ultrasonic plastic welding works when high frequency vibration produces heat to melt the plastic precisely at the interface of the parts being joined without indiscriminate heating of the surrounding material [18]. The process is fast and clean, requires no consumables, does not need a skilled operator, and lends itself to automation. Compared to ultrasonic cleaning, ultrasonic plastic welding requires a much higher power intensity to hold vibrational amplitudes constant at varying mechanical loads.

1.3.3 Metal welding

The ultrasonic metal welding process was extensively researched in 1950 [20]. The advantages of ultrasonic metal welds are as low heating and relatively low distortion. The welding temperature is typically below the melting temperature of the metals, which helps to avoid brittleness and the formation of high resistance intermetallic compounds in dissimilar metal welds. The equipment for ultrasonic metal welding can be operated in ranges between 40 kHz and 60 kHz in machines of several kilowatts output capacity.

1.3.4 Soldering

Ultrasonic soldering is the oldest of the five major processes, the original work on these faster and more uniform soldering techniques being done as early as 1936 [21]. The process is fundamentally similar to ultrasonic cleaning with cavitation in molten solder eroding surface oxides and exposing the metal. Ultrasonic soldering can be achieved without fluxes and improves wettability

under most conditions. Overall processing times with ultrasonic soldering can be improved because pre-cleaning and post-cleaning operations are eliminated.

1.3.5 Machining

The application of ultrasonic excitation to machining was discovered by Lewis Balamuth in 1942 while investigating the dispersion of solid in liquid by means of magnetostrictively vibrating nickel tube. Machining process provides high dimensional accuracy but this classic material removal process has some deficiencies. An introduction of ultrasonic technology to the machining process can be observed to reduce these problems.

In ultrasonic machining, material is removed from a surface by fine abrasive grains in slurry. The tip of the tool, called a sonotrode, vibrates at a resonance frequency with low amplitude. This vibration provides a velocity to abrasive grains between the tool and the workpiece. The stress produced by the cyclic impact of abrasive particles on the workpiece surface is high and in brittle materials, such as ceramics and carbides, these impact stresses cause microchipping and erosion of the workpiece surface [22].

In another machining process, called rotary ultrasonic machining, the abrasive slurry is replaced by a tool with metal bonded diamond abrasives which are either implanted or electroplated on the tool surface. The tool is vibrated ultrasonically and rotated while being pressed against the workpiece surface at a constant pressure. The process is similar to a face milling operation, with inserts being replaced by abrasives. Ultrasonic rotary machining substantially increases cutting rates, extends tool life, and due to the lower tool pressures, allows better dimensional control and reduces chipping [23].

1.4 Applications of power ultrasonics in current technology

Power ultrasonics is currently used in a wide variety of science and engineering applications which require load reduction, decreased friction, surface improvement, safer techniques, cost effectivesness and increased product qualities.

1.4.1 Ultrasonic in metalworking processes

The study of ultrasonics in the areas of metal forming, metal removal and metal joining saw very little activity in the 1940 to 1955 period. However, in 1955 F. Blaha and B. Langenecker stated that an acoustic softening occurred in metals under ultrasonic action, leading to a reduction in static stress necessary for plastic deformation [24]. This work was followed by other studies and led to very extensive research on ultrasonic application on metal, as well as some industrial uses [5, 25-33]. The benefits of ultrasonic assisted forming typically included lower forming forces, larger percentage deformation without tearing, and improvements in surface finish. Much research has been published in metalworking processes such as machining [34, 35], forging and compression [36-39], drawing and extrusion [30, 40-43], and welding [44]. All of these studies have shown the beneficial effects of oscillation on elastic-plastic deformation and friction at the contact surface. The studies were investigated in a wide variety of industrial metalworking operations in order to obtain an optimum manufacturing design for various commercial opportunities. A list of power ultrasonic applications in metalworking processes are summarised in Table 1-1.

Table 1-1 A variety list of power ultrasonic applications in metalworking processes

Processes	Applications	Ultrasonic significant effects
Machining	Milling, turning, threading, electrolytic, spark erosion and abrasive machining	Decrease in cutting forces, improvement in surface finish, increase in tool life, noise reduction and good machining on brittle materials
Forging and Upsetting	Hot and cold forging, with and without lubricant forging, open and closed forging	Reduction in friction, force reduction, material softening, improvement in stress superposition
Drawing and Extrusion	Axial and radial	Force reduction, improved surface finish, reduction in internal friction, higher drawing rates and less breakage
Welding	Plastic and metal	Fast, clean, economical, low heat, no pre-cleaning and weld inaccessible areas

1.4.2 Ultrasonics in medical applications

The use of ultrasonics in medicine has several strands. Diagnostic ultrasound is now being used quite extensively for the examination of organs such as the brain, eyes, breast, and liver, as well as in obstetrics. Ultrasonic cleaning baths are available commercially for the cleaning of dental and surgical instruments, while the scaling of teeth can now also be done with a commercial device using an ultrasonic probe [45].

Conventional bone cutting instruments such as burs, saw and chisels, offer limited accuracy and manoeuvrability to surgeons [46] and often result in tissue burning, formation of debris, and damage to adjacent tissue. An alternative

bone cutting device is the ultrasonic blade. In the last twenty years, improvements in transducer design and the development of more sophisticated electromechanical power control, has meant that interest in ultrasonic surgical devices has been strengthened [47].

The use of ultrasonics as a tool in medical diagnosis and measurement first appeared after World War II. New applications of ultrasonics to medical procedures were raised in the late 1950's and continue to be developed. The most important area was imaging, where the technology of non-destructive testing was adopted [48]. The use of ultrasound for surgical and dentistry procedures also appeared in this period. A list of some power ultrasonic applications in medical procedures is presented in Table 1-2.

Table 1-2 A variety list of power ultrasonic applications in medical procedures

Processes	Applications	Ultrasonic significant effects
High intensity focused ultrasound (HIFU) [49]	Treatment of cancers, tumours and fibroids	High intensity heat
Bone cutting [50]	Orthopaedic devices, orthognathic surgery and osteotomy	Elimination of swarf, improved cut quality and precision, reduced reaction force, clean and safe
Ultrasonic cleaning [51]	Dental scaling	Cavitation and micro-streaming
Ultrasonic surgery [52]	Soft tissue dissection	Higher precision, tissue temperature rised and acoustic streaming

1.4.3 Ultrasonic in chemical and liquid applications

The application of ultrasonics to liquid chemicals, sonochemistry, takes advantage of the cavitation bubbles produced by high frequency alternating pressure. The bubbles grow until they reach an unstable size before undergoing violent collapse, which produces both chemical and mechanical effects [31]. The cavitation effects depend on the type of system in which it is generated. These systems can be broadly divided into homogeneous liquid, heterogeneous solid/liquid and heterogeneous liquid/liquid system. The explanation of these systems' functions are shown in Fig. 1-2 to Fig. 1-4.

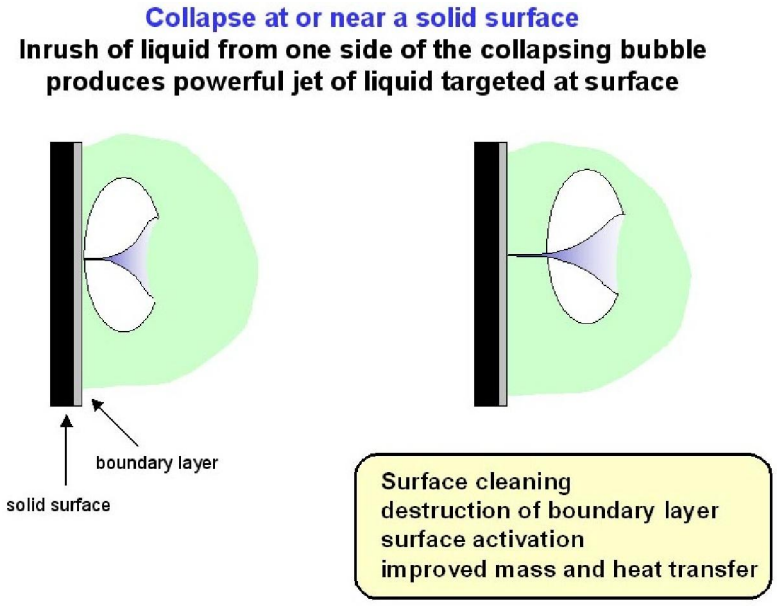

Figure 1-2 The cavitation of homogeneous liquid [53] where (a) the collapsing bubble hit to boundary layer and (b) surface cleaning after the hitting

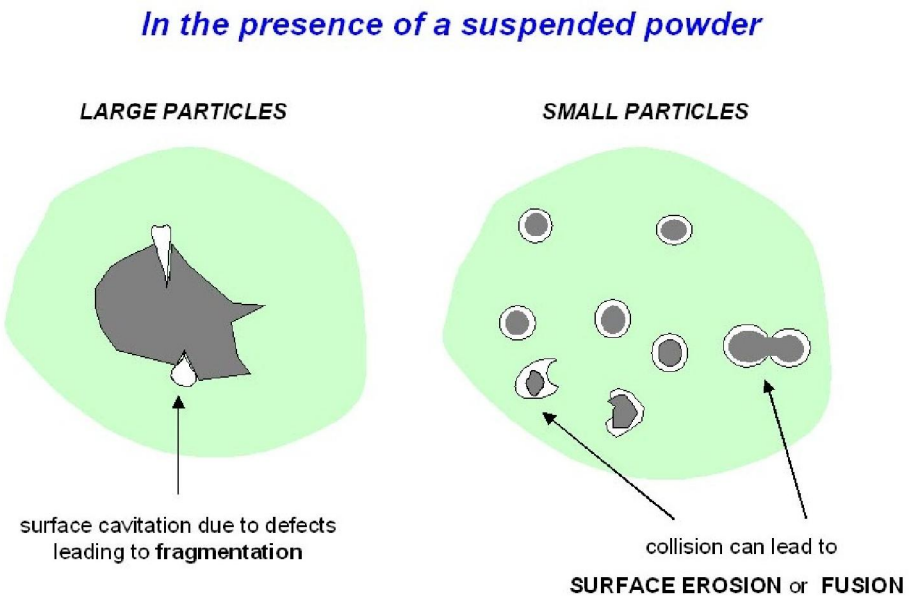

Figure 1-3 The cavitation of heterogeneous solid/liquid [53]

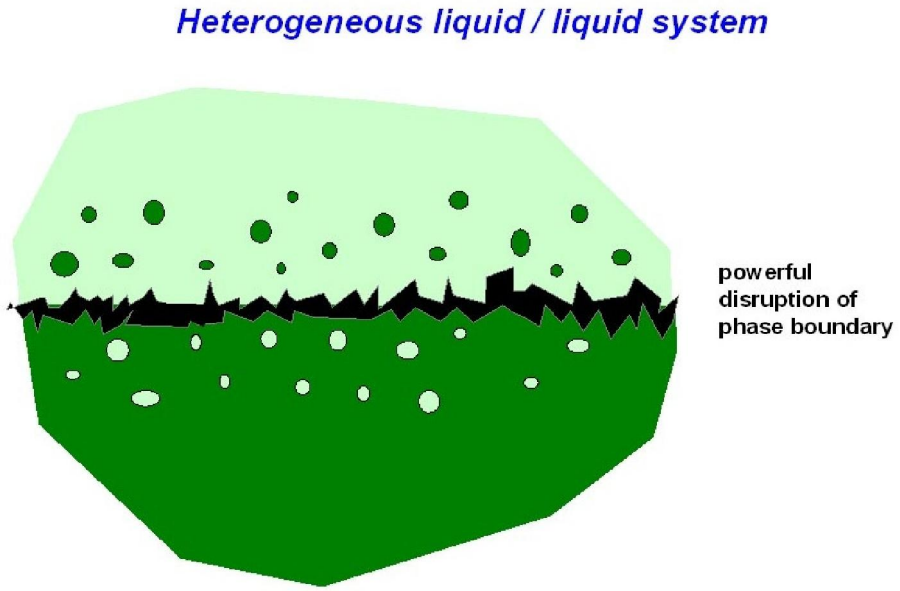

Figure 1-4 The cavitation of heterogeneous liquid/liquid [53]

Sonochemistry began in 1927 when Richards and Loomis observed the chemical effects of high frequency sound waves [54]. As the technology of ultrasonics developed it was soon realized that cavitation can produce useful effects. It is now well known that cavitation has considerable commercial importance in applications such as industrial cleaning, chemical processing and bio-chemical processes. A list of power ultrasonic applications in chemical and liquid processes is summarised in Table 1-3.

Table 1-3 A variety list of power ultrasonic applications in chemical and liquid processes

Processes	Applications	Ultrasonic significant effects
Sonochemistry [4, 55]	Material science, biotechnology and environmental protection	Decrease in reaction time, improved yields, lower operating temperatures and pressures, increased selectivity, radical formation for reaction initiation and more effective catalysts
Power ultrasound in food industry [56, 57]	Particle size control, process tomography, determination of material properties, monitoring of shelf life and preservation enhancement	Reduced impact on nutritional content, coupled with standard sterilization and pasteurization methods
Ultrasonic cleaning bath and chemical etching and irradiation [6, 58]	Reactor vessel, batch treatment and flow system	Cavitation bubbles, acoustic energy, reduce processing time, induced extreme temperatures and pressures, thermal energy, chemical and mechanical energy

1.5 Summary of work

The research reported in this thesis is based on understanding the benefits of applying ultrasonic excitation in the shaping of metal parts for manufacturing applications. Metal is chosen because of the engineering properties, and limitations that influence the choice of this material in many engineering applications. The two metals most commonly used in the manufacturing industry are steel and aluminium because of their cost, mechanical properties and flexibility in processing.

Until the early 1950s, most manufacturing operations that involved metal processing were carried out using traditional machinery such as lathes, drills, milling machines and various pieces of equipment for forming, shaping and joining materials. However, nowadays such equipment can not provide the efficiency, productivity and quality needed for industrial manufacturing competitiveness. This demand has led engineers and investigators to develop new technologies to improve efficiency and flexibility in metal processing, one such technology is power ultrasonics.

The early uses of power ultrasonics largely focused on ultrasonic cleaning until, in the 1950s, the applications of ultrasonic vibration were studied by Blaha and Langenecker [24] who described the benefits of the effects of superimposed ultrasonic excitation in the metal forming process. Since then, a large number of investigations have reported that the principal effect of an ultrasonically assisted metal forming process is a reduction in static flow stress [4, 41, 59-67]. However, the findings have not been sufficient to explain the stress reduction mechanisms, which have resulted in difficulties in optimising the applications of this technology. In particular, no detailed characterisation of the effects of superimposing ultrasonic oscillations on stress during elastic-plastic deformation in a series of ultrasonic amplitude has been carried out, and previous findings have relied on interpretations of measurement of the mean flow stress and oscillatory stress on a single material and using ultrasonic vibration amplitude. This have been insufficient to resolve the effects of ultrasonic vibration.

Research through experiments and finite element simulation studies has been carried out to gain quantitative understanding of the mechanisms of improvement in ultrasonic forming characteristics, such as a reduction in material flow stress, coefficient of friction and oscillatory stress behaviour [59, 66-69]. These studies have characterised the mechanisms by applying ultrasonic vibration to the tool and die in forming tests, and similar results have been predicted in numerical analyses. Research is now required further to characterise these behaviours and understand how they can be optimised for metal forming operations. To advance this field, this study will extend to finite element modelling to examine the characteristics of the oscillatory stress during the ultrasonic excitation.

In this work, the ultrasonic energy is produced by a piezoelectric transducer, and the vibration energy is amplified by an ultrasonic booster and horn. The traditional methods for the design of an acoustic horn are based on the equilibrium of an infinitesimal element under elastic action forces, and integration over the horn length to attain resonance at a desired frequency [70-72]. Accordingly, for practical applications, the tooling is designed for and vibrated at, or close to, the system resonance frequency [37].

Previous studies [4, 26, 43, 73-75] have shown that the effects of ultrasonic excitation on metal forming processes can be considered to be influenced by two categories of mechanism, namely volume effects and surface effects. Previous studies explained that the experimental characteristics of the volume effects and surface effects are mainly dependent on the interpretation of mean flow stress and have neglected the oscillatory stress. A study of the mean and oscillatory flow stress can be demonstrated to provide further insights into the beneficial, significant effects on metal forming process during superimposed ultrasonic excitation.

All of the previous studies showed that the application of ultrasonic excitation on metal forming was investigated in elastic-plastic deformation conditions. A detail study of superimposed ultrasonic excitation on static load during elastic deformation conditions in metal forming has not been investigated because of the effects of reversible behaviour in the material, but understanding the effects of ultrasonic excitation during the elastic deformation is an advantage.

Therefore, an investigation was carried out in the present study that uses both experimental and finite element modelling approaches, and consequently the influences of volume effects and surface effects can be predicted by simulating the ultrasonic excitation on a static forming test in the FE analysis.

Many past studies have been associated with the development of ultrasonic metalworking processes for industrial applications such as die forming, wire drawing and extrusion [59, 62, 63, 76, 77]. All of these studies interpreted the benefits of ultrasonic excitation in the forming process but their statements were focused on the measurement of mean flow stress and forming force only. The findings offered were not enough to validate the proposed stress and force reduction mechanisms.

This current study aims, therefore to investigate the effects of ultrasonic excitation on material flow stress and oscillatory stress behaviour during the elastic and plastic deformation of metals, which have not been included in any previous studies. The material flow stress and oscillatory stress behaviour parameters are investigated in stress-strain diagrams and the parameters gained from these investigation are subsequently used to developed finite element models. The simulation models are used to predict the material softening due to both volume effects and surface effects.

CHAPTER 2

LITERATURE REVIEW

2.1 The history of ultrasonic excitation in metal forming processes

Applications of ultrasonics in metal working processes have been studied since the early 1950s [24, 25, 78], beginning with the earliest studies of Blaha and Langenecker who researched the effects of ultrasonic excitation on metal plasticity [24, 73]. The ultrasonic excitation results in a stress reduction phenomenon during plastic deformation of a metal. The characteristic stress-strain curve was obtained from a tensile test of a single crystal of zinc. A significant effect was also observed by Blaha and Langenecker [73, 79, 80] when studying stress reduction during a tensile test of single crystals of aluminium, cadmium, beryllium, tungsten and stainless steel. The oscillation frequency of the ultrasonic vibration was in the range of 15 to 25 kHz. Progressing from this result, Blaha and Langenecker further observed that the magnitude of stress reduction was independent of the excitation frequency, but dependent upon the amplitude of vibration.

In 1957 Nevill and Brotzen [25] obtained similar effects when stretching a low carbon steel wire with superimposed oscillatory stress. They concluded that the yield stress decrease was independent of the frequency of vibration between 15 kHz and 80 kHz, was directly proportional to the amplitude of vibration, was independent of the elongation of strain applied, and was independent of temperature. In Nevill and Brotzen work, the vibrational amplitude was measured by the amplitude of the oscilloscope pattern which is proportional to the alternating voltage that supplied to the transducer. In this case, the amplitude of vibration was measured by the peak to peak of oscilloscope pattern. In the current technology, the transducer was provided with generator where the ultrasonic amplitude can be directly measured and controlled by the

generator display unit. The measurement of ultrasonic amplitude can be confirmed using non-contact method such as Laser Doppler vibrometer (LDV).

Later, in 1965, Konovalov and Skripnichenko [26] investigated the effect of ultrasonic excitation on the properties of metals during tensile tests. In their work, ultrasonic excitation was generated by a magnetostrictive transducer. Their results showed that the ultrasonic excitation changed the mechanical properties of the metals for the interval of excitation during the tensile test. It was also shown that the effect was practically independent of the investigated rates of loading but dependent on the amplitude of vibration.

In 1966, Izumi et al. [81] carried out a series of tests to observe the effect of ultrasonic vibration on the compressive deformation of metals. In this experiment, the ultrasonic vibration was generated by a magnetostrictive nickel transducer and was superimposed on a static compression load through an ultrasonic horn. A 22 kHz frequency was used and up to 17 μm vibration amplitude was generated on the horn interface. The research study focused on the effects of ultrasonic vibration amplitudes on material compressive stress, heat generation, compression velocity and hardness distribution. The results showed that the ultrasonic excitation reduced the flow stress of compression and material hardness. The distribution of hardness was measured on the longitudinal cross-section of copper and brass alloy. They were measured that the hardness distribution considerably difference which can be seen between the specimen compressed without vibration and that with vibration. It was observed that an uniform distribution with low hardness values was seen in the specimen compressed with a large amplitude of vibration which is apparently due to heat generation. However, the difference in hardness between the specimen with and without vibration was not very obvious. They also observed that the ultrasonic excitation generated high heat on the material when the amplitude increased. However, the effect of ultrasonic excitation was not influenced by the compressive loading rate.

In 1967, Winsper and Sansome [64] reviewed all the studies of applications of ultrasonic excitation on metal forming from 1955 until the late 1960s. All the studies showed that superimposed oscillatory stress during metal forming process significantly reduced the static flow stress. This stress reduction has

been observed under both tensile loads and compressive loads during metal-working operations. This article also reviewed the historical developments of ultrasonic excitation on metal-working processes. Research and preliminary conclusions on the effects of oscillatory stress on the mechanical properties of materials, the mechanisms of reduction in stress and the effects on friction, and also on the use of ultrasonics in various metal working processes such as forging, coining, extruding, rolling, forming and wire and tube drawing were described and discussed. At the end of the review, they suggested that the effects of superimposed ultrasonic excitation during metal-working processes can be explained by a reduction in mean flow stress, a reduction in friction force and the generation of localized heat.

Since these discoveries, many investigators [4, 37, 38, 82-89] have focused on the effectiveness of applied ultrasonic vibration in metal working processes and related the benefits of oscillatory stress to characteristics of the deformation, process speed, ultrasonic frequency, amplitude, mode of vibration, material properties and the interface friction condition in order to increase the productivity, quality and reliability of industrial processes.

Most of these research publications of ultrasonic application in metal-working processes were reported that the significant effects of ultrasonic vibration are independence to frequency, strain applied, temperature and rates of loading. All the claims and findings have been proved and supported with experimental and numerical measurements. However, it was an unclear explanation on temperature of material during superimposed ultrasonic excitation where as heating of the specimen often ignored. Some of the research works [5, 90] observed that the specimen experienced a localised heating due to friction between a relative motion of surfaces where friction at the interface causes heat generation which is generates a thermal softening.

2.2 Mechanics of oscillatory deformation

Improvements to metal-working technology, using ultrasonic vibrations to achieve advantageous effects during plastic deformation processes, are becoming more and more prominent. The equipment required for an ultrasonic system is expensive but the results obtained, if compared to conventional processes are driving a large scale use of ultrasonics in industry.

This activity was prompted by the findings of Blaha and Langenecker who reported a reduction in forming stress due to superimposed oscillatory stress. It has been reported by Winsper et al [91] that the beneficial reduction in stress can be attributed to two basic mechanisms, known as the volume effects and the surface effects. They have defined volume effects as a decrease in flow stress of the material being formed and surface effect, as a change in frictional conditions at the interface between the vibrating device and the workpiece.

The occurrence of the volume effect was discussed in the early work of Blaha and Langenecker [24] who explained that the change in mechanical properties during an ultrasonic tensile test was due to activation of dislocations. However, more explanation is required to define how ultrasonic oscillations can transmit the vibration energy to dislocate the material structure. The natural frequency of dislocations is estimated to be about 100 MHz [92], and thus the energy transmission cannot be explained in terms of resonance. This was accepted by Nevill and Brotzen [25] who argued that Blaha and Langenecker's work did not provide any correlation between the experimental and theoretical models of dislocation movement and energy absorption. Neville and Brotzen explained that the stress reduction was accounted for in terms of the superimposition of alternating acoustic stress on the stress produced externally. This superposition of stresses is schematically illustrated in Fig. 2-1, where S is a steady uniaxial stress, A is a maximum amplitude of alternating stress and S_y is necessary minimum stress to produce yielding. The superposition of stress was achieved when $S + A > S_y$,where the alternating stress is greater than that required to induce plastic deformation. At this point, the alternating stress was sufficient to activate dislocation.

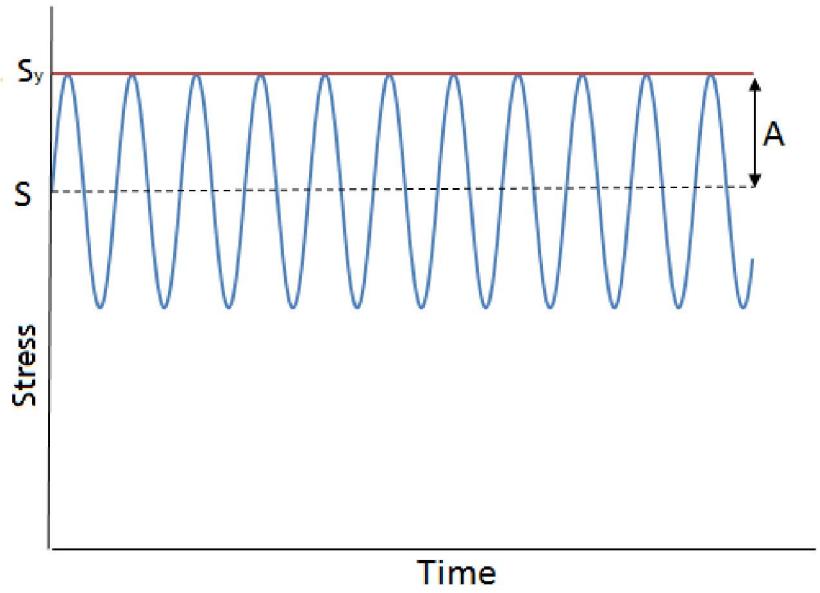

Figure 2-1 Superposition of steady and alternating stresses to cause yielding

Winsper et al. [64] reviewed the application of ultrasonic excitation to metal deformation, as carried out by a large number of investigators. All the results showed that deformation was achieved with significantly reduced stress when oscillatory stress was superimposed on static forming. Some [25, 43, 93] have accepted the stress superposition mechanism, which describes the stress in a work piece when vibrations are applied which have amplitudes of less than some critical value. The magnitude of the oscillatory stress corresponding to this threshold value is dependent on the characteristics of the material being deformed.

A measurement of the characteristics of stress reduction and oscillatory stress amplitude could instead offer a significant explanation of material softening during the superimposed ultrasonic excitation.

The phenomenon of material softening effects was reported by Blaha and Langenecker [24]. This phenomenon is therefore often referred to as the Blaha effect, or volume effect, and is also known as the acoustoplastic effect [4, 64, 74]. This acoustoplastic effect is described as a decrease in the flow stress during deformation at a constant strain rate or an increase in strain rate during plastic deformation under a constant stress.

Winsper et al. [64] reported that the material softening mechanisms can be explained by the phenomena of reduced flow stress, reduced friction conditions and heating of the workpiece. However, the mechanisms of reduced flow stress and reduced friction were most effectively obtained in the material softening during ultrasonic metal-working operations. Heating of the workpiece was often ignored since the ultrasonic excitation did not generate heat in the workpiece.

2.3 The influence of ultrasonic excitation on the processes of plastic deformation

The effect of ultrasonic excitation on the processes of plastic deformation can be described by a force-displacement diagram (Fig. 2-2) for the static compression of a specimen [94]. The diagram shows regions of elastic and plastic deformation [22]. In elastic deformation, if the load P does not exceed an elastic limit P_{yo}, the force P and the displacement h are proportional to each other through the relationship:

$$P = k_o h = \varepsilon E A, \tag{2.1}$$

where h is the deformation of the specimen, $k_o = EA/H$ is its static stiffness; A and H are the cross-section and height of the specimen respectively; E is the elastic modulus of the material and $\varepsilon = h/H$ is the strain.

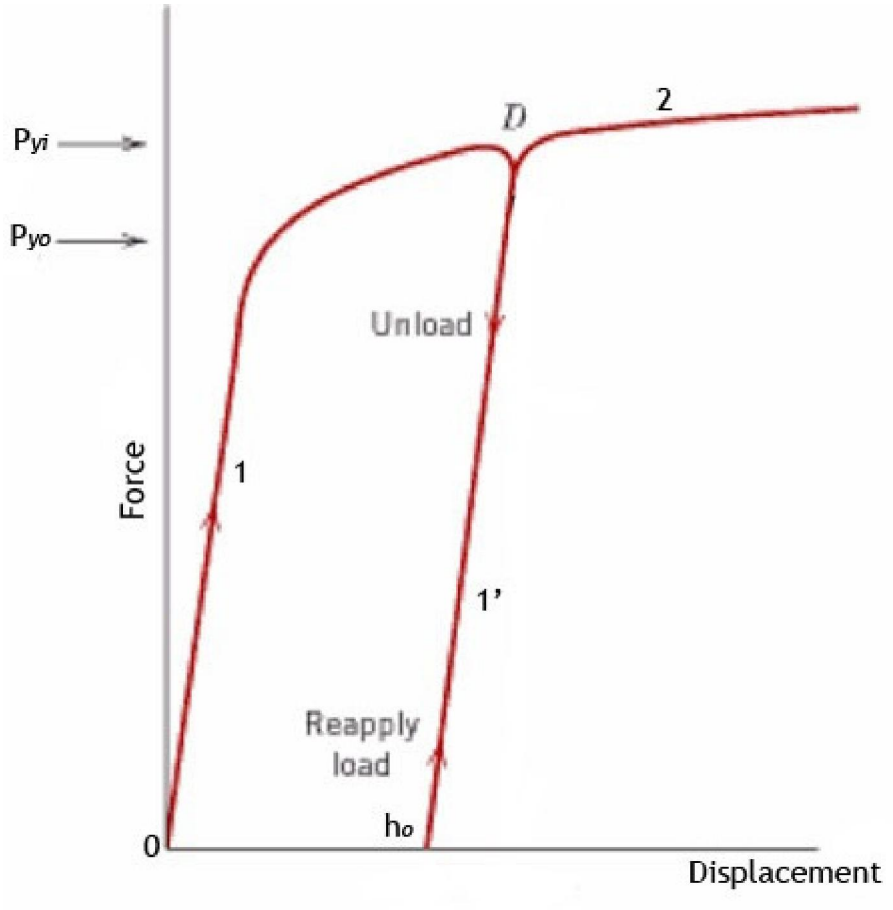

Figure 2-2 Elastic and plastic deformation [95]

In plastic deformation in which the material experiences both stress and strain, the process varies depending on whether the deformation increases or decreases: curve 1 corresponds to an increase from point 0 and curve 1' corresponds to a decrease in deformation starting from point D. Curve 1' is practically parallel to the initial part of curve 1 as shown in Fig. 2-2. After a complete loading/unloading cycle there is residual plastic deformation h_o and, during subsequent reloading, the material will be in an elastic state, described by curve 1', until the force P reaches the value P_{yi}, $P = P_{yi} = P_D$. Further loading causes a plastic deformation along curve 2.

Fig. 2-2 shows a typical diagram for an elastic-plastic material that experiences work hardening where the force in the plastic deformation zone rises as the deformation increases. During the cyclic loading of such a material, its elastic limit rises from one cycle to the next and the value at certain point in time

depends on the complete loading history. This cyclic loading effect is similar to the process of vibrational hardening during ultrasonic metal forming.

The vibrational loading processes can be described using idealized 1-D models consisting of elementary parts to describe the mechanical behaviour of a real material [94, 96, 97]. The model depicted in Fig. 2-3(a), consists of an elastic element k_o, a pair of dry friction components D connected in series, and a carriage that includes of the vibratory tool.

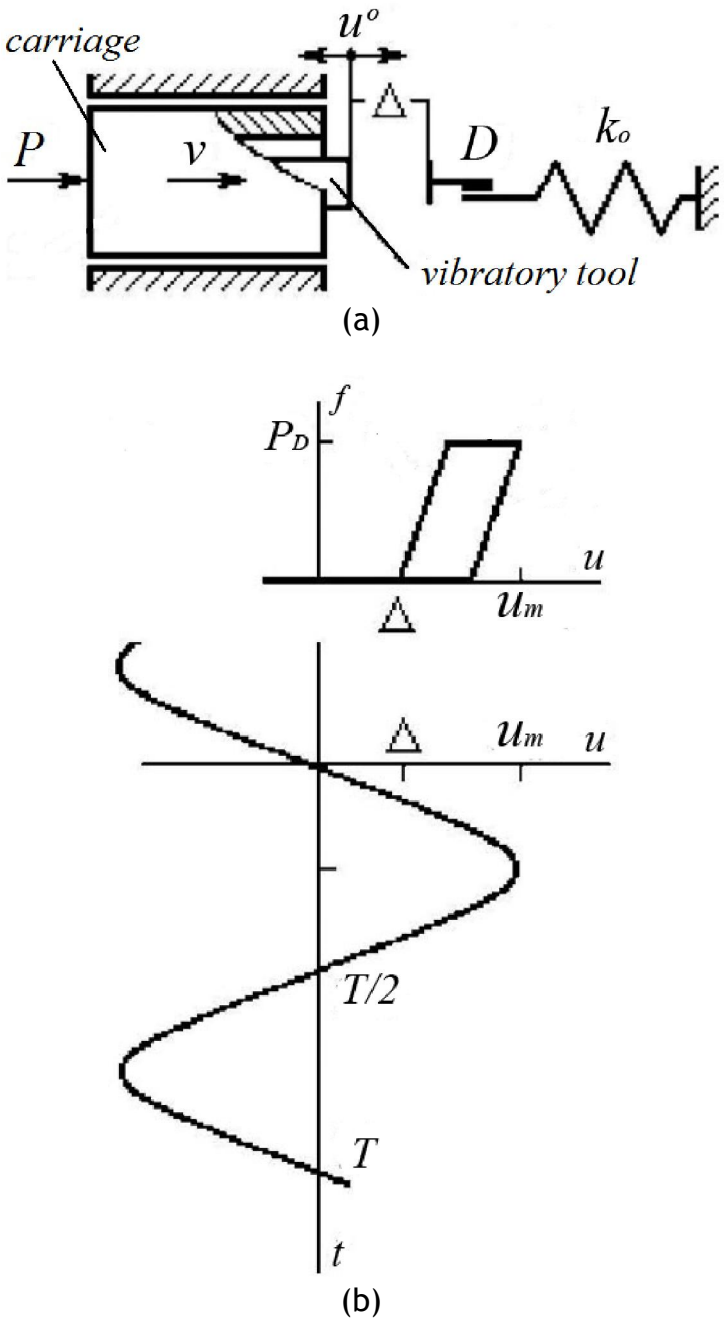

Figure 2-3 The model of vibrational loading process [98]

Let the deformation of the material result from its interaction with vibratory tool. The vibrational motion of tool with respect to the carriage obeys the law:

$$u^o = asin\omega t, \tag{2.2}$$

where a is the amplitude and ω is the angular frequency. Carriage is subject to a constant static force P and, depending on the conditions of deformation, either moves with a constant speed v, or remains in equilibrium $(v = 0)$. The full motion of the tools; carriage and vibratory tool are described as follows:

$$u(t) = vt + u^o(t) = vt + asin\omega t, \tag{2.3}$$

To simulate the deformation process, the following experiment is carried out. The force P is slowly increased and the movement of the carriage is tracked. It is assumed that, for every given value of P, the model has an oscillatory regime of deformation. This assumption allows the interaction between the tool and the material to be considered during one period of tool vibration alone. The following notation is now introduced, Δ is the distance between the centreline of the vibratory tool and the deformation of the specimen specimen; $h = u(t) - \Delta$ is the displacement of the carriage with respect to the specimen and is equal to the deformation over a period, and f is the force of interaction between the tool and the specimen. Values of $\Delta > 0$ correspond to the adjustment of the tool in which an initial clearance is set up, while $\Delta < 0$ corresponds to an initial interference between the material and the tool. The material deformation is assumed small and the elastic wave propagated along the material in a period of time shorter than the period of loading, that is $H/c \ll T = 2\pi\omega$, where c is the speed of sound in the material. Consequently, due to this assumption and based on a linear relation of Hooke's law, the dynamic characteristic $f = f(u, \dot{u})$ determines the relation between the force f, displacement u and speed $\dot{u}$ of the tool as shown in Fig. 2-3(b). The dynamic characteristic is represented as follows:

$$f = f(u,\dot{u}) = \begin{cases} 0, & u \le \Delta, \dot{u} > 0 \\ k_o(u-\Delta), & \Delta \le u \le \Delta + \frac{P_D}{k_o}, \dot{u} > 0 \\ P_D, & \Delta + \frac{P_D}{k_o} \le u \le u_m, \dot{u} > 0 \\ P_D + k_o(u-u_m), & u_m - \frac{P_D}{k_o} \le u \le u_m, \dot{u} < 0 \\ 0, & u \le u_m - \frac{P_D}{k_o}, \dot{u} < 0 \end{cases} \quad (2.4)$$

where

$$u_m = a[\sqrt{1-(\tfrac{v}{a\omega})^2} + \tfrac{v}{a\omega}\cos^{-1}(-\tfrac{v}{a\omega})] \quad (2.5)$$

which is the maximum of the function (2.3) over a period.

Hence, the force of interaction is calculated as:

$$F(t) = f[u(t), \dot{u}(t)] \quad (2.6)$$

is a periodic function of time with a period $T = 2\pi/\omega$. The constant force P and the parameters of motion of the tool are obtained as:

$$P = \frac{1}{T}\int_{t_1}^{t_1+T} F(t)dt = \frac{1}{T}\int_{t_1}^{t_1+T} f[u(t), \dot{u}(t)]dt \quad (2.7)$$

The dynamic characteristic of applied force, the motion of vibratory tool and a force-time measurement can be calculated using equation (2.7) and is shown in Fig. 2-4. The material deformation does not exceed the limits of the initial linear part of the dynamic characteristic $(0 < h \le P_D/k_o)$ and the carriage remains in dynamic equilibrium with speed $v = 0$. If the material deformation exceeds the limit $(h > P_D/k_o)$, the deformation is considered to be plastic deformation and it is assumed that the carriage moves with a constant speed v. Fig. 2-5 demonstrates the situation of dynamic deformation.

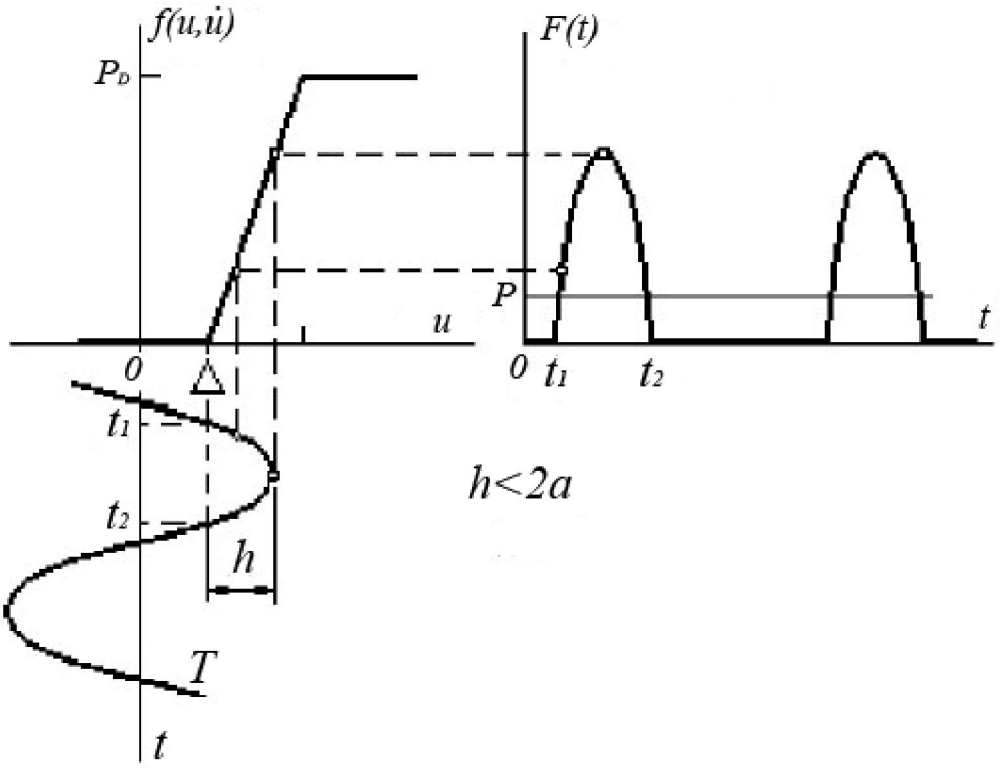

(a)

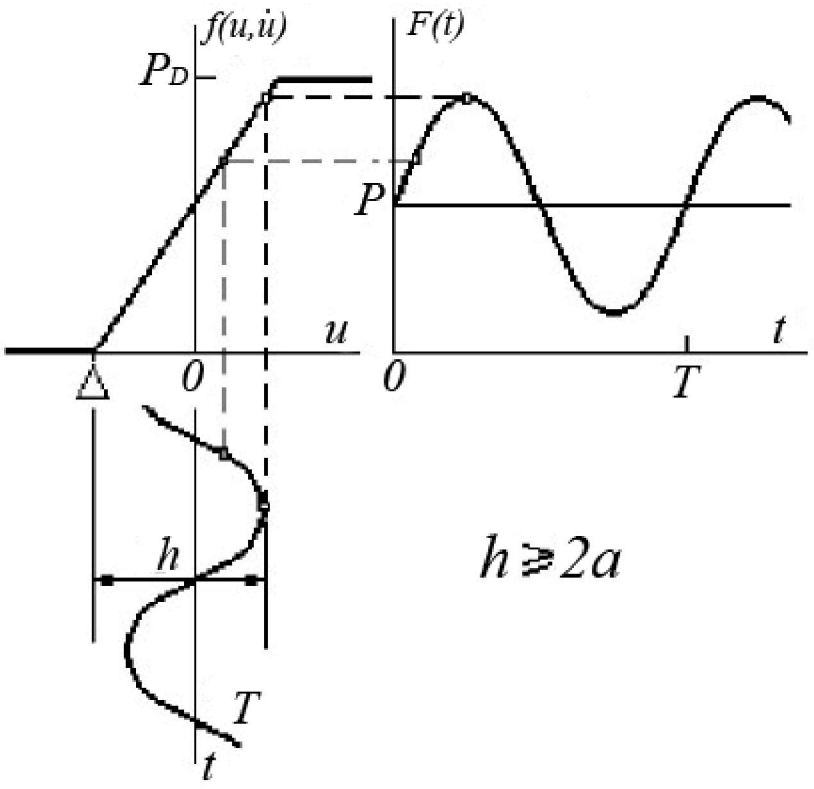

(b)

Figure 2-4 The dynamic loading characteristics $(v = 0)$ [98]

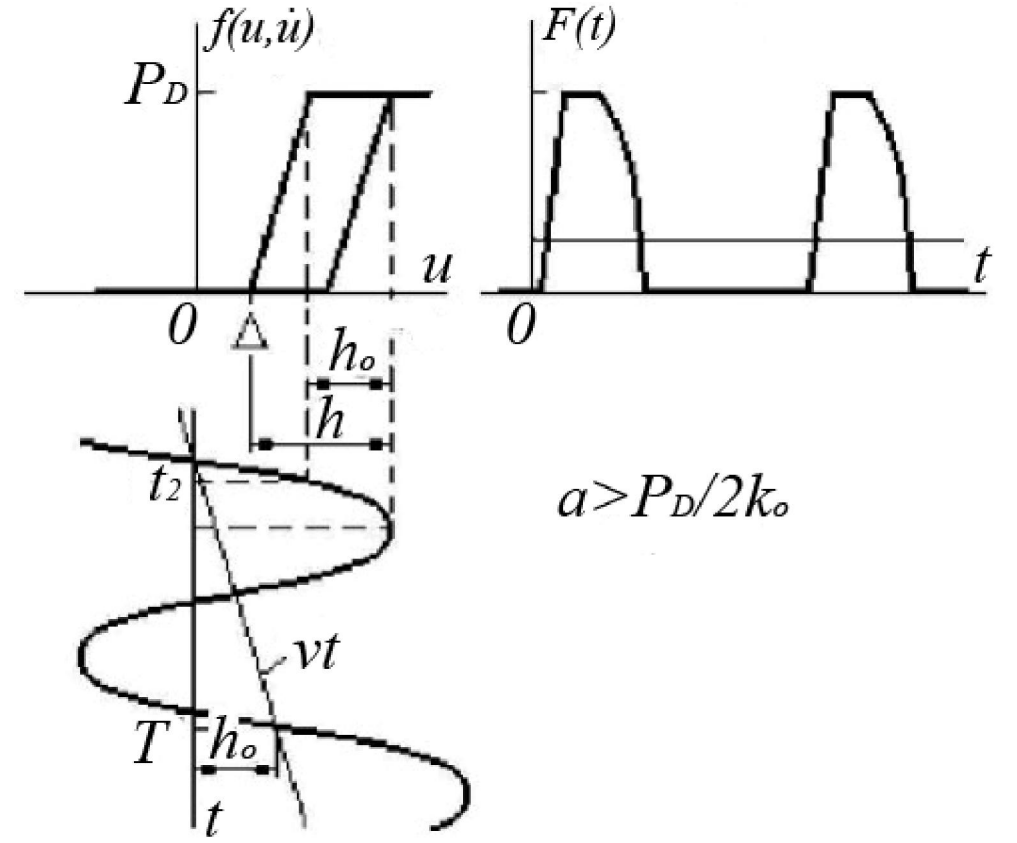

(a)

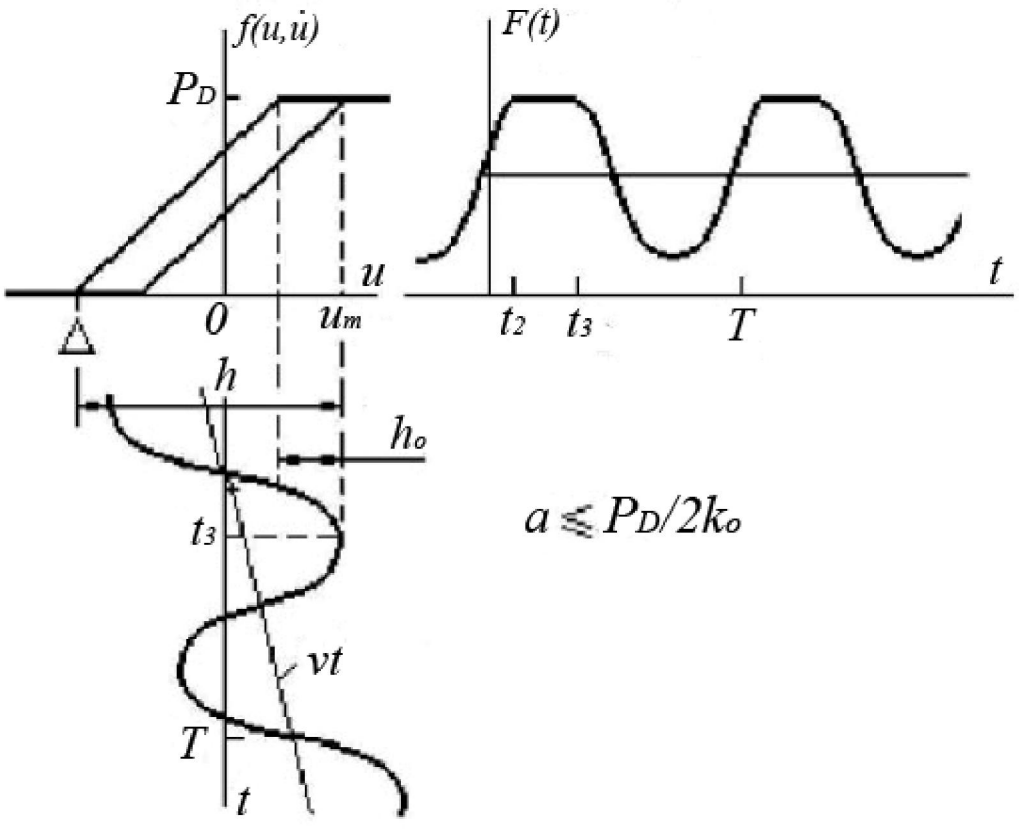

Figure 2-5 The dynamic loading characteristics (constant speed v) [98]

An experimental study by Izumi et al. [65] investigated the effect of ultrasonic excitation on compression test for different materials. The compression test was carried out for 14 mm diameter and 15 mm high specimens. The velocity of compression was kept constant and the amplitude of vibration was changed from 0 to 15 μm. This investigation resulted in a relation between an observed yield limit σ, and vibration amplitude a,

$$\sigma = \sigma_o - Ka, \tag{2.8}$$

where σ_o is the actual yield limit found in a static deformation processes and K is a material constant dependent on the material. In the case of Izumi et al. [65, 81], the investigation used a vibration amplitude, $a \leq P_D/k_o$ and deformation of displacement, $h \geq 2a$ which refers to Fig. 2-4 and Fig. 2-5 for continuous loading. If $\dot{u} > 0$, equation (2.4) shows the influence of the tool on the specimen during a periodic sequence of impulses as:

$$f(t) = k_o[u(t) - \Delta], \quad t_1 \leq t \leq t_2 \tag{2.9}$$

where $u(t) = asin\omega t$, $\Delta = a - h$, $t_1 = -\frac{\pi}{2\omega}$, and $t_2 = \frac{\pi}{\omega} - t_1$. According to equation (2.9), the constant force is equal to

$$P = k_o(h - a) \tag{2.10}$$

Dividing equation (2.10) by A and using notation $\sigma = P/A$, $\sigma_o = k_o h/A$, and also $K = k_o/A = E/H$, we obtain a relation of the equation (2.8). According to equation (2.8) and equation (2.10), various materials respond differently to ultrasonic vibration in plastic deformation. Materials with a bigger elastic modulus E and specimens with a bigger static stiffness $k_o$are more sensitive to the influence of ultrasonics [65, 98].

The significant effect of force reduction due to ultrasonic excitation during the process of plastic deformation can be shown in Fig. 2-6.

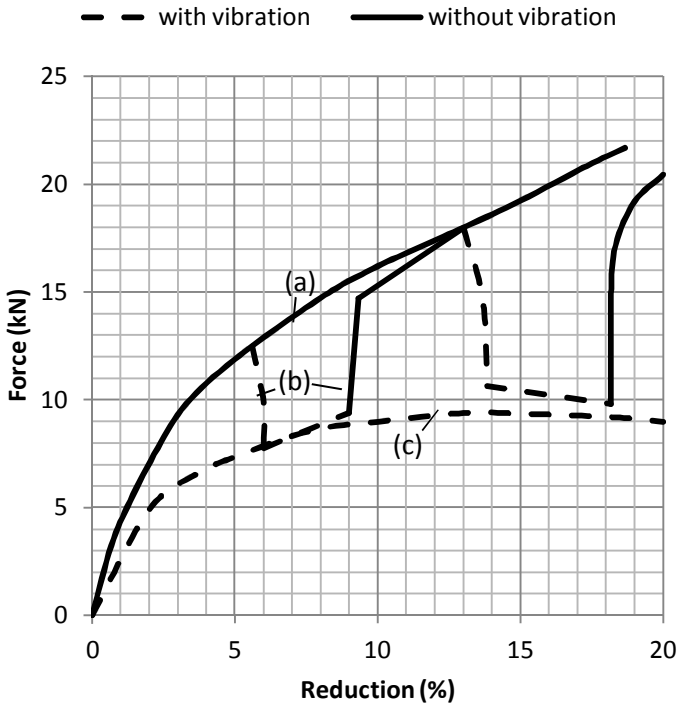

Figure 2-6 Drop of compressive load due to superimposed vibration. (a) without vibration, (b) superimposed on the direction of static compression, (c) with vibration [65]

2.4 The influence of ultrasonic excitation on interface friction

Interface friction appears during the interaction of the tool and the workpiece where the friction force is used to resist the motion between tool and workpiece. A model of an ultrasonic system can be simulated with a friction force as shown Fig. 2-7.

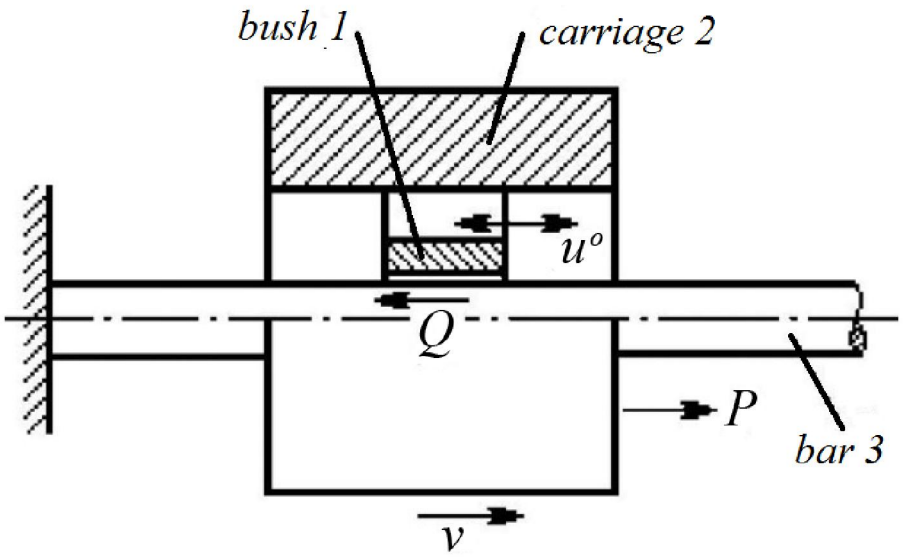

Figure 2-7 Ultrasonic friction force [98]

When carriage 2 moves, subject to a static force P, with an average speed v along the guide bar 3 then bush 1, which is connected to the carriage, is able to vibrate laterally with respect to it. A dry friction force Q is developed in the contact zone between bush 1 and bar 3 and a static force, $P = Q$, is needed to maintain the uniform motion. The influence of vibration in the contact zone on the static force necessary to overcome friction is now estimated. The steady motion of the bush 1 is considered as:

$$u(t) = vt + u^o(t) = vt + asin\omega t \tag{2.11}$$

The nonlinear dynamic characteristic of the dry friction force is presented as follows:

$$f(\dot{u}) = Q\ sgn\ \dot{u} \tag{2.12}$$

where sgn is signum function, denoted by $sgn\,\dot{u}$ is defined by

$sgn\,\dot{u} = \begin{cases} -1, & \dot{u} < 0 \\ 1, & \dot{u} > 0 \end{cases}$ which is shown in Fig. 2-8(a)

Consider the differential equation of (2.11) and substitute it into (2.12). The frictional force developed in the contact zone:

$$F(t) = f\big(\dot{u}(t)\big) = Q\ sgn\ (v + a\omega cos\omega t) \tag{2.13}$$

is a periodic function with the period $T = 2\pi/\omega$.

The relationship between the static force P and the parameters of the system's motion can be written as:

$$P = \frac{1}{T}\int_0^T F(t)dt = \frac{Q}{T}\int_0^T sgn\ (v + a\omega cos\omega t)dt \tag{2.14}$$

The characteristics of the friction present in the contact zone are shown in Fig. 2-8, with the speed and friction force as a function of time.

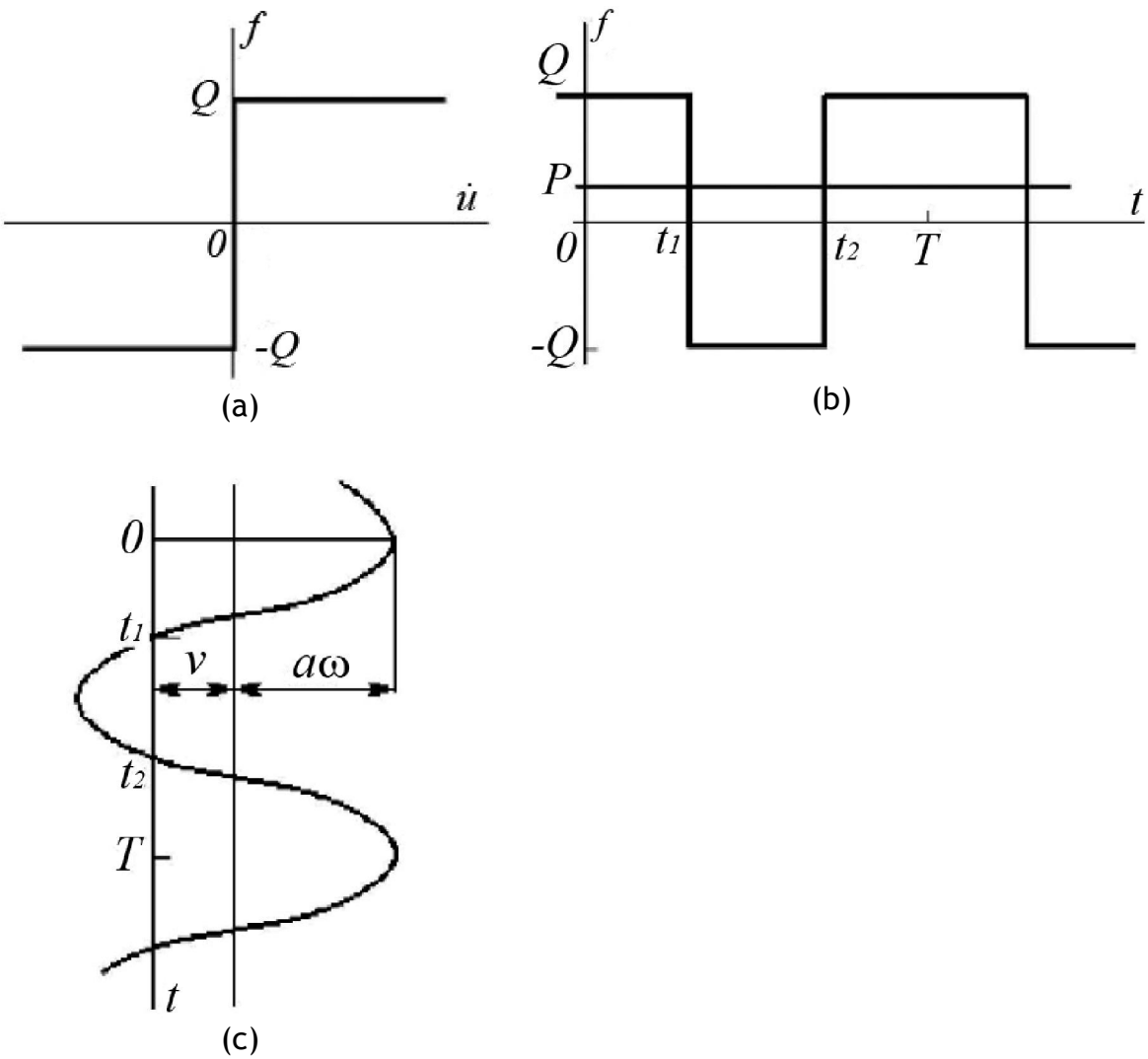

Figure 2-8 The characteristics of the frictional force [98]

Solving the equation (2.14) in a period of cyclic motion gives

$$P = \frac{Q}{\pi}[\pi - (\tau_2 - \tau_1)], \tag{2.15}$$

where

$\tau_1 = \omega t_1 = \cos^{-1}\left(-\frac{v}{a\omega}\right) = \frac{\pi}{2} + \sin^{-1} va\omega$ and $\tau_2 = \omega t_2 = 2\pi - \tau_1$

t_1 and t_2 are the instants, when the speed $\dot{u}(t)$ changed its sign in Fig. 2-8. Substituting τ_1 and $\tau_2$into equation (2.15), reveals

$$P = \frac{2Q}{\pi}\sin^{-1}\frac{v}{a\omega} \tag{2.16}$$

Considering that the carriage speed v is very small, the vibration velocity $v/a\omega$ approximates to:

$$\sin^{-1}\frac{v}{a\omega} \approx \frac{v}{a\omega} \tag{2.17}$$

and substituting (2.17) into (2.16) gives the static force required to overcome friction force as

$$P = \frac{2Q}{\pi a\omega}v \tag{2.18}$$

The force behaviour under ultrasonic influence, as considered in (2.18), is known as a vibrational smoothing [99-103].

On the other hand, vibration of bush 1 is consider applied in a sliding plane perpendicular to the velocity of the carriage v in Fig. 2-7. The sliding plane is shown in Fig. 2-9. The plane moves along the x-axis, with a speed v and performs T-periodic vibration $\dot{u}(t)$ along the y-axis direction. The friction force Q has a constant value and in a direction opposite to that of the velocity vector $v_o(t)$.

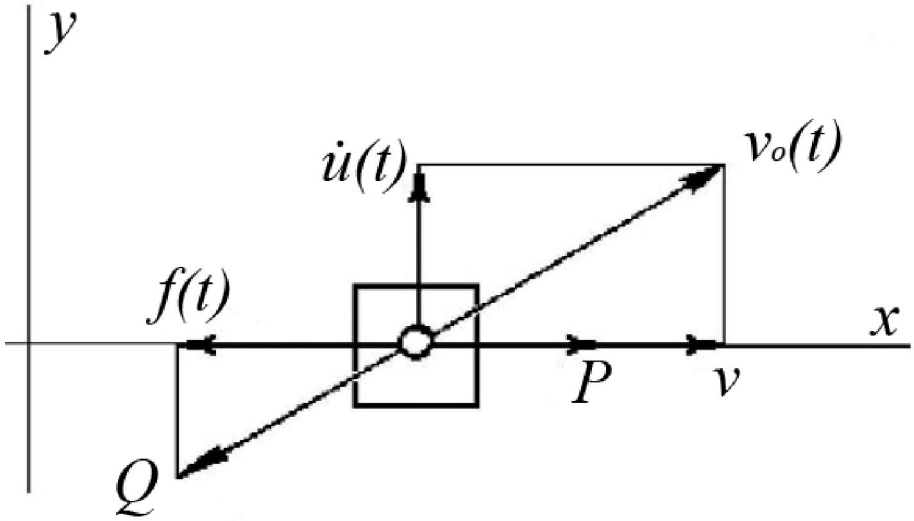

Figure 2-9 The vibratory element slides in an axis

As a result, the constant force P needed to overcome the friction force is required to be:

$$P = \frac{1}{T}\int_0^T F(t)dt = \frac{Q}{T}\int_0^T \frac{vdt}{\sqrt{v^2+[\dot{u}(t)]^2}} \tag{2.19}$$

Substituting $\dot{u}(t) = a\omega sin\omega t$ and assuming $v \ll a\omega$, the constant force gives

$$P = \frac{2}{3}Q\frac{v}{a\omega}ln\left[\frac{2\left(1+\sqrt{\left(\frac{v}{a\omega}\right)^2+1}\right)^2}{\frac{v}{a\omega}\left(1+\sqrt{\left(\frac{2v}{a\omega}\right)^2+1}\right)}\right] \tag{2.20}$$

The dependence of the static force P on the ratio of speeds $\frac{v}{a\omega}$, in accordance with equations (2.18) and (2.20), is shown in Fig. 2-10(a) and Fig. 2-10(b), respectively. The result in Fig. 2-10(a) occurs whenever the magnitude of friction and speed of forming are parallel which is shown in Fig. 2-7, conversely, if the magnitude of friction and forming speed are perpendicular in Fig. 2-9, the ratio of force $\frac{P}{Q}$ on the ratio of speed $\frac{v}{a\omega}$ is measured in Fig. 2-10(b). It can be seen that the vibration in the contact zone leads to a decrease in friction force [98]. Comparing Fig. 2-10(a) and Fig. 2-10(b), it can be seen that, for the vibration speed $a\omega$ and for a small sliding speed v, the most pronounced

decrease in friction is achieved when the direction of vibration and sliding coincide.

Fig. 2-7 shows that the frictional force is developed at the interface between the motion of the tool and the deformed material in metal forming. The work done by friction can translate into deformation, wear and heat, affecting the contact surface properties. This beneficial effect offers advantages to metal joining in some metal forming processes, but lubrication is used to prevent the wear. Consequently, the frictional force is reduced in terms of friction coefficient.

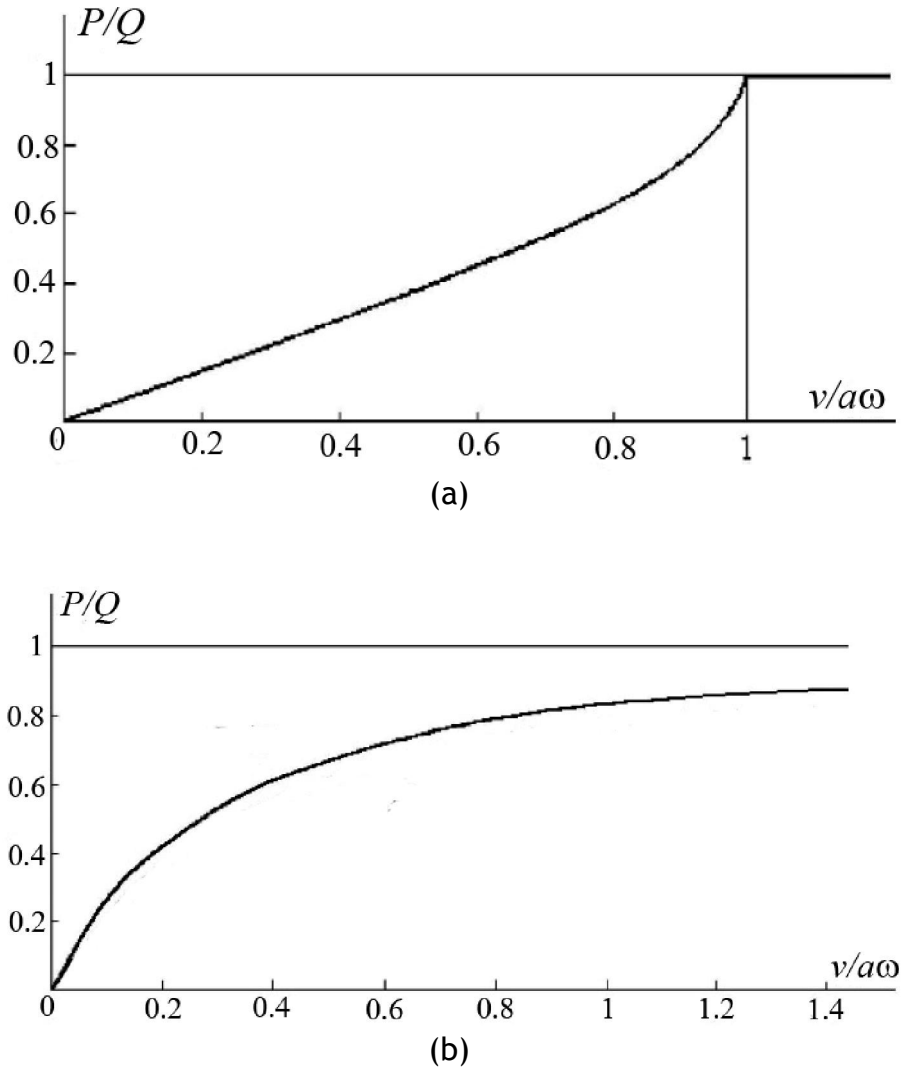

Figure 2-10 The dependence of the static force on the ratio of speeds [98] for (a) vibration motion parallel to speed and (b) vibration motion perpendicular to speed

Friction coefficient reduction influences the aspect of ultrasonic metal forming called the surface effect. Thus, the phenomena of surface effects are defined as a change in frictional conditions at the interface between the vibrating tool and the specimen. The effect of ultrasonic excitation on friction was first examined by Lehfeldt [92], who reported that a sphere excited by oscillations moves on a revolving plate and minimum friction forces are observed when the sphere vibrates tangentially to the plate surface at the maximum amplitude. Winsper et al. [64] concluded that the superimposed ultrasonic excitation on conventional metal forming effectively reduces the frictional force without requiring any lubrication. The occurrence of surface effects during ultrasonic metal forming is useful in forming difficult materials under severe frictional conditions.

Pohlman and Lehfeldt [92] summarised the reduction in forming force as being influenced by reductions of internal friction in the material and external friction at the interfaces where internal friction reduction is explained by the superimposition of the oscillatory stress on the static stress. They have measured the result of reduction in drawing force when the specimen was subjected to impulses of ultrasonic vibration at specific intervals. The suddenness of the reduction in drawing force when ultrasonic vibration is switched on indicated that the vibration has a direct influence on the internal friction of the specimen where the external friction was not occurred in the drawing process. The internal friction was defined as the force resisting motion between the elements making up a solid material while it undergoes plastic deformation. In the case of Pohlman and Lehfeldt work, as deformation occurred, internal forces opposed the applied force which mean that the internal friction was in linear proportion with forming force.

Similar results obtained by other investigators [37, 40, 41, 64, 83, 104] interpret the coefficient of friction between tool and material as being significantly reduced with the application of ultrasonic vibration. The researchers also claim that the coefficient of friction is reduced as a function of the ultrasonic amplitude, forming speed, contact pressure, viscosity of the lubricant, acceleration of the vibratory tool, contact time and material properties. Many investigators [64, 105, 106] conclude that the ultrasonic vibration reduces the coefficient of friction for unlubricated surfaces. Unexpectedly, the results demonstrate similarly shape curves of stress-strain for lubricated runs.

Recently, many researchers have defined the effectiveness of surface effects on ultrasonic forming by experimental and numerical results. Finite element results by Yoa et al. [107] demonstrate that the stress superposition is only a part of the load reduction measured under superimposed ultrasonic vibration, and observed that there was no temperature change during the process. The load reduction in the ultrasonic forming process was attributed to a combination of stress superposition and friction reduction. Other investigators [108, 109] observed finite element simulations and experiments on hot ring compression to explore the frictional effect of ultrasonic excitation. They have measured the temperature of specimen during ultrasonic vibration on ring compression test. The test results indicated that ultrasonic vibration indeed raised the temperature of the specimen. The temperature increased rapidly in the initial vibration stage and then decreased with time. They also found that the stress-strain curve obtained from ultrasonic compression test at 25^{o}C has a similar curve compared with stress-strain curve of conventional compression at 150^{o}C. Therefore the reduction in the flow stress caused by increasing the temperature to 150^{o}C was similar to that caused by applying ultrasonic vibration. However, there was no further explanation on causes of heat generated during applying the ultrasonic excitation. Consequently, the interface friction increased with the temperature of the material and indicated that the vibration also increased the interfacial friction. A simulation result by Mousavi et al.[67] predicted that the extrusion force was not affected by the friction factor in the contact interaction.

Daud et al. [66] measured a significant number of friction coefficients in ultrasonic metal forming using an ultrasonic ring test. As a result the coefficients of friction from the ultrasonic tests were identical to the coefficient of friction for static test for a dry surface. This demonstrated that any change in the interface friction condition during ultrasonic excitation was temporary and the effects were not measurable by analysis of the specimen after ultrasonic excitation is discontinued.

Later, Daud et al. predicted the behaviour of interface friction between die and specimen using an ultrasonic compression test with different lubricated surfaces. A reduction in the static stress was observed for all surface conditions. It was clear that the stress reduction was dependent on the lubricated condition but,

unexpectedly, a dry surface condition showed a higher reduction. A finite element model was developed for verification and an agreement was achieved with the experimental result if a lowered value of friction coefficient was introduced during superimposed ultrasonic excitation.

Most of the investigators above claimed that the surface effect was not thoroughly understood, although it offered greater potential to the metal forming industry.

2.5 The influence of oscillatory stress on metal characteristics

Since the work of Blaha and Langenecker in 1955, a large number of investigators [25, 26, 36, 38, 39, 65, 66, 110, 111] have studied the effect of applying oscillatory stress to metal undergoing plastic deformation. Superimpositon of oscillatory stress onto static deformation shows significant effects on the forming force, forming speed, friction condition, material temperature and material properties. Most researchers have suggested that ultrasonic excitation reduced the material flow stress in their work.

Explanations of the significant effect of superimposed oscillatory stress on material properties has become a major consideration in the study of the ultrasonic metal forming process. Choice of the appropriate material properties and metal characteristics can be dictated by the properties required for the process. The classic example involves strength and ductility; normally, a material of high strength will only have a limited ductility. A material rarely possesses the maximum or ideal combination of properties after it has been processed and thus it is necessary to trade off one characteristic for another. Consideration is made of whether any deterioration of material properties occurs during ultrasonic metal forming, such as whether a significant reduction in mechanical strength or grain size reduction for harder materials may result from the application of ultrasonics.

During ultrasonic metal forming, the vibration causes the flow stress loading of compression to be significantly lowered [38, 65]. The decrease of flow stress with increased ultrasonic vibration amplitude is called vibration sensitivity. This vibration sensitivity is exceedingly sensitive to the individual characteristics of materials such as acoustic impedence (ρc), Young's modulus (E), melting point (T_m), work hardening coefficient and stacking-fault energy (γ). Other researchers [84, 112, 113] have found that the force reduction effect by ultrasonic excitation not only occurs in metal but also in plasticine, cheese and bone. Recently, the effectiveness of flow stress reduction and improvement in material properties by superimposed ultrasonic oscillation have been investigated by more researchers in many metal forming processes, which included metal drawing [30, 37, 114], extrusion [67, 111, 115], bending [116], grinding [117], machining [118] and drilling [33, 119]. Beside the major reduction in flow stress, the researchers have also observed other beneficial effects on metal properties during processing such as material hardness, grain size and surface roughness.

2.5.1 Forming speed

In a simple ultrasonic compression test, a cylindrical specimen is compressed between a flat punch and die. Usually, the flat punch is pressed down with a constant rate to compress the specimen on the static die as shown in Fig. 2-11 [120]. a and f are the amplitude and the frequency of die vibrations, the maximum vibration speed is calculated as $V(t)_{\max} = 2\pi af$, and the speed profile is shown in Fig. 2-12.

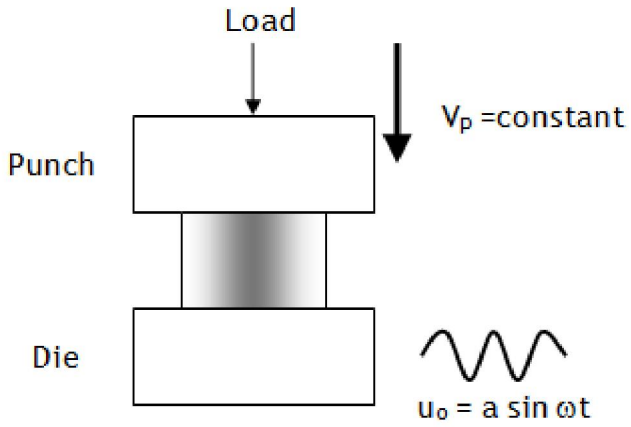

Figure 2-11 A simple ultrasonic vibration compression test

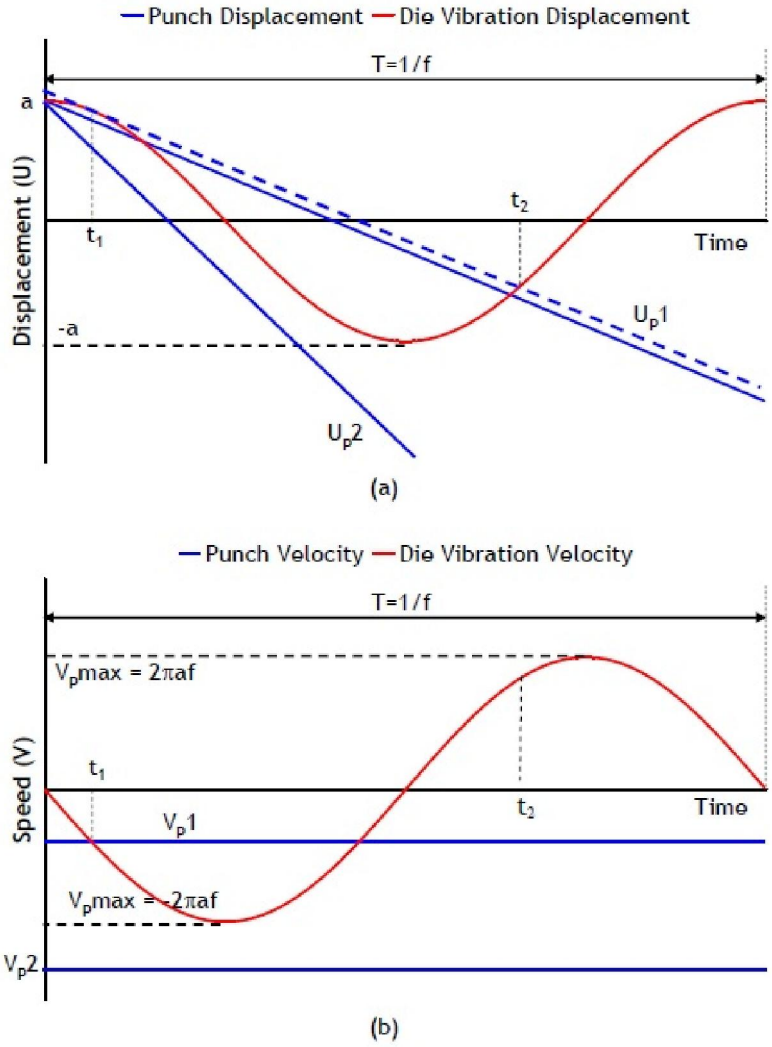

Figure 2-12 (a) Variations of punch displacement and ultrasonic vibration displacement with time (one period) and (b) variations of punch speed and ultrasonic vibration velocity with time (one period) [67]

If the punch speed is less than the maximum vibration speed (refer to figure 2-12(b) where $V_p1 < V_pmax$), the die surface separates from the specimen. Under this situation at time t_1, the die vibration rate exceeds the punch speed, V_p1, and thus the die surface is separated from the flowing material. The separation continues until the die surface and the flowing material are in contact again at time t_2. The time separation between t_1 and t_2 creates an opening without contact conditions. This occurrence results in a decrease of the punch load due to a reduction of the friction forces by the contact and separation incident [67]. On the contrary, if the punch speed is higher than the maximum speed, (refer to figure 2-12(b) where $V_p2 > V_pmax$) the contact between the die surface and specimen remains, and no separation occurs.

Another investigator, Kristoffy [37], reports that the maximum vibration speed must be at least three times the forming speed in order to achieve a force or friction reduction effect. It is also shown that a tangential vibration of the die in wire drawing operations does not change the direction of friction forces, unless the maximum vibrated velocity is larger than the drawing speed. However, Siegert et al. [30] explain that the reduction of friction force is influenced by a function of the ultrasonic amplitude and forming velocity. Unexpectedly, the friction force reduction observed reduces with the increase of forming speed. Izumi et al. [65] observe that the effect of forming speed was independent to the amplitude of superimposed ultrasonic excitation during the compression test.

2.5.2 Material hardening properties

Generally, metal hardening is defined as a strengthening of metal by plastic deformation and it is known as strain hardening or cold working. These effects occur because of dislocation movements within the crystal structure in the material. Metalworking processes which induce plastic deformation to exact a shape change are permanent. Plastic deformation occurs as a result of work performed on the material and the magnitude of the energy supplied is large

enough to break the material structure bonding. During this process, the bonds rupture and then reform.

In ultrasonic metal forming, it has been believed that the vibratory energy transported to the material is enough to dislocate the structure bonds [24]. However, ultrasonic oscillation of frequencies below 100 MHz has not enough supplied the energy to impart dynamic mobility to the dislocations. The natural frequencies of dislocations are about 100 MHz, so the energy transmission cannot be explained in terms of resonance [92]. Schmid [110] reported a reduction in material hardness and yield point with less intense ultrasonic oscillation. The results from x-ray examination showed that the thermal softening of the specimen hardened by ultrasonics excitation occurred by material recrystallisation, without essential structural changes.

Recently, Siu et al. [88] investigated the microstructure of aluminium samples after they had undergone ultrasonic assisted indentation. It was found that samples exposed to ultrasonics during indentation exhibited enhanced subgrain formation in the microstructure after the deformation process. Siu et al. observed similar subgrain formation in samples which had undergone global heating, this suggested that subgrain formation in samples exposed to ultrasound experienced localised heating. It was also observed that dislocations could travel further in a given length of time in areas containing subgrain formation, providing evidence that ultrasonics could enhance dislocation motion.

Tsujino et al. [116] reported that the vibratory tool and die decreased the metal springback, increased the bending angle and improved the bending surface conditions during ultrasonic forming. The hardness of the specimen and the elongation of the bending surface decreased and became more uniform along the bending part, while the roughness of the bending surface was decreased by ultrasonic excitation. During ultrasonic deep hole drilling by Heisel et al. [119] a clear improvement in surface quality was apparent due to the existence of ultrasonic excitation compared to the conventional process. The influence of vibration energy on the material properties of the specimen was observed as a lowering of the residual deformation and increased the density of the material. Suh et al. [121] used ultrasonic technology to increase the hardness and fatigue strength of knives. This ultrasonic forging technique was observed to affect the

grain size of the material surface. The surface hardness was increased but the compressive residual stress was decreased by the ultrasonic vibration. The study suggested that ultrasonic vibration technology effectively improved the mechanical properties and had therefore become a practical method to improve metal forming processes.

All the investigations into the effectiveness of ultrasonic excitation during metal forming processes demonstrate a significant response to the material mechanical properties during plastic deformation. The results also suggest that the flow stress of metals are softened during the ultrasonic excitation and become more useful as a result. This study of the effectiveness of ultrasonic excitation investigated during plastic deformation, and therefore, the present study will investigate the effectiveness of ultrasonic excitation during both elastic and plastic deformation. Thus, the material softening effects are modelled in an elastic-plastic equation to gain the elastic and plastic strain hardening data, and the material constant data, to describe the behaviour of the material. The material model parameters are then used to develop FE models which are used to predict the effects of a material softening mechanism.

2.5.3 Ultrasonic amplitude

In this study, ultrasonic vibration is excited in the ultrasonic horn and propagated to the material. The ultrasonic vibration amplitude is controlled by a Langevin piezoelectric transducer and generator. The Langevin transducer is widely used in high power ultrasonic applications, the transducer being used to vibrate at a tuned frequency by the generator [122]. In studies of superimposed ultrasonic excitation on metal forming processes, the major effects occurring were a lowering of the material flow stress, called volume effect, and a reduction in friction contact conditions, called the surface effect [4, 64]. The effectiveness of ultrasonic excitation is shown to be dependent on the ratio of stress reduction to the ultrasonic vibration amplitudes [61, 65]. This stress

reduction-ultrasonic amplitude ratio can be calculated and plotted in a stress – strain diagram, to show the effects on elastic-plastic material behaviour.

In earlier ultrasonic studies, Nevill and Brotzen [25] reported that the decrease in flow stress was proportional to the ultrasonic vibration amplitude in frequencies between 15 kHz and 80 kHz. This result was independent of the resonance frequency, temperature and strain range. Petukhow et al. [111] have observed that increasing the amplitude of ultrasonic vibration results in a decrease in extrusion forces. In bending work by Tsujino et al. [116] observed an increment of ultrasonic excitation amplitude halved the radius of curvature of the bending compared to forming without vibration. Mousavi et al. [67] predicted, in their simulation work, that the average extrusion force was decreased by reducing the extrusion speed and increasing the amplitude of ultrasonic excitation. The vibration frequency was also demonstrated to be less influential than vibration amplitude in reducing the extrusion force. Other investigators [110] observed that ultrasonic amplitude strongly influenced the effect of material softening in various metal deformation processes such as wire drawing, tube drawing, rolling, and deep drawing.

In conclusion, all the results obtained showed that the effect of ultrasonic vibration amplitude on the forming of sheet metal and the wider metal deformation process was related to the reduction in material flow stress. This effect was observed as stress reduction linearly increasing with increased ultrasonic amplitude. A significant explanation could be achieved by studying the effect of ultrasonic excitation on various type of metal in a range of ultrasonic amplitudes. The effect of absorption of vibratory energy by the material is reflected in the magnitude of ultrasonic amplitude. Furthermore, the ultrasonic amplitudes applied are dependent on the power of the ultrasonic transducer.

The observed effect of material flow reduction did not include the oscillatory stress in strain hardening behaviour, but the mean flow stress only. Consequently, in all these studies, the experimental characterisation on the effects of superimposed ultrasonic excitation have largely relied on interpretations of measurements of the mean flow stress and have ignored the oscillatory stress. Analysis of the oscillatory stress measurements, especially on

the maximum and mean path of oscillatory stress, could provide better information to explain the material softening effect.

2.6 Effect of Ultrasonic Oscillation in Finite Element Modelling (FEM)

Finite element modelling (FEM) is developed to overcome the difficulty of real time measurements of metal forming processes during experimental analysis. Material flow distributions and forming force characteristics can be predicted by analysing the stress-strain behaviours of the material. This numerical analysis can be performed using commercial program simulation software such as Abaqus, Deform, Ansys, Dyna and Nastran [123]. These numerical studies are compared to measured data originating from the experimental test. As a result, it has become possible to quantitatively understand the mechanisms of improved forming characteristics such as a reduction in flow stress, coefficient of friction, and heat generation.

Many physical phenomena in the material forming process can be described in terms of partial differential equations. In general, solving these equations by classical analytical methods, with many unknown parameters, is impossible. Hence, the finite element method is a numerical approach by which these partial differential equations can be solved approximately [124].

Metal forming simulation is a class of highly nonlinear continuum mechanics problems, because it is accompanied by large deformation (geometric nonlinearity), nonlinear materials behaviour (material nonlinearity in both deformation and temperature), and frictional contact (a nonlinear boundary condition). Starting in the mid-1980s, the history of FE modelling has shown significant success in axisymmetric applications of ultrasonic metal deformation. The approximation of a two-dimensional cross section in a three dimensional specimen, using the plane strain assumption, was an early option in attempting to achieve an understanding of the three dimensional forming process. Many

researchers have started to develop the axisymmetric FE model for metal forming simulation since the pioneering work [125] was presented in 1973. In this study, the three dimensional simulation of metal forming had difficulty in accomplishing the numerical task from the viewpoint of computational efficiency, solution accuracy, graphics visualization, mesh generation and automatic remeshing. However, as computer technology and software advanced, wider and more complicated metal forming processes began to be investigated. It is believed that the further development of the FE model will be continuously driven by industry needs to make the modelling more realistic, more practical, and more affordable.

Most investigators [35, 66, 68, 108, 126-128] presented a conclusion from numerical studies, that under the activation of ultrasonic excitation, the material flow stress of metal forming was decreased. Hung et al. [108] predicted in their simulation that under the activation of ultrasonic vibration, the extrusion force was decreased. The postulated reason for the force reduction was that it was caused by the increase of the material temperature by the ultrasonic vibration. The ultrasonic excitation softened the specimen material and decreased the forming stress of the material. During the numerical simulation, the material was clearly deformed and melted around the tip of the cup when the ultrasonic vibration was applied in the drawing process. Therefore, they presumed that ultrasonic vibration raised the temperature of the specimen, increased the fluidity of the material and extended the height to diameter ratio of the cup. Other researchers such as Hung et al. [109], studied the ring compression tests and analyzed them using commercial software to simulate the frictional effect of ultrasonic vibration on hot ring compression. Consequently, the friction calibration curves and friction factor were inversely derived using finite element analysis.

A three dimensional FE model to simulate a thermomechanical coupled process was developed from finite element code by Ahmed et al. [129]. This simulation demonstrated that a higher temperature and magnitude of residual stress occurred in the material when ultrasonic turning was compared to conventional turning. Finite element simulations were developed in ultrasonic tensile and compression tests using a commercial software code, Abaqus, with an implicit solution to simulate nonlinear material behaviour by Daud et al. [66]. In the FE

models an adjustment in the coefficient of friction was applied. The FE models were developed by adoption of the interface friction coefficient μ = 0.25, representing a dry surface condition for static compression, and then changed to a friction free contact by setting μ = 0 during superimposed ultrasonic excitation on the compression test. The models effectively changed the boundary conditions from a dry surface to a friction free condition, thus influencing the stress-strain result. Daud et al. suggested a more realistic representation of the simulation compression test data in modelling, by combining an adjustment in material properties with an adjustment in the friction contact conditions during the ultrasonic deformation. A consensus was achieved by Ashida et al. [59] who showed that an adjustment to the coefficient of friction between the sheet metal and die without lubrication was measured at approximately 0.5, and with ultrasonic vibration was approximately 0.15. Then during the application of ultrasonic excitation, the coefficient of friction between the sheet metal, the die with lubricant and the ultrasonic vibration was measured to be approximately 0.1. As a result, effective application of ultrasonic vibration to press forming for avoiding cracking and obtaining large deformation in press forming was achieved.

In FE modelling, there are five types of hardening behaviour models: the isotropic hardening model, a linear kinematic hardening model, the Johnson-Cook hardening model, a user-defined subroutine UHARD, and a nonlinear isotropic/kinematic cyclic hardening model [124]. These hardening models were used by investigators [130-132] in their metal forming investigations which resulted in the work hardening response. Previous studies [91, 93, 106, 133] have also shown that the amount of reduction of yield stress was directly proportional to the ultrasonic energy absorbed by the material. The material's effective softening effects are dependent upon the ultrasonic intensity and this was introduced in the relations of the isotropic and kinematic hardening model [134]. Siddiq et al. [90] implemented the user-defined subroutine UHARD model and the combined hardening model to describe a material isotropic yield response, and used the size of the yield surface to predict the response of material behaviours. Consequently, the predicted results of material behaviour were dependent on the field or state variables assigned in the hardening model. The proposed friction model was also implemented in the numerical work, to

determine a friction model based on Coulomb's friction law. The hardening variables were applied in non-linear isotropic and kinematic hardening model along with a thermomechanical coupling model of the ultrasonic welding process [90]. The hardening model was developed with material parameters that had been identified through previous studies and experiments of forming tests on materials.

Therefore, the present study has been carried out through experiments and finite element simulation analysis by applying ultrasonic excitation to the lower die in the compression test and plate forming of metals. An FE model is developed using material model parameters which are identified in the experimental data. The versatility and predictive ability of FE model are demonstrated and the effect of ultrasonic excitation on metal forming process is investigated and compared qualitatively with experimental results under a variety of test conditions such as elastic-plastic deformation, a range of metals and a series of ultrasonic vibration amplitudes.

2.7 Conclusion

Superimposed ultrasonic excitation on metal forming processes has been investigated since the early 50s. The results have shown a significant beneficial effect on material characteristics and metal forming loads. The most significant finding was that the ultrasonic excitation reduced the material flow stress during the metal deformation process. However, further clarification on mean flow stress and oscillatory stress, and how they are affected the surface effects and volume effects, have not been offered in the literature. The explanations of the oscillatory stress measurements, particularly on the mean and maximum oscillatory stress paths, have not provided adequate information on the material softening effects. In almost all of these studies, evaluations of the benefits of ultrasonic excitation relied on measurements of mean flow stress only, and not on oscillatory stress measurement.

Most investigators claim that the surface effects and the volume effects are not thoroughly understood, although they currently offer great potential in metal forming processes. This understanding can be achieved by identifying the effectiveness of both mechanisms during elastic and plastic deformation conditions.

Although the effectiveness of ultrasonic excitation on metal forming processes is experimentally and numerically proved in terms of the benefits to the forming force, an explanation of how the benefits arise is not yet available and an inability to quantify their contribution in material characteristics remains.

CHAPTER 3

DESIGN OF THE ULTRASONIC EXCITATION SYSTEM

3.1 Methodology for the design of high power ultrasonic booster and horn

The development and application of high power ultrasonic techniques in forming processes requires the use of specifically designed ultrasonic components to correctly transmit the energy from the transducer to the tool and die interface. Typical high power transducers consist of a piezoelectric or magnetostrictive element of transduction and a solid acoustic horn acting as an amplifier. Acoustic horns can be generally classified into catenoidal, exponential, conical, parabolic, hyperbolic and stepped forms, according to the decreasing rate of their cross-sectional area. The traditional methods for the design of an acoustic horn are based on the equilibrium of a small element under elastic action forces and integration over the horn length to attain resonance [70-72, 135]. The vibration can only be effectively applied if the tooling is designed for, and vibrated at or particularly close to, the system resonance frequency [37, 136]. The construction of each part of the tooling must be properly designed, accurately manufactured, tested, and (usually) corrected. The laws of sonic and ultrasonic wave propagation must be considered in the design of the tooling in order to achieve satisfactory vibration energy transmission, and avoid damage of the workpiece and tooling.

Amin et al. [72] stated the differential equation in horn design as being:

$$\frac{\partial^2 u}{\partial x^2} + \frac{\partial \ln A(x)}{\partial x}\frac{\partial u}{\partial x} + \frac{\omega^2}{c^2}u = 0 \qquad (3.1)$$

where u is the amplitude of the vibration in the axial direction, $A(x)$ is the cross-sectional area at any axial position x, ω is the angular velocity, and c is the acoustic speed of the horn material.

This equation has been confirmed by Peshkovsky et al. [137] who designed a five element bar horn and gave the equation of vibrations for displacement as:

$$\frac{\partial^2 u}{\partial x^2} + \frac{1}{A(x)} \frac{\partial A(x)}{\partial x} \frac{\partial u}{\partial x} + k^2 u = 0 \tag{3.2}$$

where $k = \omega / c$ is the wave number, $\omega = 2\pi f$ is the angular frequency of the vibrations, and f is the frequency of vibration.

In designing the horn, the difficulties in solving the general differential equation have limited the horn contour geometries. Uniform profiles such as cylinder, stepped, conical or exponential are commonly used. Exponential and conical horns have been widely used in power ultrasonics studies [72, 138]. The design for horn resonance considers the profile as unloaded. This is the standard method used in the design and calculation of the vibrating components, including the ultrasonic transducer and horns [139]. For practical applications, to drive longitudinal oscillation, the ultrasonic transducer has the same longitudinal resonance frequency as the horn, and is attached at the end of the horn which causes the horn to vibrate in the longitudinal mode. When designing a horn therefore, the dimensions of the ends are restricted by the size of the transducer stack and the outer tool diameter.

The next step is to choose the horn profile according to the displacement magnification required. Then the resonant length is obtained through solution of the differential equation. This length depends on the working frequency and has little effect on the magnification. Hence, the main variable that affects the magnification is the horn profile. The theory of acoustic horns is based on the problem of longitudinal vibration of multi-element rods that have cylindrical elements and elements of variable cross sections. The rod model is well suited to determine the approximate vibration behaviour, provided that the maximum cross-sectional dimension of the transducer and horn are less than a quarter-wavelength of the frequency of interest. For a multi-element rod, the ultrasonic

horn design approach by Petshkovsky et al. [137] also agreed that for all practical purposes, it is sufficient to require that the maximum cross-sectional dimension of any portion of a resonant horn does not exceed a quarter-wavelength at the horn's resonance frequency.

Another theory suggested by Heisel et al. [119] is that the vibration dimensioning of ultrasonic tools is carried out by half-wave synthesis. In this process, the smallest unit is a so-called $\lambda/2$ longitudinal mode horn. In this unit, the mode form is represented by half a wavelength and the system is designed for a given resonant frequency. Then, longer ultrasonic tools can be obtained by connecting several $\lambda/2$ vibrators together, all tuned to the same resonant frequency. In this way, it is established that the whole system is in resonance at the given frequency as well. An example of a multi-element horn designed by a mathematical equation for the characteristics of a five-element horn [137] is shown in Fig. 3 –1.

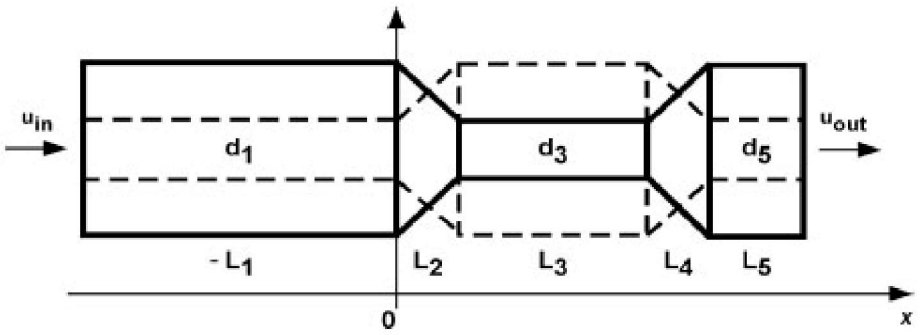

Figure 3-1 Five element horn [137]

The gain factor of the horn can be expressed as:

$$\text{Gain factor} = \left|\frac{u_{out}}{u_{in}}\right| \tag{3.3}$$

where u_{in} is the input ultrasonic vibration amplitude from the transducer and u_{out} is the output ultrasonic vibration amplitude measured at the end of horn.

From the theory of longitudinal vibration of rods, equations for conical, exponential and catenoidal rods are derived by Merkulov [140]. The principles describe how to obtain the resonant length for several types of horn. An illustration of these axisymmetric horn profiles is shown in Fig. 3-2.

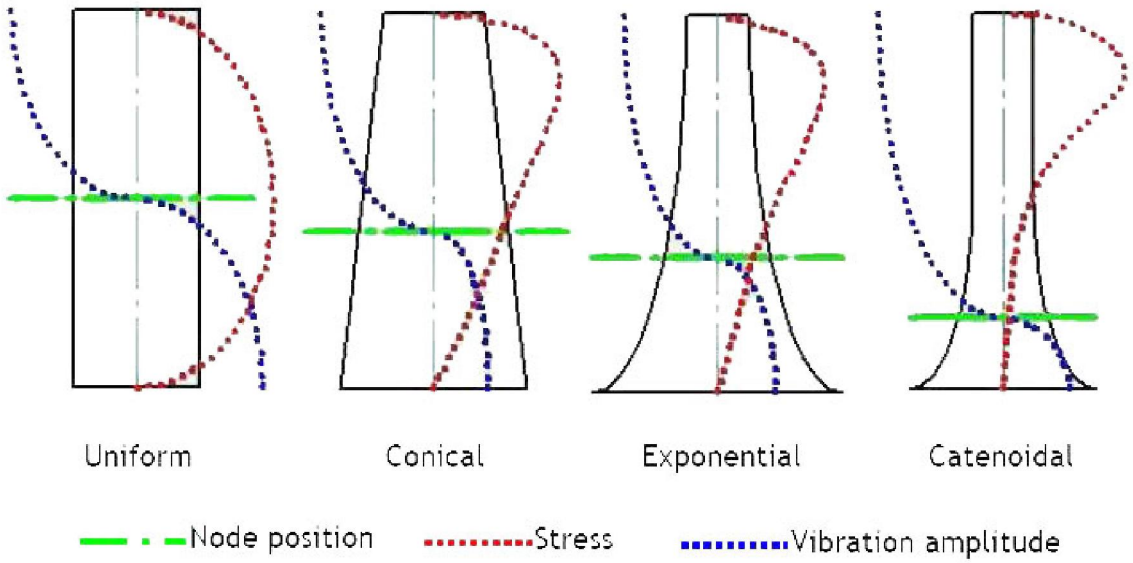

Figure 3-2 Common axisymmetric horn profiles illustrating node position, stress distribution and vibrational amplitude along the length of the ultrasonic component [141]

The application and the ultrasonic amplitude required for the process were considered in order to design the most suitable horn profile. The horn profile was a compromise of component reliability and gain. The catenoidal profile produced a larger gain than the other three profiles but also exhibited higher stress for the same material. Manipulation of the profile line between the two ends of the rod can shift the node position, which is the location of the zero displacement, which can be removed from the high stress zone. This tends to reduce the value of maximum stress [140].

In this study, a 20 kHz transducer is used to provide amplitude of up to 10 μm peak-to-peak, depending on the generator setting. The horn is designed to provide a range of amplitudes up to 20 μm peak-to-peak. This horn is also used as a tool and die in the study of ultrasonic metal forming. Since the ultrasonic

vibrations are applied by a longitudinal transducer, the horn is tuned to the longitudinal mode at the operating frequency. The horn profile is designed to produce both higher and smaller amplitudes and is known as a booster or de-booster horn. The booster horn is designed using the five element horn configuration as described by Peshkovsky [137]. It is possible to design the horn with high gain while ensuring both horn ends have the same cross sectional area. The horn has been divided into five sections with the complete rod length following half wave length conditions according to equation (3.4):

$$l = \frac{c}{2f_n} \tag{3.4}$$

with c = the speed of the stress wave in a solid medium and f_n = the driving frequency of the ultrasonic generator

Equation (3.4) is valid for components whose length is considerably larger than their diameter. For guidance, the diameter, D, to length, l, ratios should be in the region of $D/l < 1$. In accordance with equation (3.4), a titanium (Ti-6Al-4V), rod component with c = 4989 ms^{-1} should have an axial length of 0.125 m to resonate longitudinally at 20 kHz. This result is applied for the first longitudinal mode of vibration and defines the length of the half wavelength component.

In this study, the five element horn is designed based on the characteristics of a Peshkovsky ultrasonic horn and has a different profile for each part the horn, as in Fig. 3-2. The advantage of five elements configuration can be seen whenever the dimensions of the ends are restricted design by the size of the transducer stack and the outer tool and die diameter. Therefore, the behaviours of five element horn configuration can be manipulated by resizing the profile of each element in the configuration. This requirement cannot be achieved if using a single horn profile such as in Fig. 3-2. Using this design, the gain can be adjusted by modifying the parameters of the curved sections, while the frequency of the longitudinal mode can be adjusted by the steepness of the linear taper sections, thus allowing the design criteria to be met such as gain, longitudinal mode frequency, node position and both ends of horn diameter matched with diameter of the transducer. The horns are manufactured from titanium (Ti-6Al-4V) and modelled fully with 3D quadratic elements in Abaqus. The titanium alloy has

been chosen as the material for tool and die to ensure the ultrasonic system is able to operate efficiently and is suitable to be used without failure under high loading conditions. Gain and stress distributions are determined using a frequency analysis, carried out by determining the modal characteristic and a steady state response. The stresses are calculated to ensure it operates within acceptable limits. As a result, the FE model predicted the maximum gain that can be achieved is gain 2 to meet the design criteria such as longitudinal mode at 20 kHz, both ends of diameter 32 mm and half-wave length of 125 mm. Two profiles of horn were designed, in order to provided a high gain ultrasonic horn. Both horns were designed with a criteria of longitudinal mode close to 20 kHz, gain 2 and half-wave length of 125 mm. The horns can be bolted together which gave the characteristics of gain 4 and longitudinal mode close to 20 kHz. In this study, the first horn is known as the booster and the second profile is known as the horn. The final profile designs for the booster and horn are shown in Figures 3-3 and 3-4. The booster and horn are used as an ultrasonic die in the experimental tests which provide ultrasonic vibration to the material.

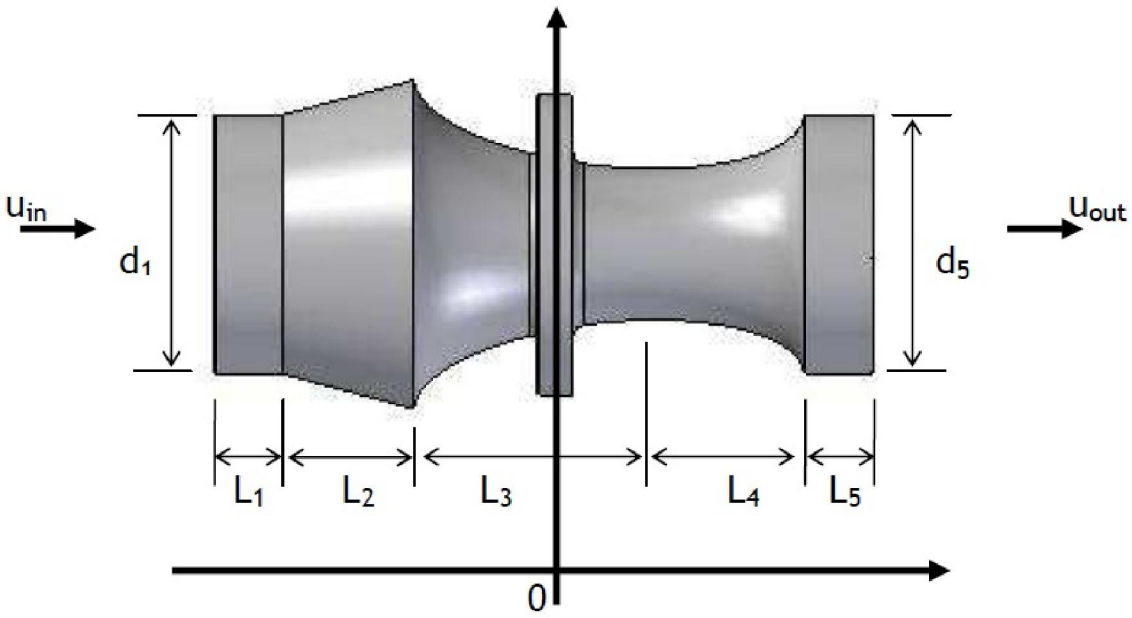

Figure 3-3 Designed profile - booster

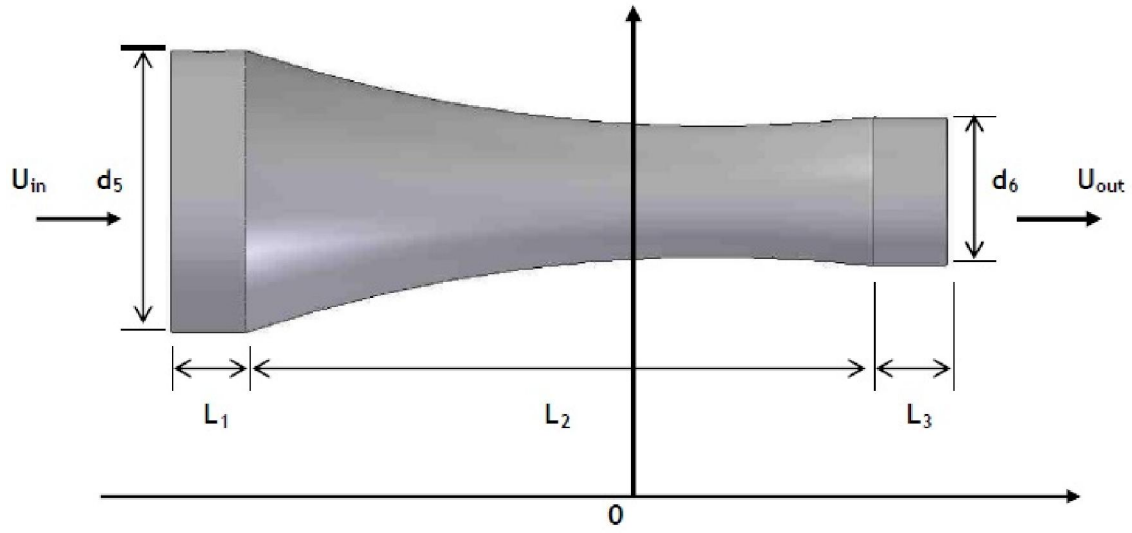

Figure 3-4 Designed profile - horn

In this study, a punch tool is used to compress the metals to the die shape. The punch tool is connected to the cross-head of the test machine. Three types of punch tools are used, as shown in Fig. 3-5.

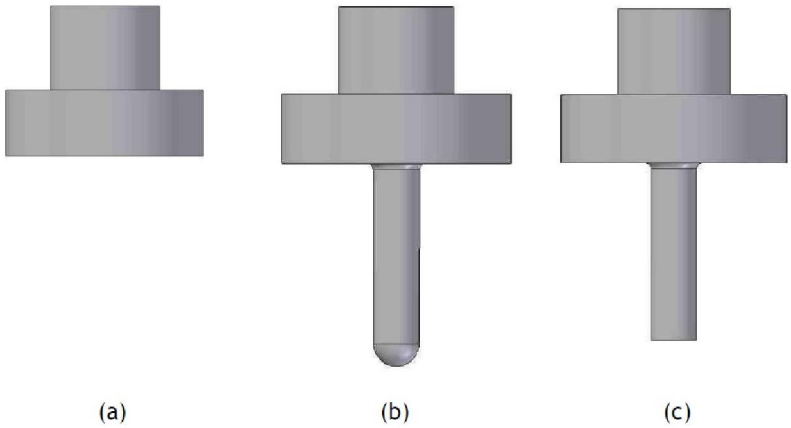

Figure 3-5 Three types of punch (a) flat punch for compression test (b) round punch, and (c) flat punch for forming test

All the ultrasonic tools were connected to the mounting rigs that can be fixed to the test machine. This ultrasonic excitation system consists of the booster, die

horn, transducer, generator and mounting rigs. The design of the ultrasonic excitation system is shown in Fig. 3-6. The mounting rig is constructed of four pillar bars used to connect to the base of the test machine and a plate holder to attach to the flange which is located at the nodal mounting point on the booster. The pillar height is based on the size of the transducer used. All the ultrasonic tools devices, such as the mounting rig, plate holder, booster and horn are made from titanium alloy grade 5 (Ti-6Al-4V) due to the high strength and acoustic properties.

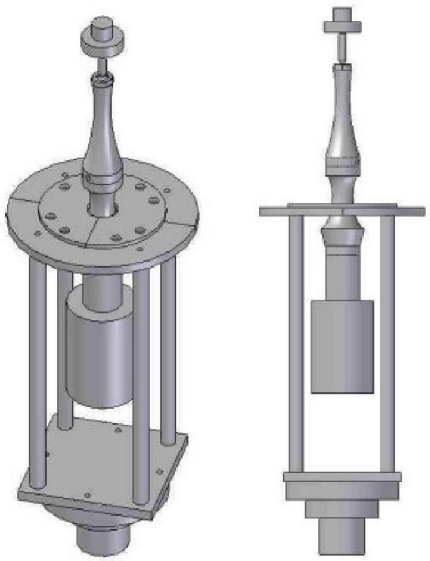

Figure 3-6 The design of the ultrasonic excitation system, in isometric and front views

3.2 Transducer

A transducer is the name for a device capable of converting one form of energy into another, a simple example being a loudspeaker which converts electrical energy to sound energy. Ultrasonic transducers are designed to convert either mechanical or electrical energy into high frequency sound and there are three main types such as gas driven, liquid driven and electromechanical. In the study of superimposed ultrasonic excitation on metal working process, an

electromechanical transducer provides the ultrasonic vibration amplitudes required for the process. The two main types of electromechanical transducers are categories based on either the piezoelectric or the magnetostrictive effect. The most commonly used are piezoelectric transducers.

Quartz was the piezoelectric material originally used in devices such as the very early types of underwater ranging equipment. Quartz is not a particularly good material for this purpose because of its mechanical properties, it is a somewhat fragile and difficult to machine. Modern transducers are based on ceramics containing piezoelectric materials. Currently, the most frequently employed piezoelectric piezoceramic contains lead zirconate titanate, commonly referred to as PZT.

Such materials have two complementary piezoelectric properties; by the direct effect and inverse effect. The direct effect is defined by pressure applied across the large surfaces of the section resulting in a charge generated on each face of equal size but of opposite sign. This polarity is reversed if tension is applied across the surfaces. The inverse effect is defined by a charge applied to one face of the section and an equal but opposite charge to the other face resulting in the whole section of crystal either expanding or contracting depending on the polarity of the applied charges. Thus on applying rapidly reversing charges to a piezoelectric material, fluctuations in dimensions will be produced. This effect can be harnessed to transmit ultrasonic vibrations from the crystal section through whatever medium it is in contact with.

The most common form of transducer is a disc with a central hole. In a power transducer it is normal practise to clamp two of these piezoelectric discs between metal blocks which serve both to protect the delicate crystalline material and to prevent it from overheating by acting as a heat sink. Fig. 3-7 shows an example of piezoelectric transducer. The unit is generally one half wavelength long or multiples of this can be used. The peak-to-peak amplitudes generated by such systems are normally of the order of l0 to 20 μm and they are electrically efficient. Such transducers are highly efficient, and depending on dimensions can be used over the whole range of ultrasonic frequencies from 20kHz to several MHz.

In this study, a generator uses mains electricity to generate a high frequency ultrasonic signal to drive the transducer, which is tuned to a specific frequency of 20 kHz and typically provides a maximum axial vibration of 10 μm amplitude. The ultrasonic generator has electronic circuitry incorporated in the system which can track the exact resonance frequency and control the amplitude of vibration to allow tuned operation even under high loads.

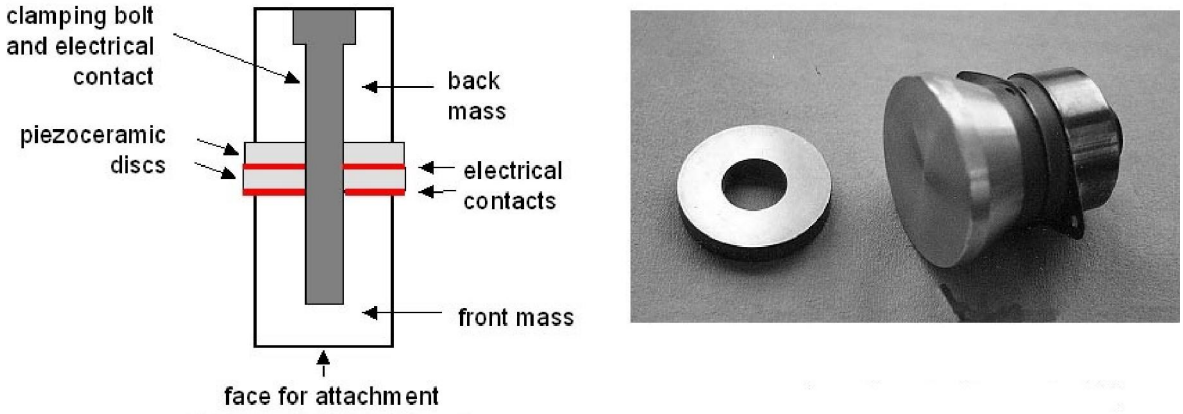

Figure 3-7 The form of piezoelectric transducer

3.3 Finite element modelling

Finite element analysis (FEA) is one of the most flexible and powerful computational tools available for solving engineering problems concerning the deformation of solids. Finite element modelling (FEM) can be applied to systems with any geometric configuration or boundary conditions. FEM was first developed in 1943 by R. Courant, who utilized the Ritz method of numerical analysis and minimization of variation calculus to obtain approximate solutions to vibration systems [142]. By the early 70's, FEM was limited to expensive mainframe computers generally owned by the aeronautics, automotive, defense

and nuclear industries. Since the rapid decline in the cost of computers and the phenomenal increase in computing power, FEM has been developed to an incredible precision. Present day supercomputers are now able to produce accurate results for all kinds of parameters. FEM consists of a computer model of a structure or design that is stressed and analysed for specific results.

FEM uses a system of points called nodes which then form elements which create a grid called a mesh. The material and structural properties which define how the structure will react to certain loading conditions are assigned to the mesh.

In FEM, a variety of meshing techniques exist to mesh models of different topologies. The different meshing techniques provide varying levels of automation and user control. In this study, the meshing technique is free meshing with tetrahedral elements which are used to simplify complex profile shapes so that the FE software can be used to generate a high quality mesh, without the need for partitioning. This type of element is chosen because it supports free meshing of three-dimensional solids. Free meshing with tetrahedral elements is the software default mesh generation algorithm which is significantly more robust for complex shapes and allows for increase in the size of the interior elements thus increasing the computational efficiency.

In FEM, the model is meshed with elements. The number of elements in the model is controlled initially by the global size and accommodating structural features. A mesh convergence study is then conducted by varying the element density of the structure model to provide confidence in the accuracy of the FE modelling technique. The static and dynamic responses of loaded structures can be analysed computationally using FE packages using a frequency analysis to determine the natural frequencies and mode shapes. For example, Fig. 3-8 depicts mode shapes of the first longitudinal, bending and torsional mode of vibration of a uniform rod analysed using 0.0054 global size elements with free boundary conditions.

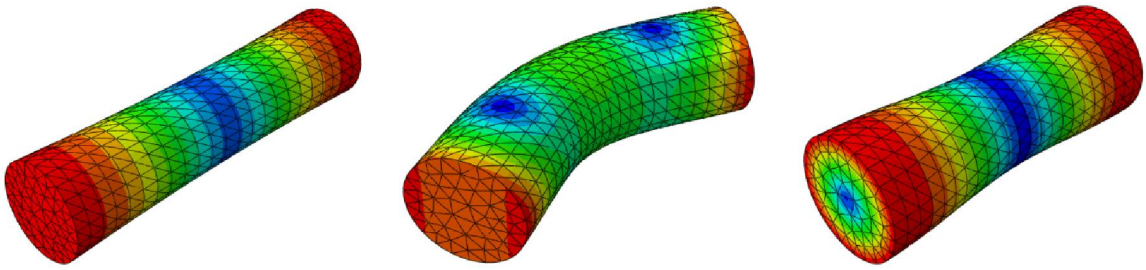

(a) (b) (c)

Figure 3-8 Mode shape diagrams with contours of displacement for (a) 1st longitudinal (b) 1st bending and (c) 1st torsional mode of vibration.

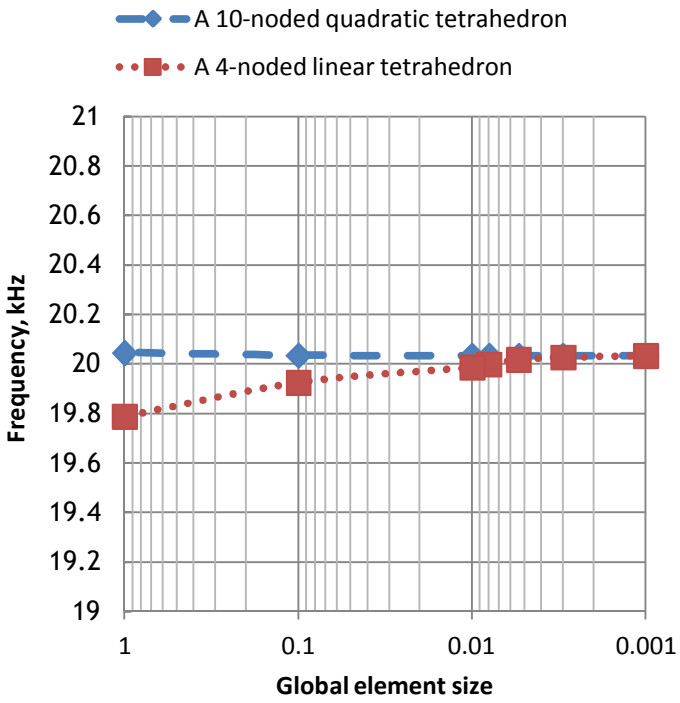

Figure 3-9 Mesh convergence study for a uniform rod using 3D tetrahedron element.

Fig. 3-9 illustrates a mesh density study using 4-node linear and 10-node quadratic tetrahedron elements by varying the global size number for the rod. The natural frequency of the first longitudinal mode using the FE package Abaqus is calculated to be 20 kHz and mesh convergence is achieved by both of the elements type. The 10-node quadratic tetrahedron element results in a convergence to the tuned frequency with less number of elements while the 4-node linear tetrahedron element needed a higher number of elements to converge. These solutions show that the FE package is sufficiently accurate to provide a solution for a relatively low number of elements thus providing

confidence in the modelling approach for determination of natural frequencies and mode shapes.

The finite element package Abaqus is used to calculate the natural frequencies, gain and stress distribution of the horn. In Abaqus, a complete finite element analysis usually consists of three distinct stages: pre-processing, simulation and post-processing. In the pre-processing stage, the horn is defined as a model of the physical problem, and an Abaqus input file is created. The model is created graphically using Abaqus/CAE or another pre-processor such as Solid Edge or AutoCad. In the simulation stage, the software solves the numerical problem which was defined in the pre-processing stage. To conduct a vibrational analysis in Abaqus two prescribed steps are applied, firstly a frequency step using either the Lanczos or subspace eigensolver to extract natural frequencies within the frequency range of interest, and secondly a steady-state dynamics direct step to predict the steady-state amplitude and phase of the system under a predefined loading of a harmonic excitation at a specified frequency. The frequency step allows natural frequencies and mode shapes of the system to be calculated and the steady-state dynamics direct step allows stress and displacement amplitude of the system to be predicted for the applied loading condition. The results can be evaluated once the simulation has been completed and the displacements, stresses or other fundamental variables have been calculated. In the post-processing stage the results can be displayed in a variety of options, such as colour contour plots, animations, deformed shape plots and X-Y plots. In this study, the booster profiles were meshed using 3D quadratic tetrahedrons in Abaqus and the distributions of displacement amplitude and stress on the booster are shown in Fig. 3-10. The stress distribution in the booster was plotted using the Von-mises and Hencky criteria [143].

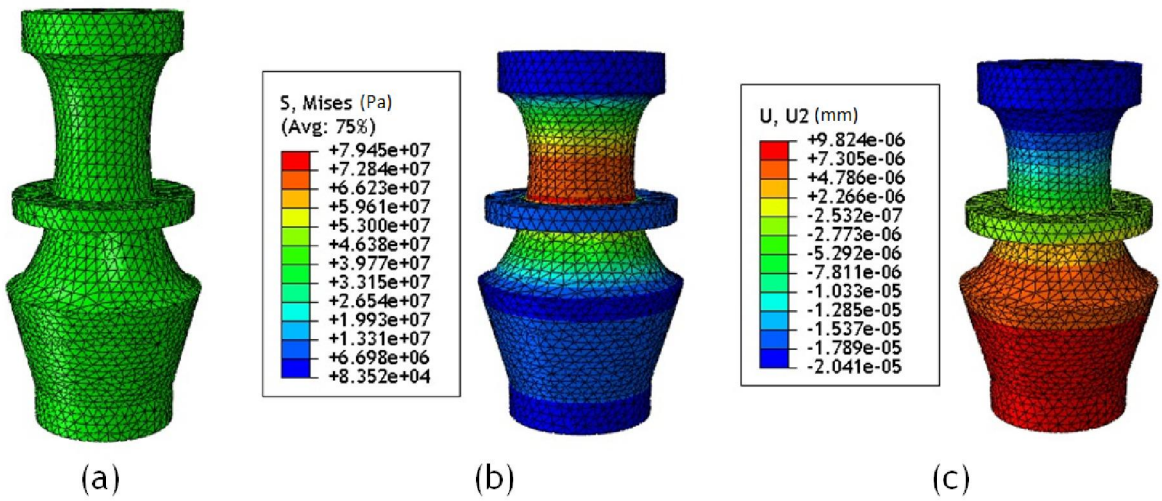

Figure 3-10 Booster contour for (a) element mesh (b) von-mises stress distribution (c) amplitude displacement distribution

By plotting the Mises stress along the centre line of the titanium booster at the excited tuned frequency, it is possible to identify the maximum stress location along the longitudinal axis of the booster. Similarly, the displacement amplitude distribution can also be determined along the longitudinal axis and these are shown in Fig. 3-11.

The combination of a booster and horn is used to obtain a higher gain. As mentioned in the previous section, the end diameter of the booster is equal to the end diameter of the ultrasonic transducer, in order to achieve interface continuity and transfer ultrasonic energy efficiently. When the booster and transducer are joined together, the transducer provides a 10 μm peak-to-peak vibration amplitude, so that the end of booster produces 20 μm of peak-to-peak ultrasonic vibration amplitude. This was sufficient to provide the range of ultrasonic amplitudes needed in this ultrasonic forming test study. However, the range of ultrasonic amplitudes can be increased by designing a second horn, having similar characteristics to the first horn; in this case a booster and horn. The combination of the booster and horn provides a gain of 4. In addition, the booster is used as a holder between the mounting rig and transducer. The tuned booster is included to allow a flange to be incorporated to provide a nodal mounting to the test machine. This ensures that the mounting rig does not affect the vibratory motion of the horn, booster or transducer. The distribution of von-Mises stress and displacement for the booster and horn combination are calculated using FEM. The combination profiles are meshed using a 3D 10-node

quadratic tetrahedron element, as shown in Figure 3-12, and the distributions of displacement amplitude and stress along the booster and horn axes are shown in Figure 3-13.

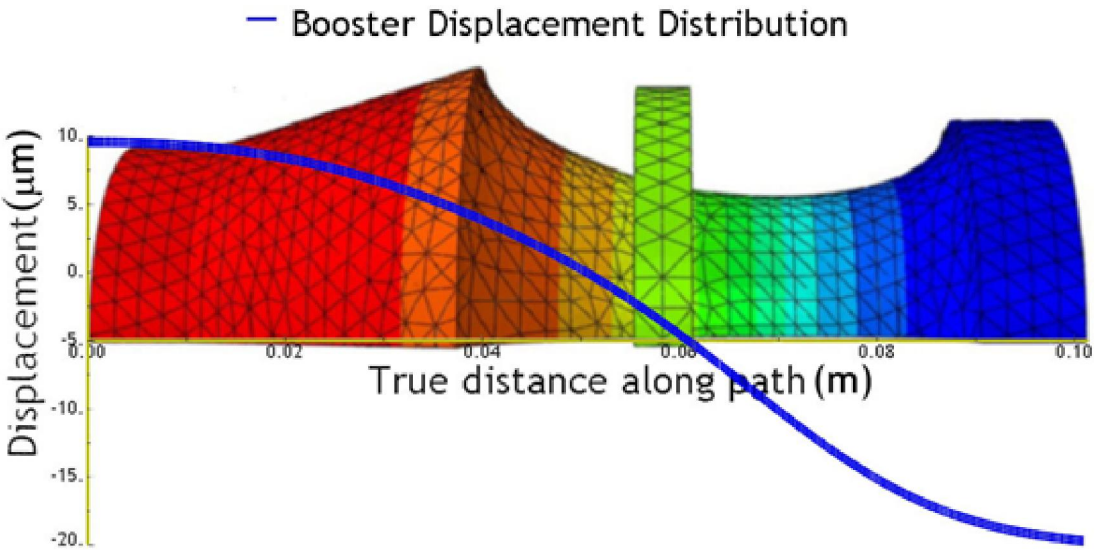

(a)

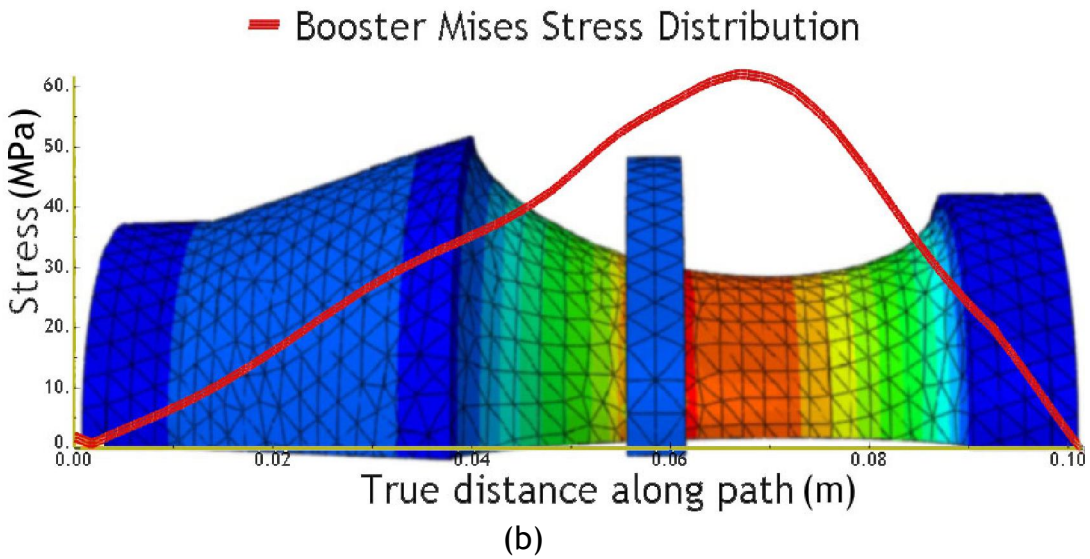

(b)

Figure 3-11 Graphical representation of (a) displacement and (b) Mises stress distribution along the centre axis of the booster

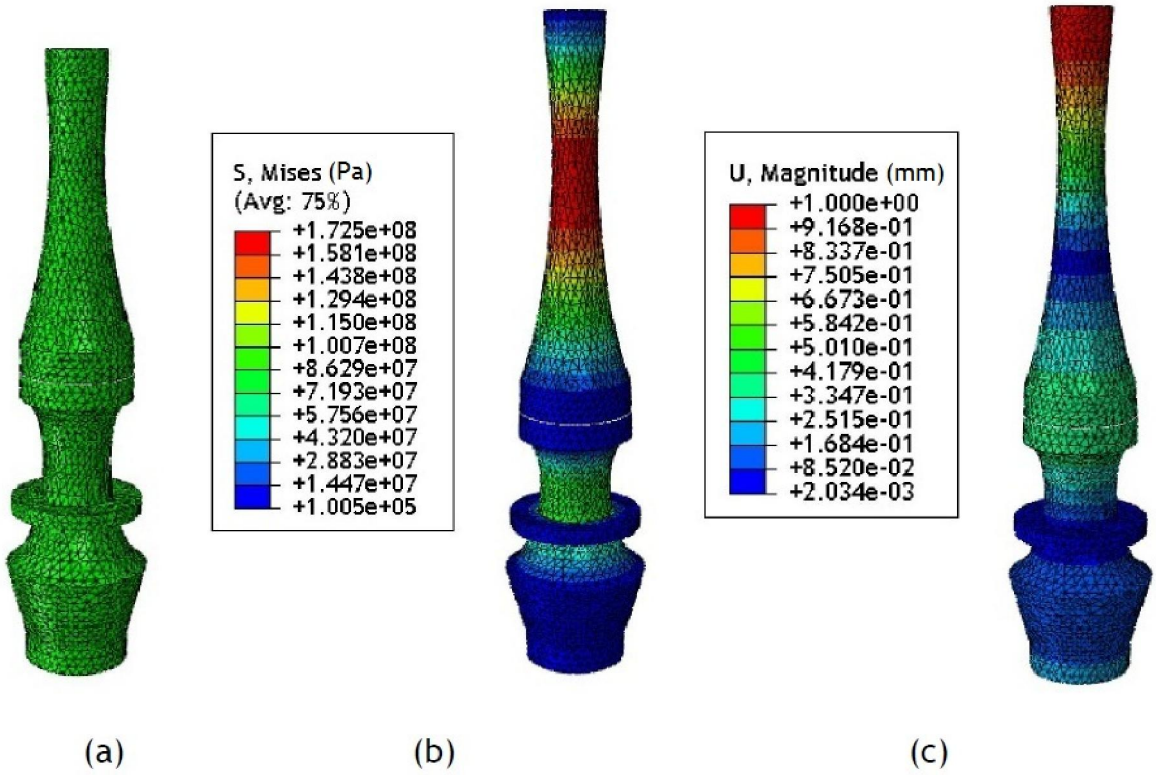

(a) (b) (c)

Figure 3-12 Booster and horn contours of (a) element mesh (b) Mises stress distribution (c) amplitude displacement distribution

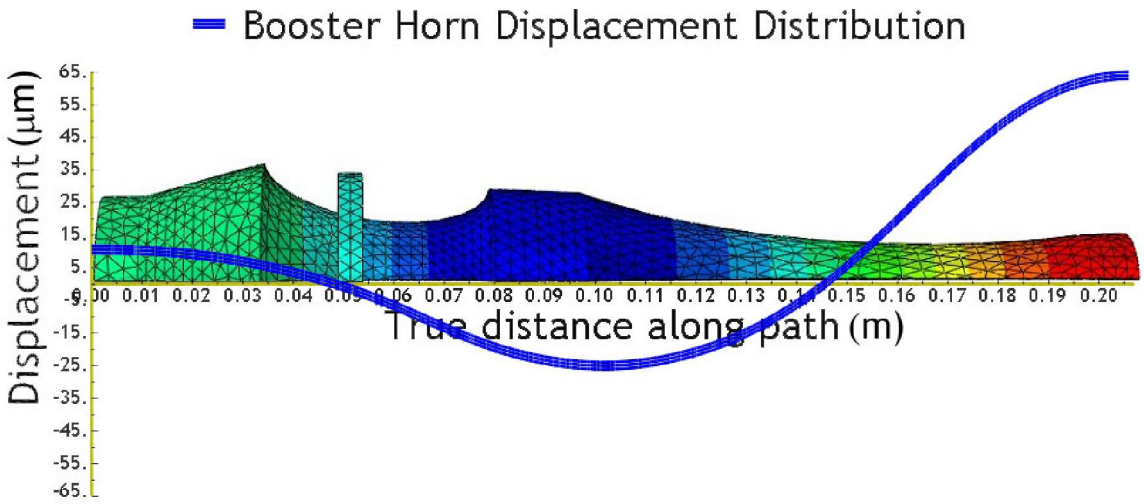

(a)

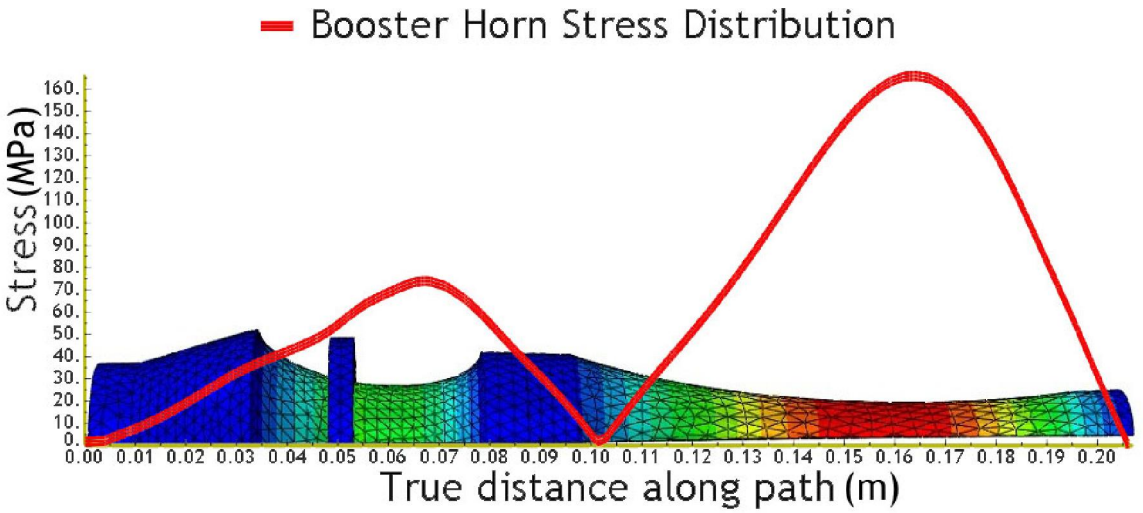

(b)

Figure 3-13 Graphical representation of (a) displacement and (b) Mises stress distribution along the centre axis of the combination of booster and horn

From FE analysis, the maximum stress location along the longitudinal axis of the ultrasonic booster and horn was predicted by plotting the Mises stress along a centre line of the profiles at the excited natural frequency. Similarly, the nodal position can also be determined along the centre line of booster and horn. Two tuned ultrasonic horns were designed, using the procedure described previously to resonate in the longitudinal mode at 20 kHz. The maximum Mises-stress for the combined booster and horn was calculated to be 160 MPa.

In this study, titanium alloy grade 5 (Ti-6Al-4V) has been chosen as the material for the booster and horn due to its high strength, high toughness, anti-corrosiveness, durability and low acoustic loss. The material selection for ultrasonic components is critical to ensure the ultrasonic system is able to operate efficiently and is suitable to be used under high loading conditions without failure. High strength and high toughness are most important factors for the design of ultrasonic components especially ultrasonic horns where the structures experience high loading. All the ultrasonic components were assembled using threaded studs. Ideally for ultrasonic systems, an acoustic loss factor of zero is perfect and there should be no energy losses but in reality every ultrasonic component will experience acoustic losses and reduction of energy in the system particularly at joining surfaces and stud locations. The acoustic loses in the material can be quantified from the quality factor. Higher quality factor indicates a lower energy loss. Another factor that influences the energy transfer in material is the acoustic impedance. The acoustic impedance of all components should be matched as closely as possible to ensure energy transfer is maximum between joining components and to ensure the vibration is transferred effectively between one component and the next. Consequently, titanium alloy is used in design of the ultrasonic components. The material properties for the Titanium alloy are tabulated in Table 3-1. The maximum stress in both of the horns designed in this study are significantly lower than the yield strength of the titanium alloy, from Table 3-1. It is safe to assume from the FE analysis that the ultrasonic horns operate within a safe operating regime in terms of stress levels.

Table 3-1 Material Properties of Titanium Ti-6Al-4V (Grade 5)

Titanium Ti-6Al-4V (Grade 5)	
Density	4430 kg/m^3
Hardness, Vickers	349
Tensile Strength, Ultimate	950 MPa
Tensile Strength, Yield	880 MPa
Modulus of Elasticity	113.8 GPa
Compressive Yield Strength	970 MPa
Poisson Ratio	0.342
Melting Point	1604 - 1660^{o}C
Shear Strength	550 MPa

3.4 Experimental modal analysis (EMA)

Experimental modal analysis (EMA) is a form of vibration testing of an object whereby the natural (modal) frequencies, modal masses, modal damping ratios and mode shapes of the object under test are determined. EMA works when energy is supplied to the system with known frequency content. Where structural resonances occur there will be an amplification of the response, clearly seen in the response spectra. By analysis of the response spectra and force spectra, a transfer function can be obtained. The transfer function or frequency response function (FRF) is often a curve fitted to estimate the modal parameters. Commonly FE modelling is also used to calculate these modal parameters but validation of the FE simulations is carried out using EMA. EMA is used in this study to confirm the FE predicted modal parameters for the ultrasonic horns.

3.4.1 FRF measurements

The frequency response function (FRF) is a fundamental measurement that exhibits the inherent dynamic properties of a mechanical structure following EMA, frequency, damping and mode shape are obtained from a set of FRF measurements. The FRF describes the input-output relationship between two points on a horn as a function of frequency, as in equation (3.5);

$$F(\omega) \times [H(\omega)] = X(\omega) \tag{3.5}$$

where $H(\omega)$ is the motion parameter response per unit of excitation force at an input degree of freedom (DOF). $F(\omega)$ and $X(\omega)$ are the input force function and an output motion parameter response, respectively. This equation shows that the FRF is defined as the ratio of the Fourier transform of an output response ($X(\omega)$) divided by the Fourier transform of the input force ($F(\omega)$) that caused the output.

The FRF is simply defined by a curve representing the output to input ratio. The input applied force and output response of the horn as either displacement, velocity or acceleration can be measured. The measurement is captured in the frequency domain using a fast Fourier transform (FFT) algorithm. During the transformation the functions become complex and contain real and imaginary components and use both magnitude and phase to describe the FRF response.

3.4.2 Dynamic signal processing

The Fast Fourier Transform (FFT) is an algorithm for transforming data from the time domain to the frequency domain. Because of the many calculations involved in transforming domains, the transform must be implemented on a digital computer if the results are to be sufficiently accurate. The frequency domain cannot be calculated directly from a measurement in a continuous

manner but instead must be calculated by sampling and digitizing the time domain input. This means that the algorithm transforms digitized samples from the time domain to samples in the frequency domain.

When the measurement signals have been gathered at various target locations on the structure by the response measuring device in this case a laser vibrometer, the data is collected and processed using a spectrum analyser. To extract the natural frequencies and mode shapes of the system, FRF's are calculated from Fast Fourier Transforms (FFT). Fourier transforms convert response signals from the measurement devices in the time domain to spectral properties in the frequency domain using digital Fourier transform (DFT) analysis, a form of the FFT algorithm developed by Cooley and Tukey in the 1960s [144]. Erroneous results can be produced using digital Fourier analysis by aliasing. Aliasing is a problem where the discretisation of the continuous time history is misinterpreted if the sampling rate is too slow, and high frequency signals can be misinterpreted as low frequency signals and can cause a distortion of the measured spectrum using DFT. This phenomenon can be avoided by using anti-aliasing filters where the original time signal is subjected to a low-pass sharp cut-off filter. Leakage is a problem where a sample of the signal is taken using a finite length of time history coupled with the Periodicity Principle. The Periodicity Principle considers all signals to be periodic but unfortunately signals such as random excitation are not. If the signal sampled is ideal and is precisely periodic the resulting spectrum will display a single line at the frequency of the sine wave but if the signal is not ideally periodic several lines will appear surrounding the single frequency and as such the spectrum produced does not indicate the single frequency which the time signal processed. This problem can be minimised or avoided by changing the duration of the measurement period, using zero padding where zeros are added to the end of the measured sample and by using the windowing technique where a prescribed profile, such as hanning, cosine taper, hamming or exponential window is used on the time signal. Filtering is also a solution that can be used on its own or alongside the windowing technique on the sample in the frequency domain instead of the time domain. Common filters include high-pass, band limited, narrow band and notch.

The FRF's of the manufactured horns were generated in this study using a hanning window and also a high pass sharp cut off filter to minimise leakage and

aliasing. The FRF results during the EMA of the horns were also improved by collecting 30 responses during the analysis for each measurement point and averaging the FRF results to reduce the noise content in the final FRF.

3.4.3 Laser doppler vibrometers

Laser Doppler Vibrometers are optical devices that are able to detect the instantaneous velocity of the structure [145]. A LDV works upon two principles, the Doppler shift and optical inferferometry. The Doppler shift describes how the frequency of a wave will change if the source of the wave is moving relative to an observer. Since light can be treated as a wave, this principal can be applied to laser light. Thus the wavelength of reflected light is slightly different to the wavelength of the incident beam for moving objects. If the object were stationary the reflected beam would be of exactly the same frequency and wavelength. However if the object is moving toward the incident beam then the reflected beam has a shorter distance to travel and since the speed of light remains constant, the wavelength of the reflected beam must decrease. The opposite is true if the object is moving away from the source, the wavelength will increase. The difference between the wavelength of the source beam and reflected beam can be used to determine the velocity of the object. Fig. 3-14 shows how typical vibrometer is constructed.

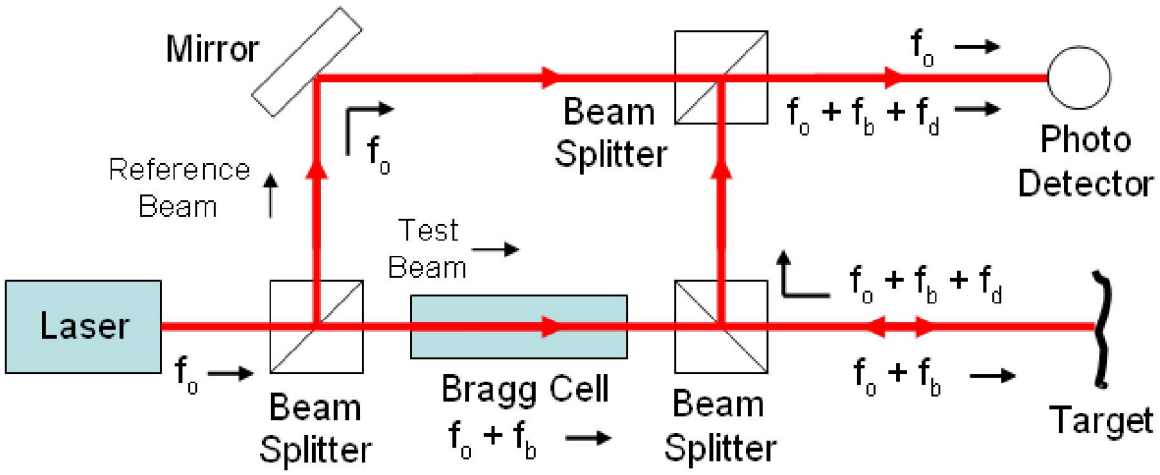

Figure 3-14 Basic components of a laser Doppler vibrometer [146]

The beam from the laser, which has a frequency f_o, is divided into a reference beam and a test beam with a beam splitter. The test beam then passes through the Bragg cell, which adds a frequency shift f_b. This frequency shifted beam then is directed to the target. The motion of the target adds a Doppler shift to the beam given by $f_d = \frac{2v(t)cos\alpha}{\lambda}$, where $v(t)$ is the velocity of the target as a function of time, α is the angle between the laser beam and the velocity vector, and λ is the wavelength of the light. Light scatters from the target in all directions, but some portion of the light is collected by the LDV and reflected by the beam splitter to the photo detector. This light has a frequency equal to $f_o + f_b + f_d$. This scattered light is combined with the reference beam at the photo-detector. The initial frequency of the laser is very high (>10^{14} Hz), which is higher than the response of the detector. The detector does respond, however, to the beat frequency between the two beams, which is at $f_b + f_d$ (typically in the tens of MHz range). The output of the photo detector is a standard frequency modulated (FM) signal, with Bragg cell frequency as the carrier frequency, and the Doppler shift as the modulation frequency. This signal can be demodulated to derive the velocity versus time of the vibrating target.

3.4.4 EMA measurement system

The experimental testing equipment and operating configuration used in this study consists of a SignalCalc ACE hardware unit, an amplifier, an ultrasonic transducer, a 3D Laser Doppler Vibrometer (Polytec, 3D CLV-3D) and LDV signal processing unit and computer which consists a dynamic signal analyser using SignalCalc ACE data acquisition software, Data Physics Corp. The tuned horn was excited between 0 and 40 kHz using a random excitation as input signal created at low power by a function generator of SignalCalc ACE hardware unit that has a sample rate of 204.8 kHz and 51200 spectral lines with resolution of 0.78 Hz for measurements taken between the range of 0 and 40 kHz. The amplifier amplifies the signal from the function generator. The ultrasonic transducer converts the electrical signal from the amplifier to mechanical vibration through the piezoelectric effects, thus exciting the horn by the vibration supplied from the transducer. During the excitation of the horn, a laser beam from the 3D LDV is pointed at the horn surface to measure the vibration velocities response of the surface. This time domain data was recorded and transformed to the frequency domain using the Fast Fourier Transform (FFT) to generate the frequency response function (FRF) which was produced using a dynamic analysis analyzer in the computer. It is possible to determine the maximum magnitude of response when the excitation frequency is at the resonant frequency of the horn. These measurements were then analysed using ME'Scope VES modal analysis software to measure the modal parameters such as resonance frequencies and mode shapes of the ultrasonic horn. The EMA measurement system setup is illustrated in Fig. 3-15.

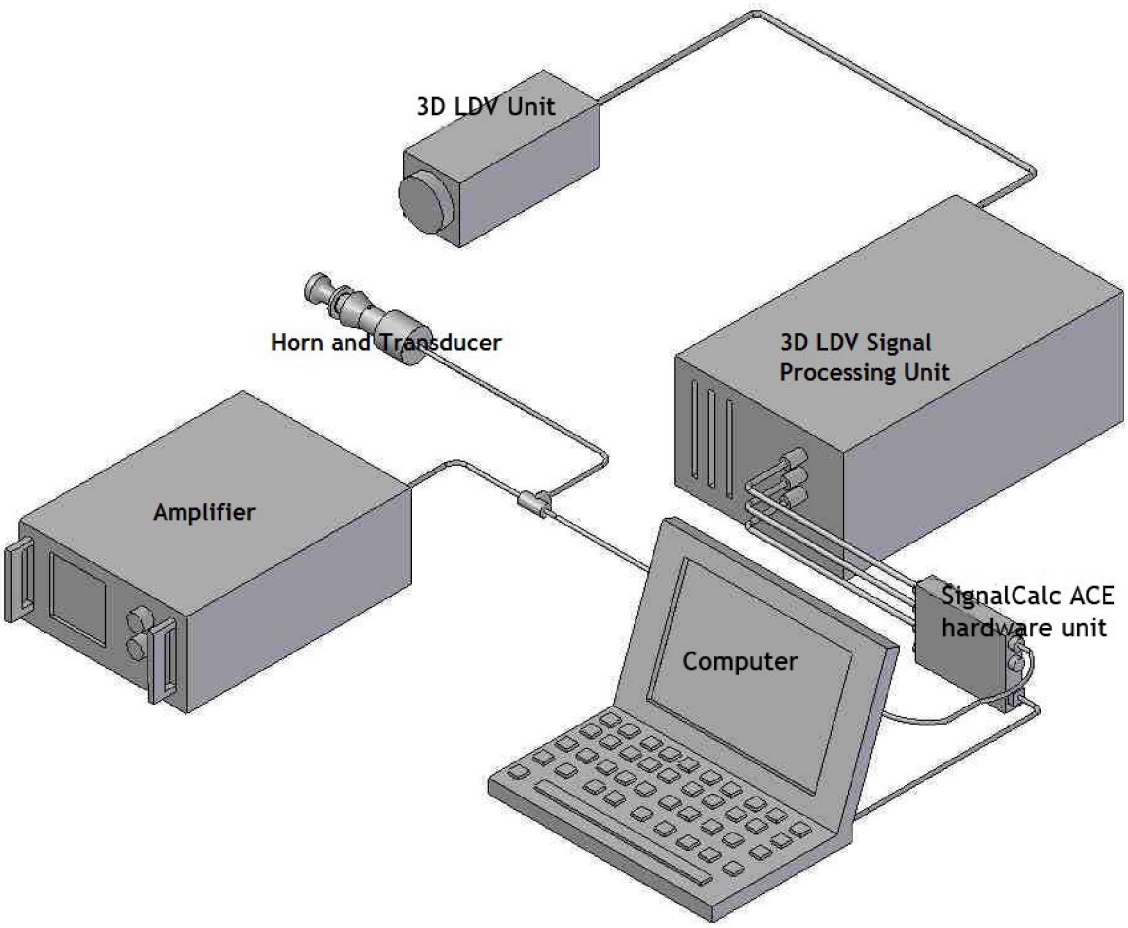

Figure 3-15 EMA Hardware Setup

3.5 Validation

The tuned ultrasonic booster and horn use precision engineering equipment to manufacture accurately the ultrasonic components to the required size to ensure the component is tuned precisely. The booster and horn were manufactured using computer aided manufacture (CAM) technology for modelling before machining using a CNC machine. The ultrasonic excitation system is shown in Fig. 3-16, and consists of the ultrasonic transducer, a booster, and an ultrasonic horn, all tuned to their first longitudinal mode of vibration at a nominal 20 kHz. The forming die in this study constitutes the output end of the ultrasonic horn. The die horn and booster were designed using finite element analysis (FEA), and

the modal frequencies and associated mode shapes were subsequently confirmed using experimental modal analysis (EMA).

Figure 3-16 Ultrasonic transducer, booster and die horn

To validate the FE modelling approach for ultrasonic booster and horn design, the longitudinal mode shape from the FEM was analysed for the combined booster and horn and compared to the mode shapes from the EMA analysis on the booster and horn. The EMA was conducted creating a mesh of points on the outer surface, sufficient to capture the movement of the booster and horn in any mode shape. The FEM and EMA mode shape results for the ultrasonic booster and horn are shown in Fig. 3-17. This figure shows the FEM and EMA modal responses for the designed ultrasonic booster and horn in the longitudinal mode at frequency close to 20 kHz. In this study, FEM predicted the resonance frequency of the designed booster and horn to be 20.74 kHz, while EMA measured the frequency at 20.8 kHz. Fig. 3-18 shows the frequency response measured and predicted by EMA and FEM, respectively. As mentioned previously, the transducer alone was setup to longitudinal mode at the resonant frequency of 20 kHz and it can be read from the monitor display unit. However, the longitudinal mode of combination booster and horn was measured in EMA at resonant frequency of 20.8 kHz which is used as a driving frequency for the ultrasonic experiments. There is no tuning procedure has been taken placed, however, during the experiments the tuned frequency, acoustic power and ultrasonic amplitude are monitored in order to ensure the system maintained same performance throughout experiments even under high loading conditions.

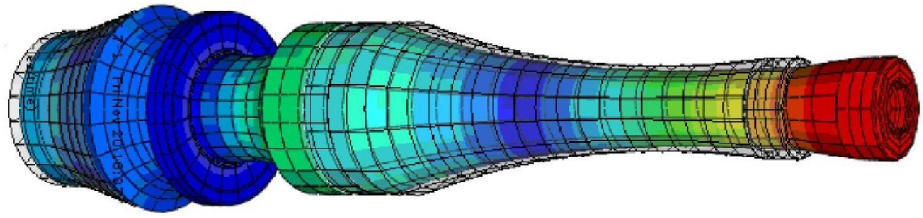

(a) 20.74 kHz FE predicted

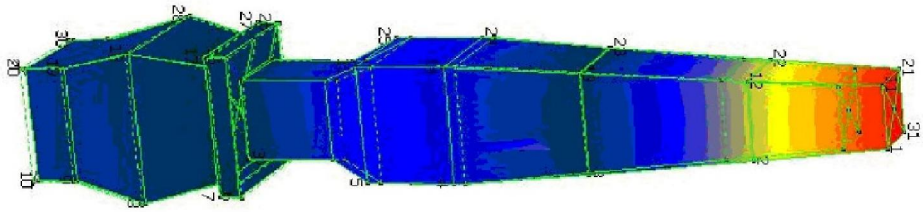

(b) 20.8 kHz EMA measured

Figure 3-17 Comparison of (a) FE predicted and (b) EMA measured longitudinal mode shape and modal frequency

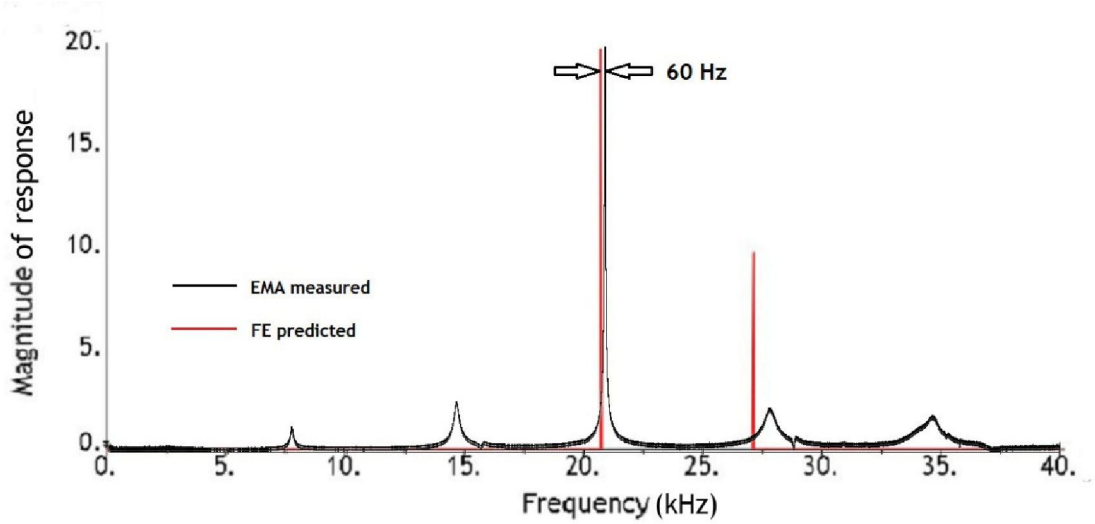

Figure 3-18 Natural frequencies measured and predicted by EMA and FEA for ultrasonic tools at 20 kHz tuned frequency

3.6 Conclusion

This chapter has shown the process of designing an ultrasonic excitation system that includes an ultrasonic transducer, a booster and an ultrasonic horn, all tuned to their first longitudinal mode of vibration at 20 kHz. The system was designed using numerical finite element analysis and was verified by experimental modal analysis. The tuned booster was used to allow a flange to be incorporated between the transducer and the die horn, to provide a nodal mounting to the test machine. This ensures that the mounting rig does not affect the vibratory motion of the horn, booster or transducer. The forming die in this study constituted the output end of the ultrasonic system and was incorporated into the end of the horn. The die horn and booster were designed using finite element modelling (FEM), and modal frequencies and associated mode shapes were subsequently confirmed using experimental modal analysis (EMA). The ultrasonic booster was designed using the five-element horn configuration as reported by Peshkovsky [137]. The transducer can only provide ultrasonic amplitudes up to 10 μm, depending on the generator setting, therefore the profile of the booster and horn are designed to amplify the amplitude and allow a range of ultrasonic amplitudes to be excited. The ultrasonic system has been measured and calculated as having a longitudinal mode of vibration at 20.8 kHz and to provide a gain of four.

CHAPTER 4

STATIC-ULTRASONIC UPSETTING OF METALS SPECIMENS UNDER PLASTIC DEFORMATION CONDITIONS

4.1 Introduction

Metal upsetting is a measurement procedure to determine the behaviour of materials under compression loads. Usually a cylindrical specimen is used. The compression test is one of the primary tests and has been the most highly developed, especially in the study of the workability behaviour of metals [147]. The specimen is compressed and deformation at various loads is recorded. The load necessary to produce a given displacement is monitored as the specimen is crushed in compression at a constant rate. A load-versus-displacement curve is the immediate result of such a test. Material properties are obtained from the stress-strain diagram. The compressive stress and strain are calculated from the measured force-displacement data and plotted as a stress-strain diagram which is used to determine elastic-plastic region, yield stress σ_y, and modulus of elasticity E. A stress-strain diagram for a material under compression load is shown in Fig. 4.1. The relationship between the load-displacement curve and stress-strain curve can be expressed as

$$\sigma = \frac{P}{A}(1 + \frac{h}{H}), \tag{4.1}$$

and

$$\varepsilon = ln(1 + \frac{h}{H}) \tag{4.2}$$

where P is the applied load, A is the cross-sectional area of the specimen, h is compression displacement and H is the height of the specimen.

Metal upsetting is usually used in the workability test to define the level of deformation that can be achieved in a metalworking process without inducing an undesirable condition, such as fracture, buckling, or the formation of laps. In this investigation, metal upsetting is used as a metal forming process to study the effects of superimposed ultrasonic excitation on material characteristics that can be plotted in the stress-strain diagram.

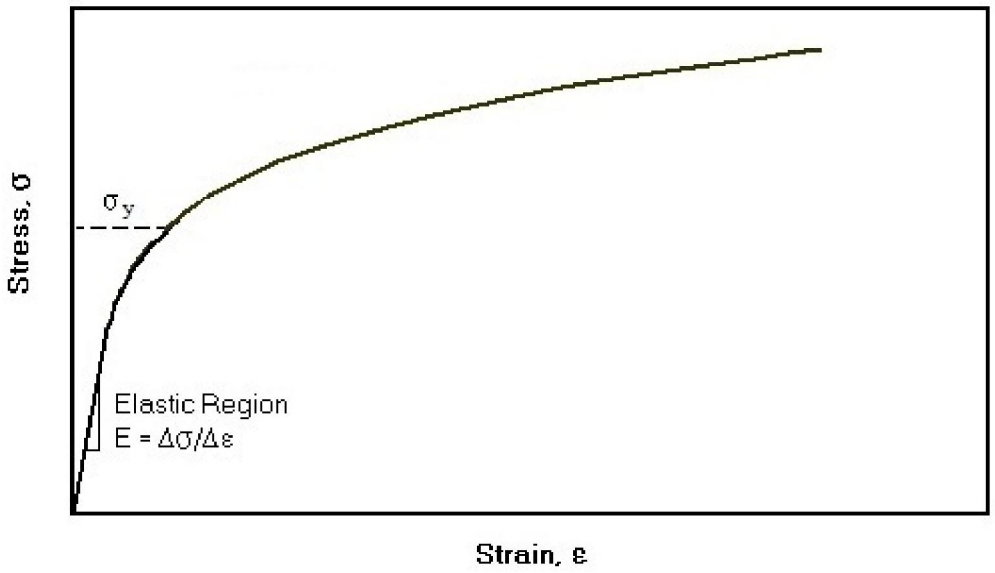

Figure 4-1 Stress-strain diagram

As discussed in chapter 2, early studies concluded that the influence of vibrations on metal forming processes could be considered in two specific areas, volume effects and surface effects. The compression of the specimen during metal upsetting results in a flow of material towards the outside of the flat dies. At the same time, friction forces are generated on the contact surface influencing deformation. Ultrasonic excitation prevents the accumulation of shear stresses, meaning that the influence of the friction forces on the contact surfaces of the specimen and die are reduced. This reduction in friction forces is defined as the surface effects. This effect occurs together with a decrease in static force required for deformation, known as the volume effect. The volume effect was defined as the reduction in flow stress or applied load during ultrasonic excitation of the material being formed [75, 85]. More recently, studies [39, 66] have shown the beneficial effects of volume and surface

mechanisms during ultrasonic excitation on upsetting. Daud et al. [66] investigated the effects of the application of longitudinal and radial ultrasonic excitation in compression tests of aluminium specimens, and finite element models were developed to numerically investigate the material and friction effects of ultrasonically assisted compression. The results showed that the compression stress was reduced by an effective softening mechanism of ultrasonic excitation on the material under dry surface friction conditions. Daud et al. matched the numerical result to the experimental result by adopted an effective softening mechanism of ultrasonic excitation to the FE models which reduced the material properties and adjusted the contact conditions.

The results of the experiment by Izumi et al. [81] are shown in Fig. 4.2. Curve 1 shows a force-strain diagram, obtained for a static compression of an aluminium cylindrical specimen. The strain $\varepsilon = \ln\left(1 + \frac{h}{H}\right)$ is shown on the horizontal axis, where h is the compression displacement and H is the height of specimen. Curve 2 shows the change in static force P whilst compressing a similar specimen in the presence of ultrasonic excitation. Curve 3 shows the difference of static force whilst compressing the specimen, between two intervals of ultrasonic excitation. In all these cases, the compression process was carried out with the same constant speed $v = 0.5\ mm/min$ and the vibration was employed at a frequency of $22\ kHz$. The amplitude of vibration at the tip of the horn was $10\ \mu m$. From this result it was observed that a softening of the material and a change in its elastic-plastic behaviour appears under the influence of ultrasonic excitation. The influence of ultrasonic excitation in curve 3 is confirmed by the observation in curve 1 and curve 2 when the vibration is applied and re-applied during the compression deformation. It was observed that curve 3 nearly followed curve 2 in the presence of ultrasonic excitation and returns to curve 1 when the vibration is stopped. Similar effects were explained by Daud et al. [148] when investigating the influences of oscillatory stress in compression tests of aluminium.

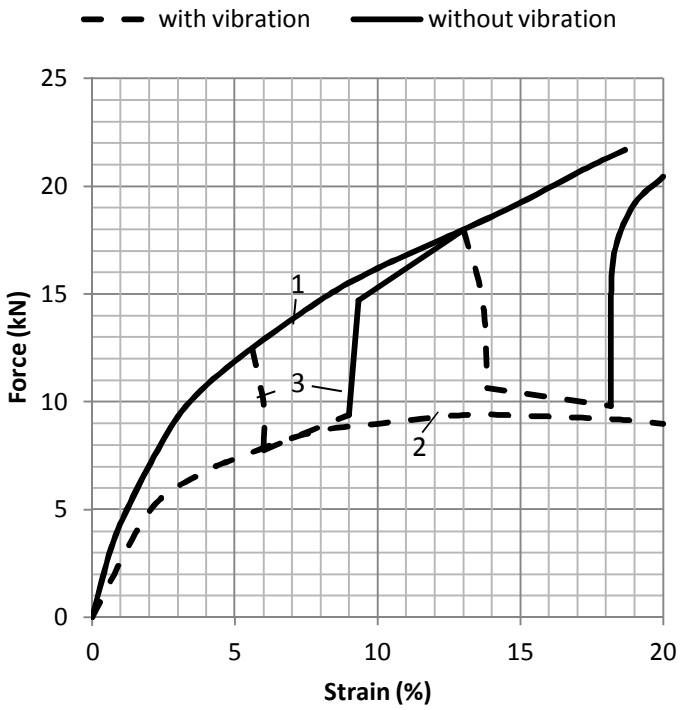

Figure 4-2 Changes in compression load in the presence of ultrasonic excitation [81]

More recently, an investigation by Siddiq et al. [5] studied the effects of ultrasonic excitation on a metal upsetting process. The study was carried out by developing a finite element model that predicted the ultrasonic softening effects when ultrasonic energy was applied during deformation. Material model parameters were identified via inverse modelling using experimental data. The study demonstrated the predictive ability of the FE model of ultrasonically assisted upsetting of aluminium alloy at room temperature, in confirming experimental results previously reported by Hung et al. [39]. The results showed that the ultrasonic energy reduced the stress-strain response of the material during the upsetting process due to material softening. The results showed a very good agreement between the experimental and simulated response.

The review of previous studies of superimposed ultrasonic excitation on upsetting showed that most of the experimental characterisations of the volume effects mainly depended on an interpretation of measurements of the mean flow stress, and have neglected the oscillatory stress. This chapter aims to characterise the oscillatory stress on the material behaviour in plastic deformation when superimposed ultrasonic excitation is applied on a static compression test under dry friction.

4.2 Apparatus

A schematic of the apparatus is shown in Fig. 4-3. The resonant ultrasonic system is set up between the cross-head and the table of the 250 kN Zwick Roell material testing machine with 100 Hz sampling rate, which is capable of controlling the cross-head speed. The designs of the system have been divided into three sections: an ultrasonic excitation system, a holder structure and the punch device. The ultrasonic excitation system consists of a 500 Watt piezoelectric transducer, a booster and a die horn. The holder structure consists of plates and pillars that can be connected between the ultrasonic excitation system and the table of the Zwick Roell material testing machine. The punch device consists of a punch tool and a piezoelectric force transducer which was attached to the cross-head of the Zwick Roell machine. During the ultrasonic experiments the temperature of material is not monitored that based on previous studies demonstrated that there was no temperature change during the ultrasonic forming process [66, 107].

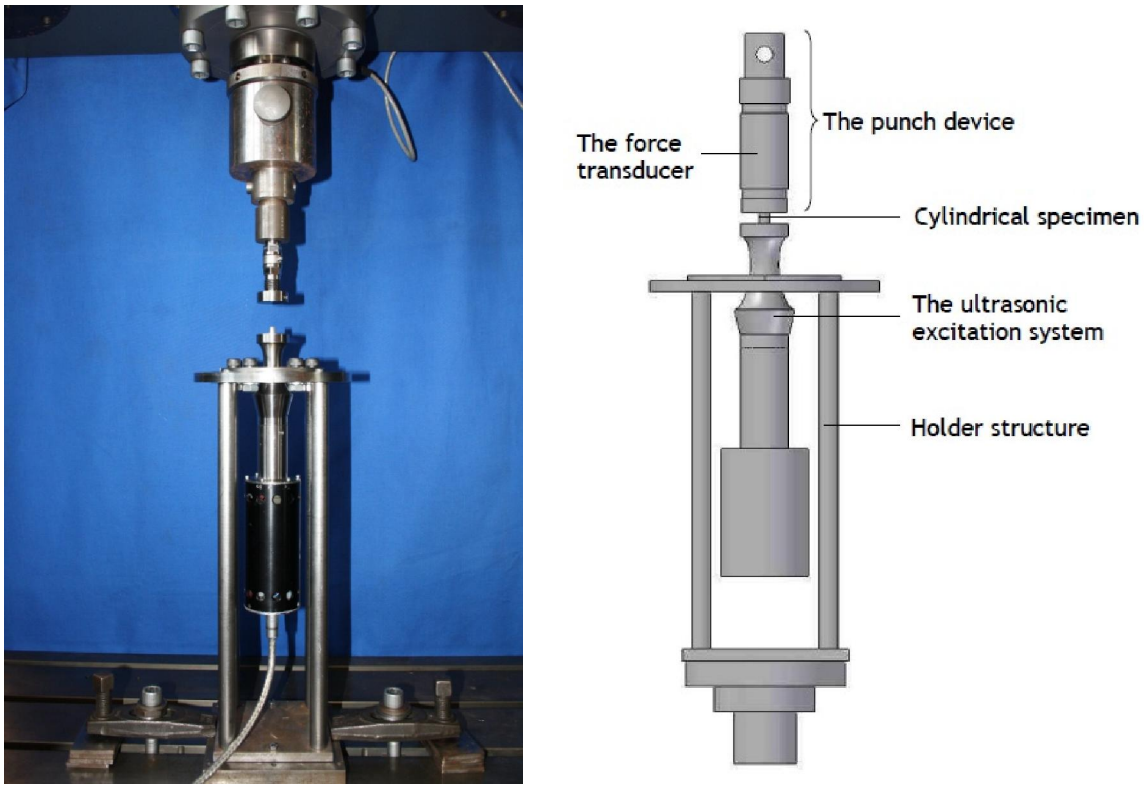

Figure 4-3 A schematic of the apparatus for static and ultrasonic upsetting tests (a) attached to Zwick Roell testing machine and (b) designed in Solid Works

4.2.1 A 500 W ultrasonic generator and piezoelectric transducer

The ultrasonic generator used in this study can deliver a 20 kHz signal at a potential power output of up to 500 Watts is shown in Fig. 4-4(b). This generator offers the facility of constantly monitoring both amplitude and acoustic power. During the ultrasonic experimental test, the amplitude and acoustic power were monitored to ensure the parameters are consistently at same level of point throughout experiment even under high loading conditions. The transducer used in this study is based on a bolted Langevin transducer design. In this construction, a number of piezoelectric discs are bolted between a pair of metal end masses. The piezo elements are of a pre-polarized lead zirconate titanate (PZT) composition. The PZT discs generate the inverse piezoelectric effect such that if a charge is applied to one face of the disc and an equal but opposite charge to the other face, the discs are either expanded or contracted depending on the polarity of the applied charges. Thus on applying a rapidly reversing charge to the piezoelectric material fluctuations in dimensions are produced. This effect can be harnessed to transmit ultrasonic vibrations from the piezo elements through whatever medium with which it is in contact. The overall length of the transducer is one half-wave at the required frequency of 20 kHz. The piezoelectric transducer has potential efficiencies of 98% when employed in a mode of continuous operation. Maximum peak to peak displacements at the transducer radiating face are in the range of up to 12 μm.

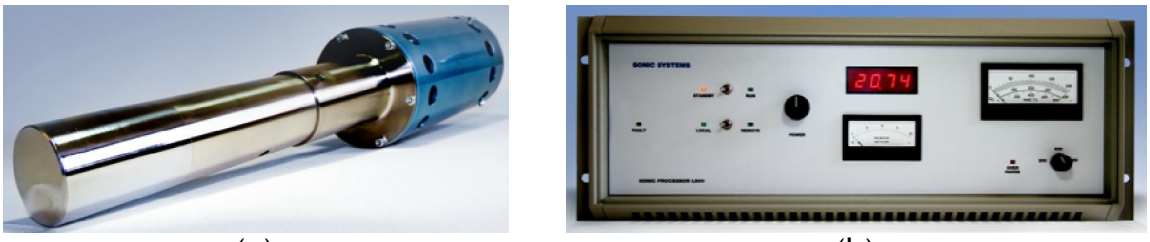

(a) (b)

Figure 4-4 (a) Ultrasonic transducer and (b) ultrasonic generator

4.2.2 Data analysis apparatus

There are various methods of measuring the amplitude response of vibrating elements. One of the most common used is piezoelectric transducer. A piezoelectric transducer is a device that uses the piezoelectric effect to measure pressure, acceleration, strain or force by converting them to an electrical charge. In this study, there are two types of transducer used to measure the static-oscillatory force response during superimposed ultrasonic excitation on upsetting test. The transducers are referred to as the piezoelectric force transducer and the machine load cell.

4.2.2.1 Piezoelectric force transducer

The piezoelectric force transducer is the simplest form of measurement transducer which contains a piezoelectric element sandwiched between two electrical contacts. The piezoelectric force transducer is mounted under preload between the punch tool and machine cross-head. Once the transducer is subjected to vibration, stress is applied to the piezoelectric element and the resultant strain within the element generates an electrical charge through the direct piezoelectric effect. The generated charge is directly proportional to a known amplitude of force. The charge signal is fed to a charge amplifier as an output voltage. The voltage signal is acquired by the SignalCalc ACE data acquisition hardware and software for data processing. The piezoelectric force transducer can measure static and dynamic force responses. Table 4-1 shows the technical data for the Kistler piezoelectric force transducer used in this study.

Table 4-1 Technical Data of Kistler Force Transducer

Type	10 kN Force Transducer
Maximum Range of Load, kN	± 10
Natural Frequency, kHz	≈ 55
Weight, g	90
Sensitivity, charge/N	≈ -4
Operating Temperature Range, ^{o}C	-40 to 120

4.2.2.2 Data analysis hardware and software

SignalCalc ACE, powered by Quattro is used as the hardware to receive the output voltage signal which is collected from the charge amplifier. The hardware is capable of real-time measurements to record data on all channels at a rate of 204.8 ksamples/sec. The vibrational force responses obtained by the force transducer in voltage are channelled into the Quattro for processing, analysis and then conversion into readable data using SignalCalc ACE dynamic signal analyser software. The vibrational force responses are continuously recorded in the time and frequency domain in the software analyzer. It is much more practical to convert the force responses versus time to the parameter of interest such as, static-oscillatory stress versus strain. In order to obtain these parameters, a simple mathematical model is developed using Matlab R2010a commercial software to compute the parameter of static flow stress, oscillatory stress and strain.

4.2.2.3 Zwick Roell test machine load cell

The machine load cell is typically a stiff and precise spring that outputs a relatively large electrical signal directly proportional to the force on the device. Applying a force to this spring produces strain that causes small deformations in the load cell. These deformations directly transfer to strain gauges strategically bonded to the load cell. In turn, the dimensional change of the bonded strain gauges produces a resistance change in each individual gauge. The resistance change produces an electrical charge that is proportional to the compression load. The machine load cell can only measure static force responses. Consequently, an applied force versus displacement diagram can be directly measured from the machine software. Then, the force-displacement diagram is converted to a stress-strain diagram using the Matlab R2010a software.

4.2.3 Materials and specimens

Two types of metal specimens are used in the upsetting tests. All the specimens are machined to a cylinder of 8 mm in diameter and 8 mm in height, giving an aspect ratio of 1. The use of specimens having aspect ratio more than two should be avoided to prevent buckling and shearing modes of deformation. All specimen surfaces were sanded and polished to provide a uniform surface roughness. The interfaces between the specimens, die horn and flat punch tool are in dry conditions. For modelling purposes, the coefficients of friction, μ, at the interfaces were estimated from static ring compression tests where for a dry surface $\mu = 0.25$ [66]. Compression tests were performed on specimens of commercial grade metals; aluminium and magnesium. The mechanical properties of the metals specimens measured from experimental test are shown in Table 4-2.

Table 4-2 The mechanical properties of the metals specimens used in the compression tests

Material Properties	Unit	Metals	
		Aluminium	Magnesium
Density	kg/m^3	2705	1770
Compressive Strength, Yield	MPa	60	124
Modulus of Elasticity	GPa	1.45	1.7
Poissons Ratio		0.33	0.35

4.3 Experimental procedure

In these experiments, metals cylindrical specimens are compressed between a flat die and a flat punch tool. The die is the end surface of the ultrasonic horn. The die horn consists of a tuned longitudinal mode horn of 20.7 kHz, for the experiment which superimposes axial ultrasonic vibration on the static deformation process, providing a uniform nominal vibration peak to peak amplitude in a range of 5 μm to 20 μm on the flat die surface depending on the ultrasonic generator setting. The flat punch tool is connected to the cross-head of the Zwick Roell testing machine which provides a constant cross-head speed of 5 mm/min for these experiments. In ultrasonic deformation tests, the ultrasonic excitation is applied after 1 mm displacement deformation of the specimen height which assumes that the material is deforming beyond the yield limit in plastic hardening deformation. Both static and ultrasonic deformations are performed at a constant cross-head speed of 5 mm/min under dry surface conditions until 50% of specimen height is reached. Previous studies [5, 39, 65] showed that the strain rate did not influence the significant effect of ultrasonic excitation under room temperature. However, when the material temperature was increased, the loading force was expected to decrease as the strain rate was

lowered. The temperature rise occurred due to frictional heating when relative motion of the interface exists. In this study, a speed of 5 mm/min was chosen in order to observe the effect of ultrasonic excitation on specimen behaviours during the experimental test and FE simulation. The other constraints were due to apply time of ultrasonic excitation and the appearance of frictional heating. It was measured that the observation can be done for 24s during the ultrasonic excitation tests.

4.4 Metal stress-strain diagrams

The behaviour of materials under compression loads can be obtained by plotting the stress-strain diagram. The diagram is generated by calculating the true stress and strain of compression deformation under static loading. Fig. 4-5 shows the stress-strain diagram for aluminium and magnesium. These curves are used to determine the material properties of the metals shown in Table 4-2.

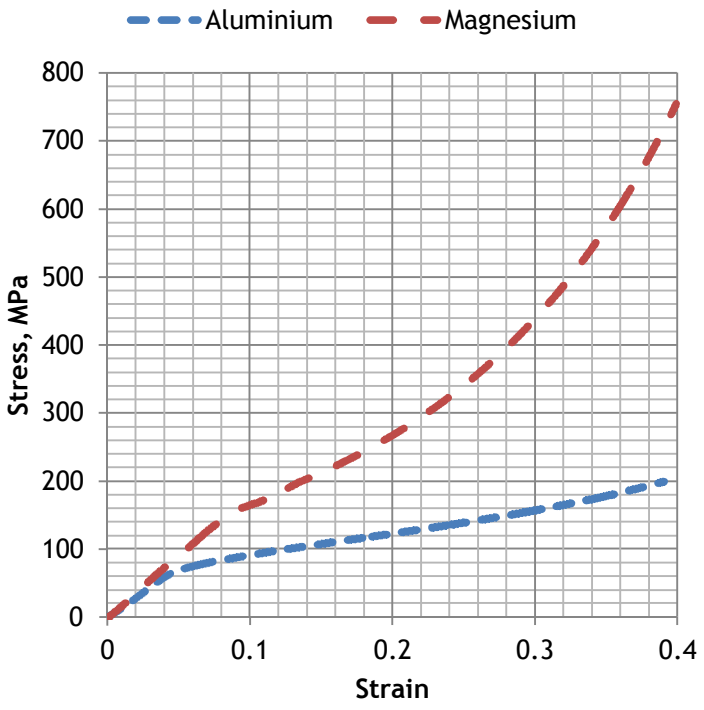

Figure 4-5 Metal stress-strain diagram

The resulting stress-strain diagram gives a direct indication of material properties such as modulus of elasticity, yield point and ultimate strength. The modulus of elasticity is defined as the ratio of stress to strain within the elastic region of the stress-strain curve. It is a measure of the stiffness of the material and is also known as Young's Modulus. The Young's Modulus of aluminium and magnesium were determined in Table 4-2 that shows the values of material stiffness are much lower than standard figures of 69 GPa and 45 GPa for aluminium and magnesium, respectively. Experimentally, the behaviour of materials was obtained using the experimental procedure that has been discussed previously. Generally, the Zwick-Roell testing machine was measured the deformation (strain) of an elastic material is directly proportional to the amount of force applied to the material (stress) and the Young's Modulus is calculated to measure the stiffness of material. However, the results shown in Table 4-2 was affected by the compliance of the ultrasonic system structure included rig, tool and die that attached to the machine. It was expected that in this case, the elastic modulus measured is an extensive property of the solid body dependent on the material, the structure and boundary conditions. This has resulted repercussion in the oscillatory stress predictions particularly in FE models.

Commercially material properties of aluminium A1050 and magnesium AM50 are a shown in Table 4-3. Initially, these properties were used as a material model in FE to simulate the static compression test and resulted the stress-strain curves which shown in Fig. 4-6. The stress-strain curves of standard material properties were compared against the experimental results presented the FE model prediction show a variation with experimental results. Data improvement has been applied to the material model in FE in order to obtain a good comparative agreement with the experimental results by adjusted the material properties of Young's Modulus and Yield stress. The adjusted material properties was shown in Table 4-2. The comparison results for adjusted material properties in FE model with experimental are shown in Fig. 4-6. However, the application of adjusted material properties in FE model was affected the prediction of oscillatory stress during the superimposed ultrasonic excitation. The measurement of oscillatory stress for standard and adjusted material properties in FE model are shown in Fig. 4-7. Fig. 4-7 shows a prediction of oscillatory

stress using material model of adjusted and standard properties of material against ultrasonic vibration amplitude. In Fig. 4-7(a) and (b) the slope of oscillatory stress to ultrasonic amplitude using standard material properties was observed higher than the slope of oscillatory stress to ultrasonic amplitude in experimental and using adjusted material properties in FE model has a lower slope of oscillatory stress to ultrasonic amplitude. Consequently, correction on ultrasonic vibration amplitude was applied to correlate the prediction of oscillatory stress in FE model as to achieve a good comparative agreement with experimental slope of oscillatory stress against ultrasonic amplitude. From Fig., the coefficient of ultrasonic amplitude was identified where the amplitude was amplified four times in FE model as correlated to the experimental results for both materials. The correction in ultrasonic amplitude resulted a good agreement between the gradient of oscillatory stress to ultrasonic amplitude in experimental result and using adjusted on material properties and vibration amplitude in FE model which showed in Fig. 4-7(a) and (b).

Table 4-3 The mechanical properties of the commercial metals (standard)[149]

Material Properties	Unit	Metals	
		Aluminium	Magnesium
Density	kg/m^3	2705	1770
Compressive Strength, Yield	MPa	90	130
Modulus of Elasticity	GPa	69	45
Poissons Ratio		0.33	0.35

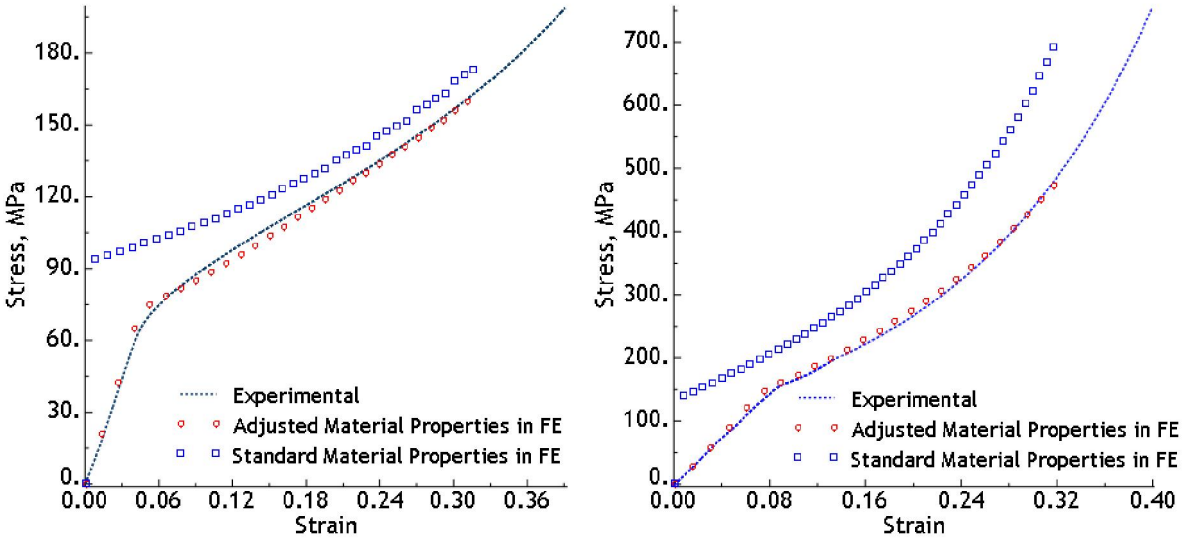

Figure 4-6 Comparison of experimental and simulation data with standard and adjusted material properties for static compression test for (a) aluminium and (b) magnesium

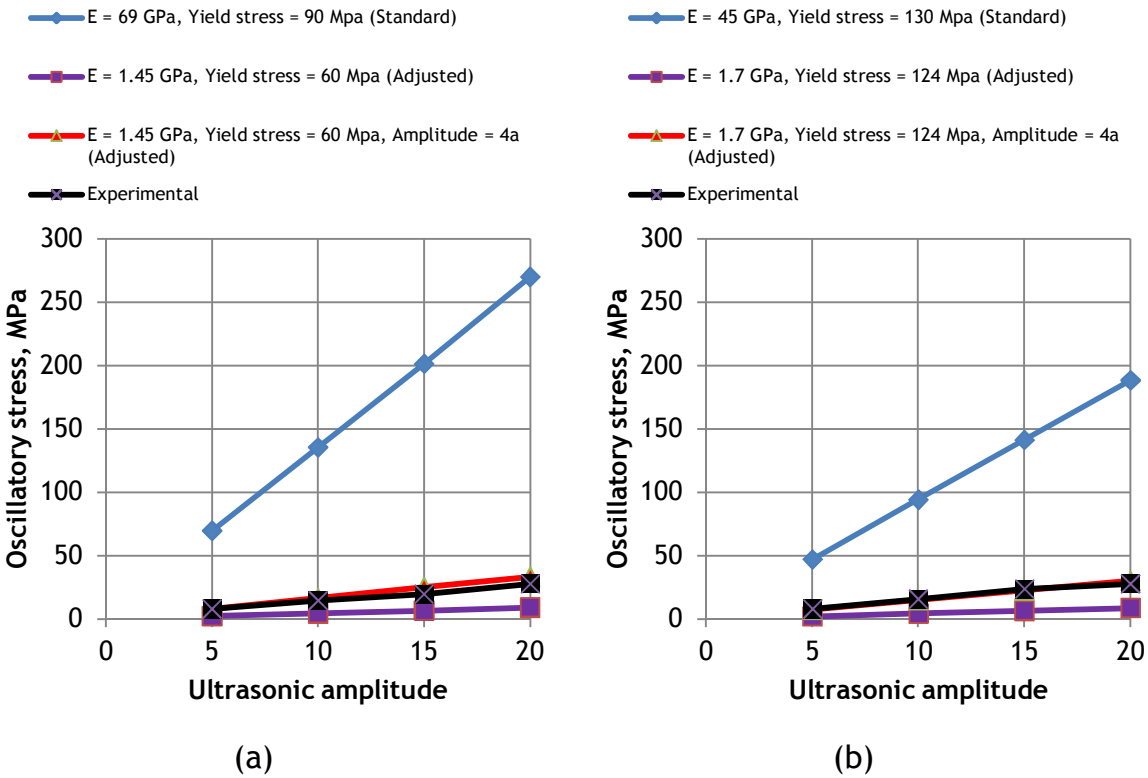

Figure 4-7 Comparison of experimental and simulation ratio of oscillatory stress to ultrasonic amplitude with standard and adjusted material properties for (a) aluminium and (b) magnesium

In this study, the measurement of Young's Modulus and yield stress of the specimen was not properly determined the actual properties of material. Subsequently, in future works the determination of specimen material properties such as Young's Modulus and compression yield stress limit during compression test should be considered. As suggestion, a suitable device to measure the actual material properties is the electrical resistance strain gauge [150]. The device can be used to determine Young's Modulus and Poisson's ratio and most widely used for measuring elastic strains.

4.5 Ultrasonic upsetting finite element model and boundary conditions

The ultrasonic upsetting model is developed using the commercial finite element code Abaqus. The material properties model applied in the ultrasonic upsetting model is referred to in Table 4-2, along with boundary conditions parameters such as interface contact conditions, compression speed and ultrasonic amplitudes. The identification of these material and boundary condition parameters is performed using an inverse modelling method. In this method experimental stress-strain curves are compared with the simulated stress-strain curves and the difference between the experimental and simulated stress-strain curves is minimized by the variation of these parameters. The process is repeated until a good agreement is achieved between experimental and simulated stress-strain curves.

4.5.1 Stages of Finite Element Modelling

The construction of the FE model was developed using Abaqus commercial software. The stages followed in the modelling processes in Abaqus are shown in Fig. 4-8.

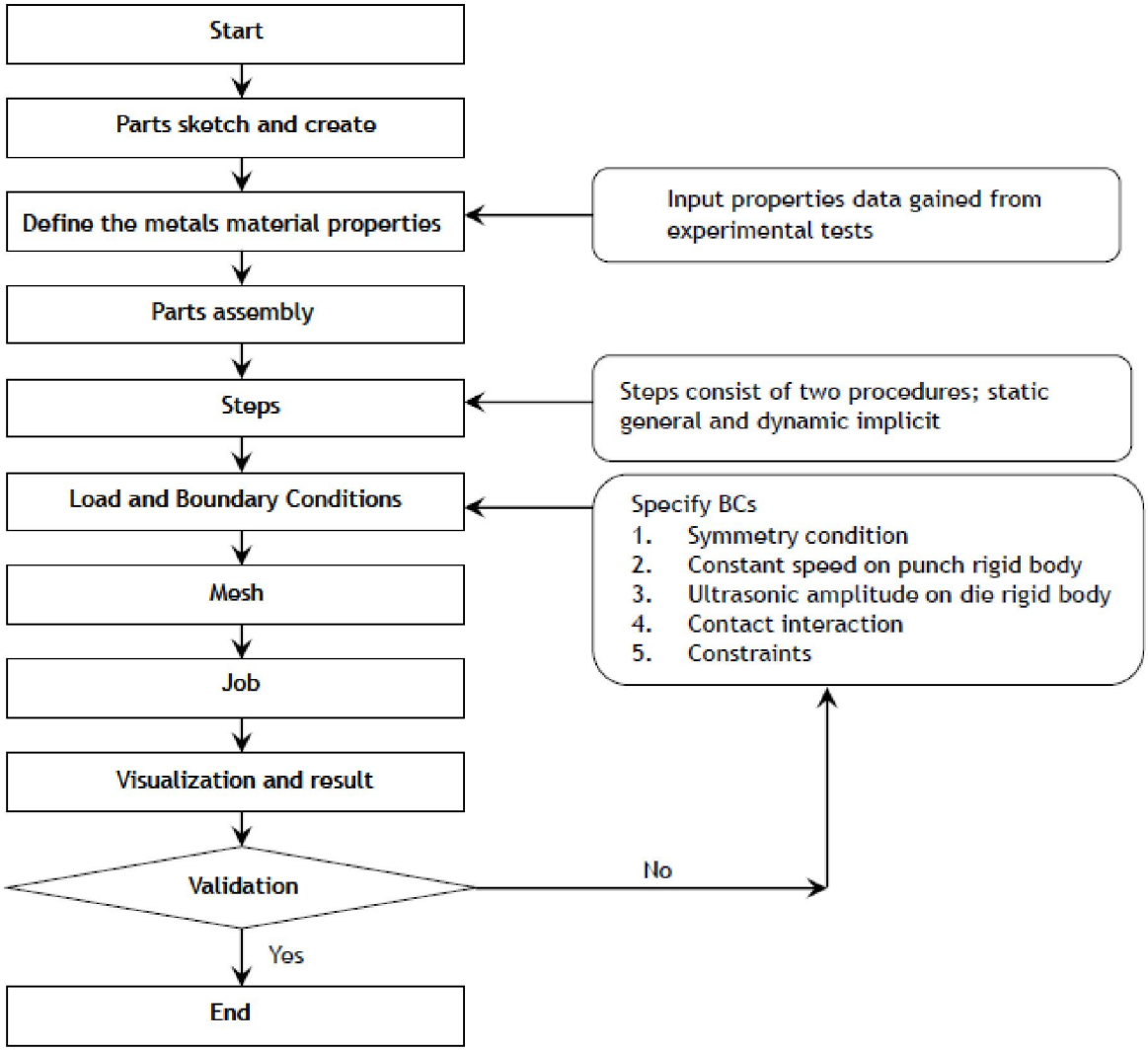

Figure 4-8 Stages of numerical analysis in FE modelling

The modelling process was initiated by creating individual parts by sketching their geometry directly into Abaqus in its parts module. Punch and die tools were modelled as rigid bodies, and the specimen was modelled as an axisymmetric deformable body. The material properties of the deformable specimen were defined in the second stage of the FE modelling. The material properties definition was assigned as elastic-plastic behaviour. The elastic and post-yield parameters of the material used the classical metal plasticity model in the simulation. The initial yield stress at zero plastic strain was defined in the model. The elastic-plastic behaviour data was obtained from the static and ultrasonic compression test. Fig. 4-5 measured the initial yield stresses at zero plastic strain are 60 Mpa and 120 Mpa for aluminium and magnesium,

respectively. Ten other data points through the curves of plastic stress-strain conditions are measured included Young's Modulus, Poisson's Ratio and density of the materials which were shown in Table 4-2. All the data points are defined in FE material model as material behaviours. The static stress-strain curves were plotted from FE model simulation and matched with the experimental results. As a result, a better correlation between the experimental and FE data was achieved. All parts were assembled in a global coordinate system. Rigid body tools were used because of their advantages over deformable bodies with regard to degrees of freedom and this produced significant computational time savings without affecting the overall results.

The analysis procedures, loading, and output request options were defined in the Abaqus steps. General static and implicit dynamics procedures were introduced in the step analysis. The first step used is general static to calculate the elastic-plastic behaviour when a static load is applied then the procedure is continued in implicit dynamics as a second step. A static analysis is sufficient to obtain a response in static compression until a certain displacement deformation occurs. However, for superimposed ultrasonic excitation, a nonlinear dynamic analysis must be performed. In a nonlinear dynamic response, the equations of motion must be integrated directly. The direct integration of the equations of motion is performed in Abaqus as an implicit dynamics procedure. An automatic incremented control was used in the steps so that Abaqus automatically adjusts the size of the load increments and solves nonlinear problems easily and efficiently.

The most critical stage in the process is designating the load and boundary conditions. The conditions applied in the deformation of the FE model followed the experimental procedures. The FE loading and boundary conditions are discussed later in this section. The contact simulation is assigned to identify the area of surfaces that are in contact and to calculate the contact pressure generated. In this analysis, the contact simulation has to be able to detect when two surfaces are in contact and to apply the contact constraints. Similarly, the analysis must be able to detect when two surfaces separate and remove the contact constraints, especially during the dynamic analysis. The interaction between contacting surfaces consists of two components, normal to the surfaces and tangential to the surfaces. In those normal to the surface, a hard contact

behaviour was used. The behaviour shows where a dramatic change in contact pressure occurred and also shows when a contact condition is changed from open (clearance) to closed (clearance equal to zero) and vice-versa. In those tangential to the surface, a coulomb friction model is used to describe the interaction of contacting surfaces. The model characterises the frictional behaviour between the two surfaces using a coefficient of friction, μ. The axisymmetric deformable specimens are meshed using four node quadrilateral elements, as it is necessary to use a sufficiently refined mesh to ensure the results are adequate; coarse meshes can yield inaccurate results. The suitable mesh can be demonstrated as producing converged results. Lastly, the job was created to complete the FE model process stage. In the 'visualization and results' stage, the results of displacements and reaction forces are obtained in the history output database file for each increment of the simulation. These results are used to create the stress-strain diagrams.

The results calculated in the FE model were matched to the experimental test results to attain close agreement outcomes. In this case, the static stress-strain curve predicted by FE model was matched to the static stress-strain curve measured from the experimental test. If acceptable agreement was achieved, this marked the end of the process stages. However, if the results were not well matched, the process returned to the load and boundary condition stage. An adjustment can be made in material properties data or the definition of load and boundary conditions to gain a better match, but the adjustment made should be referred to the experimental results. The process is repeated until the results correlation is satisfactory.

4.5.2 The FE loading and boundary conditions

The finite element method requires dividing of the analysis region into many sub-regions. These small regions are the elements, which are connected with adjacent elements at their nodes. Mesh generation is a procedure of generating the geometric data of the elements and their nodes, and involves computing the

coordinates of nodes, defining their connectivity and thus constructing the elements. In this study, the FE model was constructed from only half of the specimen diameter and was meshed using axisymmetric four node elements, taking advantage of symmetry. An axisymmetric model is a way to analyze a revolved part as a 2D model where the part and loads are symmetrical. The axisymmetric elements deform as if each element was a solid ring, so that an axisymmetric solid element is modelled like a 2D element. The axisymmetric four-node element is shown in Fig. 4-9. By reducing a 3D model to a 2D plane, there can be orders of magnitude reduction in solution time and file size.

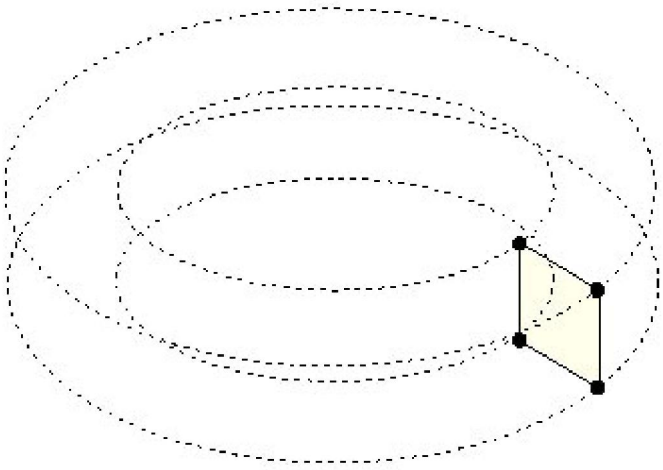

Figure 4-9 The axisymmetric four-node element

The FE model consists of three main parts; the flat punch and die as axisymmetric analytical rigid bodies, and the axisymmetric deformable metal specimen. The geometry of the model for the specimen has dimensions of 4 mm $\times$ 8 mm. The deformed and undeformed mesh profiles of an upsetting test simulation are shown in Fig. 4-10:

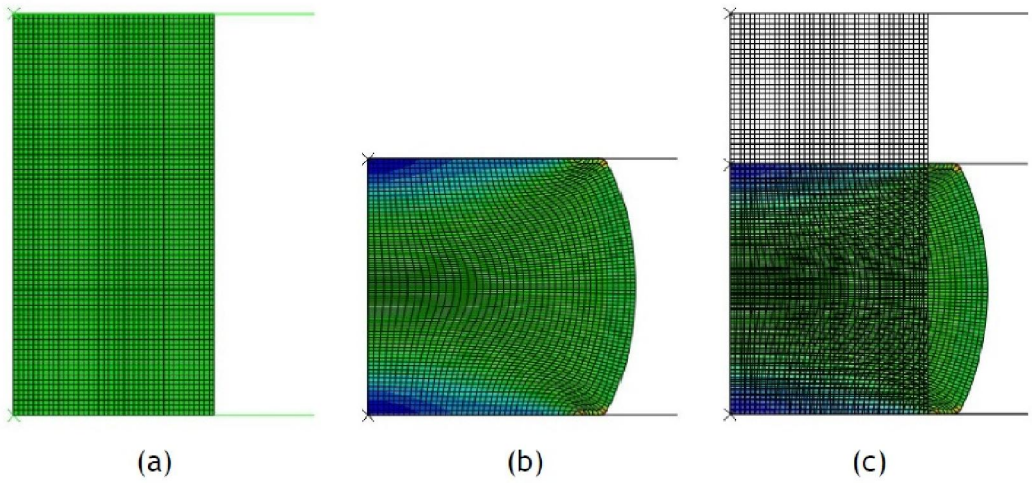

Figure 4-10 Mesh profile for (a) undeformed (b) deformed (c) multiple view of meshing for the upsetting FE model

The speed of the punch and vibration amplitudes are applied in the simulation through a reference point associated with the rigid bodies of punch and die, as shown in Fig. 4-11. A constant velocity of 5 mm/min is applied in a vertical direction at the punch reference point while the centre line is defined as a fixed symmetry in the horizontal direction. The ultrasonic vibration is applied using displacement boundary conditions, with a periodic sinusoidal curve; $u_o = asin\omega t$, where a is the amplitude of vibration and ω is the angular frequency. The contact interaction conditions are defined as a surface to surface method between all the rigid bodies and specimen interfaces. Tangential and normal behaviour are defined as contact properties with a friction coefficient of 0.25 for dry surfaces and hard contact, respectively. Isotropic elastic-plastic properties are used to describe the behaviour of metal specimens. All the material properties parameters of the metals used are shown in Table 4-2.

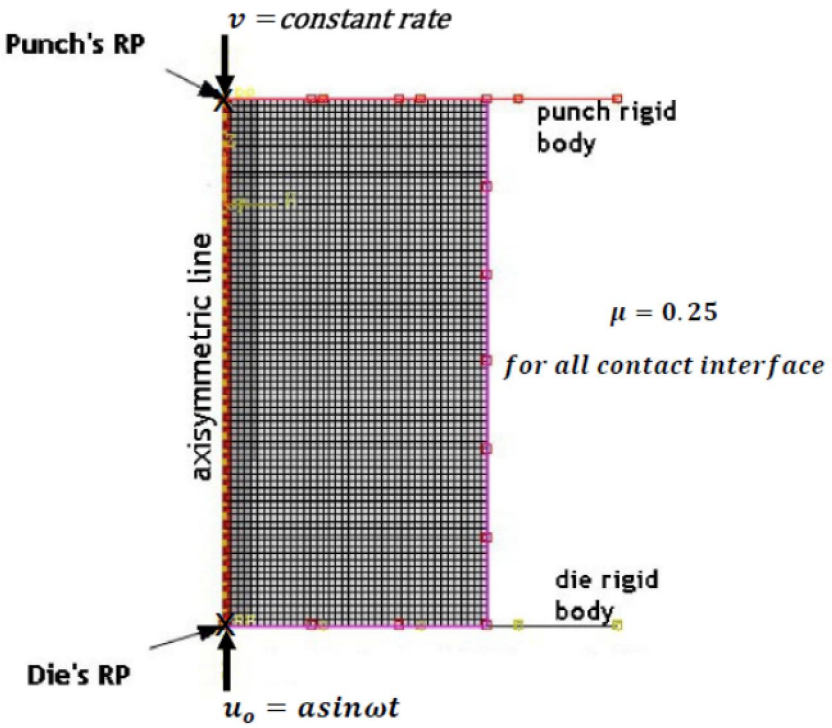

Figure 4-11 FE model boundary conditions

To demonstrate the performance of the current FE model, a compression test of soft grade aluminium with and without ultrasonic excitation is simulated and validated against the experimental and numerical results [66]. In Fig. 4-12, black solid and dash line show the stress-strain relationship from experimental and FE simulated static compression tests for a cylinder specimen with dry interface. Hence, the red solid line shows the stress-strain relationship from the current FE model of a static compression test with using the material properties model measured in the experimental test by Daud et al., such as material elastic-plastic behaviour data, coefficient of friction of 0.25 for dry contact surface which measured in the material ring compression test, constant crosshead speed at 5 mm/min and compressed until 50% of the specimen height. Model prediction show a good agreement with the experimental and previous numerical results.

For identification of the oscillatory stress behaviour, the simulation test conditions were using the same material properties model applied with a constant velocity of 5 mm/min to the punch, with and without the ultrasonic excitation. The ultrasonic excitation was introduced with a frequency of 20 kHz

and longitudinal vibration amplitude of 10 μm at 22% reduction of the specimen height. Fig. 4-13 shows the oscillatory stress behaviour from the FE model compared to the model by Daud. Fig. 4-13(a) shows an 11 MPa reduction in the mean stress and the peak to peak oscillatory stress amplitude is 23 MPa. Close FE prediction results are shown in Fig. 4-13(b) where the mean stress is reduced by 13 MPa, and the peak-peak oscillatory stress amplitude is 24 MPa. However, the experimental results by Daud et al. measured a reduction in mean stress of 40 MPa and a peak-to-peak oscillatory stress amplitude of 24 MPa during the superimposed ultrasonic excitation on compression. It is clearly shown that the agreement is not so close for the mean stress reduction but for the oscillatory stress amplitude the experimental and FE result was the same. For more realistic representation of the compression test data, they suggested combining a temporary adjustment in material properties with a temporary adjustment in the friction contact condition during ultrasonic excitation in the FE model. Since the simulation of the deformation process is matched validated with previous study, the process has expanded the materials and the amplitudes of vibration used were varied for the other metals with vibration of 5 μm to 20 μm applied on the die in this study.

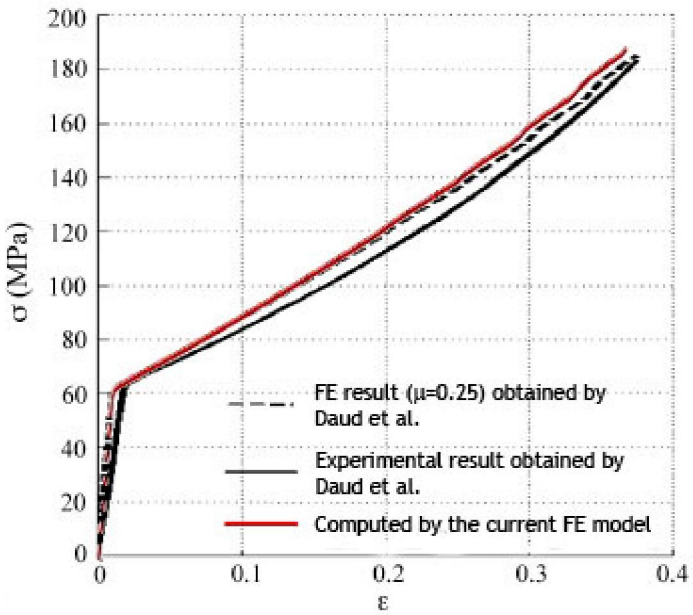

Figure 4-12 Comparison of FE stress strain data with previously published for FE and experimental results.

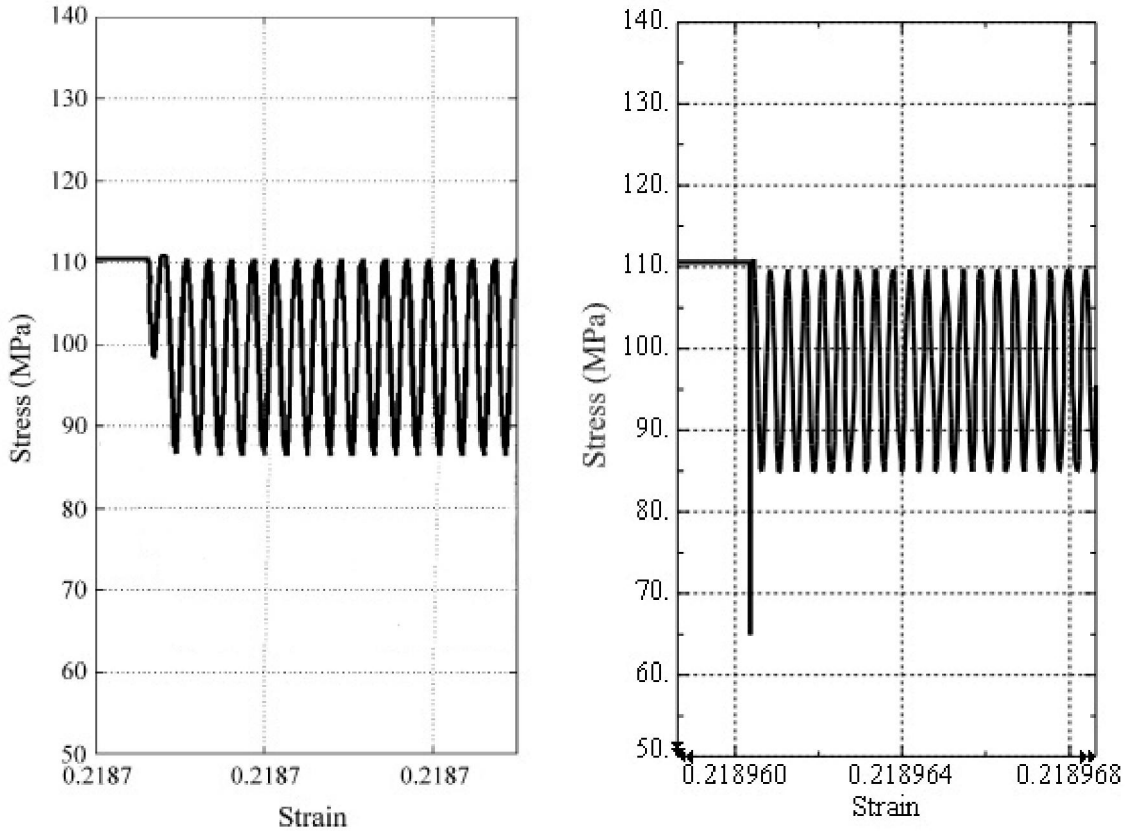

Figure 4-13 Results of (a) ultrasonic loading obtained by Daud et al. [66] and (b) ultrasonic loading computed by the current FE modelling

4.6 The effects of ultrasonic excitation on experimental results

The effects of material properties behaviour during the superimposed ultrasonic excitation on compression test can be illustrated in the stress-strain curve. The effects can be explained in terms of flow stress reduction, oscillatory stress, mean flow stress, a path of maximum peak of oscillatory stress, and a path of minimum peak of oscillatory stress in the stress-strain diagram. All the term annotations are shown in Fig. 4-14.

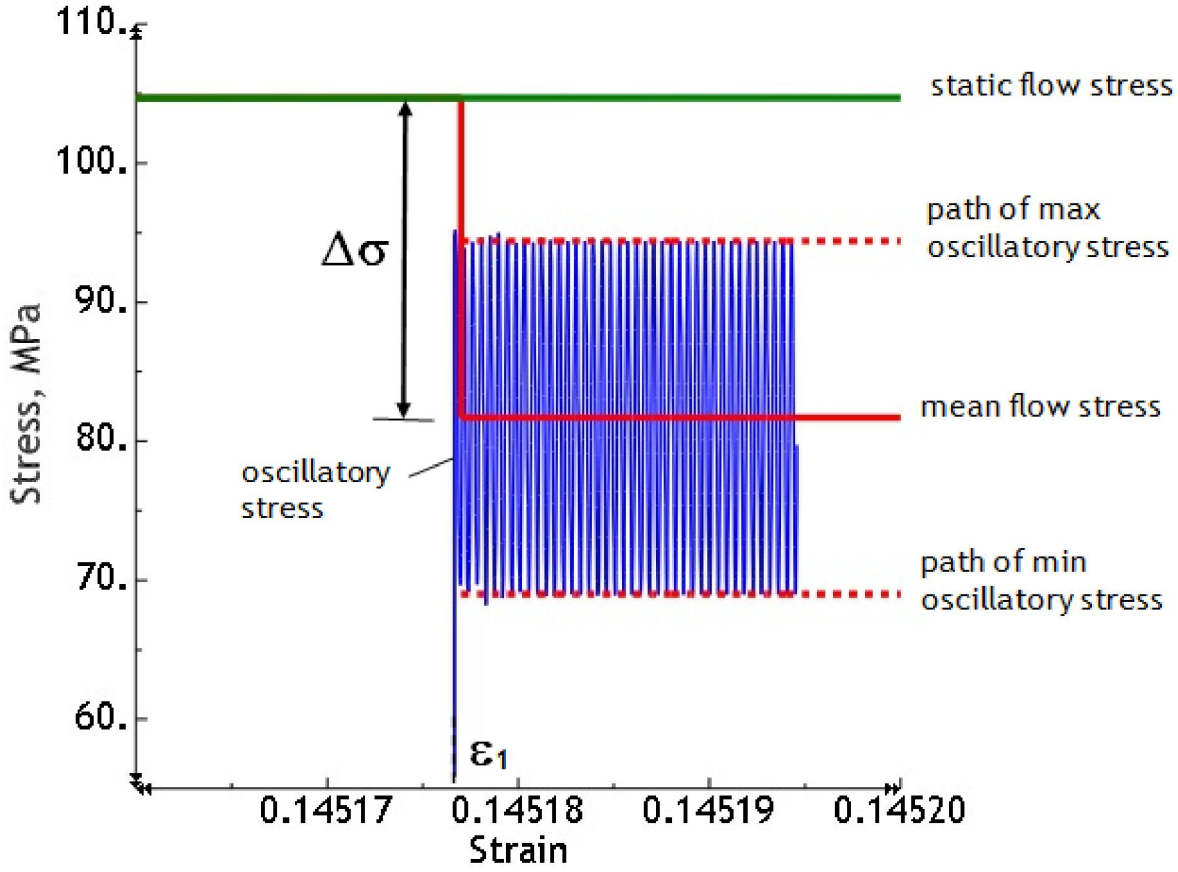

Figure 4-14 Annotation of stress-strain diagram

Static flow stress is defined from the curve of material flow behaviour in the stress-strain diagram during elastic-plastic deformation under a constant compression rate. Oscillatory stress is defined as the sinusoidally varying stress that occurs when the ultrasonic excitation is introduced. Fig. 4-14 shows the ultrasonic excitation introduced at strain ε_1. The path of maximum oscillatory stress is defined as a connection of the maximum peak points of oscillatory stress. Hence, the path of minimum oscillatory stress is defined as a connection of the minimum peak points of oscillatory stress. The mean flow stress is defined as the mean value of the oscillatory stress and can be calculated as

$$\bar{\sigma} = \frac{\hat{\sigma} - \check{\sigma}}{2}; \tag{4.4}$$

where $\hat{\sigma}$ is the maximum peak of oscillatory stress and $\check{\sigma}$ is the minimum peak of oscillatory stress.

Stress reduction is defined as the reduction of static flow stress to the mean flow stress in the presence of ultrasonic excitation at strain ε_1. At this point, the stress reduction can be calculated as

$$\Delta\sigma = \sigma_{static} - \bar{\sigma}\,; \tag{4.5}$$

where $\bar{\sigma}$ is the mean flow stress and σ_{static} is static flow stress at strain ε_1

In this investigation, the stress reduction is determined in terms of a percentage that can be defined as

$$\Delta\sigma = \frac{\sigma_{static} - \bar{\sigma}}{\sigma_{static}} \times 100\%; \tag{4.6}$$

These terms are used to explain the effects of superimposed ultrasonic excitation on upsetting in the following sections.

As reported in previous studies [39, 65, 66], the flow stress of compressive deformation can be remarkably reduced by superimposing ultrasonic vibration on the static load in compression tests. Researchers have concluded that softening of the material and a change of its elastic-plastic properties take place under the influence of ultrasonic excitation, and that such a softening effect can only be observed in the presence of vibration. This effect was confirmed in numerous later research studies and experiments [5, 77, 107]. The studies also explained the influence of friction on material flow in ultrasonic upsetting tests. During the upsetting process, the condition of plastic deformation changes as the geometry of the cylinder specimen changes. The movement of the flat punch causes the changes, and is an important feature in the compression process. The punch and die are subjected to both deformation and friction forces. The frictional forces act in the direction tangential to the surface of the punch and die, opposite to the relative velocity between the punch, die and the specimen. As shown in the previous studies, ultrasonic excitation of the die leads to a decreases in the mean load required to overcome frictional forces, which are described in terms of a coefficient of friction.

The influence of volume effects in the flow stress reduction was investigated experimentally by Izumi et. al [65]. This resulted a relationship between an observed yield limit σ, and vibration amplitude a;

$$\sigma = \sigma_o - Ka; \tag{4.8}$$

where σ_o is the actual yield limit found in a static deformation processes and K is a material constant.

The influence of surface effects on the coefficient of friction was investigated experimentally by Rozner [41]. This investigation demonstrated that a maximum reduction in the coefficient of friction of 40% could be achieved in a study of ultrasonic strip drawing. In this current study, aluminium and magnesium are the metals studied as cylinder specimens. Aluminium and magnesium are considered to be soft metals and can be easily shaped by any of the main industrial metalworking processes. Mostly aluminium has been the subject of research studies [5, 27, 39, 45, 64, 77, 81, 109, 148]. Most of these studies performed the application of ultrasonic vibration to metalworking processes for a dry surface condition.

During the upsetting tests, two sets of forming force measurement data are recorded. The first set of force-displacement data is recorded by the machine load cell. This set of data includes a mean load and static force measurement in a series of ultrasonic excitation loading tests with excitation amplitudes of 5 μm, 10 μm, 15 μm and 20 μm. The second set of data are recorded using the piezoelectric force transducer mounted between the punch tool and the machine cross-head. This set of data consist of a static force measurement and a series of oscillatory force measurements with excitation amplitudes of 5 μm, 10 μm, 15 μm and 20 μm. Both data sets are measured simultaneously during static and ultrasonic metal upsetting. All the force responses are processed and analysed using SignalCalc ACE data acquisition hardware and software and Matlab R2010a software to provide stress-strain material behaviour. All the material behaviours are presented in stress-strain diagrams for the aluminium and magnesium specimens in the following section.

4.6.1 Aluminium

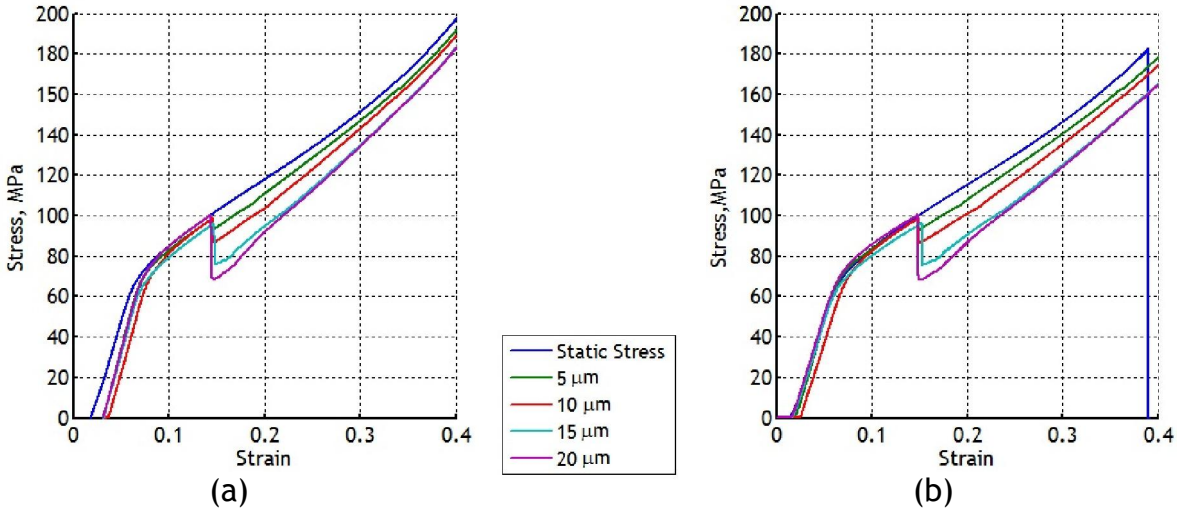

Figure 4-15 Comparison of stress-strain results measured by (a) machine load cell and (b) piezoelectric force transducer for aluminium specimens

Table 4-4 Comparison of the percentage reduction in compressive flow stress

Sensor	Reduction in mean flow stress for amplitudes of			
	5 μm	10 μm	15 μm	20 μm
Machine Load Cell	6 %	12.4 %	21 %	31.7 %
Piezoelectric Force Transducer	6 %	12.5 %	21 %	31.6 %

Fig. 4-15 shows the stress-strain results which were measured for static and static-ultrasonic compression tests on aluminium cylinder specimens. Fig. 4-15 shows two sets of data recorded by the test machine and the piezoelectric force transducer. The data was used to confirm agreement between the two sensors

for both the static and ultrasonic stress response measurements. The results in Table 4-4 show that the mean flow stress is recorded similarly by both of the force transducers, and clearly exhibits a reduction in the static flow stress in all tests under ultrasonic excitation. The percentage reduction in mean flow stress increases with ultrasonic amplitude.

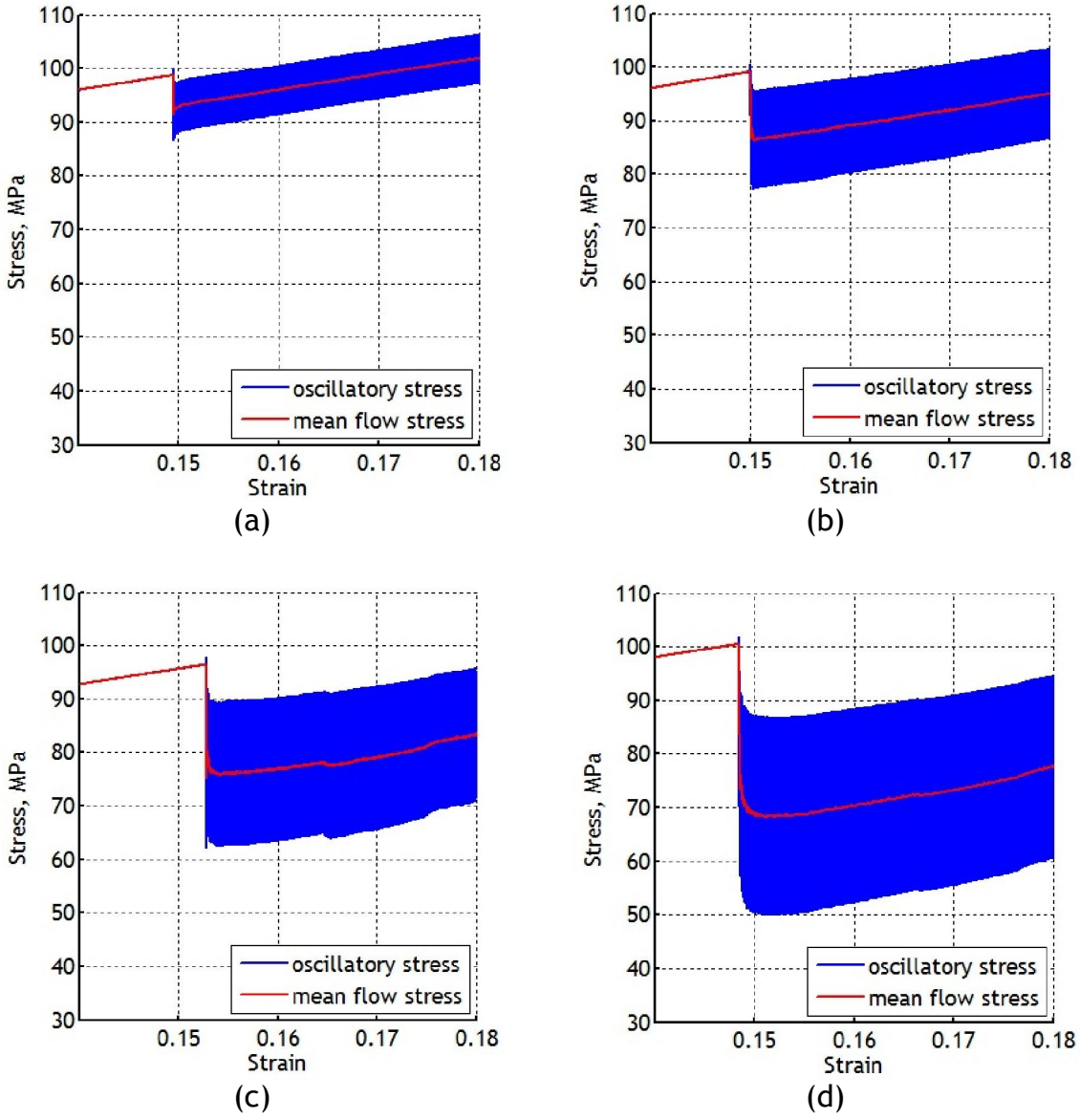

Figure 4-16 Mean flow stress and oscillatory stress measured by piezoelectric force transducer for (a) 5 μm, (b) 10 μm, (c) 15 μm and (d) 20 μm ultrasonic amplitude

Measurement of the flow stress without reference to the oscillatory stress behaviour does not provide very meaningful interpretations of the effects of ultrasonic excitation, because this relies on a reduction in the mean flow stress alone as being a direct measure of a beneficial effect. The measurements of the oscillatory stress are presented in Fig. 4-16 for a series of ultrasonic amplitudes between 5 μm and 20 μm. For each measurement, the peak to peak amplitude of the oscillatory stress during the ultrasonic excitation of the die horn is recorded and these results are summarised in Table 4-5.

Table 4-5 Stress reduction and amplitude of peak to peak oscillatory stress

Ultrasonic amplitude	Reduction in mean flow stress	Amplitude of peak to peak oscillatory stress
5 μm	6 %	7.952 MPa
10 μm	12.5 %	14.712 MPa
15 μm	21 %	19.881 MPa
20 μm	31.6 %	27.833 MPa

4.6.2 Magnesium

Similar procedures and methods are employed in the superimposition of ultrasonic excitation on compression tests for cylindrical die cast magnesium AM50. The compression tests are carried out via experimental procedures using the Zwick Roell material testing machine. The ultrasonic compression test procedure is repeated for four different ultrasonic amplitudes of vibration that are applied at the die surface. The material properties of magnesium, derived from a static compression test, are shown in Table 4-2, and the plastic flow characteristic of the material is obtained by the measurement of a true stress-strain curve as shown in Fig. 4-5. Two sets of data are measured, from the

machine load cell and the piezoelectric force transducer. Fig. 4-17 and Table 4-6 show two sets of data recorded by the load cell of the test machine and the piezoelectric force transducer. Fig. 4-17 and Table 4-6 are used to confirm agreement of the measurement of mean flow stress between the machine load cell and piezoelectric force transducer. The measurements of the oscillatory stress are presented in Fig. 4-18 for a series of ultrasonic amplitudes between 5 μm and 20 μm. For each measurement, the peak to peak amplitude of the oscillatory stress during ultrasonic excitation of the die horn is recorded and these results are summarised in Table 4-7.

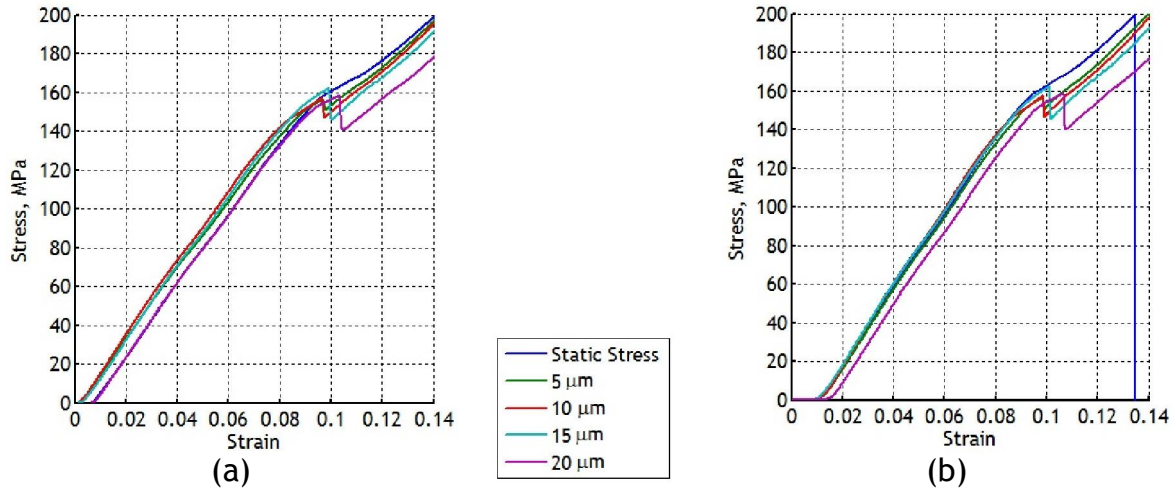

Figure 4-17 Comparison of stress-strain results measured by (a) machine load cell and (b) piezoelectric force transducer for magnesium specimen

Table 4-6 Comparison of the percentage reduction in compressive flow stress

Sensor	Reduction in mean flow stress for amplitudes of			
	5 μm	10 μm	15 μm	20 μm
Machine Load Cell	3.4 %	6.3 %	9.6 %	11.4 %
Piezoelectric Force Transducer	3.8 %	6.3 %	10 %	12.5 %

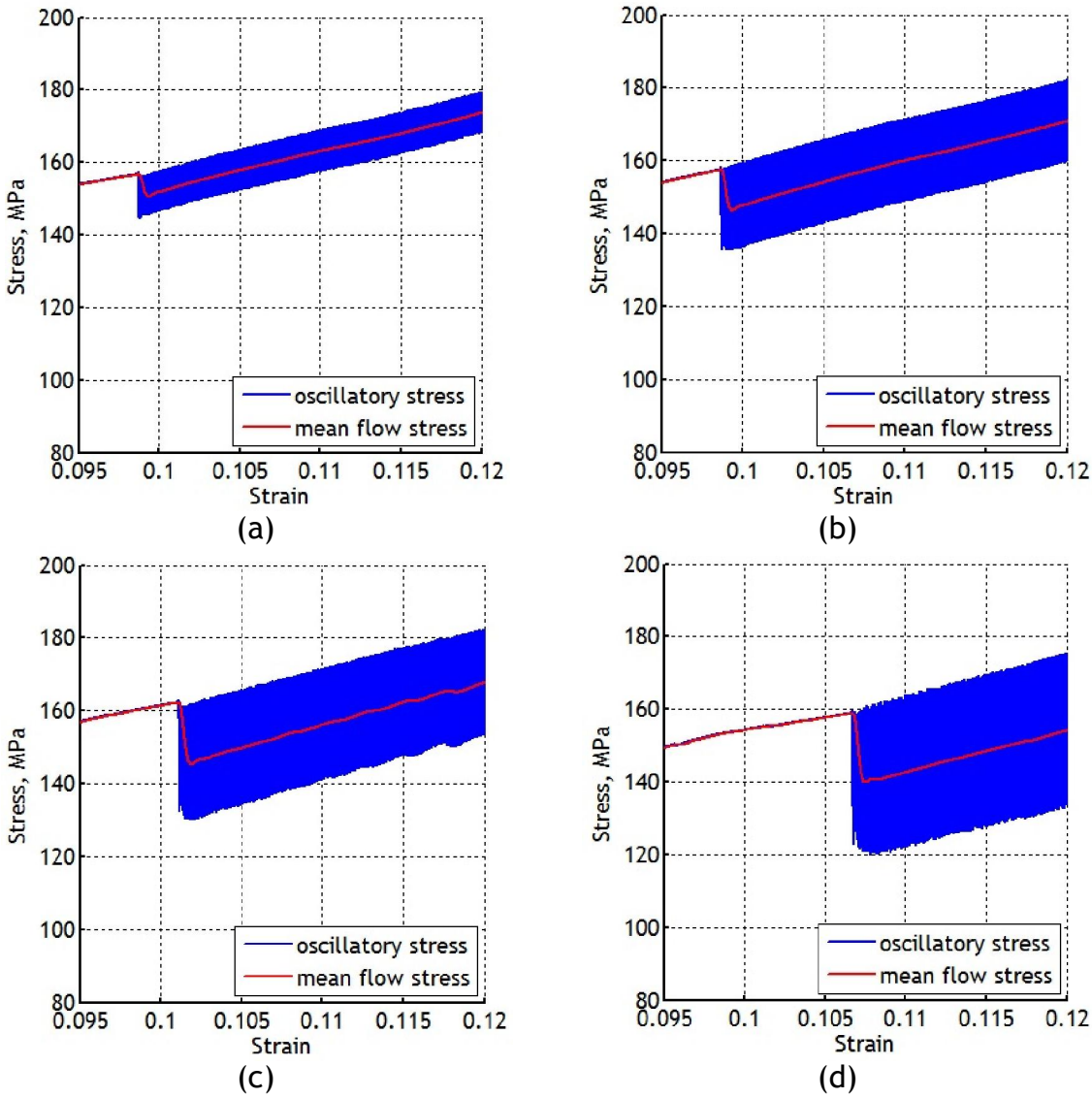

Figure 4-18 Mean flow stress and oscillatory stress measured by piezoelectric force transducer for (a) 5 μm, (b) 10 μm, (c) 15 μm and (d) 20 μm ultrasonic amplitude

Table 4-7 Force reduction and amplitude of peak-peak oscillatory stress

Ultrasonic amplitude	Reduction in mean flow stress	Amplitude of peak to peak oscillatory stress
5 μm	3.8 %	7.952 MPa
10 μm	6.3 %	15.904 MPa
15 μm	10 %	23.857 MPa
20 μm	12.5 %	27.833 MPa

4.6.3 The material softening mechanism

In all of these upsetting processes the results showed that the static flow stress of compressive deformation was considerably lowered by the ultrasonic vibration superimposed on the static load. When ultrasonic vibrations were superimposed on static compression during plastic deformation, the flow stress dropped immediately. This phenomenon has been referred as the Blaha effect and is also known as the acoustoplastic effect or volume effect. This effect during superimposed ultrasonic excitation has been described as a decrease in the flow stress during deformation at a constant strain rate or an increase in strain rate during plastic deformation under a constant stress [4, 74]. The relationship between the stress reduction, $\Delta\sigma$, and ultrasonic vibration amplitude during the compression of aluminium and magnesium is shown in Fig. 4-19. The results in Fig. 4-19 show how the percentage stress reduction for the same ultrasonic amplitude are highly dependant on the metal of the specimen, with softer metals allowing larger stress reductions to be achieved, and that stress reduction increases nearly linearly with ultrasonic amplitude in the range of this study (5 μm to 20 μm).

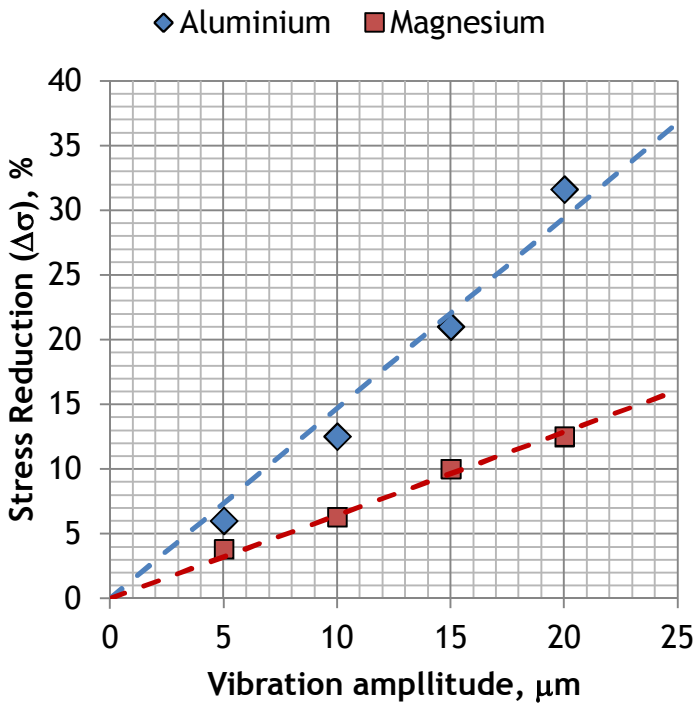

Figure 4-19 The relationship between stress reduction and vibration amplitude

The magnitude of compressive yield stress reduction by ultrasonic vibration amplitude can be measured during the superimposed ultrasonic excitation at a specific strain. These results can be seen in Fig. 4-20, in which the compressive yield stress reduction was measured at strain, ε = 10 %. It was found that within the ultrasonic amplitude range, the compressive yield stress is observed to decrease in proportion to the amplitude. This relationship can be expressed as an equation (4.8). The values of material constant, K, slope of the line in Fig. 4-20, depend on the type of metal as shown in Table 4-8 (a). The K values show good agreement, for the two metals used with those in Table 4-8 (b) from research reported by Izumi et al. [65].

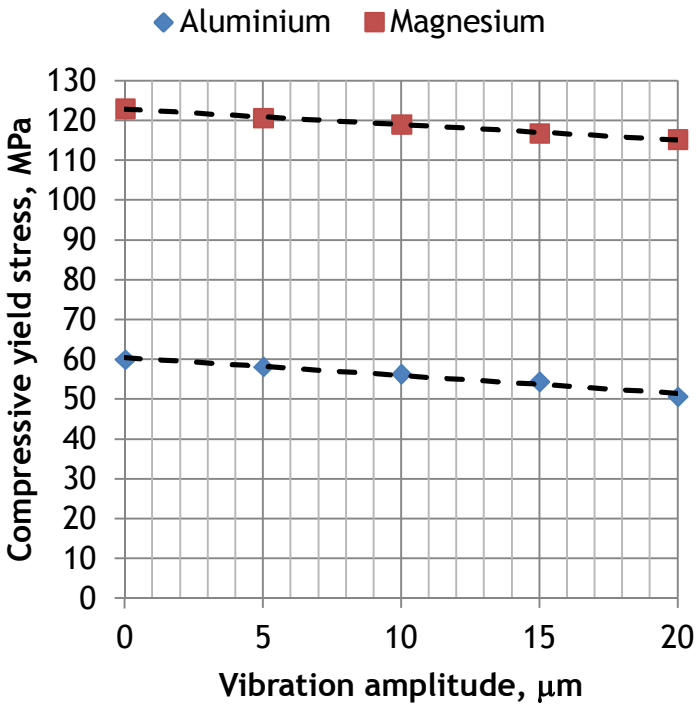

Figure 4-20 Compressive flow stress at $\varepsilon \approx 10\%$ in relation to ultrasonic vibration amplitude

Table 4-8 The value of slope K calculated by (a) current study and (b) Izumi et al.[65]

Material	Material dependent constant, K
Aluminium	0.447
Magnesium	0.38376

(a)

Material	Material dependent constant, K
Aluminium	0.40
Magnesium	0.37

(b)

Since contact conditions exist between the specimen, the ultrasonically oscillating die and the punch, the presence of friction cannot be neglected. Many previous studies [38, 40, 83] have suggested that the application of ultrasonic excitation in metal forming processes reduces the coefficient of friction at the tool or die-specimen interface. Based on indirect measurements, these reports concluded that the reduction in coefficient of friction in metal forming is related to the measured reduction in material flow stress. This claim was not fully proven because of the lack of ability to measure the coefficient of friction accurately. However, the coefficient of friction was directly estimated from the experimental data in ultrasonic drawing experiments [40, 41]. By comparing ultrasonic and conventional drawing, it was reported that the friction coefficient in ultrasonic drawing was approximately reduced by 30% to 40%.

4.7 Incorporating ultrasonic excitation in the numerical model

An FE model is developed using material model parameters which were identified from experimental data. The stress-strain data and material behaviour were obtained from the stress-strain diagram in Fig. 4-5. The material behaviour model was defined in the FE model by introduced the initial yield stresses at zero plastic strain, data points of plastic stress-strain conditions, Young's Modulus, Poisson's Ratio and material density which can be measured from Fig. 4-5. In this study, the compression tests have used a dry specimen interface as the contact condition and a coefficient of friction of 0.25 for a dry surface condition is adopted in the FE model. The specimen was deformed under static-ultrasonic loading by applying a constant velocity of 5 mm/min to the reference point of the punch rigid body. General static and implicit dynamics procedures were used in the step analysis to simulate the static-ultrasonic loading. The first step, general static, is to calculate the elastic-plastic behaviour when a static load is applied, then the procedure is continued in implicit dynamics as a second step to predict an oscillating plastic behaviour. By controlling the total time step, the specimen was compressed for 12 s in the first step in static loading and

continued in ultrasonic loading for 0.001 s in the second step analysis to allow for manageable computational time. Ultrasonic loading was superimposed at the reference point of the die rigid body at a frequency of 20 kHz and longitudinal vibration amplitude of 5 to 20 μm. This gave 20 cycles of oscillation, with each cycle containing 20 data points. It was computed so that the superimposed ultrasonic excitation was introduced at strain, $\varepsilon = 11.8\,\%$ during plastic deformation. The versatility and predictive ability of FE modelling is demonstrated and the effect of ultrasonic excitation on upsetting process is investigated and compared with the experimental results.

For the second series of FE models, changes were made to the material model and boundary conditions to simulate the effects of reduction in flow stress and interface contact conditions. The reduction in flow stress followed equation (4.8) with the values of material dependent constant, K being 0.447 and 0.38376 for aluminium and magnesium, respectively. In this series, the adjustment of material behaviour properties was carried out on the initial yield stress and data points of plastic stress-strain conditions by referred to the equation (4.8). The material flow stress reductions were calculated for a series of ultrasonic vibration amplitudes from 5 to 20 μm. The reduction in coefficient of friction is set to a value of 0.15 during superimposed ultrasonic excitation in the second step analysis procedure. A friction value of 0.15 was chosen because it is consistent with reductions reported in previous studies. This value represents the maximum reduction in the coefficient of friction of 40% which has been reported [41]. This contact condition adjustment was applied to the ultrasonic deformation for ultrasonic vibration amplitudes between 5 and 20 μm. In all of these processes, the analysis procedure was repeated as for the first series of FE models.

For the third series of FE models, the effect of a reduction in the material flow stress during superimposed ultrasonic excitation was investigated. In this case, the changes only considered a reduction of flow stress in order to investigate the influence of the volume effect alone during ultrasonic plastic deformation.

For the fourth series of FE models, the effect of a change in the numerical value of the coefficient of friction during superimposed ultrasonic excitation was

investigated. The adjustment only considered the coefficient of friction, to predict the influence of the surface effect alone during ultrasonic vibration.

For comparison, the results of the first series and second series of FE models are presented alongside the experimental results for superimposed ultrasonic excitation at ultrasonic vibration amplitudes of 5 μm to 20 μm. The results are shown in the following section according to the materials used in this study.

Previously from the experimental result, the material stiffness was measured has a lower value than the actual material stiffness for aluminium and magnesium. Consequently, the adjustments on ultrasonic amplitudes were applied in the FE models as equated to the experimental results. The relationship can be determined from an equation (2.8) which showed that the material with a bigger elastic modulus E and specimens with a bigger static stiffness k_o is more sensitive to the influence of ultrasonics. Subsequently, the equation shows the elastic modulus E is inversely proportional to ultrasonic amplitude. The adjustment of amplitudes applied was relied on the reduction in elastic modulus of material from 69GPa to 1.45GPa for aluminium A1050 and from 45GPa to 1.7GPa for magnesium AM50, the vibration amplitudes were increased fourfold in FE models. The measurement of adjusted ultrasonic amplitudes was determined from Fig. 4-7. A compression test of aluminium and magnesium with and without ultrasonic amplitudes were simulated and validated against the current experimental results to demonstrate the performance of modified amplitudes. Consequently, the FE model predictions show a good agreement with the experimental results.

4.7.1 Aluminium

The predictive measurements of the first series and second series of FE models, presented in Fig. 4-21 to Fig. 4-24, show a comparison of the mean flow stress and oscillatory stress measured from the piezoelectric force transducer and the results predicted by the numerical analysis during static and ultrasonic

deformation. The ultrasonic die horn is excited at amplitudes between 5 μm and 20 μm and the test results are shown in the figures. For each measurement, the stress reduction and the peak to peak amplitude of the oscillatory stress during ultrasonic excitation of the die horn are summarised in Table 4-9.

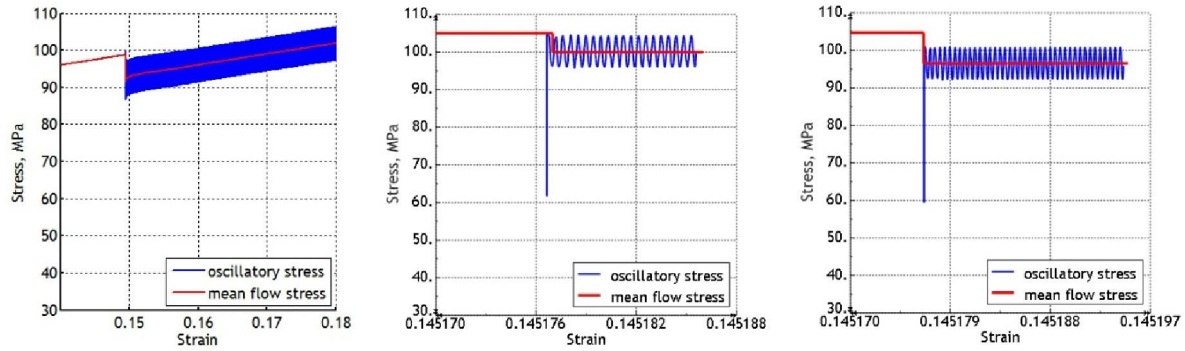

Figure 4-21 Comparison of stress-strain data (a) measured by the piezoelectric force transducer, (b) predicted in the first series of FE models and (c) predicted in the second series of FE models for 5 μm ultrasonic amplitude

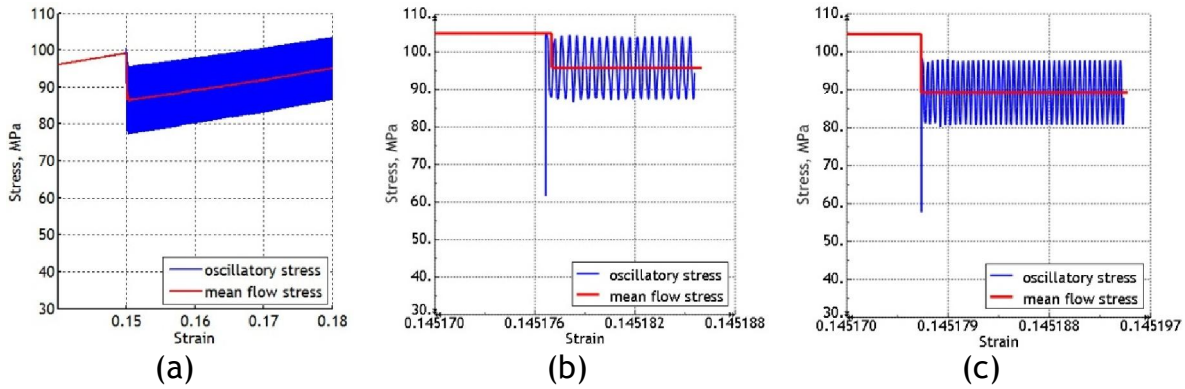

Figure 4-22 Comparison of stress-strain data (a) measured by the piezoelectric force transducer, (b) predicted in the first series of FE models and (c) predicted in the second series of FE models for 10 μm ultrasonic amplitude

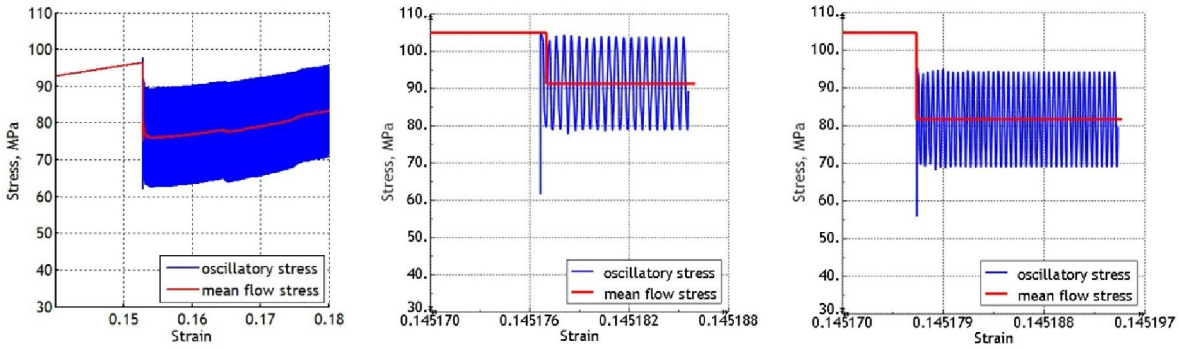

Figure 4-23 Comparison of stress-strain data (a) measured by the piezoelectric force transducer, (b) predicted in the first series of FE models and (c) predicted in the second series of FE models for 15 μm ultrasonic amplitude

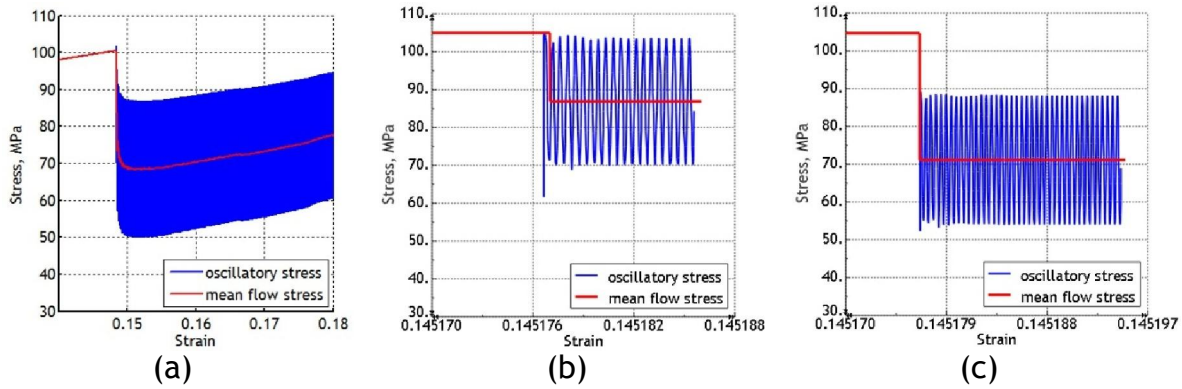

Figure 4-24 Comparison of stress-strain data (a) measured by the piezoelectric force transducer, (b) predicted in the first series of FE models and (c) predicted in the second series of FE models for 20 μm ultrasonic amplitude

Table 4-9 Stress reduction and amplitude of peak-peak oscillatory stress

Vibration amplitude	Stress reduction (%)			Peak-peak oscillatory stress		
	Piezoelectric force transducer	The first series of FE Model	The second series of FE Model	Piezoelectric force transducer	The first series of FE Model	The second series of FE Model
5 μm	6.0 %	4.0 %	7.8 %	7.952 MPa	8.350 MPa	8.349 MPa
10 μm	12.5 %	8.0 %	14.8 %	14.712 MPa	16.998 MPa	16.998 MPa
15 μm	21.0 %	12.5 %	22.0 %	19.881 MPa	25.249 MPa	25.249 MPa
20 μm	31.6 %	16.5 %	32.0 %	27.833 MPa	33.399 MPa	33.398 MPa

All of these figures show the effects of the flow stress and oscillatory stress during superimposed ultrasonic excitation for four different ultrasonic vibration amplitudes. The results from the piezoelectric force transducer show the ultrasonic excitation was introduced after 1.3 mm displacement of the cross-head, which quates to a strain, $\varepsilon = 15\%$, and then loading was continued until 50% reduction of specimen height was achieved. However, in the FE model the ultrasonic excitation was introduced after 15 s of static loading which equates to a strain of 14.5 % and loading was continued for 0.001 s to 0.002 s. During this time, the stress is observed to oscillate about a constant mean value.

For the third series of FE models, that considers adjustment of flow stress alone during plastic deformation, the results are shown in Fig. 4-25. For the fourth series of FE models, that consider adjustment on coefficient of friction alone during plastic deformation, the results are shown in Fig. 4-26. For each measurement, the stress reduction and the peak to peak amplitude of the oscillatory stress are calculated and the results of both series of FE models are summarised in Table 4-10.

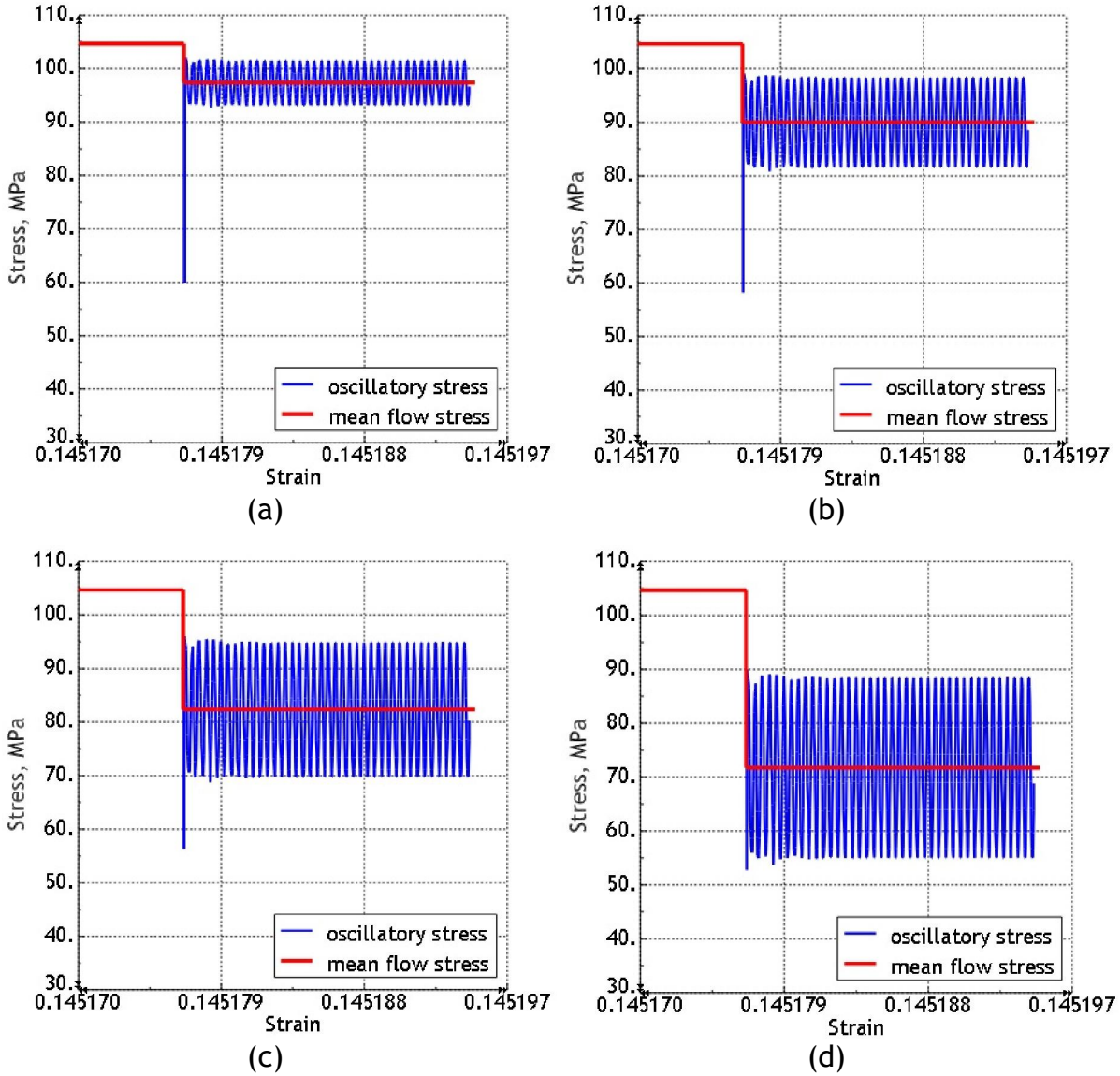

Figure 4-25 Stress reduction and oscillatory stress in aluminium, for FE model incorporating flow stress adjustment for (a) 5 µm (b) 10 µm (c) 15 µm and (d) 20 µm ultrasonic amplitudes

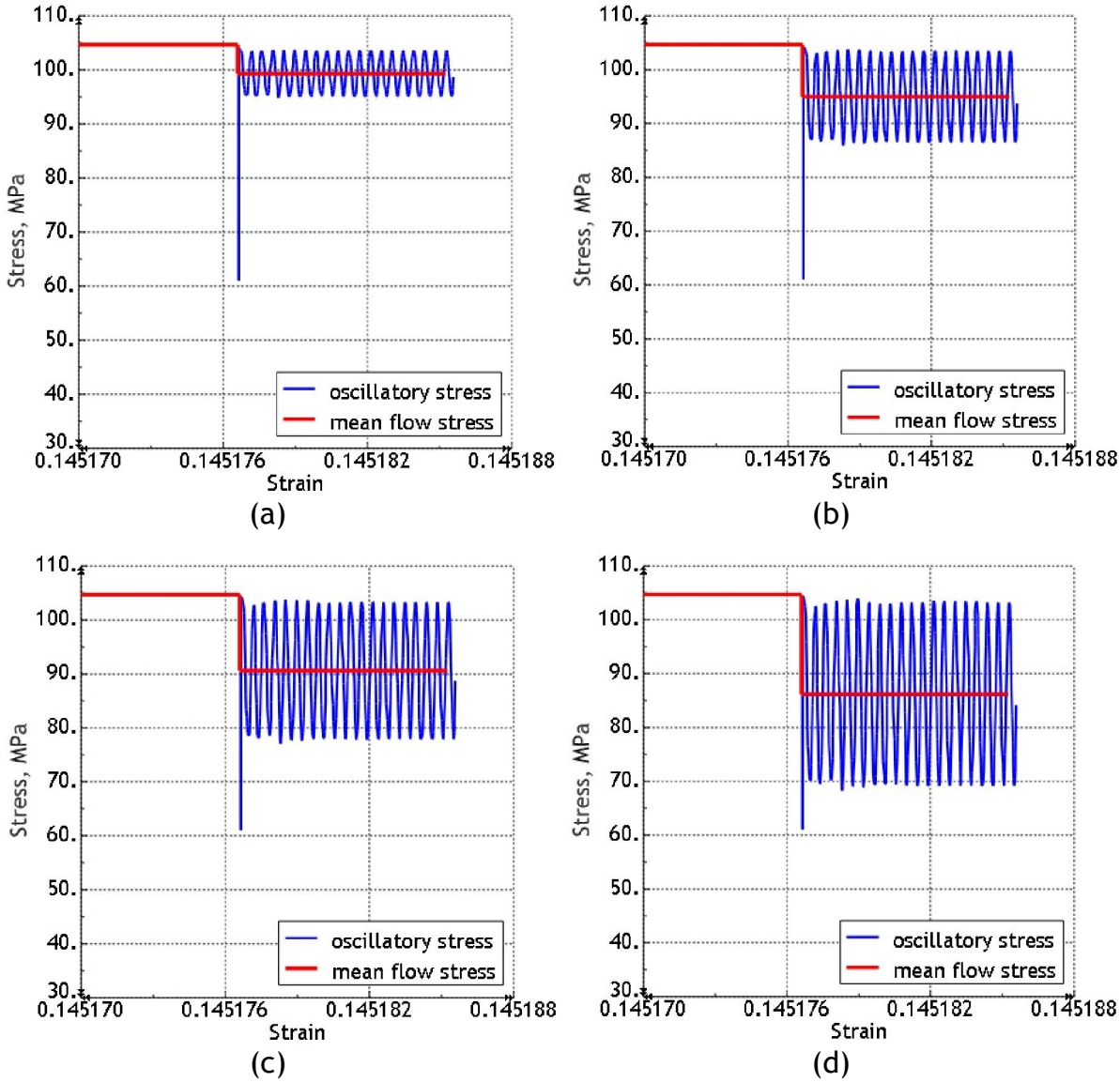

Figure 4-26 Stress reduction and oscillatory stress in aluminium, for FE model incorporating coefficient of friction adjustment for (a) 5 μm (b) 10 μm (c) 15 μm and (d) 20 μm ultrasonic amplitudes

Table 4-10 Stress reduction and amplitude of peak-peak oscillatory stress

Vibration amplitude	Stress Reduction		Peak-peak oscillatory stress	
	The third series of FE Model	The fourth series of FE Model	The third series of FE Model	The fourth series of FE Model
5 μm	7.0 %	5.2 %	8.349 MPa	8.449 MPa
10 μm	14.0 %	9.3 %	16.699 MPa	16.899 MPa
15 μm	21.4 %	13.5 %	25.049 MPa	25.308 MPa
20 μm	31.5 %	17.6 %	33.399 MPa	34.314 MPa

4.7.2 Magnesium

The same series of simulations was then performed for magnesium compression models, as described in the previous section. The predictive measurements of the first series and second series of FE models, presented in Fig. 4-27 to Fig. 4-30, show a comparison of the mean flow stress and oscillatory stress measured from the piezoelectric force transducer and the results predicted by the numerical analysis during the static and ultrasonic deformation. Then, for each measurement, the stress reduction and the peak to peak amplitude of the oscillatory stress during ultrasonic excitation of the die horn are summarised in Table 4-11.

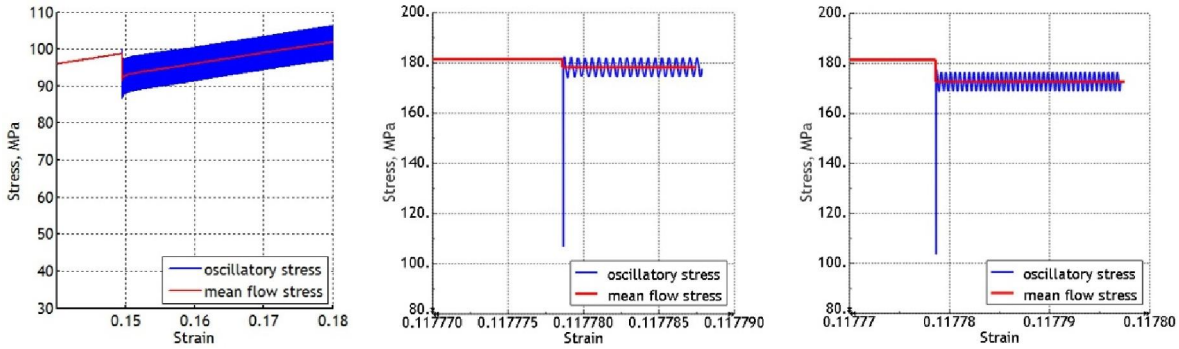

Figure 4-27 Comparison of stress-strain data (a) measured by the piezoelectric force transducer, (b) predicted in the first series of FE models and (c) predicted in the second series of FE models for 5 μm ultrasonic amplitude

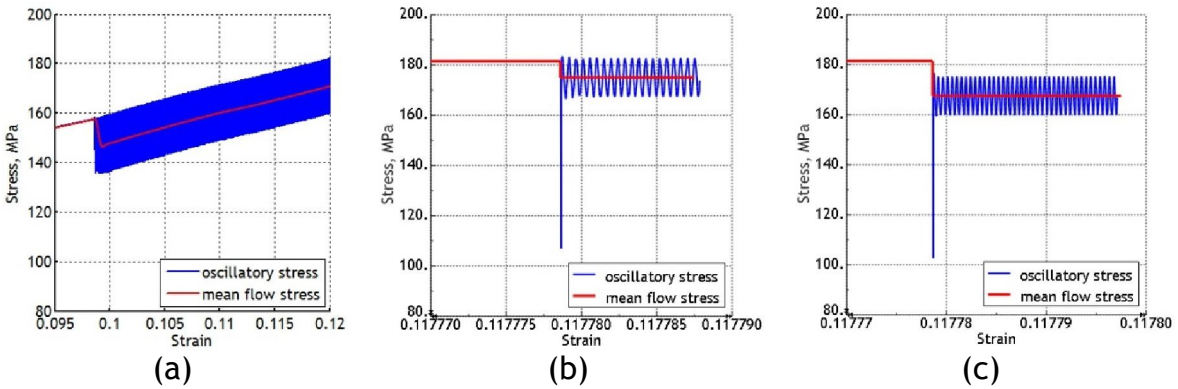

Figure 4-28 Comparison of stress-strain data (a) measured by the piezoelectric force transducer, (b) predicted in the first series of FE models and (c) predicted in the second series of FE models for 10 μm ultrasonic amplitude

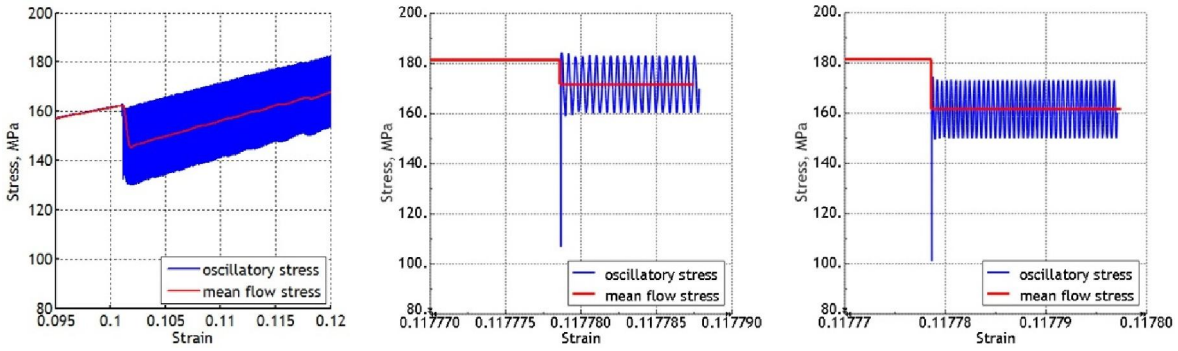

Figure 4-29 Comparison of stress-strain data (a) measured by the piezoelectric force transducer, (b) predicted in the first series of FE models and (c) predicted in the second series of FE models for 15 μm ultrasonic amplitude

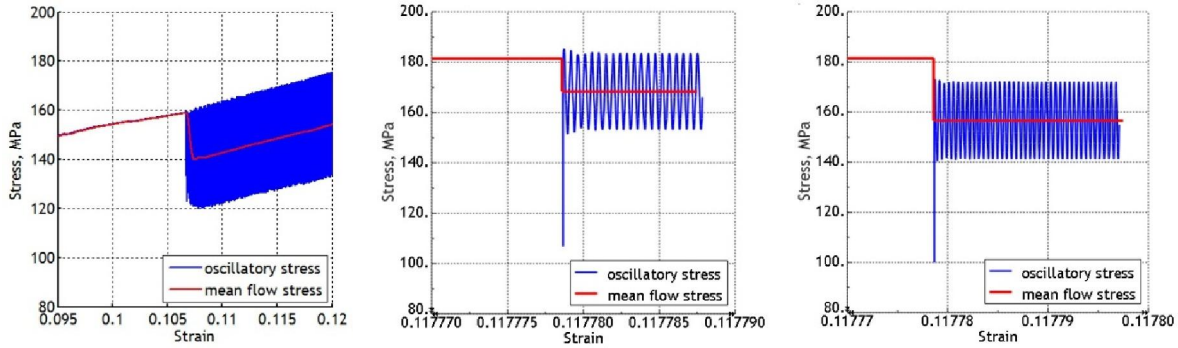

Figure 4-30 Comparison of stress-strain data (a) measured by the piezoelectric force transducer, (b) predicted in the first series of FE models and (c) predicted in the second series of FE models for 20 μm ultrasonic amplitude

Table 4-11 Stress reduction and amplitude of peak-peak oscillatory stress

Vibration amplitude	Stress reduction			Peak-peak oscillatory stress		
	Piezoelectric force transducer	The first series of FE Model	The second series of FE Model	Piezoelectric force transducer	The first series of FE Model	The second series of FE Model
5 μm	3.8 %	2.0 %	4.8 %	7.952 MPa	7.555 MPa	7.674 MPa
10 μm	6.3 %	3.6 %	8.8 %	15.904 MPa	15.109 MPa	15.427 MPa
15 μm	10.0 %	5.4 %	11.0 %	23.857 MPa	22.684 MPa	23.101 MPa
20 μm	12.5 %	7.2 %	13.7 %	27.833 MPa	30.239 MPa	30.855 MPa

For the third series of FE models, that considers adjustment of flow stress alone during plastic deformation, the results are shown in Fig. 4-31. For the fourth series of FE models, that considers adjustment on coefficient of friction alone during plastic deformation, the results are shown in Fig. 4-32. For each measurement, the stress reduction and the peak to peak amplitude of the oscillatory stress are calculated both series of FE models are summarised in Table 4-12.

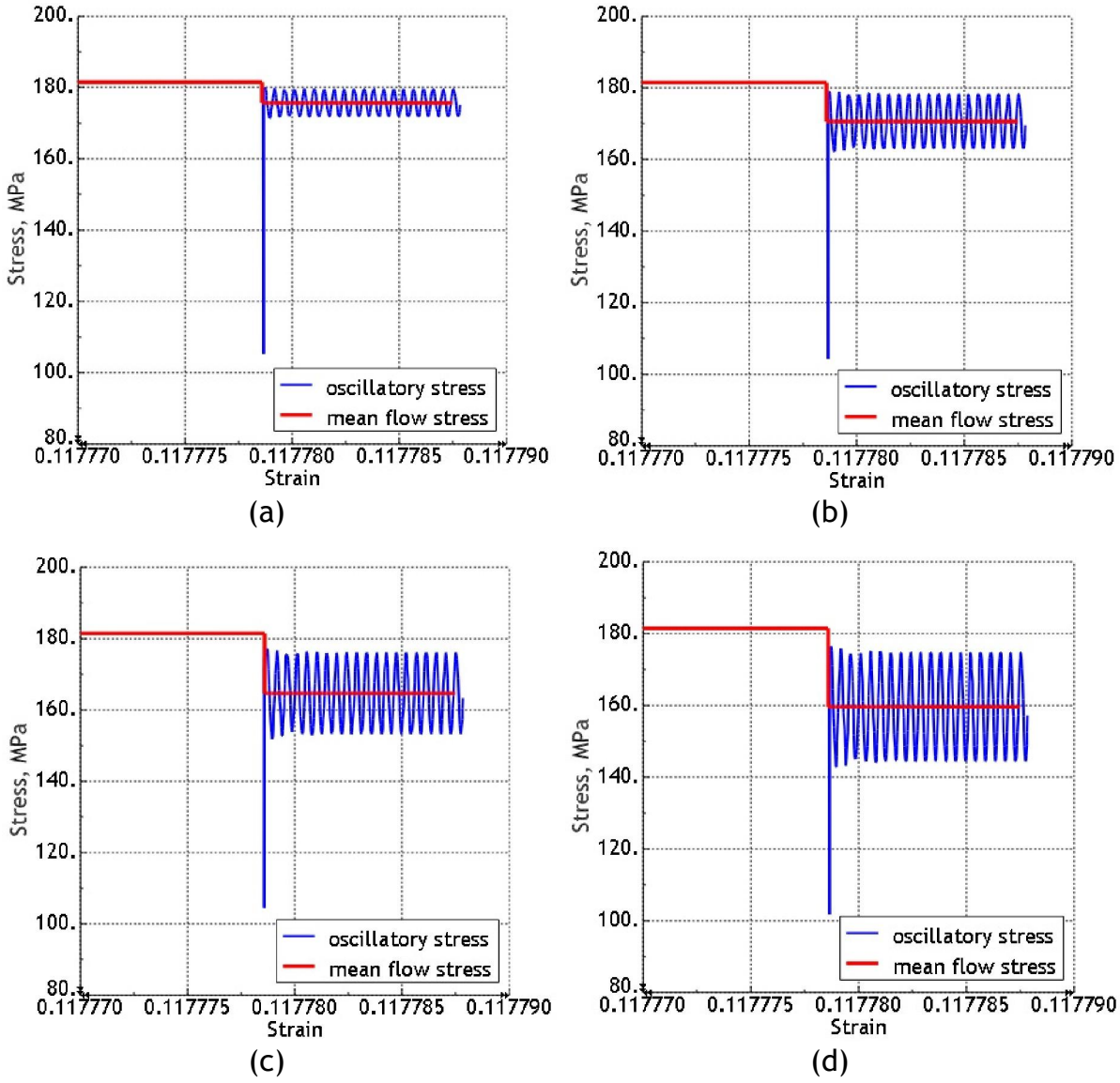

Figure 4-31 Stress reduction and oscillatory stress in magnesium, for FE model incorporating flow stress adjustment for (a) 5 μm (b) 10 μm (c) 15 μm and (d) 20 μm ultrasonic amplitudes

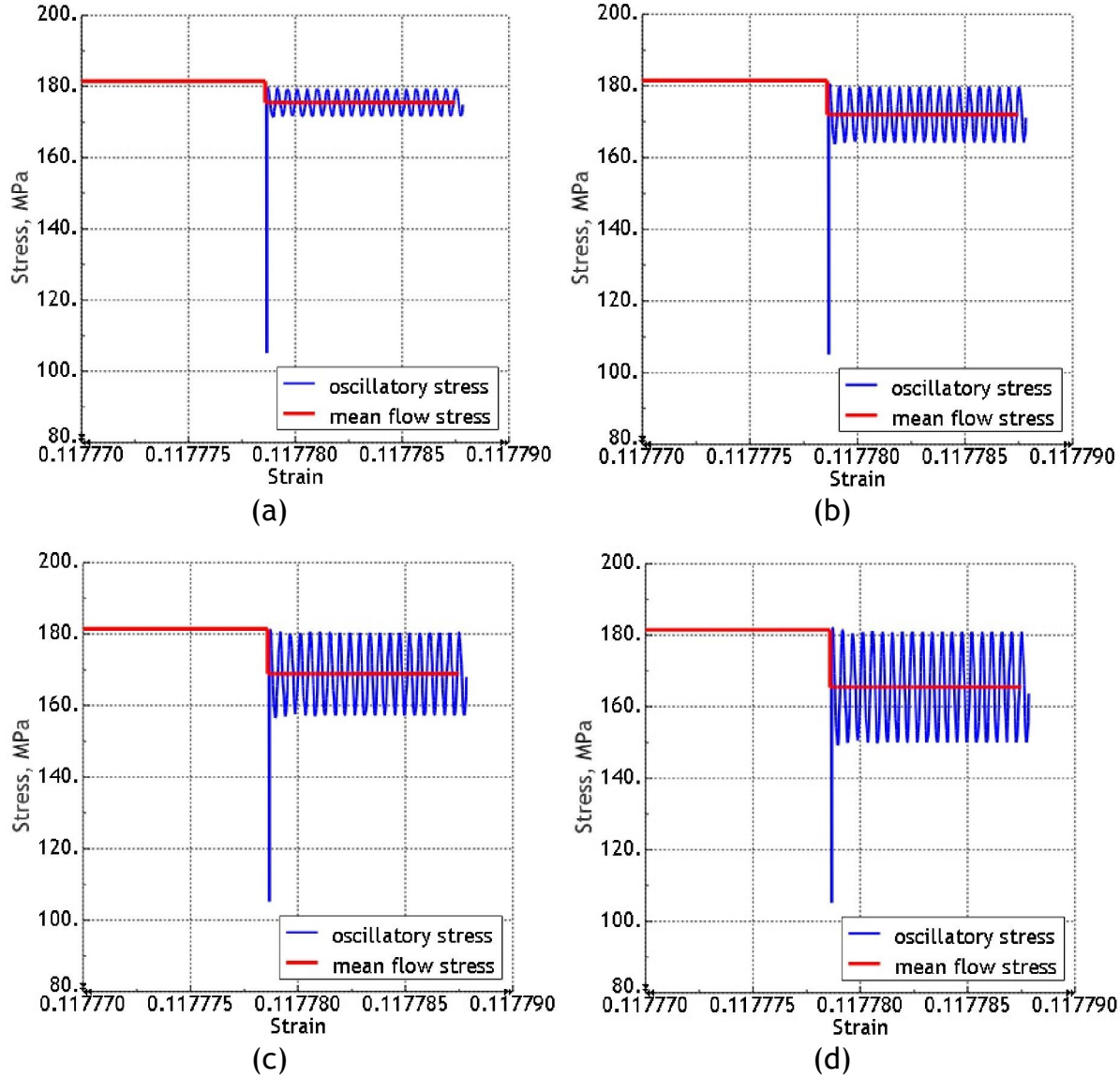

Figure 4-32 Stress reduction and oscillatory stress in magnesium, for FE model incorporating coefficient of friction adjustment for (a) 5 μm (b) 10 μm (c) 15 μm and (d) 20 μm ultrasonic amplitudes

Table 4-12 Stress reduction and amplitude of peak-peak oscillatory stress

Vibration amplitude	Stress Reduction		Peak-peak oscillatory stress	
	The third series of FE Model	The fourth series of FE Model	The third series of FE Model	The fourth series of FE Model
5 μm	3.2 %	3.3 %	7.575 MPa	7.674 MPa
10 μm	6.0 %	5.2 %	15.129 MPa	15.427 MPa
15 μm	9.3 %	7.0 %	22.903 MPa	23.101 MPa
20 μm	12.0 %	9.0 %	30.239 MPa	30.855 MPa

4.8 Experimental and numerical results discussion

In this study, the effects of ultrasonic excitation on the stress-strain behaviour for dry contact conditions were investigated. The stress-strain relationships were derived from the measured load-displacement data using a piezoelectric force transducer and predicted data using finite element modelling. During superimposed ultrasonic excitation, the oscillatory stress, static flow stress, mean flow stress and stress reduction can be extracted from the stress-strain diagram.

Measured and predicted data from the experimental and numerical analysis for aluminium and magnesium are shown in figures in previous section. For discussion purposes, the results from the experimental and numerical tests on aluminium during superimposed ultrasonic excitation for an ultrasonic vibration amplitude of 20 μm are presented in Fig. 4-33.

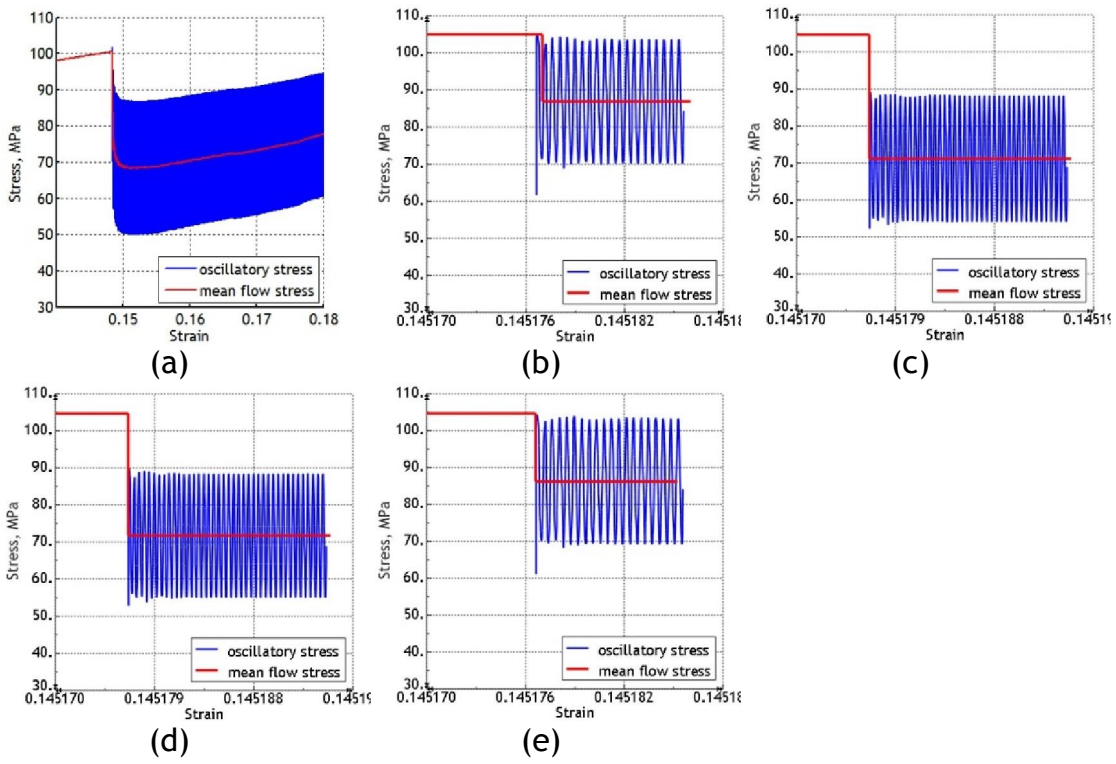

Figure 4-33 Oscillatory stress for aluminium specimen and 20 μm ultrasonic amplitude, (a) measured by piezoelectric force transducer, (b) from FE analysis, (c) from FE analysis with adjustments to material flow stress and coefficient of friction, (d) from FE analysis with adjustments to material flow stress only and (e) from FE analysis with adjustments to coefficient of friction only.

Comparison of Fig. 4-33(a) and (b) shows that measurement of the flow stress without reference to the oscillatory stress behaviour does not provide a very meaningful measure of the effects of ultrasonic excitation, especially since the deviation between the results of the FE model and measurements is best illustrated by the change in the path of the maximum oscillatory stress. It can be observed for both the experimental and FE data that the path of the mean oscillatory stress is significantly reduced from the path of the static flow stress when ultrasonic excitation is introduced, but the path of the maximum oscillatory stress is also significantly reduced in the measurements but not in the FE results. This change in behaviour, characteristic of an effective material softening, is a result of the acoustoplastic effect [4, 74]. This volume effect is then incorporated into the FE model by applying an adjustment to the material flow stress properties at the onset of ultrasonic excitation in Fig. 4-33(c) and (d). This involves calculation of a material dependent constant, K which can be estimated from the measured oscillatory stress as the decrease of flow stress per unit amplitude as described by Izumi [65]. In this study, the material dependent constant, K was measured as 0.447 and 0.38376 for aluminium and magnesium, respectively.

However, it has also been shown previously that ultrasonic excitation additionally alters the friction contact condition between the specimen and upper and lower test machine platens [5, 66, 90]. This surface effect is included in the FE model as a 40% reduction in the coefficient of friction, consistent with the maximum achievable friction reduction generally agreed in the literature [40, 41]. The resulting stress-strain relationship is shown in Fig. 4-33(c) and (e). The results clearly show that a close match between the experiment and the FE model data is achievable by modelling the effects of superimposed ultrasonic excitation as a combination of an adjustment of material flow stress properties and interfacial friction in Fig. 4-33(c). Fig. 4-33(d) and (e) show the effects of superimposed ultrasonic excitation predicted by the FE model by adjustment of (d) material flow stress properties only and (e) interfacial friction only.

Similar measurement and FE modelling procedures were employed for studying the effects of ultrasonic excitation on compression tests for magnesium metal specimens for the range of ultrasonic amplitudes. Fig. 4-34 show the results for

an ultrasonic amplitude of 20 μm. Similar measurement results to those for aluminium, illustrating both a reduction in the mean flow stress and a reduction in the path of the maximum oscillatory stress from the path of the static flow stress, were obtained in all tests. Therefore, the FE models were developed to match the experimental results by combining an adjustment in the material properties with an adjustment in the friction contact condition during ultrasonic excitation.

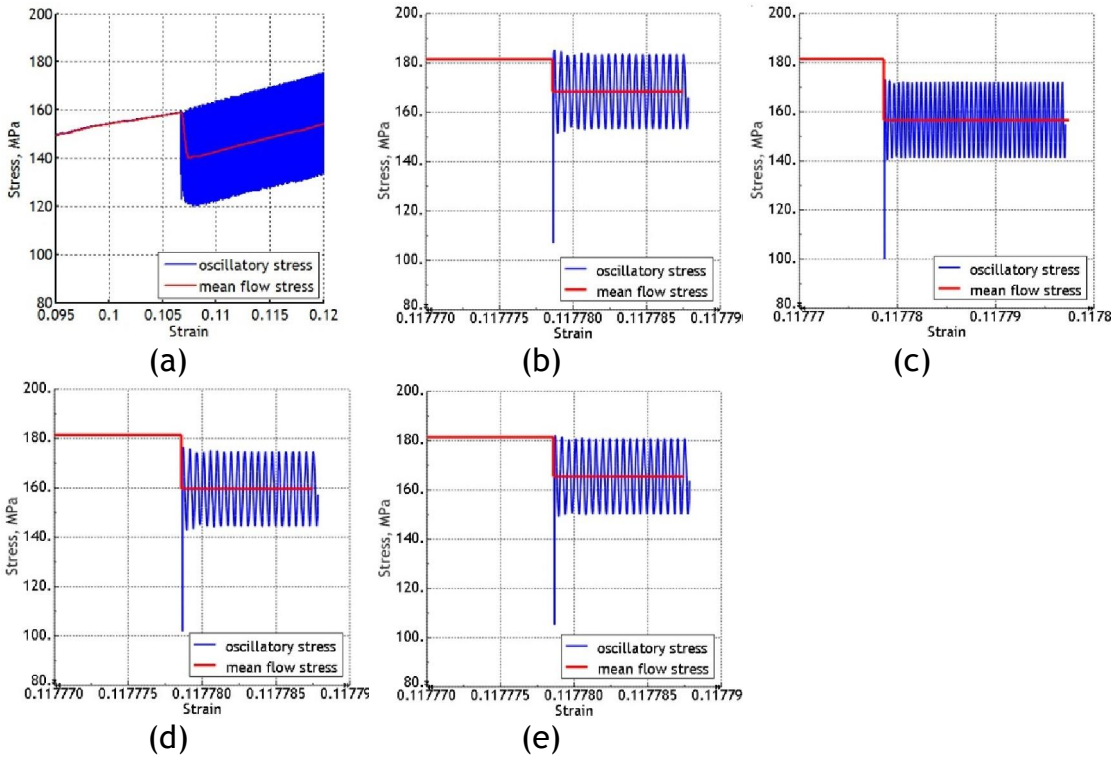

Figure 4-34 Oscillatory stress for magnesium specimen and 20 μm ultrasonic amplitude, (a) measured by piezoelectric force transducer, (b) from FE analysis, (c) from FE analysis with adjustments to material flow stress and coefficient of friction, (d) from FE analysis with adjustments to material flow stress only and (e) from FE analysis with adjustments to coefficient of friction only.

The results have also shown that the percentage reduction in the mean flow stress from the static flow stress increases linearly with ultrasonic amplitude. These results are summarised in Fig. 4-35. The results in Fig. 4-35 show how the percentage stress reductions for the same ultrasonic amplitude are highly dependant on the metal of the specimen, with the softer metal allowing larger stress reductions to be achieved, and that stress reduction increases linearly

with ultrasonic amplitude in the range of this study (5 μm to 20 μm). Fig. 4-35(b) shows that the predicted percentage reduction in static flow stress is a close match with the experimental results. The influence of surface effects and volume effects were predicted by plotting the percentage in static flow stress reduction against vibration amplitude from FE analysis with adjustment to material properties only and from FE analysis with adjustment to contact conditions only. This relationship is shown in Fig. 4-36. Therefore, the slope of the graph can be measured and is called the $\Delta\sigma - USA$ value. In this case, the $\Delta\sigma - USA$ value is defined as a ratio of the percentage of stress reduction to ultrasonic vibration amplitude. The ratio of stress reduction to ultrasonic amplitude ($\Delta\sigma$-USA) is adopted as a measure of the separate and combined contribution of volume effects, in terms of adjustment in material properties, and surface effects, in terms of adjustment to the friction contact condition. The measurement of the $\Delta\sigma - USA$ value is summarised in Table 4-13. The results are presented as a bar chart in Fig. 4-37. The bar chart shows that for plastic deformation, the volume effect of effective material softening dominates the stress-strain behaviour during superimposed ultrasonic excitation.

A similar result was achieved by Yoa et al [107] who reported that the dominate mechanism contributing to stress reduction in the plastic condition was the volume effect. It is known that the mechanism of stress reduction by superimposed ultrasonic excitation can be accounted for by a combination of three effects; stress superposition, surface effect and volume effect. However, through FE simulation in the report's result suggested that a reduction in friction only resulted in a minor decrease in stress, when compared to the influence of the volume effect.

Sources behind the material softening effect induced by high-frequency vibration have been investigated by various researchers [5, 66, 107] and it has been reported that the effect is temporary and that only limited permanent effect was detected from the stress-strain recovery behaviour. The factors which cause this softening effect have been attributed to various factors; including thermal effects due to heat generation [65], energy absorption from the sound wave through thermoelastic energy conversion [133], energy transformation by inelastic scattering [133], and motion of dislocation [88, 133].

Siu et al. [88] investigated the microstructure of samples that had undergone indentation with and without the application of ultrasonic excitation, finding that samples exposed to ultrasonic contained subgrain formations while those indented without ultrasonic did not. The subgrain formation is evidence of dislocation which from previously studies [24, 133, 151-153] have reported that dislocations are able to freely cross-guide due to the contraction of the extended dislocations. This provides evidence, contrary to Nevill et al. [25] and Pohlman et al. [92] that the material softening effect stems from dislocation behaviour and not from the superimposition of alternating stress on the stress produced externally.

Siu et al. [88] also observed the surface temperature increased due to heating effect in the sample from the ultrasonic energy. Therefore, to be able to compare samples indented with and without ultrasonic vibration, and understand the relationship between ultrasonic vibration and surface temperature, samples which were indented without ultrasonic vibration were heated during and after the indentation process. After the process, both samples were analysed, finding that the heated sample showed a similar degree of subgrain formation as the sample intended with ultrasonic vibration. This result shows a relationship between material softening and thermal softening, however, experimental results [24, 133, 151] reported that the ultrasonic energy required to produce the same amount of softening was extremely lower than the required thermal energy. This is due to the fact that ultrasonic energy was absorbed in the regions of dislocations while thermal energy absorbed uniformly in the sample [5]. Therefore the processes which involve ultrasonic energy supplied to the sample can be simulated using constitutive models that incorporate acoustic softening effects or volume effects. Furthermore, if relative motion of surface exists, softening due to friction should also be incorporated as surface effects and therefore in order better simulate ultrasonic processes, both volume and surface effects must be incorporated in the material model [90].

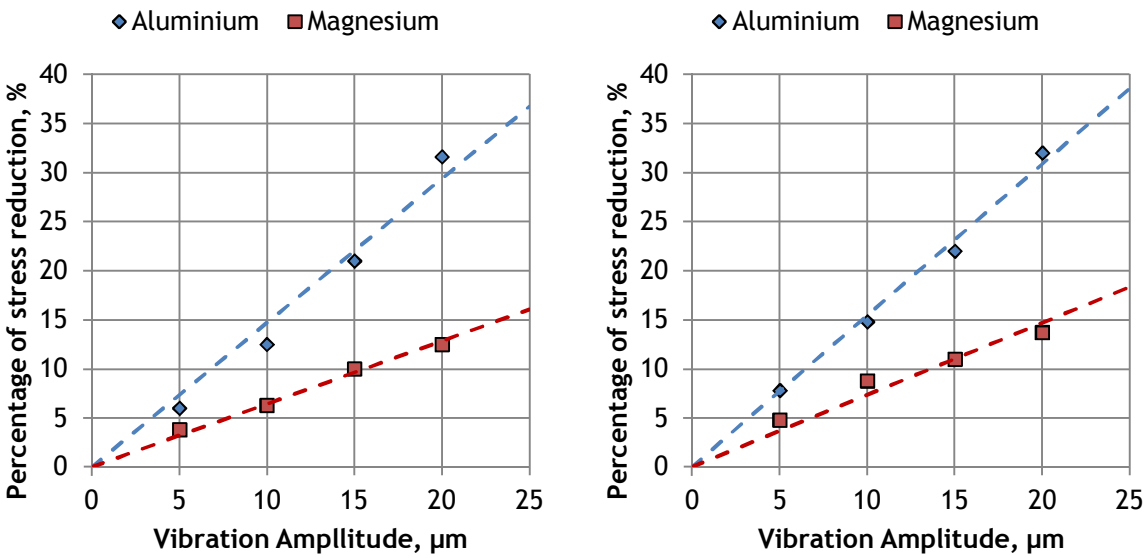

(a) (b)

Figure 4-35 Reductions in static flow stress to mean flow stress during ultrasonic excitation from (a) experiment and (b) FE analysis

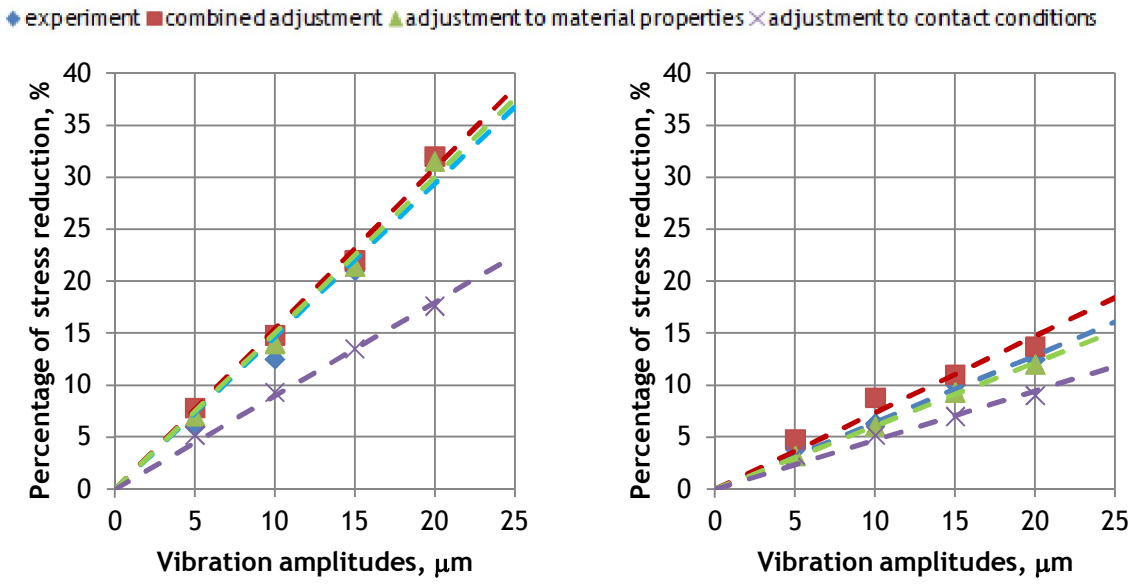

(a) (b)

Figure 4-36 The percentage of stress reduction in adjustments of material flow stress and contact conditions for (a) aluminium and (b) magnesium

Table 4-13 The predicted of $\Delta\sigma - USA$ value

Material	$\Delta\sigma - USA$ value, mm^{-1}			
	experiment	combined adjustment	adjustment to material properties	adjustment to contact conditions
Aluminium	14.7	15.4	15.0	9.0
Magnesium	6.4	7.3	6.1	4.7

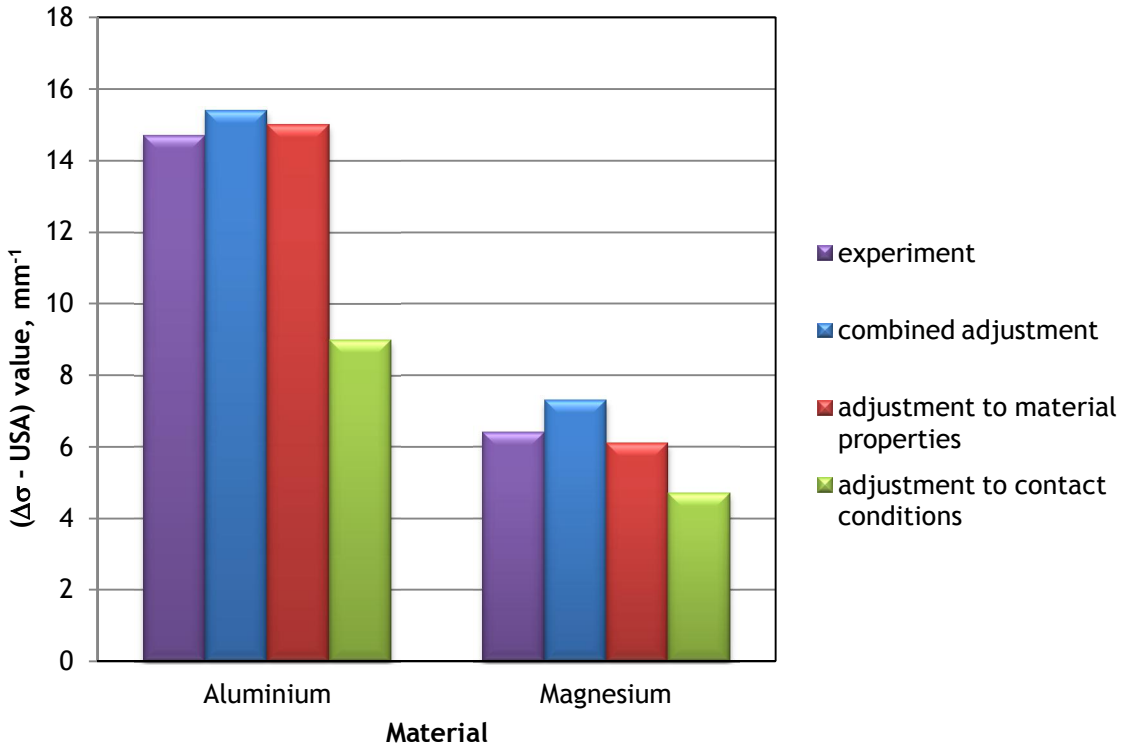

Figure 4-37 The contribution to stress reduction of volume and surface adjustments in the FE model

The influence of oscillatory stress amplitude was investigated in the stress-strain diagram during superimposed ultrasonic excitation on plastic deformation of aluminium and magnesium. The stress-strain diagram was plotted and the ultrasonic oscillatory stress was represented by the oscillating stress amplitude from which the maximum, mean and minimum peak of the stress amplitude were measured. This can be seen in the experimental and numerical test results

in the previous section. The results show that the mean value of the oscillatory stress is significantly reduced at the onset of ultrasonic excitation and follows a path parallel to the static stress path. The paths of maximum and minimum oscillatory stress also follow a path parallel to the static stress. The measurement of peak to peak oscillatory stress to ultrasonic vibration amplitude is shown in Fig. 4-38. The results show that the magnitude of peak to peak oscillatory stress linearly increases with the amplitude of ultrasonic vibration and the value is very similar for aluminium and magnesium. A similar result was obtained in numerical results, the peak to peak oscillatory stress amplitude was not changed by the adjustment to material properties and contact conditions in the FE analysis.

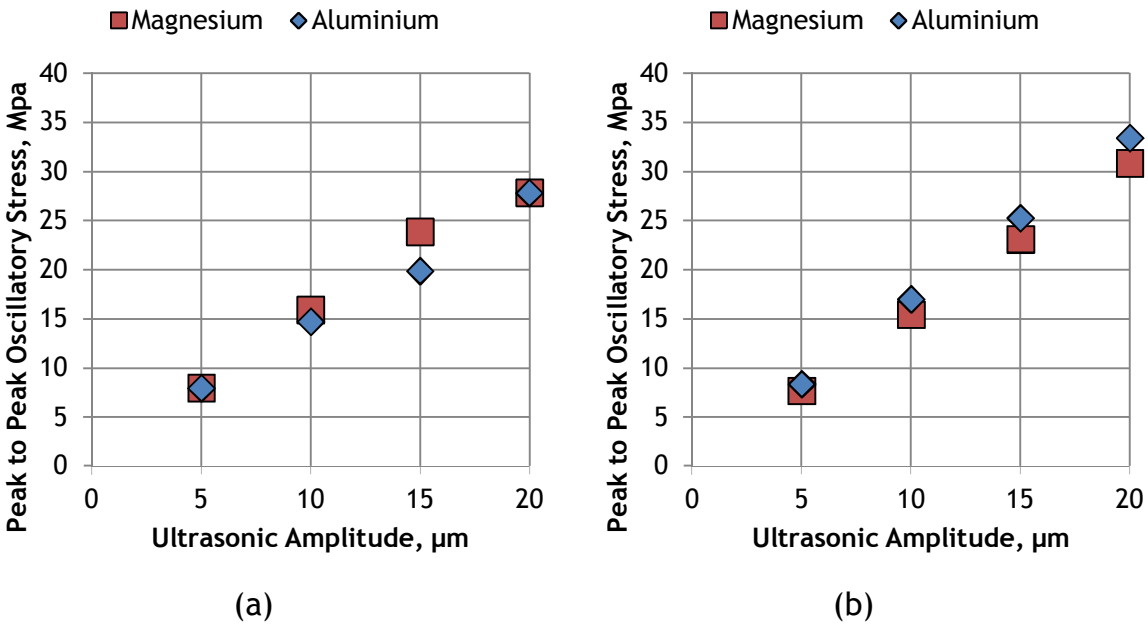

Figure 4-38 Peak-peak oscillatory stress amplitude from (a) experiment and (b) FE analysis

4.9 Conclusion

A study of the effects of superimposed ultrasonic excitation on compression of aluminium and magnesium cylindrical specimens has been carried out. During plastic deformation, longitudinal mode ultrasonic oscillations were superimposed on the flat die, where dry surface conditions were applied. Finite element models were developed using material model parameters which were identified from an experimental analysis. The finite element models were used to investigate numerically the material parameter effects and friction effects of ultrasonically assisted compression. The numerical model was adjusted at the onset of and during ultrasonic excitation by a combination of adjustment to the material properties and the contact friction. This allowed close agreement to be obtained between experimental and FE data illustrating the effects of reduction in the mean flow stress and, additionally, a reduction in the path of the maximum oscillatory stress from the path of the static flow stress due to ultrasonic excitation of the die. The influence of volume and surface effects were investigated separately in the FE model and it was shown that the reduction in mean flow stress is dominated by the effective material softening during ultrasonic excitation.

CHAPTER 5

STATIC-ULTRASONIC UPSETTING OF METALS SPECIMENS UNDER ELASTIC DEFORMATION CONDITIONS

5.1 Introduction

Previously in the literature [36, 64, 66, 109], the effects of ultrasonic excitation were studied by applying the oscillatory energy to a metal undergoing plastic deformation. A study of superimposed ultrasonic excitation on a static load during elastic deformation in metal working was not investigated. Therefore, a study of characterisation of mean flow stress and oscillatory stress behaviour could explain further insight s into the effects on metal forming process during elastic condition.

In Chapter 4, the effect of material softening mechanism in plastic deformation during superimposed ultrasonic excitation was characterised. In this chapter, the aim is to investigate the oscillatory stress behaviour in the ultrasonic compression test of cylinder metal specimens during elastic deformation, by examining the paths of the maximum and minimum oscillatory stress. The mean flow stress and stress reduction can be measured in the stress-strain diagram. Finite element (FE) models were developed to predict the effects of superimposed ultrasonic excitation during elastic deformation, allowing the contact condition and material flow stress behaviour data to be investigated.

In earlier investigations [24, 25, 64, 65, 73], the study of the effect of oscillatory stress on the mechanical properties and behaviour of metals has focused on the application of ultrasonic excitation on plastic deformation. Blaha and Langenecker [24], who discovered that there was a reduction in material flow stress while tensile testing single crystals of zinc, reported that when an oscillatory stress is superimposed on a constant level of applied stress, a stress

reduction in elastic deformation region was shown in the stress-strain diagram, whilst a continuous application of oscillatory energy from the initial strain deformation. Another study, by Izumi et al. [81], monitored the reduction of the static compressive stress due to the superimposed ultrasonic excitation on static compression and is depicted in Fig. 5-1.

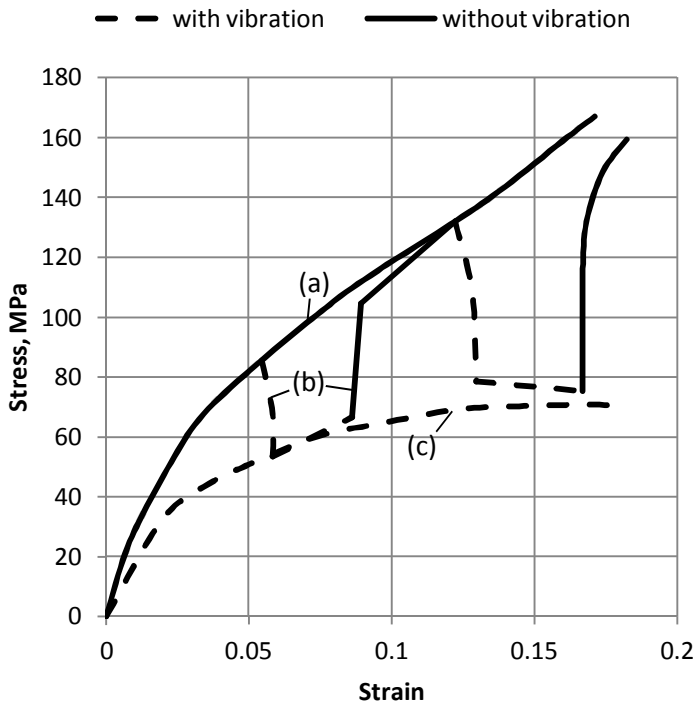

Figure 5-1 Reduction in compressive stress due to superimposed ultrasonic excitation. (a) without ultrasonic excitation, (b) interval of two ultrasonic excitation, (c) with continuous ultrasonic excitation [81]

Fig. 5-1(c) illustrates that ultrasonic excitation was applied prior to reaching the yield limit, and as a result, the stress immediately dropped after the superimposing. The stress reduction increased up to the yield stress limit and continued with increasing deformation after the yield limit. It was believed that the effect was influenced by the reduction in the material flow stress and coefficient of friction. Therefore, a series of FE models was developed to investigated the influences of the volume effect, such as the reduction in material flow stress, as well as surface effect, such as the reduction in the interface contact conditions.

Theoretically, in elastic deformation the material deformation does not exceed the limit of the initial linear part of the dynamic characteristic $\left(0 < h \leq P_{yo}/k_o\right)$ and the load P does not exceed an elastic limit P_{yo} which can be in Fig. 2-2. In this elastic deformation, it was concluded that the strain is recoverable. By referring to equation (2.10) and similar assumptions were used in Chapter 2 , this investigation resulted in a relation between a constant force P, and vibration amplitude a over a period of cycle is:

$$P = k_o(h - a) \tag{5.1}$$

where k_o is a material static stiffness, h is the material deformation and because of the material deformation does not exceed the yield limit and strain recoverable, the influence of $k_o a$ value is small where in term of the stress superposition was not achieved. Since the constant force P is lower than the elastic limit P_{yo}, the material will not yield, the mechanism of stress superposition will not attain and the force reduction will not occur.

The influence of surface friction is a mechanism of reduced the forming force during ultrasonic metal working processes since the motion of interface between the tool and specimen are existed. Theoretically, the influence of ultrasonic excitation on interface friction was previously discussed in Chapter 2. This chapter explained that the frictional force is developed at the interface between motion of the tool and specimen and the work done by this friction can be translated into force reduction. The force P needed to overcome the friction force can be described as:

$$P = \frac{2}{3} Q \frac{v}{a\omega} ln \left[\frac{2\left(1+\sqrt{\left(\frac{v}{a\omega}\right)^2+1}\right)^2}{\frac{v}{a\omega}\left(1+\sqrt{\left(\frac{2v}{a\omega}\right)^2+1}\right)} \right] \tag{5.2}$$

From the explanation above showed that the force P in equation (5.1) was not effectively contributed to the reduction in forming force, but in contrast to the force P in the equation (5.2), it was determined that the force P needed to overcome frictional force is more effective to generate the significant effect of ultrasonic excitation in the elastic deformation conditions.

5.2 Experimental procedure

A 20 kHz axially resonant ultrasonic system, consisting of a piezoelectric transducer and half-wavelength ultrasonic horn, was positioned to form the lower platen on a Zwick Roell test machine as shown in the Chapter 4. In these experiments, cylindrical metal specimens were compressed between a flat die and punch. Two types of metal specimen were used in the tests, with all specimens machined to a cylindrical bar of 8mm in diameter and 8mm in height, giving an aspect ratio of 1. Specimen surfaces were sanded and polished to provide a uniform surface roughness and the interfaces between the specimens, while die horn and punch tool were not lubricated. Compression tests were performed on specimens of commercial grade metals of aluminium and magnesium. The ultrasonic horn provided a uniform nominal vibration amplitude in the range of 5 to 20 μm, which was controlled by the ultrasonic generator. The flat punch was connected to the cross-head of the test machine which provided a constant cross-head speed of 5 mm/min. For measuring the static-oscillatory force response, a piezoelectric force transducer was mounted between the punch and machine cross-head. For each test, ultrasonic excitation was applied prior to yield limit, in order to investigate the effect of ultrasonic excitation in elastic deformation. In this case, a cylinder specimen was compressed conventionally in the testing machine, under static loading until it reached half of the specimen height to obtain the static material flow stress data. Subsequently, for the static-ultrasonic compression tests, ultrasonic vibration amplitudes were applied to the ultrasonic die surface prior to yield during elastic deformation. In order to investigate the effects of material softening mechanisms in the elastic region, the ultrasonic excitation was introduced between 0.2 mm and 0.3 mm of the cross-head displacement. The ultrasonic excitation was continued throughout loading until the material yield limit was exceeded. This process was repeated for a series of ultrasonic vibration amplitudes between 5 μm and 20 μm. A finite element model was developed using axisymmetric four node elements, taking advantage of symmetry. The model material properties and boundary conditions applied aim to simulate the experiments for static and ultrasonically assisted deformation.

5.3 Finite element modelling

The FE model was developed using Abaqus commercial software, as explained in Chapter 4. FE model was developed using material model parameters which were identified in experimental data. The effect of ultrasonic excitation on the upsetting process is investigated and compared with experimental results. The FE loading and boundary condition also followed the same procedure as in Chapter 4. The model of half of the cylinder specimen was meshed using 2D axisymmetric four node elements, while the ultrasonic die and punch tool were assumed as rigid bodies. The 2D cylinder specimen was modelled as an axisymmetric deformable body, assigned as an elastic-plastic isotropic material model. A constant velocity of 5 mm/min was applied to the punch rigid body. Four sets of FE models were simulated to investigate the material softening mechanisms during upsetting test simulation on elastic deformation.

In the first FE models, the specimen was deformed under static loading for 2.4 seconds in static general procedure. The time was calculated to be exactly the same timing as the application of ultrasonic excitation with the experimental test. Then, the deformation for 0.01 seconds in dynamic implicit procedure under vibrated displacement boundary conditions on the die rigid body was continued. This FE model was simulated for ultrasonic vibration amplitudes between 5 μm and 20 μm. The coefficient of friction of 0.25 was applied during the static and ultrasonic deformation.

In the second, third and fourth FE models, the same procedure as Chapter 4 were followed.

5.4 The effects of ultrasonic excitation in experimental results

The results from the static and ultrasonic compression tests were constructed in stress-strain diagrams. The stress-strain data followed the test procedure discussed in Chapter 4, where the static, mean and oscillatory force response was measured by the piezoelectric force transducer, while the load cell of Zwick-Roell testing machine was used to measure the static and mean forming force only. The results from the machine load cell result can be used to validate the results obtained by the piezoelectric force transducer. The force-displacement data was processed and analysed in SignalCalc ACE dynamic signal analyser software while Matlab R2010a was used to plot stress-strain curves.

5.4.1 Aluminium

The ultrasonic excitation superimposed on static compression test has been carried out for cylinder specimens of aluminium. During the upsetting tests, two sets of stress-strain data were recorded. The first set of data was measured by the machine load cell during static flow stress test and a series of mean flow stresses which excited by ultrasonic vibration amplitudes of 5 μm, 10 μm, 15 μm and 20 μm. The second set of data were recorded using the piezoelectric force transducer mounted between the punch tool and the machine cross-head. The content of this data consisted of a static flow stress, mean flow stress and oscillatory stress from excitation at ultrasonic vibration amplitudes between 5 μm and 20 μm. Both data sets are measured simultaneously during the static and ultrasonic metals upsetting.

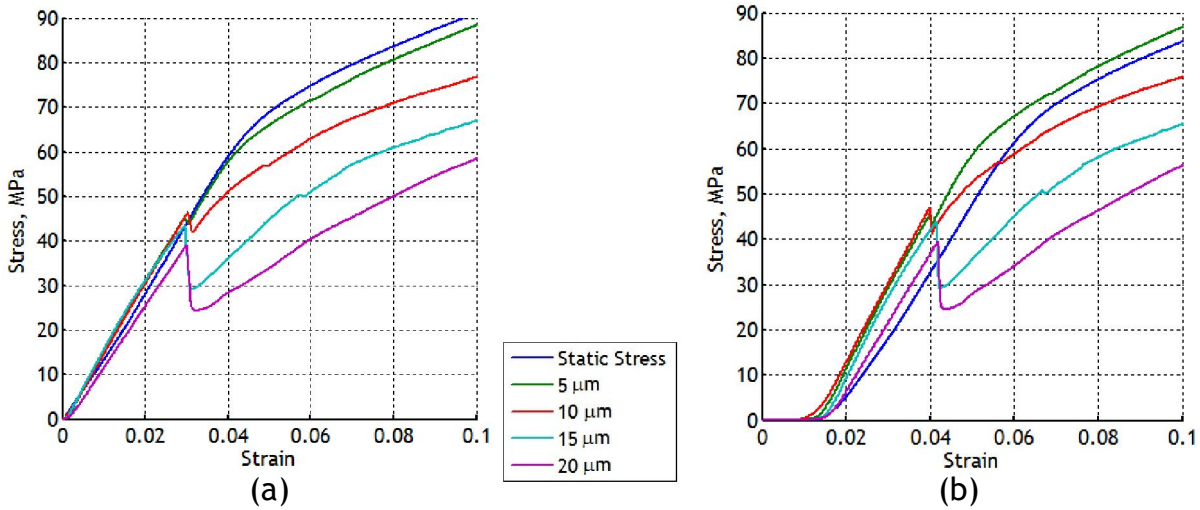

Figure 5-2 Comparison of stress-strain results measured by (a) machine load cell and (b) piezoelectric force transducer for aluminium specimen

Table 5-1 Comparison of the percentage reduction in compressive flow stress

	Reduction in mean flow stress for amplitudes of			
	5 μm	**10 μm**	**15 μm**	**20 μm**
Machine Load Cell	5 %	10 %	20 %	35 %
Piezoelectric Force Transducer	5 %	10 %	20 %	35 %

Fig. 5-2 shows the stress-strain diagram which were measured for static and static-ultrasonic compression tests on the aluminium cylinder specimen. This figure shows two sets of data recorded by the machine load cell and the piezoelectric force transducer. Both diagrams were used to confirm agreement between the two sensors for both the static and ultrasonic stress response measurement. Fig. 5-2(b) shows a delay in strain deformation, this can be accounted to an error in the timing synchronisation of the load application during the experimental tests. The results in Table 5-1 show the comparison of the percentage reduction in mean flow stress measured between the machine load cell and piezoelectric force transducer. The table shows that stress

reduction is the same for both of the force transducers, and that a clear reduction in the static flow stress in all tests condition under ultrasonic excitation exists. It can also be observed that the percentage of reduction in static flow stress increases as ultrasonic vibration amplitude increases during elastic deformation.

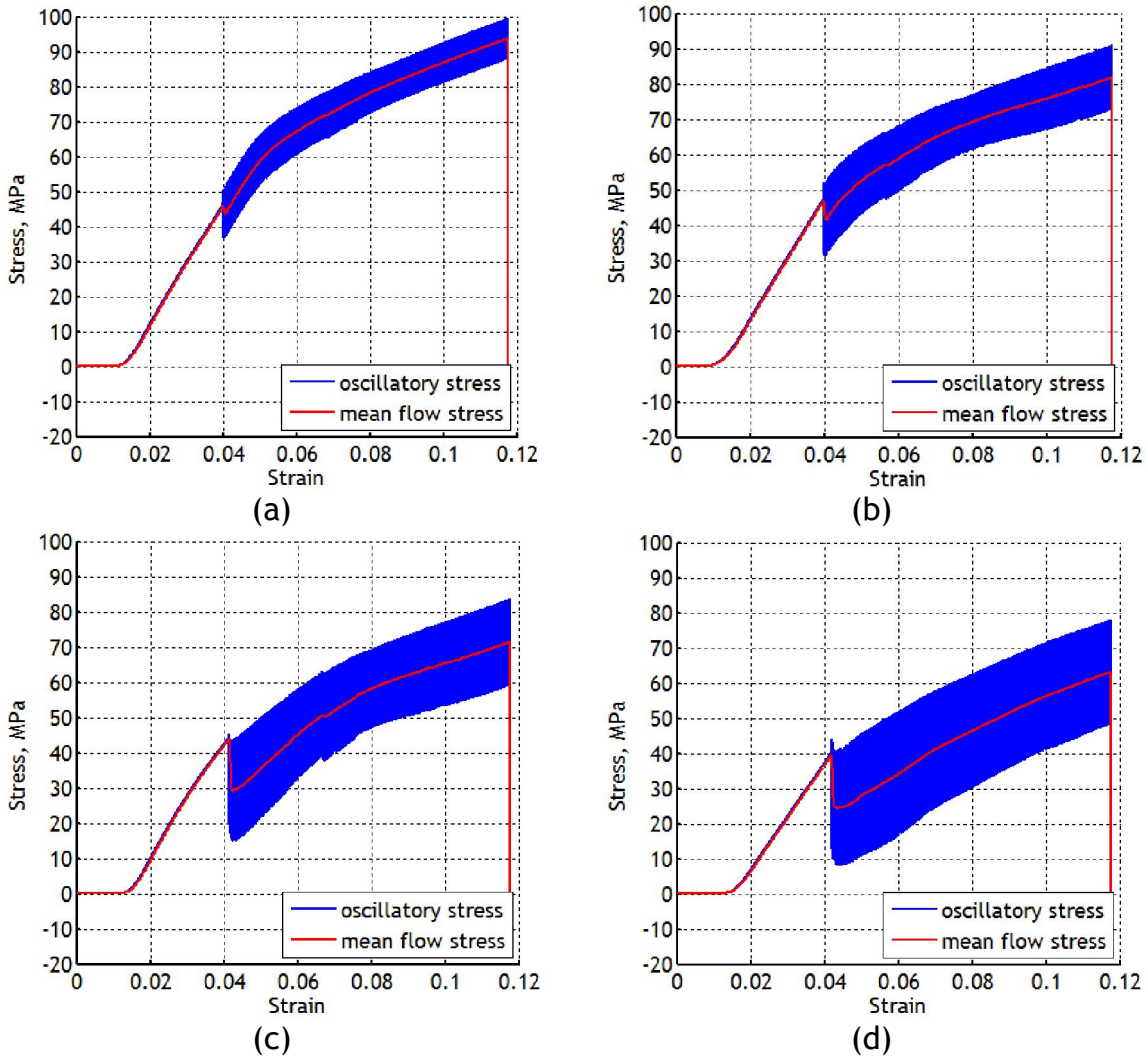

Figure 5-3 Mean flow stress and oscillatory stress measured by piezoelectric force transducer for (a) 5 μm, (b) 10 μm, (c) 15 μm and (d) 20 μm ultrasonic amplitude

Fig. 5-3 shows the oscillatory and mean flow stresses measured during compression tests. These show that the static flow stress immediately reduced once the ultrasonic excitation was introduced. The lowering in flow stress was

observed for the duration of applied ultrasonic excitation. Fig. 5-3 shows the path of maximum oscillatory stress exceeds the static flow stress at some vibration amplitudes. The calculated stress reduction and peak to peak oscillatory stress are demonstrated in Table 5.2.

Table 5-2 Stress reduction and the magnitude of peak-to-peak oscillatory stress

Ultrasonic amplitude	Reduction in mean flow stress	Amplitude of peak to peak oscillatory stress
5 μm	5 %	9.940 MPa
10 μm	10 %	15.904 MPa
15 μm	20 %	23.857 MPa
20 μm	35 %	27.833 MPa

5.4.2 Magnesium

Superimposed ultrasonic excitation on static compression tests has been carried out for cylinder specimens of magnesium and similarly to those processes applied during the compression of aluminium samples. Fig. 5-4 shows the first data set and consists of a comparison of the stress-strain measurements between the machine load cell and the piezoelectric force transducer.

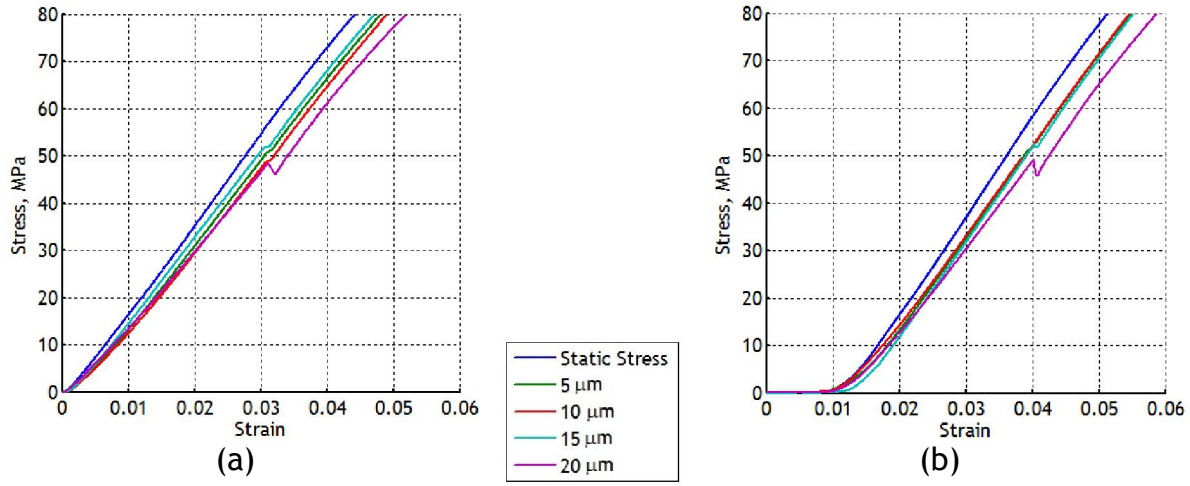

Figure 5-4 Comparison of stress-strain results measured by (a) machine load cell and (b) piezoelectric force transducer for magnesium specimen

Table 5-3 Comparison of the percentage reduction in compressive flow stress

Sensor	Reduction in mean flow stress for amplitudes of			
	5 μm	10 μm	15 μm	20 μm
Machine Load Cell	1 %	1.5 %	2.5 %	5 %
Piezoelectric Force Transducer	1 %	1.5 %	2.5 %	5 %

Fig. 5-4 and Table 5-3 confirm agreement in the measurement of mean flow stress between the machine load cell and piezoelectric force transducer. The investigation of the effects of ultrasonic excitation on the mean flow stress and the oscillatory stress are presented in Fig. 5-5 and are studied for various ultrasonic amplitudes between 5 μm and 20 μm. For each measurement, the peak to peak amplitude of the oscillatory stress during the ultrasonic excitation of the die horn is recorded and these results are summarised in Table 5-4.

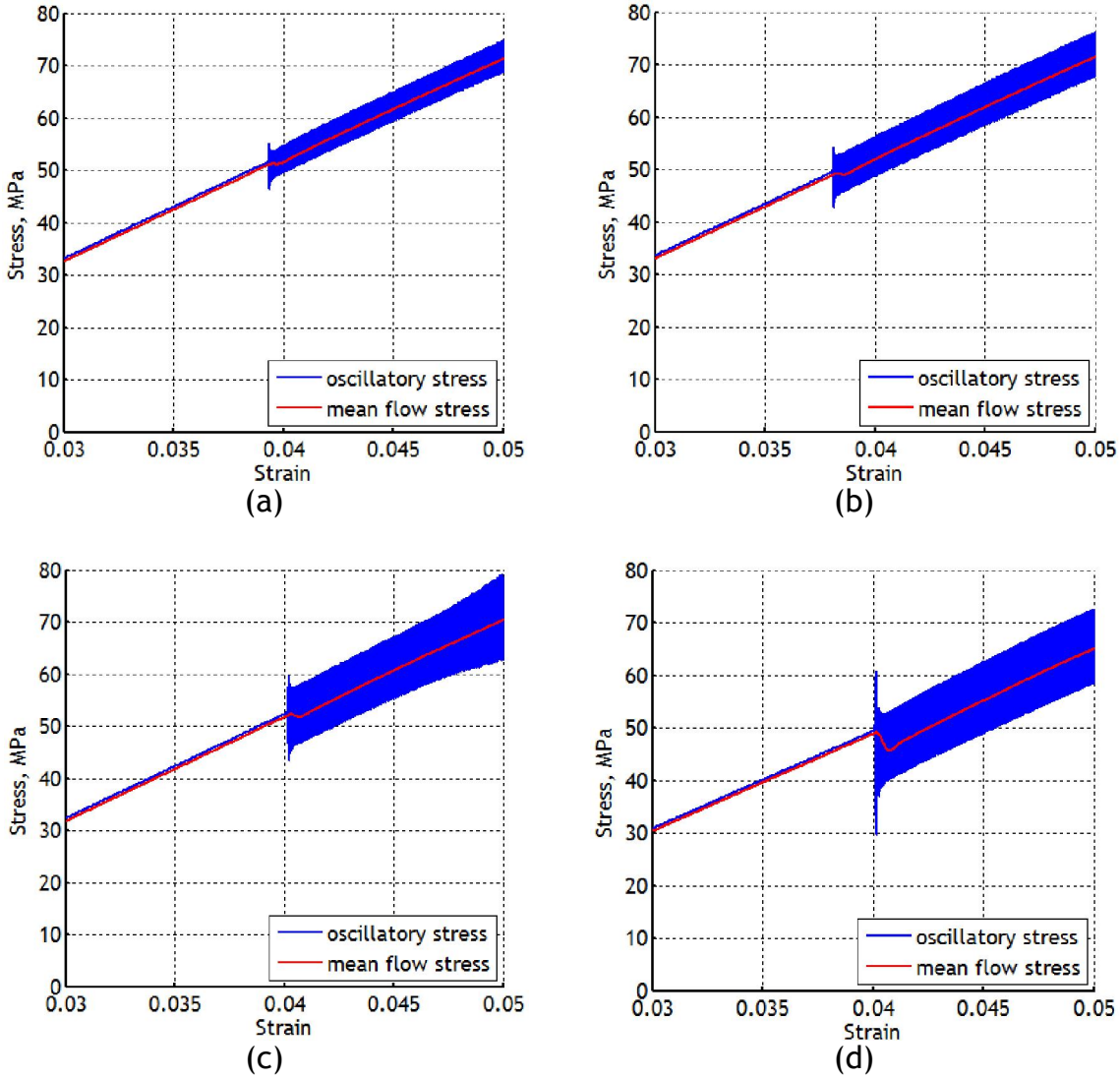

Figure 5-5 Mean flow stress and oscillatory stress measured by piezoelectric force transducer for (a) 5 μm, (b) 10 μm, (c) 15 μm and (d) 20 μm ultrasonic amplitude

Table 5-4 Stress reduction and the magnitude of peak-to-peak oscillatory stress

Ultrasonic amplitude	Reduction in mean flow stress	Amplitude of peak to peak oscillatory stress
5 μm	1 %	7.952 MPa
10 μm	1.5 %	13.917 MPa
15 μm	2.5 %	23.857 MPa
20 μm	5 %	29.821 MPa

Fig. 5-5 shows the static flow stress reduced when the ultrasonic vibration was introduced during the compression tests and it was also seen that the stress reduction is increased with ultrasonic vibration amplitude. The path of maximum oscillatory stress observed exceeds the static flow stress in all tests condition of elastic deformation for this material, however, the mean flow stress is lower than the static flow stress. The magnitude of peak-to-peak oscillatory stress is increased with ultrasonic vibration amplitudes.

5.4.3 The material softening mechanism

The effect that ultrasonic excitation has during the upsetting tests on aluminium and magnesium were investigated. In the stress-strain diagram, the ultrasonic vibration amplitudes were shown to have lowered the static flow stress during elastic deformation under dry contact conditions. The reduction in static flow stress increased with the ultrasonic vibration amplitude, and can be seen in Fig. 5-6 for both tested materials, aluminium and magnesium.

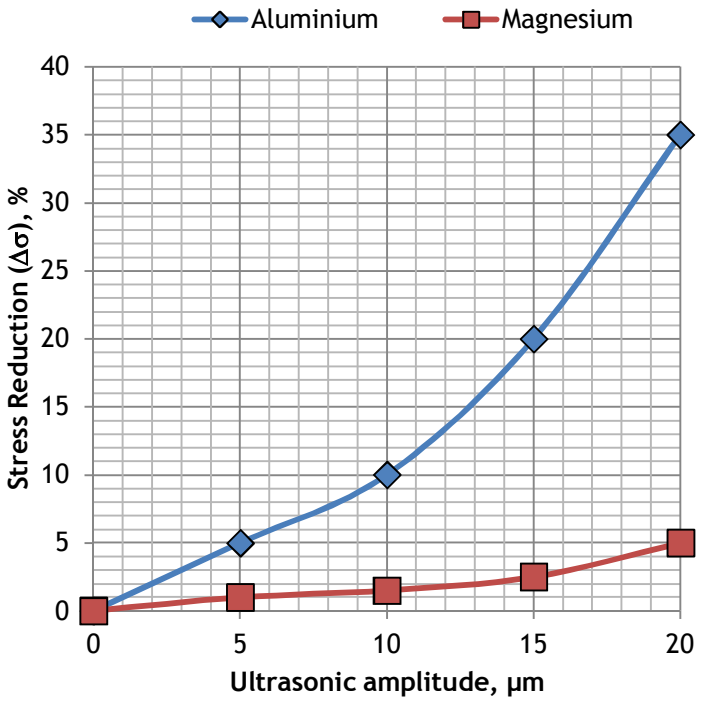

Figure 5-6 The relationship between stress reduction and ultrasonic vibration amplitudes

Fig. 5-6 shows the relationship between stress reduction, $\Delta\sigma$, and vibrational amplitudes during compression testing of aluminium and magnesium. The results in Fig. 5-6 shows that the percentage stress reductions are highly dependant on the metal of the specimen, as the softer metal exhibits larger stress reductions. It can also be seen that stress reduction increases with ultrasonic amplitude in the range of this study (5 μm to 20 μm) during elastic deformation.

Fig. 5-5 shows that the maximum peak of oscillatory stress exceeded the static flow stress, however, the mean flow stress and the path of minimum oscillatory stress are lower than the static flow stress at the onset of ultrasonic excitation. The magnitude of the peak-to-peak oscillatory stress was measured and is shown in Fig. 5-7, and shows a linear increase with ultrasonic vibration amplitude between 5 μm and 20 μm. The magnitude of oscillatory stress is highly dependant on the vibration amplitude but this relationship is the same for both metals tested.

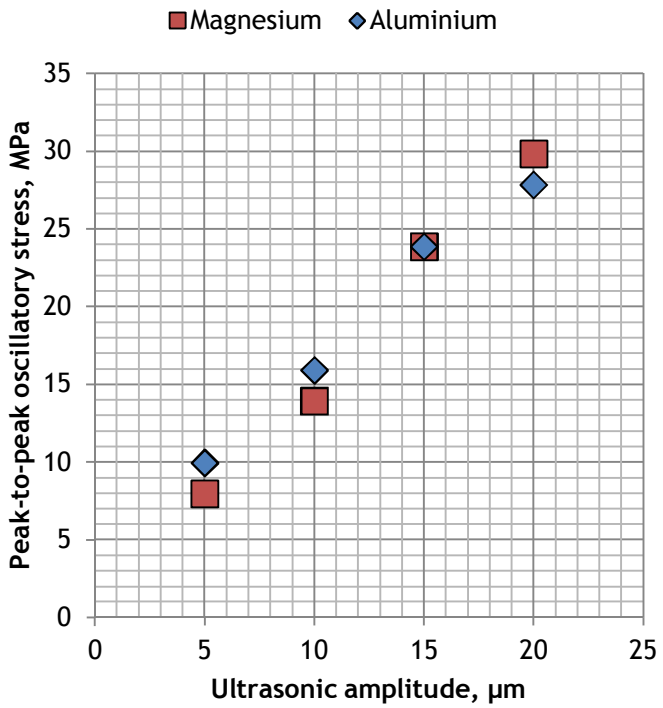

Figure 5-7 The measurement of peak-to-peak oscillatory stress in the experimental test

To investigate the influence that volume and surface effects have on material softening during the experimental compression tests, a series of FE models were developed. The FE models adopted material softening effects in order to simulate realistic stress reduction compared with experimental results. The significant stress reduction in FE analysis was obtained by adjusting the yield stress and contact condition parameter that provided realistic predictions of the volume effect and surface effect. The adjustment in the yield stress and coefficient of friction for this study are followed the previous FE material model in Chapter 4.

5.5 Incorporating ultrasonic excitation in the numerical model

The effects of longitudinal ultrasonic excitation on the stress-strain relationship for elastic deformation were predicted in the FE analysis. A series of FE models was developed to investigate the influence of the material softening mechanism during superimposed ultrasonic vibration on the static compression test. For comparison, the results of the first and second FE models are presented with experimental results where ultrasonic excitation is superimposed at ultrasonic vibration amplitudes from 5 μm to 20 μm. The third and fourth FE models are presented individually, and are shown in the following section according to the material used in this study.

5.5.1 Aluminium

Fig. 5-8 to Fig. 5-11 show the mean flow stress and oscillatory stress that were experimentally measured and numerically predicted during superimposed ultrasonic excitation. The numerical results were predicted in the first and second FE models. For each measurement, the stress reduction and the peak-to-

peak amplitude of the oscillatory stress during ultrasonic excitation of the die horn are summarised in Table 5-5.

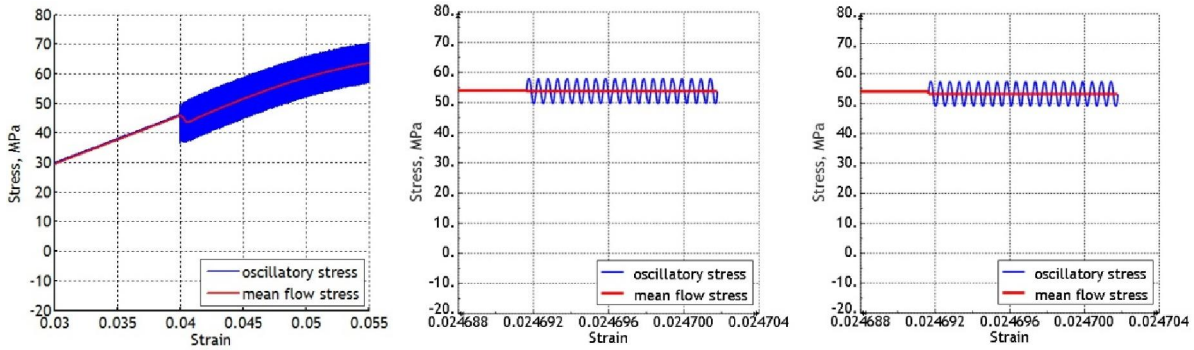

(a) (b) (c)

Figure 5-8 Comparison of stress-strain data (a) measured by the piezoelectric force transducer, (b) predicted in the first FE models and (c) predicted in the second FE models for 5 μm ultrasonic amplitude

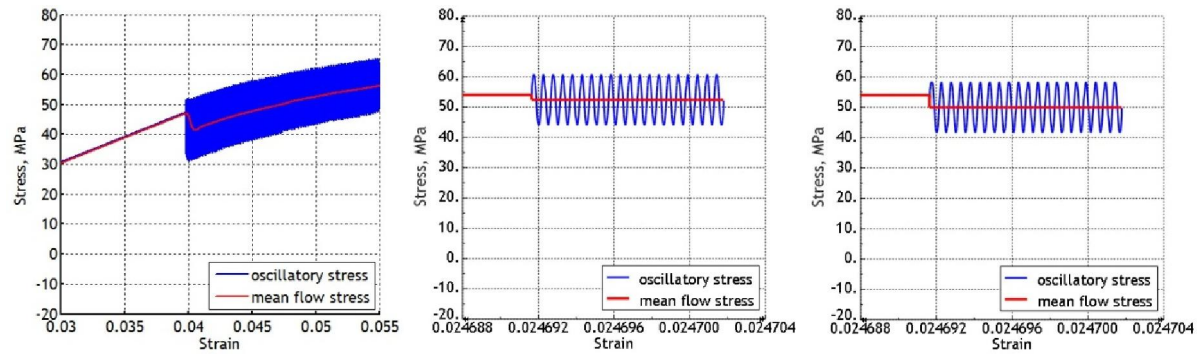

(a) (b) (c)

Figure 5-9 Comparison of stress-strain data (a) measured by the piezoelectric force transducer, (b) predicted in the first FE models and (c) predicted in the second FE models for 10 μm ultrasonic amplitude

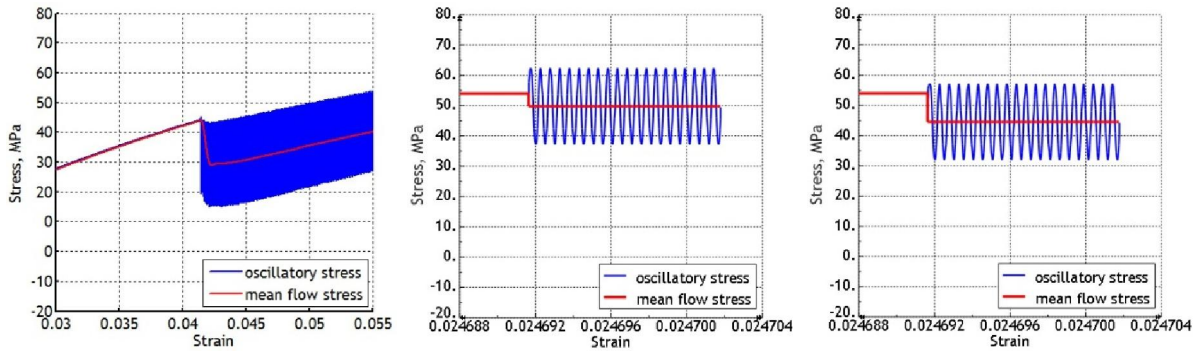

(a) (b) (c)

Figure 5-10 Comparison of stress-strain data (a) measured by the piezoelectric force transducer, (b) predicted in the first FE models and (c) predicted in the second FE models for 15 μm ultrasonic amplitude

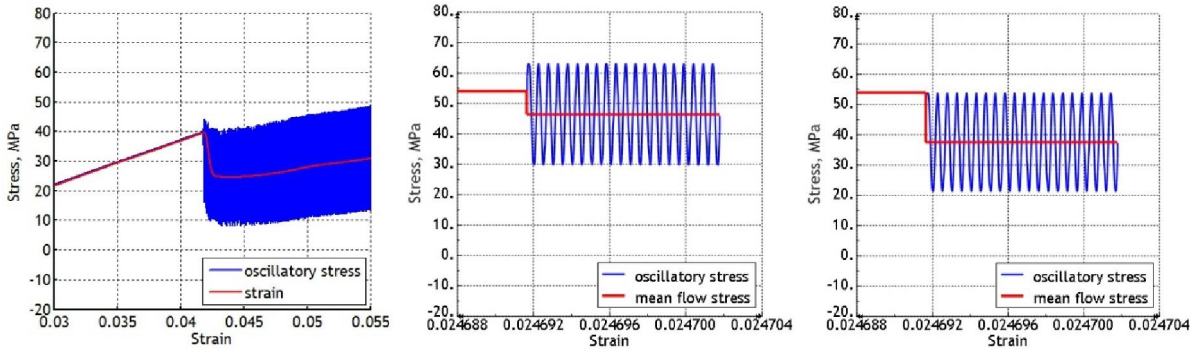

Figure 5-11 Comparison of stress-strain data (a) measured by the piezoelectric force transducer, (b) predicted in the first FE models and (c) predicted in the second FE models for 20 μm ultrasonic amplitude

Table 5-5 Stress reduction and amplitude of peak-to-peak oscillatory stress

Vibration amplitude	Stress reduction			Peak-to-peak oscillatory stress		
	Piezoelectric force transducer	The first FE Model	The second FE Model	Piezoelectric force transducer	The first FE Model	The second FE Model
5 μm	5 %	0.42 %	2 %	9.940 MPa	8.398 MPa	8.398 MPa
10 μm	10 %	2.99 %	7.5 %	15.904 MPa	16.793 MPa	16.789 MPa
15 μm	20 %	7.86 %	17.5 %	23.857 MPa	25.184 MPa	25.129 MPa
20 μm	35 %	14.07 %	30.5 %	27.833 MPa	33.565 MPa	32.660 MPa

It can be seen that the results predicted in first FE model differed with the results measured by the piezoelectric force transducer. The results of the second FE model clearly show that a close match between the experiment and the FE model data is achievable by modelling the effects of superimposed ultrasonic excitation as a combination of an adjustment of material flow stress properties and interfacial contact condition.

The third and fourth FE models were used to repeat the second FE model by introducing an adjustment to yield stress and coefficient of friction in order to predict the influences of volume effect and surface effect separately during the compression simulation. The predictive effects of superimposed ultrasonic

excitation on the adjustment to flow stress alone during elastic deformation are shown in Fig. 5-12. Meanwhile, the predictive effects of superimposed ultrasonic excitation of the adjustment on coefficient of friction alone during elastic deformation are shown in Fig. 5-13. For each measurement, the stress reduction and the peak-to-peak amplitude of the oscillatory stress are summarised in Table 5-6.

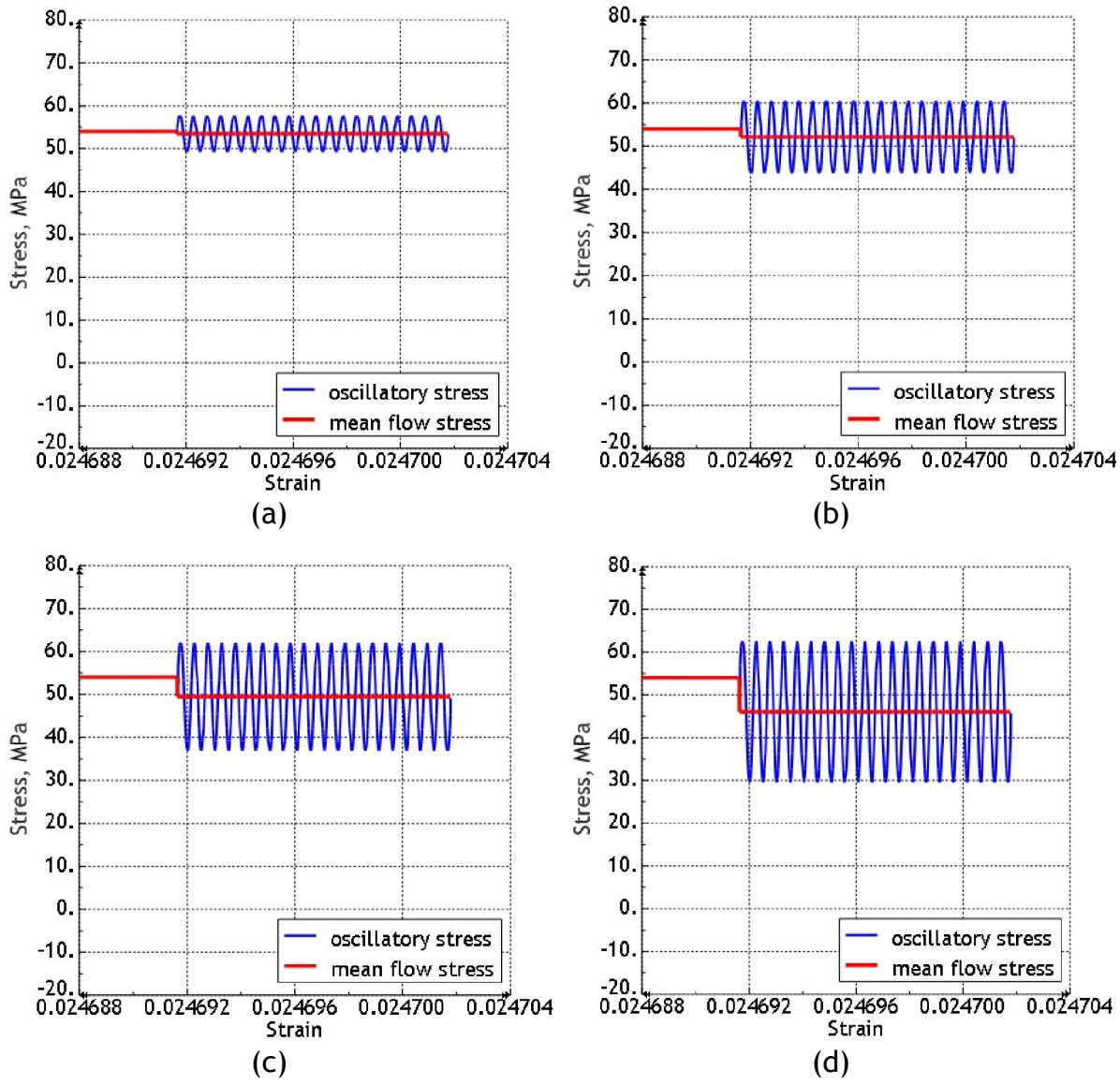

Figure 5-12 Stress reduction and oscillatory stress in aluminium, for FE model incorporating flow stress adjustment for (a) 5 μm (b) 10 μm (c) 15 μm and (d) 20 μm ultrasonic amplitudes

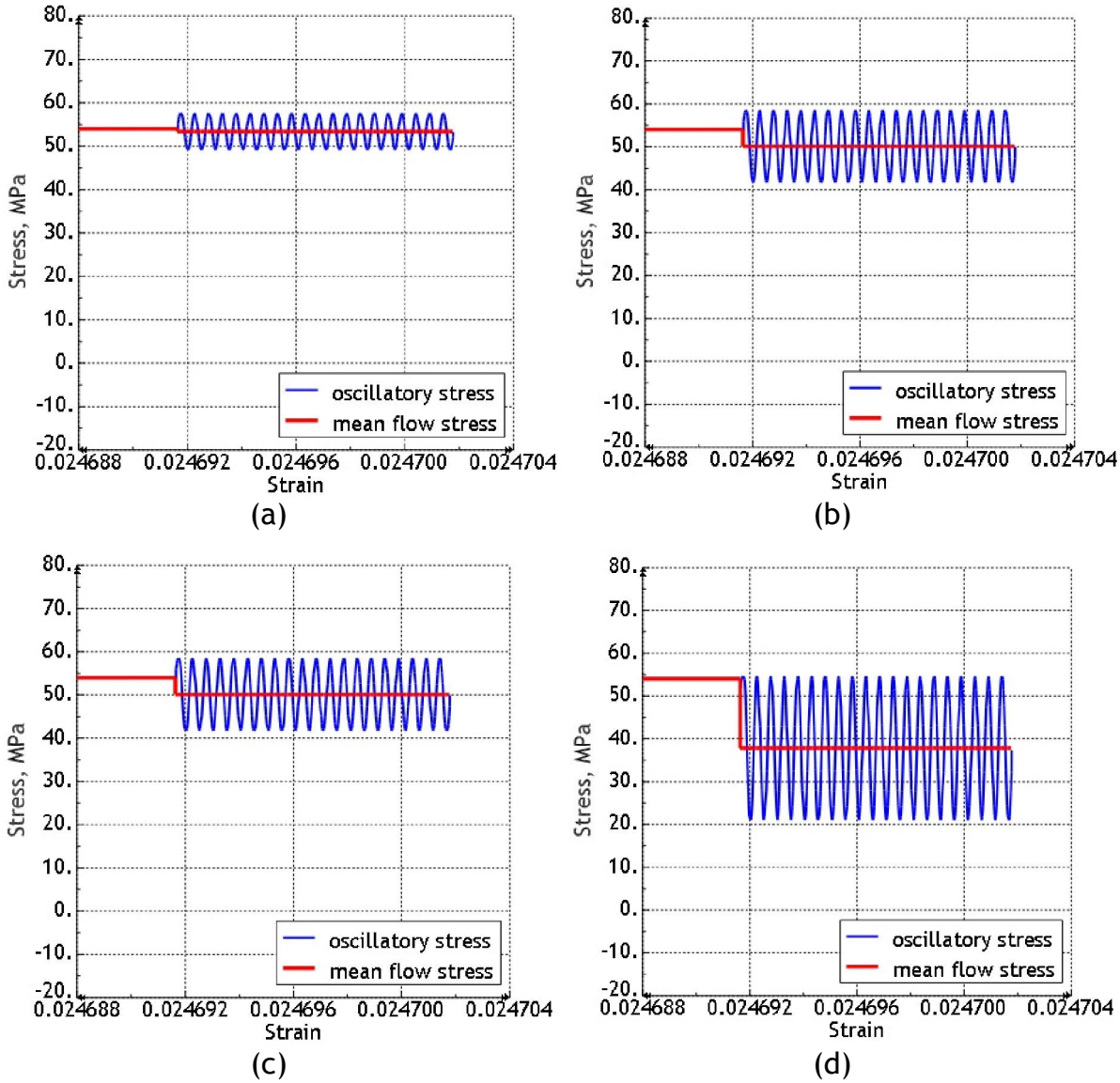

Figure 5-13 Stress reduction and oscillatory stress in aluminium, for FE model incorporating coefficient of friction adjustment for (a) 5 μm (b) 10 μm (c) 15 μm and (d) 20 μm ultrasonic amplitudes

Table 5-6 Stress reduction and amplitude of peak-to-peak oscillatory stress

Vibration amplitude	Stress Reduction		Peak-to-peak oscillatory stress	
	The third FE Model	The fourth FE Model	The third FE Model	The fourth FE Model
5 μm	1 %	1.17 %	8.398 MPa	8.397 MPa
10 μm	3.44 %	7.24 %	16.795 MPa	16.789 MPa
15 μm	8.43 %	16.75 %	25.155 MPa	25.172 MPa
20 μm	14.78 %	30 %	32.905 MPa	33.539 MPa

5.5.2 Magnesium

A series of FE models simulating the compression test were adjusted by including effective material softening during superimposed ultrasonic excitation on magnesium. A comparison of results consisting of stress-strain curves for experimental result, and a first and a second FE models are shown in Fig. 5-14 to Fig. 5-17. The models consisting of a simulated compression test were developed without and with the adjustment to material yield stress and coefficient of friction. For each measurement, the stress reduction and the peak-to-peak amplitude of the oscillatory stress during ultrasonic excitation of the die horn are summarised in Table 5-7.

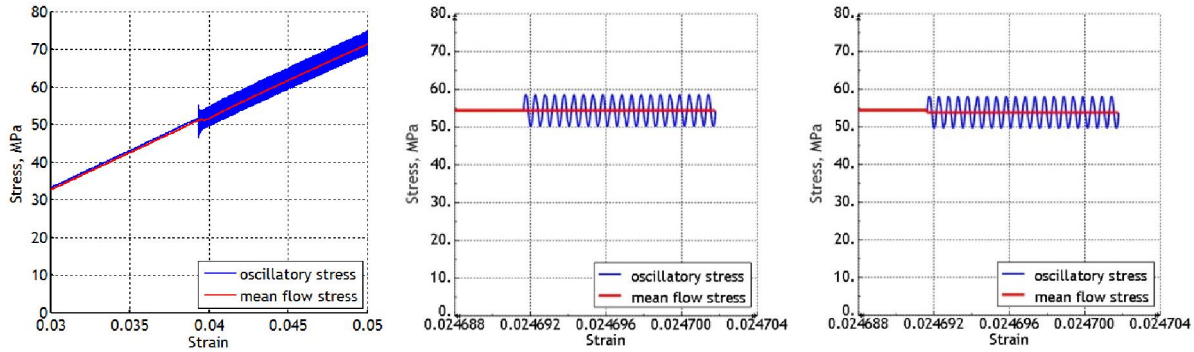

Figure 5-14 Comparison of stress-strain data (a) measured by the piezoelectric force transducer, (b) predicted in the first FE models and (c) predicted in the second FE models for 5 μm ultrasonic amplitude

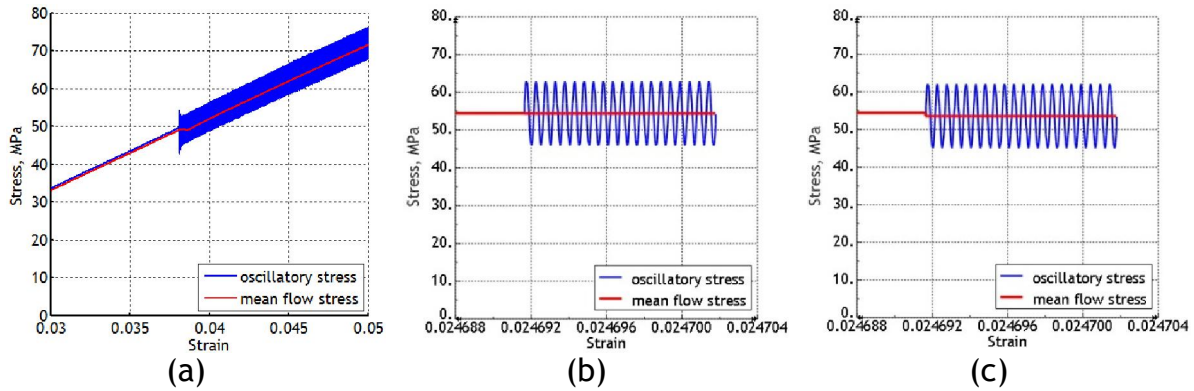

Figure 5-15 Comparison of stress-strain data (a) measured by the piezoelectric force transducer, (b) predicted in the first FE models and (c) predicted in the second FE models for 10 μm ultrasonic amplitude

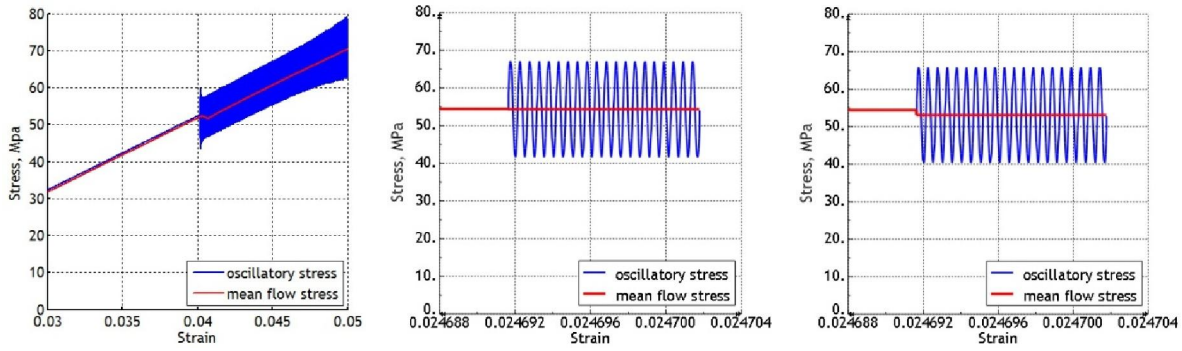

Figure 5-16 Comparison of stress-strain data (a) measured by the piezoelectric force transducer, (b) predicted in the first FE models and (c) predicted in the second FE models for 15 μm ultrasonic amplitude

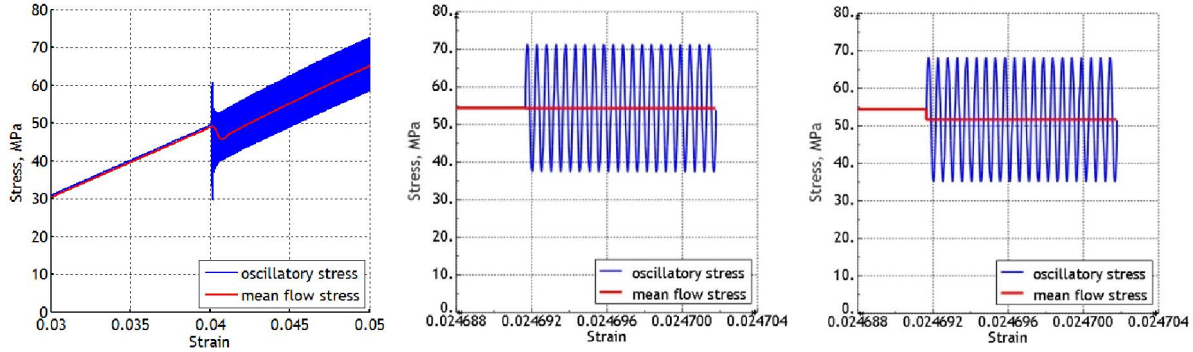

Figure 5-17 Comparison of stress-strain data (a) measured by the piezoelectric force transducer, (b) predicted in the first FE models and (c) predicted in the second FE models for 20 μm ultrasonic amplitude

Table 5-7 Stress reduction and amplitude of peak-to-peak oscillatory stress

Vibration amplitude	Stress reduction			Peak-to-peak oscillatory stress		
	Piezoelectric force transducer	The first FE Model	The second FE Model	Piezoelectric force transducer	The first FE Model	The second FE Model
5 μm	1 %	0.04 %	1.1 %	7.952 MPa	8.497 MPa	8.497 MPa
10 μm	1.5 %	0.1 %	1.63 %	13.917 MPa	16.995 MPa	16.996 MPa
15 μm	2.5 %	0.14 %	2.5 %	23.857 MPa	25.494 MPa	25.487 MPa
20 μm	5 %	0.17 %	5.05 %	29.821 MPa	33.995 MPa	33.238 MPa

For the third FE models, that considers adjustment of flow stress alone during elastic deformation, the results are shown in Fig. 5-18. For the fourth FE models, that considers adjustment on coefficient of friction alone during elastic deformation, the results are shown in Fig. 5-19. For each measurement, the stress reduction and the peak to peak amplitude of the oscillatory stress are summarised in Table 5-8.

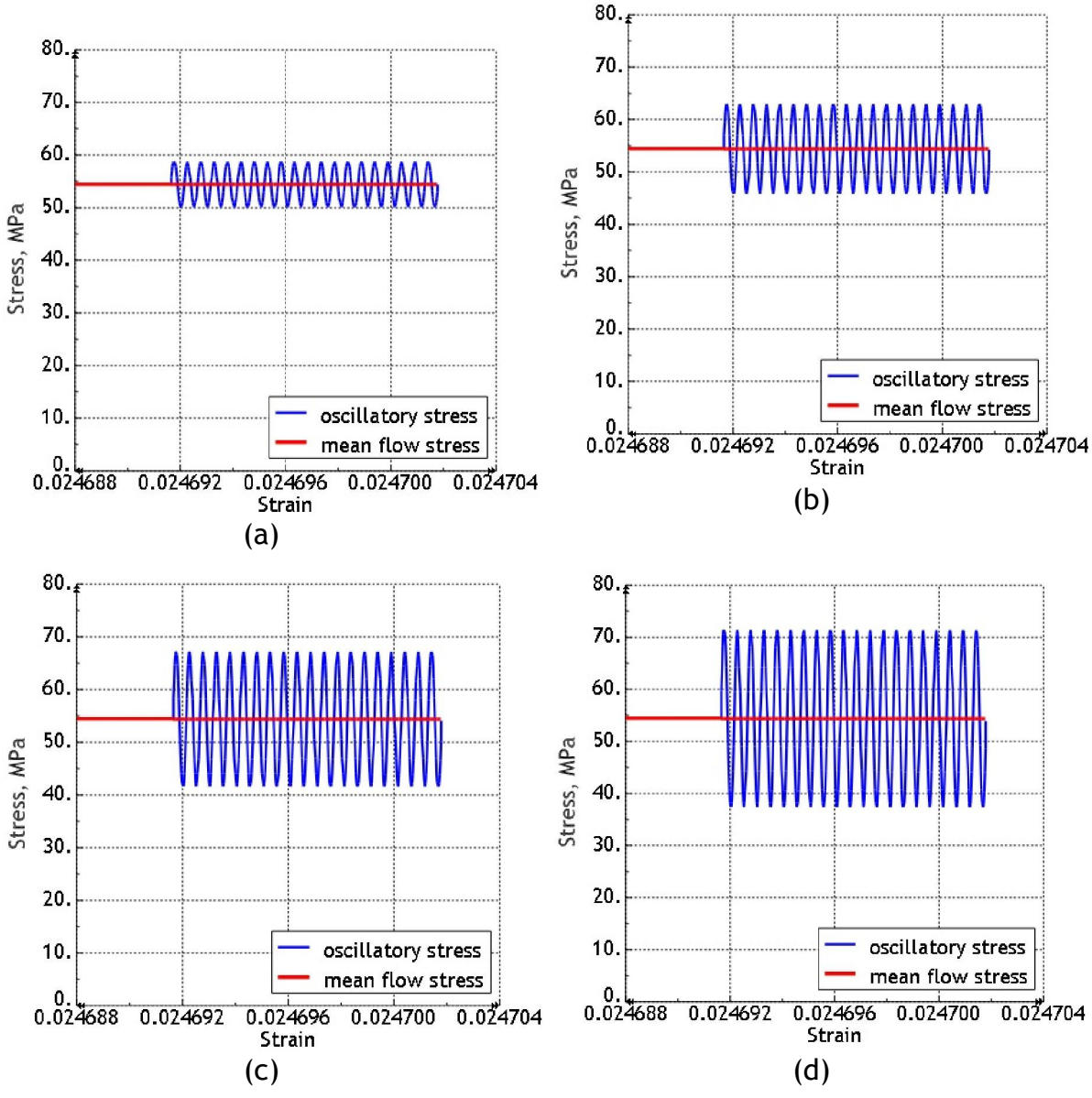

Figure 5-18 Stress reduction and oscillatory stress in magnesium, for FE model incorporating flow stress adjustment for (a) 5 µm (b) 10 µm (c) 15 µm and (d) 20 µm ultrasonic amplitudes

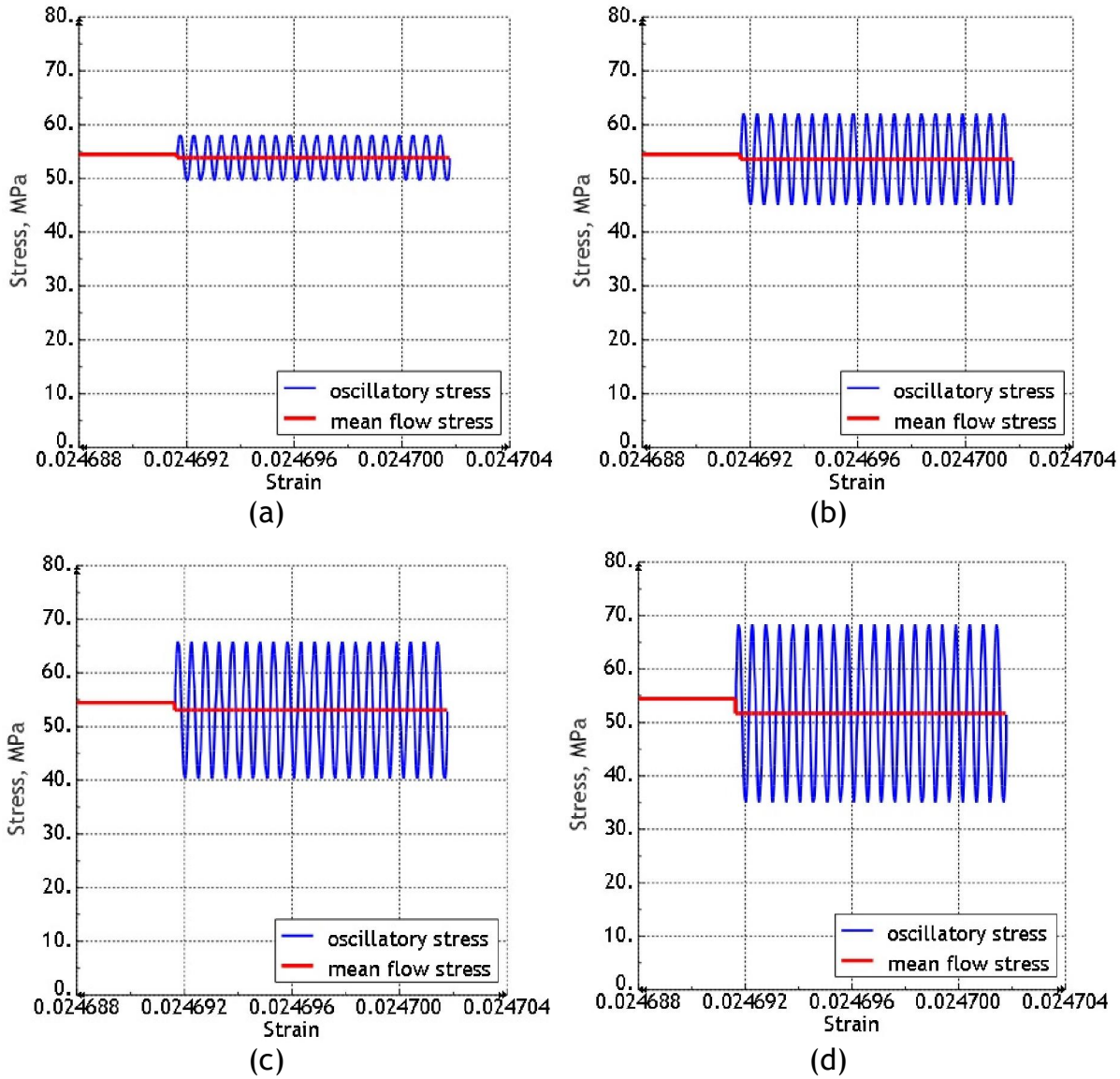

Figure 5-19 Stress reduction and oscillatory stress in magnesium, for FE model incorporating coefficient of friction adjustment for (a) 5 μm (b) 10 μm (c) 15 μm and (d) 20 μm ultrasonic amplitudes

Table 5-8 Stress reduction and amplitude of peak-to-peak oscillatory stress

Vibration amplitude	Stress Reduction		Peak-to-peak oscillatory stress	
	The third FE Model	The fourth FE Model	The third FE Model	The fourth FE Model
5 μm	0.04 %	1.1 %	8.497 MPa	8.497 MPa
10 μm	0.097 %	1.63 %	16.995 MPa	16.998 MPa
15 μm	0.14 %	2.506 %	25.495 MPa	25.487 MPa
20 μm	0.17 %	5.05 %	33.994 MPa	33.238 MPa

5.6 Discussion: The effects of superimposed ultrasonic excitation on elastic deformation

An investigation into the effects of superimposed ultrasonic excitation on the static deformation of metals for aluminium and magnesium specimens was performed through experimental tests and FE simulations. The study was carried out by introducing the ultrasonic vibration prior to reaching the yield stress limit on the static compression test. The results shown in the previous section were characterised as the behaviours of material properties parameters under elastic deformation. The results were presented in four sets of FE models in order to observe the contributions of the effects which focused on two categories of mechanism, namely volume effect and surface effect. The mechanism effects can be predicted by simulating the ultrasonically assisted metal compression in the FE analysis.

5.6.1 The ultrasonic excitation effects on stress reduction

The results presented in this chapter shows that a flow stress reduction was measured on the elastic deformation for each of the test metals. Although, the static flow stress was reduced when the ultrasonic excitation was introduced, the percentage of stress reduction is slightly lower compared to the results which were shown in the findings for ultrasonically assisted metal compression during plastic deformation in Chapter 4. It was believed that the percentage of stress reduction was affected by the material reversible conditions during superimposed of ultrasonic excitation in elastic deformation.

Finite element models were developed to predict the effects of stress reduction mechanisms in numerical terms. Four sets of FE models were developed in the FE analysis, which consisted of a combined adjustment to material flow stress and interface friction coefficient, adjustment to material flow stress only, adjustment to coefficient of friction alone and without any adjustment to flow

stress or coefficient of friction. As a result, the influence of the volume effect and surface effect could be predicted in terms of the stress reduction mechanisms. The stress reductions measured in the experimental test and predicted in the second FE models can be seen in Fig. 5-20, for aluminium and magnesium cylindrical specimens during ultrasonic deformation. This figure shows that the aluminium produced a higher percentage stress reduction compared to the magnesium.

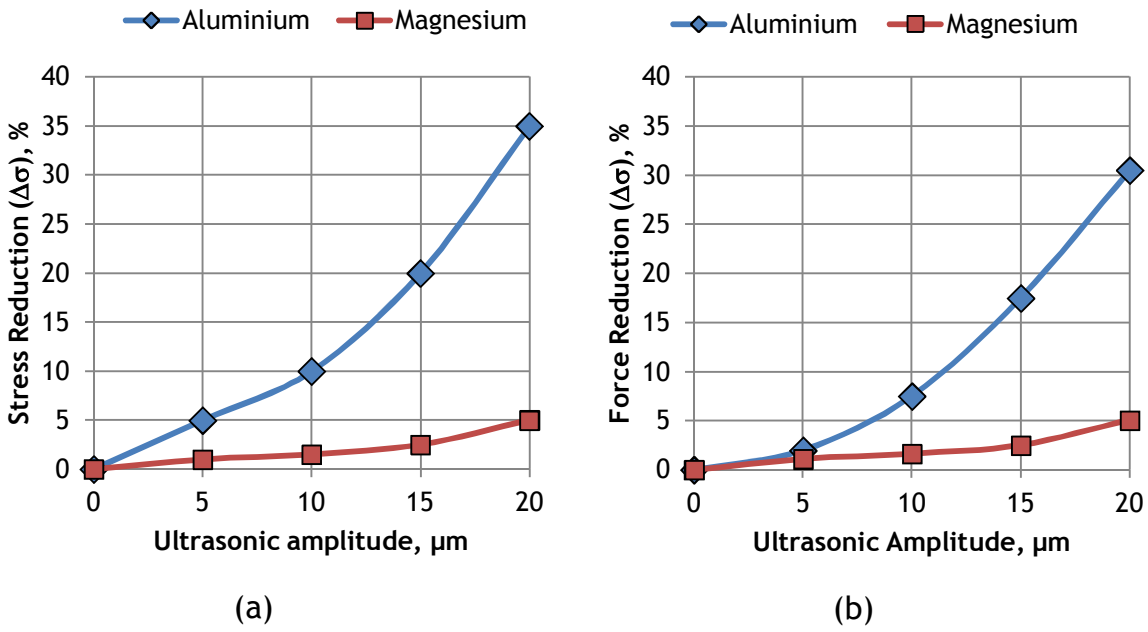

(a) (b)

Figure 5-20 Reductions in static flow stress to mean flow stress during ultrasonic excitation from (a) experiment and (b) FE analysis

5.6.2 The ultrasonic excitation effects on oscillatory stress

An investigation of the peak-to-peak oscillatory stress during ultrasonic compression can provide significant information of the stress reduction effects. Observation of the oscillatory stress in experimental and FE analysis results demonstrated that the path of maximum oscillatory stress exceed the static flow stress, but the mean flow stress and the path of minimum oscillatory stress are

lower than the static flow stress. This phenomenon is exhibited in aluminium and magnesium specimens. The path of maximum oscillatory stress was affected by the material deformation condition either in elastic or plastic region. The superimposed ultrasonic excitation during elastic deformation resulted on the path of maximum oscillatory stress exceeding the static flow stress, while the path of maximum oscillatory stress was lower than static flow stress if the ultrasonic excitation was applied in plastic deformation. The magnitude of peak-to-peak oscillatory stress is plotted in Fig. 5-22.

However, Fig. 5-3(c) and (d) for aluminium seem to have a lower path of maximum oscillatory stress during superimposed ultrasonic excitation at 15 μm and 20 μm. This can be explained in Fig. 5-21 which shows that the stress-strain results during the superimposed ultrasonic excitation at amplitude of 20 μm. The ultrasonic excitation was introduced at 3% strain at which the specimen is expected to deform under elastic condition. During the superimposed ultrasonic excitation, oscillatory stress was measured and presented in terms of the path of maximum, minimum and mean oscillatory stress as Fig 5-10(a). An FE model was then used to simulate the mean flow stress and oscillatory stress, Fig. 5-10(c). These results implied that the static flow stress and mean flow stress are presented as two different material behaviours. Although ultrasonic was applied at 3% strain at all excitation levels at vibrational amplitudes of 15 μm and 20 μm it was found that the mean static flow stress was in the plastic region of deformation. At these vibrational amplitudes to ensure that both mean and static flow stress was within the elastic region, ultrasonic should have been applied at 2.4% strain.

Experimental results reported by Izumi [81] are shown in Fig. 5-1. Izumi found that as strain levels increased that widening between static flow stress and mean flow stress occurred, however, when compared to Fig. 5-21 this behaviour was not observed. Izumi observed that above an vibrational amplitude threshold specimen experienced a significant increase in temperature and it was concluded that was accountable for the widening between the traces of static and mean flow stress. Although in this study, the specimen temperature was not measured the stress-strain behaviour did not show the widening. Therefore, it

can be determined that the compression test did not reach the vibrational amplitude that would induce significant heating observed by Izumi.

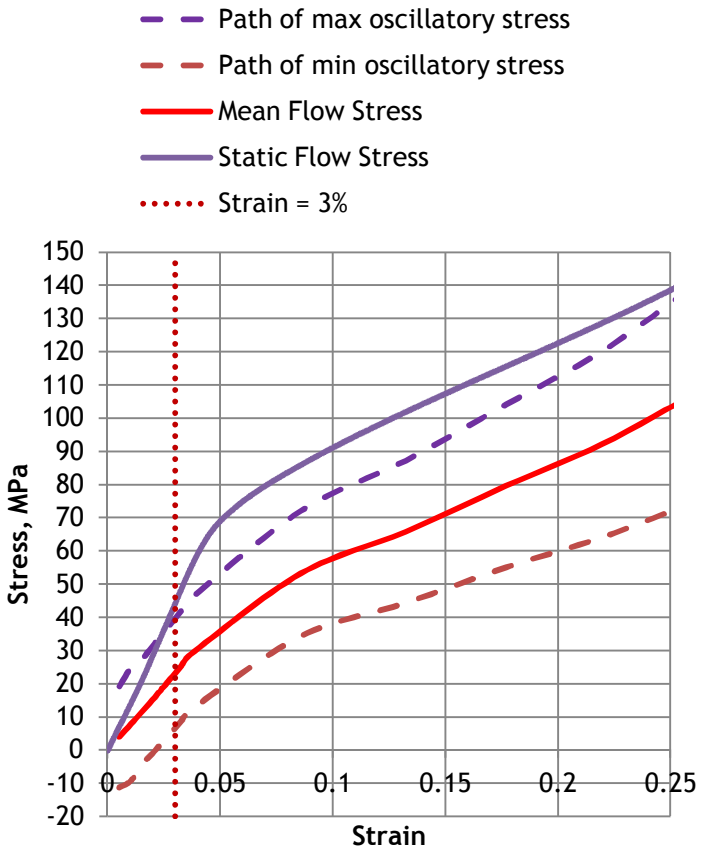

Figure 5-21 Stress-strain results during superimposed ultrasonic excitation at amplitude of 20 μm

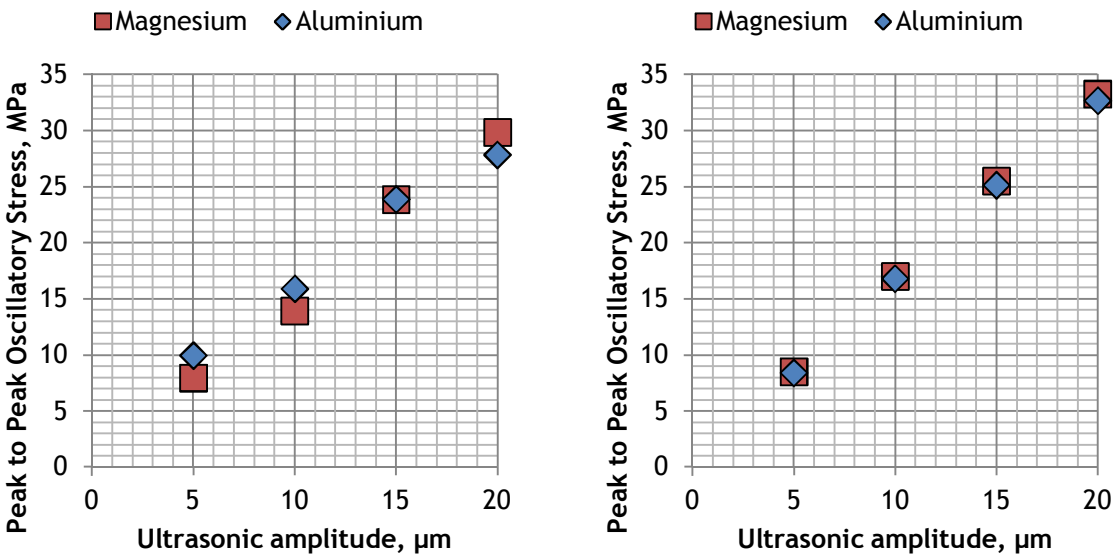

Figure 5-22 Peak-peak oscillatory stress amplitude from (a) experiment and (b) FE analysis

Fig. 5-22 shows the effectiveness of oscillatory stress with a series of ultrasonic vibration amplitudes employed. The oscillatory stress are observed to almost linearly increase with the ultrasonic vibration amplitudes for both analytical and numerical methods. Fig. 5-22 also shows that the magnitude of peak-to-peak oscillatory stress was in the same result for each ultrasonic vibration amplitude applied in the aluminium and magnesium.

5.6.3 The influence that amplitude of vibration has on stress reduction mechanisms

Volume effect and surface effect can be predicted by simulating the superimposed ultrasonic excitation on static compression during an elastic deformation in the numerical analysis. The adjustment to the material flow stress and the coefficient of friction in FE model can predict the contributions of each mechanism. Similar to Chapter 4, the influence that surface effect and volume effect has on material softening was predicted by plotting the percentage of stress reduction to vibration amplitude. This relationship is shown in Fig. 5-23. The measurement of the $\Delta\sigma - USA$ value is summarised in Table 5-

9. The results are presented in Fig. 5-24 and show that for elastic deformation, the surface effect of effective material softening dominates the stress-strain behaviour during superimposed ultrasonic excitation.

The effect of material softening has been considered by most investigators to be a combination of three effects; stress superposition, friction reduction and acoustic softening during elastic-plastic deformation [4, 5, 64, 107], Fig. 4-14. However, the mechanism of material softening in the elastic deformation has not been adequately explained. Nevill and Brotzen [25] believed that reduction in stress can be explained by a mechanism of superimposition of steady and alternating stress, while other investigators [24, 88, 133] have suggested that the stress is reduced because of vibrational energy is absorbed at dislocation sites. As mentioned in literature, the superposition of stress was achieved when the oscillatory stress is greater than the required stress to induce plastic deformation, however, if the oscillatory stress is lower than the required stress the specimen will not yield, the mechanism of stress superposition will not attain and the stress reduction will not occurr. Nevill and Brotzen also observed that the decrease in stress was independent of the prior strain for a value of average permanent elongation up to 15% during ultrasonic tensile testing of wire. This result showed that the mechanism of stress reduction was measured in the absence of surface effect. Stress superposition usually occurred due to material's elastic-plastic property. If only the stress superposition is in effect without acoustic softening, the path of the maximum oscillatory stress was consistent with the static stress without vibration in plastic deformation [107].

Therefore, in this study, the contribution of friction reduction and stress reduction have been predicted with respect to stress superposition. However, the mechanism of the superposition of stress was not achieved during superimposed ultrasonic excitation in the elastic deformation and the FE simulation in the result predicted that a reduction in flow stress resulted in a minor decrease, when compared to the influence of the friction reduction. This account that the surface effect is a dominant contribution of stress reduction in the upsetting operation. Since, the mechanism of stress superposition was not significant in elastic region caused the reduction in mean flow stress was very small compared to the amount of peak-to-peak oscillatory stress resulted the path of maximum oscillatory stress exceeded than static flow stress.

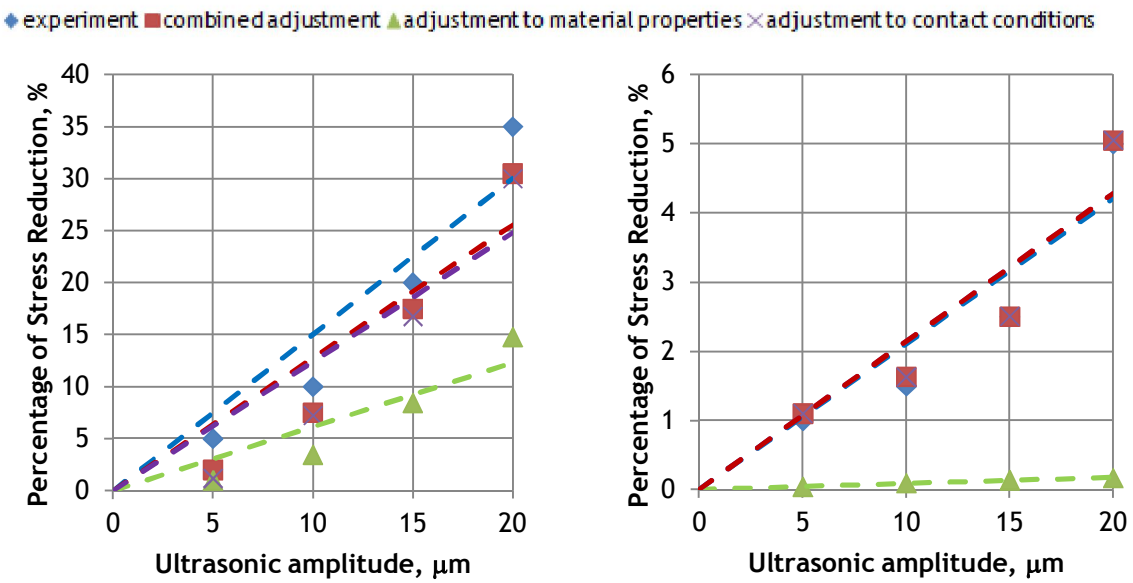

Figure 5-23 The percentage of stress reduction in adjustment to material flow stress and contact conditions for (a) aluminium and (b) magnesium

Table 5-9 The measurement of Δσ - USA value

Material	Δσ - USA value, mm^{-1}			
	experiment	combined adjustment	adjustment to material properties	adjustment to contact conditions
Aluminium	15.00	1.28	6.15	12.39
Magnesium	2.10	2.14	0.09	2.14

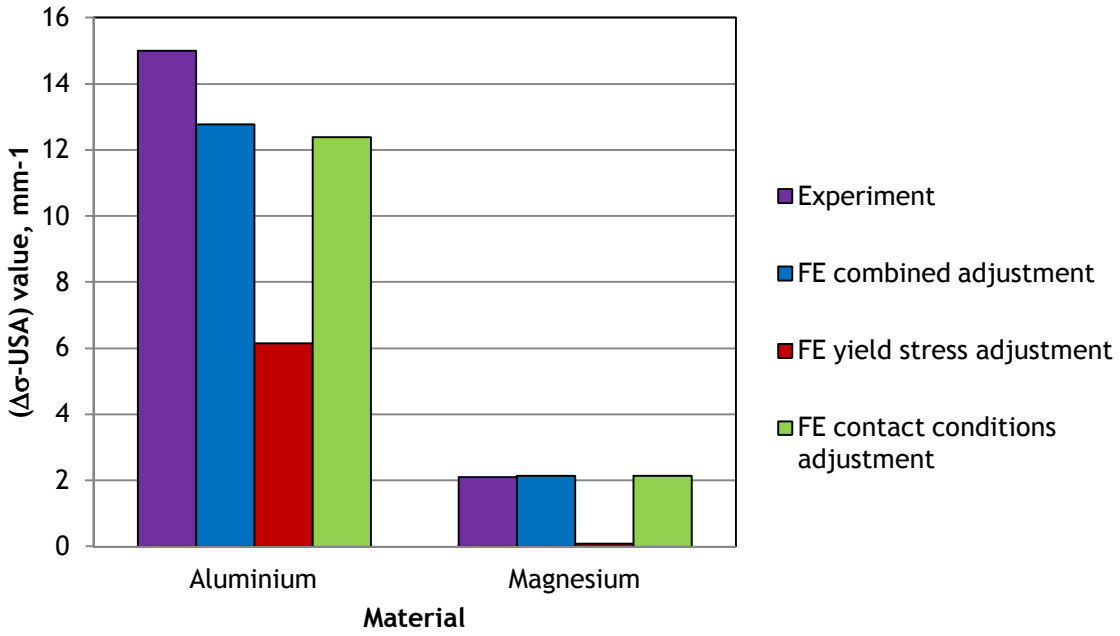

Figure 5-24 The contribution to stress reduction of volume and surface adjustments in the FE model

5.7 Conclusion

Superimposed ultrasonic excitation on elastic compression has been carried out for aluminium and magnesium cylinder specimens, and the effects of this the excitation on metal specimens has been investigated. Previously, in Chapter 4, superimposed ultrasonic excitation applied during plastic deformation had discussed the influence of surface effect and volume effect in stress reduction mechanisms. Elastic deformation was known to have material reversible conditions during the deformation, therefore the explanation in reduction mechanisms was interpreted differently in elastic deformation. It was shown that the path of maximum oscillatory stress was exceeded the static flow stress. An investigation aiming to characterise the materials behaviour during the superimposed ultrasonic excitation on elastic deformation can explain the reduction mechanisms, namely volume effect and surface effect. As a result, a reduction in static flow stress was shown in ultrasonically assisted metals compression on elastic deformation and the results were exhibited using experimental and numerical analysis for all of the metals used.

The effectiveness of the reduction mechanisms on volume effect and surface effect has been studied, and it can be concluded that the surface effect mechanism has dominated the stress reduction during the metals upsetting test on elastic deformation. It is believed that it did not affect the volume effects mechanism because of the material strain recovery factor in elastic deformation. The effectiveness of the reduction mechanisms were also considered to be dependent on the compressive strength of the metal samples, where the softer material exhibited a higher percentage of stress reduction than harder material.

CHAPTER 6

STATIC-ULTRASONIC EXCITATION IN METAL PLATE FORMING

6.1 Introduction

Metal forming processes are among the most common material processes in manufacturing technology. It is a manufacturing process by which parts or components are forming from a plate, sheet, bar, rod, wire or tubing of various cross-sections. Metal-working of a plate is generally known as a sheet metal forming process. Meanwhile, the term of press-working or press forming is used commonly in industry to describe sheet-forming operations, because they typically are performed on presses using a set of dies. The most well known metal forming processes in industry are; rolling, forging, extrusion, drawing, sheet metal forming and joining. In order to reduce the manufacturing cost of a serviceable part, thorough knowledge of all possible methods of producing the part is required in order to select the best process or combination of processes. Since these operations occur within a high-volume industry, even small improvements in material properties, simulations, and manufacturing costs will translate into substantial savings. Power ultrasonics has the potential to benefit these manufacturing process. Blaha and Langenecker [24] first investigated the benefits of superimposing ultrasonic excitation during the metal forming process. A large number of investigations have since clearly reported that the principal effect of an ultrasonically assisted metal forming process is a reduction in forming load [41, 59-63].

In the fields of high power ultrasonics, the oscillatory systems which consists of an ultrasonic transducer, horn and working tool can be designed with various shapes and excited to vibrate in different vibrational modes such as longitudinal mode, torsional mode, flexural mode and composite vibrational mode [154]. The ultrasonic transducers are used to convert the electrical input signal from an

ultrasonic generator into ultrasonic vibration, the ultrasonic horn connected to the transducer is used to amplify the vibration amplitude, and the working tool is used to radiate ultrasonic energy into the workpiece. As described in Chapter 3, the ultrasonic vibration amplitude generated by the ultrasonic transducer is based on the piezoelectric effect which occurs if a rapidly reversing charge is applied to a piezoelectric material to expand or contract the material. The amplitude of material fluctuations will depend on the applied charge voltage.

The effect of ultrasonic excitation on the deformation behaviour of metals has been under investigation for many decades [24]. It was found that during deformation, the application of power ultrasonic excitation to the specimen reduces the yield strength of the material, thus reducing the forming force. Other reports in 1970s [152, 153, 155] discussed experiments on different materials to study the effect of applying ultrasonic excitation during deformation. Material softening effects were observed and it was found that the reduction in yield strength is proportional to the applied ultrasonic vibration amplitudes. Rozner [41] performed experimental studies on ultrasonic assisted strip drawing and reported reduction in forming load and coefficient of friction. They observed that the ultrasonic excitation did not affect mechanical properties or microstructure of the drawn metal. In 1998 Jimma et al. [62] investigated an ultrasonic deep drawing process and found that ultrasonic energy not only reduces the drawing force, but also increases the limiting drawing ratio. Later, Murukawa et al. [63, 114] performed experimental studies on ultrasonic assisted wire drawing by applying ultrasonic excitation in both the radial and axial directions, finding that radial vibration was more effective in decreasing the drawing force and increasing the drawing speed than axial vibration. In 2007 Ashida and Aoyama [59] performed experimental studies of press forming by using superimposed ultrasonic excitation of the die, and found that by applying ultrasonic vibration, wrinkling and cracking could be avoided.

However, these findings have not offered a conclusive explanation of the load or stress reduction mechanism. Previously, in the literature, Blaha and Langenecker [24] explained that the flow stress reduction was due to activation of dislocations during superimposed ultrasonic excitation. However, Nevill and Brotzen [25] argued that Blaha and Langenecker's work did not provide any correlation between the experimental and theoretical models of dislocation

movement and energy absorption. They proposed a model of superimposition of alternating acoustic stress to explain the stress reduction mechanism. In their study, a model of stress superposition effect was introduced as in Fig. 6-1. This model that explained to induce yield, a minimum stress, $S_{y,}$ is required. For the case of $S_y > S + A$, where S is static flow stress and A is the stress amplitude, the material would not yield. For the case of $S_y < S + A$, the material for a portion of the vibration cycle, is subjected to a total stress greater than that required to induce plastic deformation. The stress superposition effect was clarified by Kirchner et al. [36] for low frequency oscillation applied in a series of compression tests. They reported that the path of the maximum oscillatory stress will follow the path of static flow stress curve and the path of mean flow stress will be lower than and parallel to the static flow stress curve in a strain rate independent material. In a strain rate dependent material, the path of the maximum oscillatory stress will be parallel to, but can be higher than the static flow stress. This two descriptions are shown in Fig. 6-2.

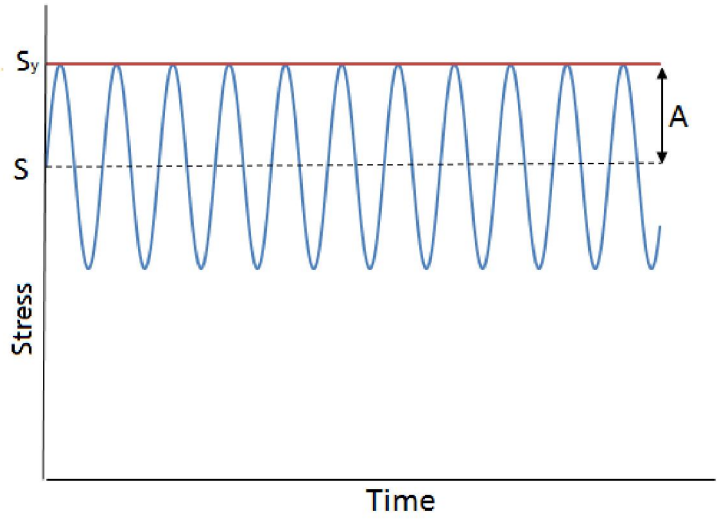

Figure 6-1 Stress superposition effects [25]

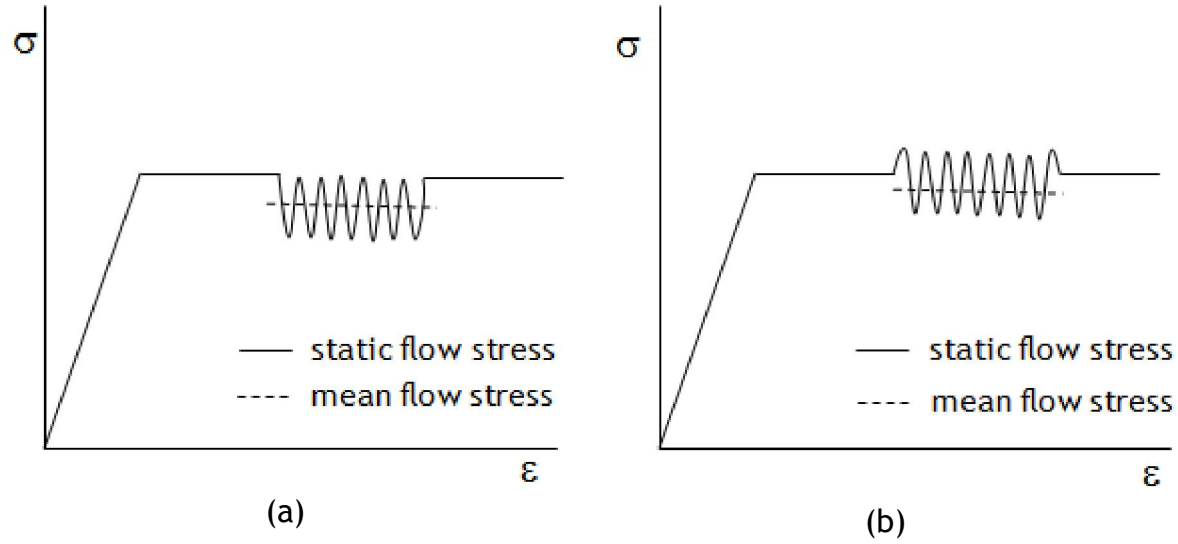

Figure 6-2 Superimposition principle where an oscillatory stress is superimposed on a static flow stress, showing (a) rate independent and (b) rate dependent elastic-plastic material [36]

This chapter aims to further the understanding behind these finding through investigating a forming test to measure the effects that superimposing ultrasonic vibrations on the die, which is tuned to a longitudinal mode at 20.8 kHz, has on the force-displacement measurements. The reason is the measurements can be directly measured from the piezoelectric force transducer and machine load cell which it does not effected by changes of contact area between punch, specimen and die when measured in the stress-strain data. Earlier studies [28, 74, 75, 81, 156] focused on the influence of ultrasonic oscillations on the internal stresses during the plastic flow of metal and as well as interfacial friction effects. Many of these studies have been associated with the development of ultrasonic metalworking processes related to industrial applications such as die forming, wire drawing and extrusion [59, 62, 63, 76, 77]. In all of these studies, the evaluation of the benefits of ultrasonic excitation relied on measurements of the mean forming force only and not on measurement of the oscillatory force during ultrasonic excitation.

Therefore, this study explains the results of a simple forming test where samples of flat sheet metals are forced into a shaped die by a shaped plunger on a test machine. The die is part of a tuned ultrasonic horn, therefore ultrasonic excitation can be applied during the tests but, crucially, tests can be performed with and without ultrasonic excitation. The design and tuning of the ultrasonic horn is achieved using finite element modelling (FEM) and experimental modal

analysis (EMA). During experimental forming tests both the plunger and piezoelectric force transducer are attached to the cross-head of the test machine of which the latter is used to measure the static-oscillatory force. The results will illustrate how ultrasonically assisted metal forming can lower the static forming force during ultrasonic excitation of the die and, further, investigate the oscillatory force during an ultrasonic forming process.

In this chapter, four sets of forming test setup were used to investigate the effect of ultrasonic excitation on the metal forming process. The design of the experiment setup was based on the forming of a single plate of metal between a shaped die and plunger. Each set of experimental setup and results is discussed in a separate section. These differences forming the test setup were used to examine the significant effects between exciting the die and exciting the punch.

6.2 The static-ultrasonic metal forming test on excited die

6.2.1 Experimental setup

In this experiment, the specimen was formed between two types of punch and die setup. The ultrasonic forming test setup is shown in Fig. 6-3 and consists of an ultrasonic transducer, a booster and an ultrasonic horn, all tuned to their first longitudinal mode of vibration at 20.8 kHz. The system was held in a structure that allowed it to be connected to the table of the Zwick Roell test machine, while the punch device consists of a punch tool and a piezoelectric force transducer which was attached to the cross-head of the Zwick Roell machine.

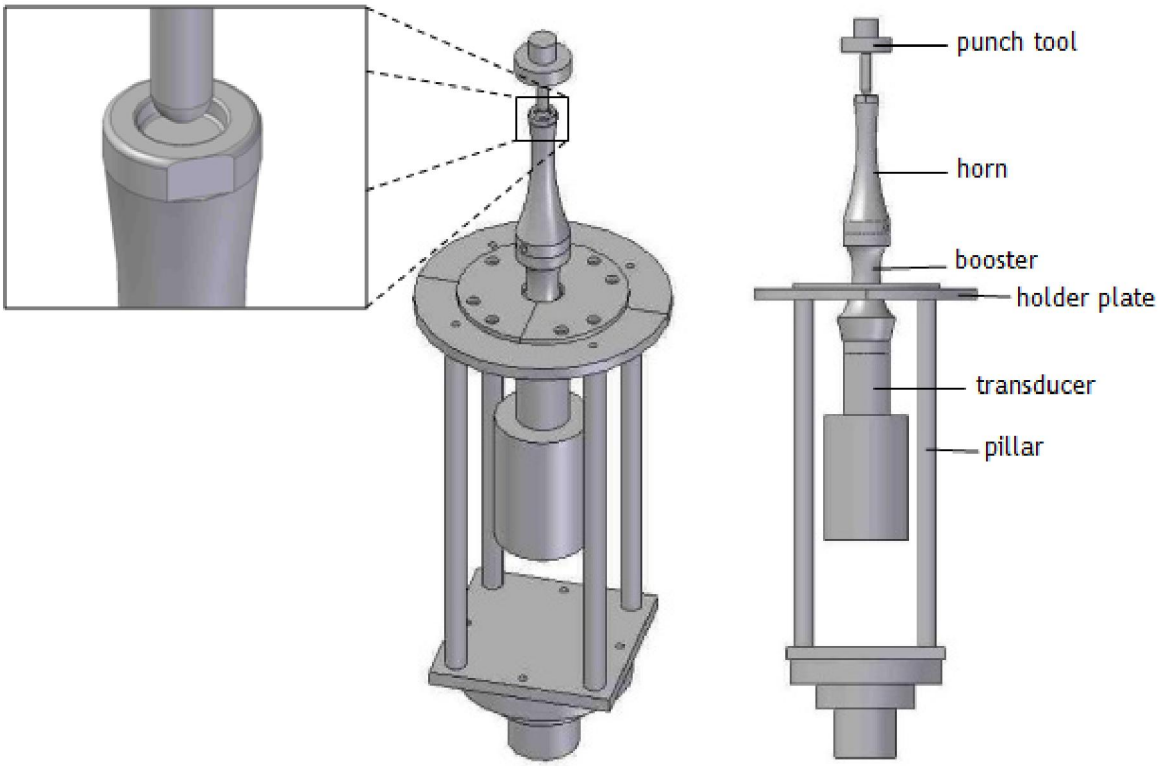

Figure 6-3 A schematic illustration of the apparatus for static and ultrasonic forming tests with insert zoom at punch tool and ultrasonic die horn.

The tuned booster was included to allow a flange to be incorporated between the transducer and the die horn in order to provide a nodal mounting to the test machine. The forming die in this study was the output end of the ultrasonic horn and is shown in the zoomed insert in Fig. 6-3. The die horn and booster were designed using FE modelling, with the booster designed using the five-element horn configuration described by Peshkovsky [137]. The die horn and booster are manufactured from titanium alloy (Ti-6Al-4V) and were modelled fully with 3D quadratic elements in Abaqus. The FE model predicted that the longitudinal mode of the booster plus die horn was 20.74 kHz, while the modal frequency determined experimentally from EMA was found to be 20.8 kHz for the longitudinal mode. The horn and booster details were discussed in Chapter 3. The ultrasonic transducer can provide ultrasonic amplitudes of up to 10 μm, depending on the generator setting, therefore the profile of the booster and horn are designed to amplify this amplitude and further allowing higher ultrasonic amplitudes to be achieved. The system was connected to a booster plate holder and four titanium alloy pillars that can be fixed to the test machine.

6.2.2 Experimental procedure

In these experiments, flat sheet metal specimens are compressed between a small bowl-shaped die and a round and a flat-nosed punch. The die consists of a tip of the ultrasonic horn tuned to a longitudinal mode at 20.8 kHz and is excited by a piezoelectric transducer. The punch tool is connected to the cross-head of a Zwick-Roell test machine which provides a constant cross-head speed of 5 mm/min. The punch profile used, shown in Fig. 6-4, consists of a round punch and a flat punch tool. A Kistler force transducer is mounted between the punch and the cross-head, as shown in Fig. 6-5, to measure the static-oscillatory force response during each test. The recorded signal response is acquired using SignalCalc ACE hardware and software for data processing. The forming tests where conducted on two different commercial metals, aluminium and die cast magnesium, so the effects of ultrasonic excitation on the forming loads could be compared.

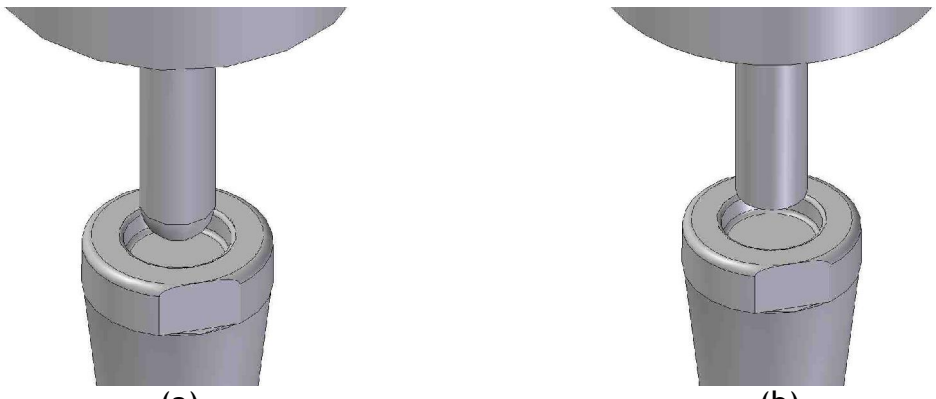

Figure 6-4 The profiles of (a) round punch and (b) flat punch tool

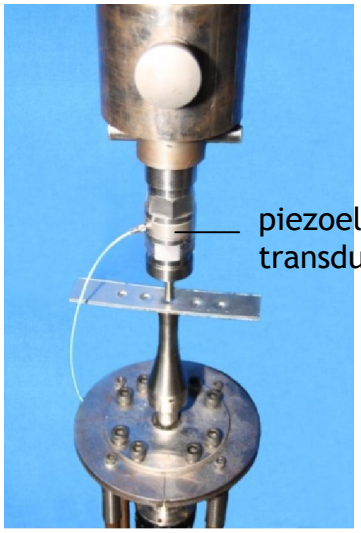

Figure 6-5 Ultrasonic metal forming test set-up

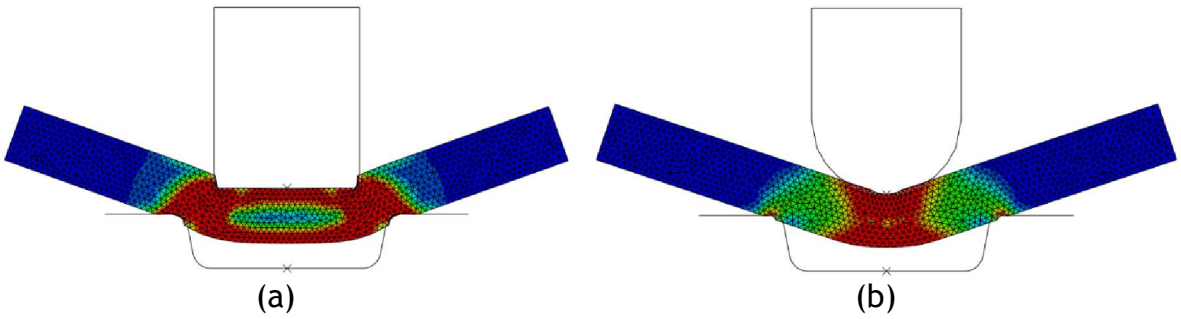

Figure 6-6 The specimen deformation by (a) flat punch and (b) round punch

The specimen was placed between the punch and die during the deformation, and is illustrated in the FE model, Fig. 6-6. Each specimen of 3 mm thick plates was cut to a size of 30 mm × 30 mm. The configuration was chosen in order to reduce the plate oscillations at its free ends. A series of static and ultrasonic forming tests were performed at a constant cross-head speed under dry surface conditions. The plate was compressed to approximately 1 mm displacement, as measured by the machine cross-head, at which point the ultrasonic excitation was applied by the ultrasonic horn. It was measured that the superimposed ultrasonic excitation is applied in the plastic deformation region.

Two sets of data were recorded during the test. The first set of force data was recorded from the load cell in the cross-head of the machine for four ultrasonic amplitudes of the horn; 5 μm, 10 μm, 15 μm and 20 μm. The second set of data was recorded for these ultrasonic amplitudes, and the forces were measured using the piezoelectric force transducer mounted between the punch and the machine cross-head. For all of the tests reported here, the tests were stopped at a cross-head displacement of 3 mm due to the die bowl height. However, the testing machine is programmed to stop if the applied load is close to exceeding the maximum limit of the piezoelectric force transducer.

6.2.3 Experimental results

Two sets of data are presented for the ultrasonic assisted forming tests. The data sets consist of a result from the test machine load cell and a couple of results from the Kitsler force transducer.

6.2.3.1 Force measurement using machine load cell on the flat punch forming test

Fig. 6-7 depicts the force-displacement curves measured for static and static-ultrasonic forming tests on the two different metal specimens. During ultrasonic excitation of the die, approximately at displacement between 1mm and 1.5mm, the mean forming force is recorded by the machine load cell and clearly exhibits a reduction in the static forming force in all tests, which was increased with ultrasonic vibration amplitude. The results in terms of the percentage reduction in the static forming force are summarised in Table 6-1.

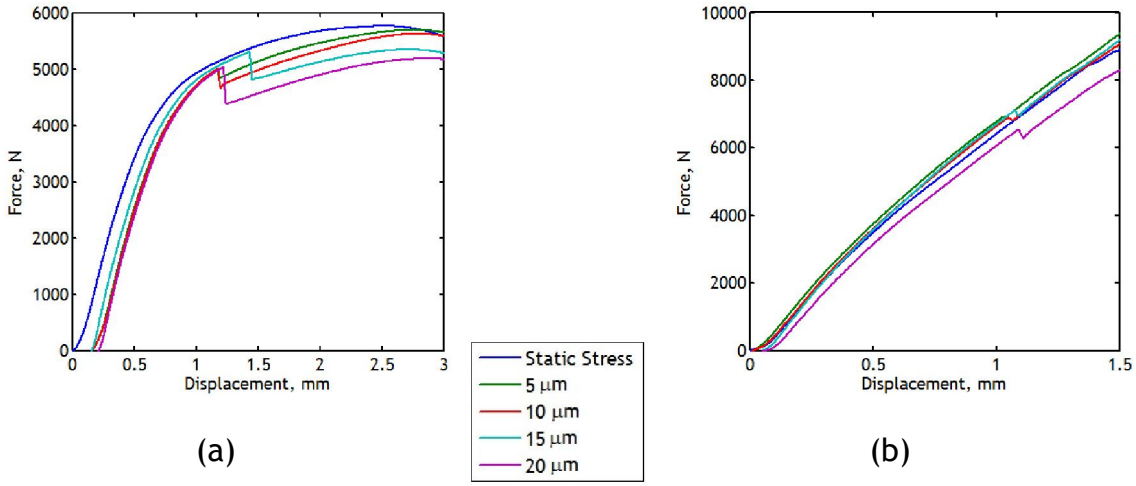

Figure 6-7 Flat punch forming tests with and without ultrasonic excitation of the die on (a) aluminium and (b) magnesium

Table 6-1 Reduction in the static forming force for the flat punch forming test

Material	Reduction in static forming force for amplitudes of			
	5 μm	10 μm	15 μm	20 μm
Aluminium	3.5 %	7 %	9.5 %	13 %
Magnesium	1.4 %	2 %	2.8 %	4.5 %

6.2.3.2 Force measurement using machine load cell on the round punch forming test

Fig. 6-8 shows force-displacement results measured by the machine load cell during static and static-ultrasonic excitation of the die for aluminium and magnesium. During the test, the static forming force was reduced by the introduction of ultrasonic excitation on the die at displacement of 1mm and the force reduction clearly increased with ultrasonic amplitude. The results in terms of the percentage reduction in static forming force when using the round punch are summarised in Table 6-2. As seen in Fig. 6-8(b) the force-displacement

curves appear in smooth line at the beginning of the deformation until displacement of 2mm, the curves start to ripple. The reason is the plate specimen starts to break after 2mm of the displacement but the punch continues deform until to the end of deformation.

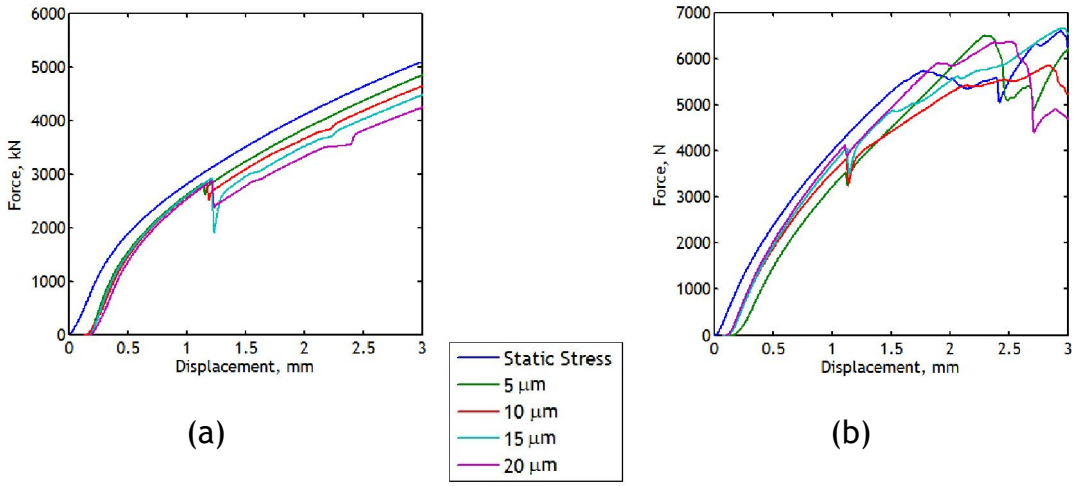

Figure 6-8 Round punch forming tests with and without ultrasonic excitation of the die on (a) aluminium and (b) magnesium

Table 6-2 Reduction in static forming force for the flat punch forming test

Material	Reduction in static forming force for amplitudes of			
	5 μm	10 μm	15 μm	20 μm
Aluminium	3.5 %	7.5 %	12 %	20 %
Magnesium	1.6 %	2.2 %	4.5 %	7 %

6.2.3.3 Mean forming force and oscillatory force measurement on the flat punch forming test using the piezoelectric force transducer

The measurement data presented in Fig. 6-9 and Fig. 6-10 show the oscillatory force and mean forming force measured by the piezoelectric force transducer for a series of ultrasonic vibration amplitudes. For each measurement, the peak-peak amplitudes of the oscillatory force during ultrasonic excitation of the die horn are summarised in Table 6-3.

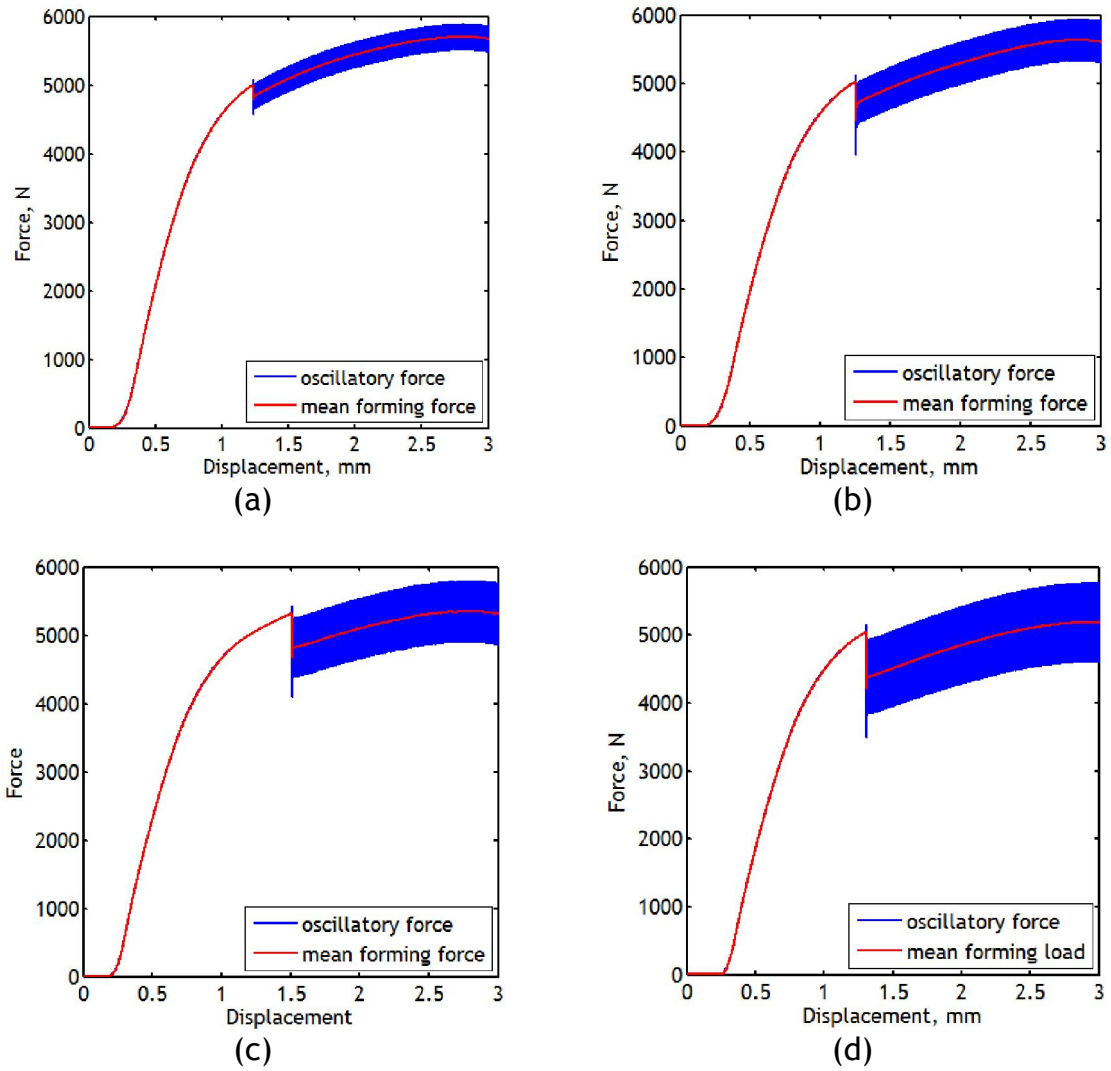

Figure 6-9 Flat punch forming tests showing the measured mean forming force and oscillatory force on aluminium for (a) 5 μm, (b) 10 μm, (c) 15 μm and (d) 20 μm ultrasonic amplitude

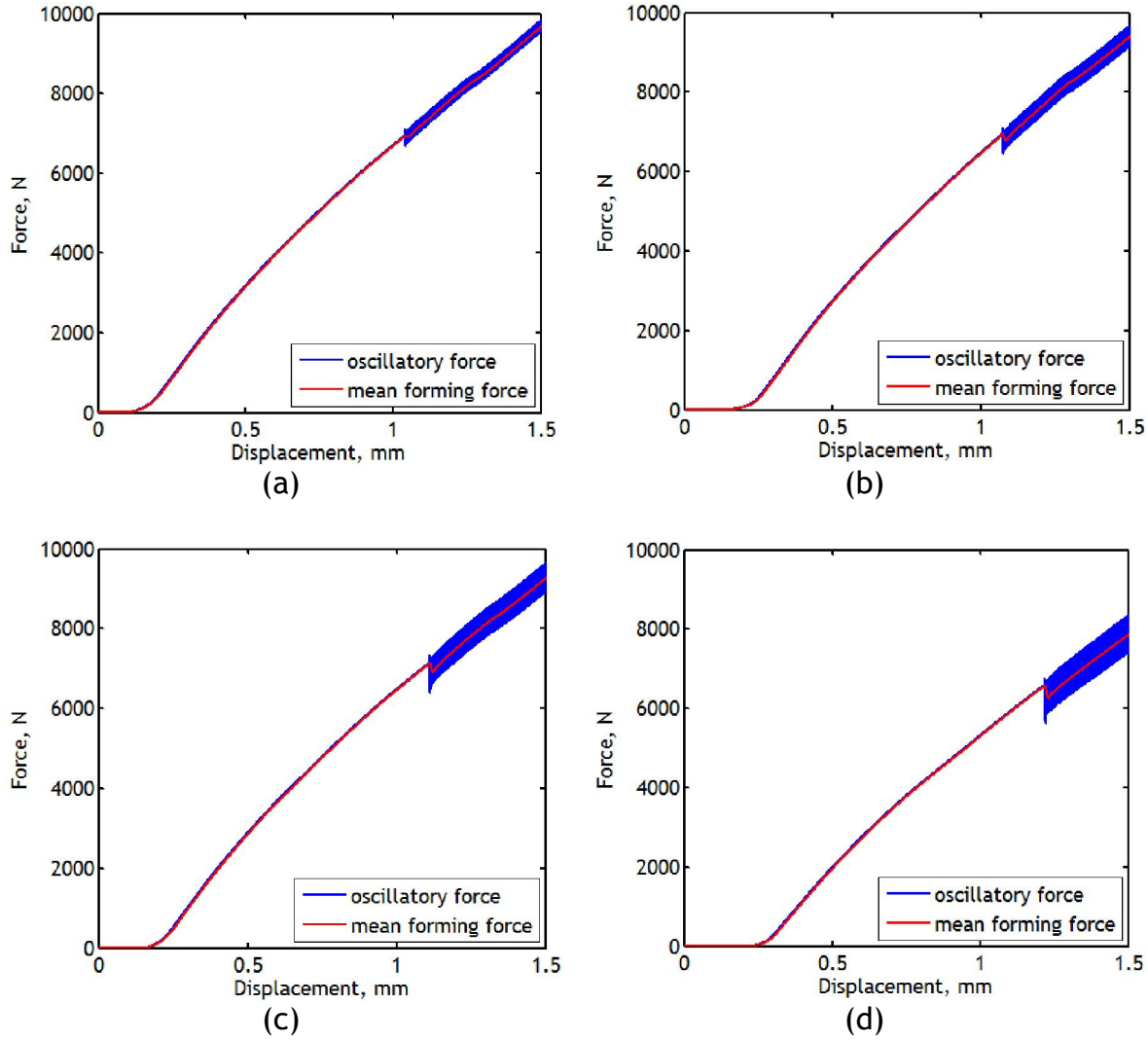

Figure 6-10 Flat punch forming tests showing the measured mean forming force and oscillatory force on magnesium for (a) 5 μm, (b) 10 μm, (c) 15 μm and (d) 20 μm ultrasonic amplitude

Table 6-3 Amplitude of peak to peak oscillatory force on the flat punch forming test

Material	Peak to peak oscillatory force for amplitude of			
	5 μm	10 μm	15 μm	20 μm
Aluminium	440 N	740 N	1060 N	1400 N
Magnesium	350 N	700 N	1000 N	1200 N

6.2.3.4 Mean forming force and oscillatory force measurement on the round punch forming test using the piezoelectric force transducer

Measurement of mean forming force and oscillatory force using a piezoelectric force transducer was repeated for the round punch forming test. Observation of oscillatory force behaviour during the forming test could be used to interpret the beneficial effects of static forming force. Fig. 6-11 and Fig. 6-12 show the force-displacement diagrams for the measurement of the mean forming force and oscillatory force during the test of aluminium and magnesium, respectively. Calculations for the peak to peak oscillatory force are summarised in Table 6.4.

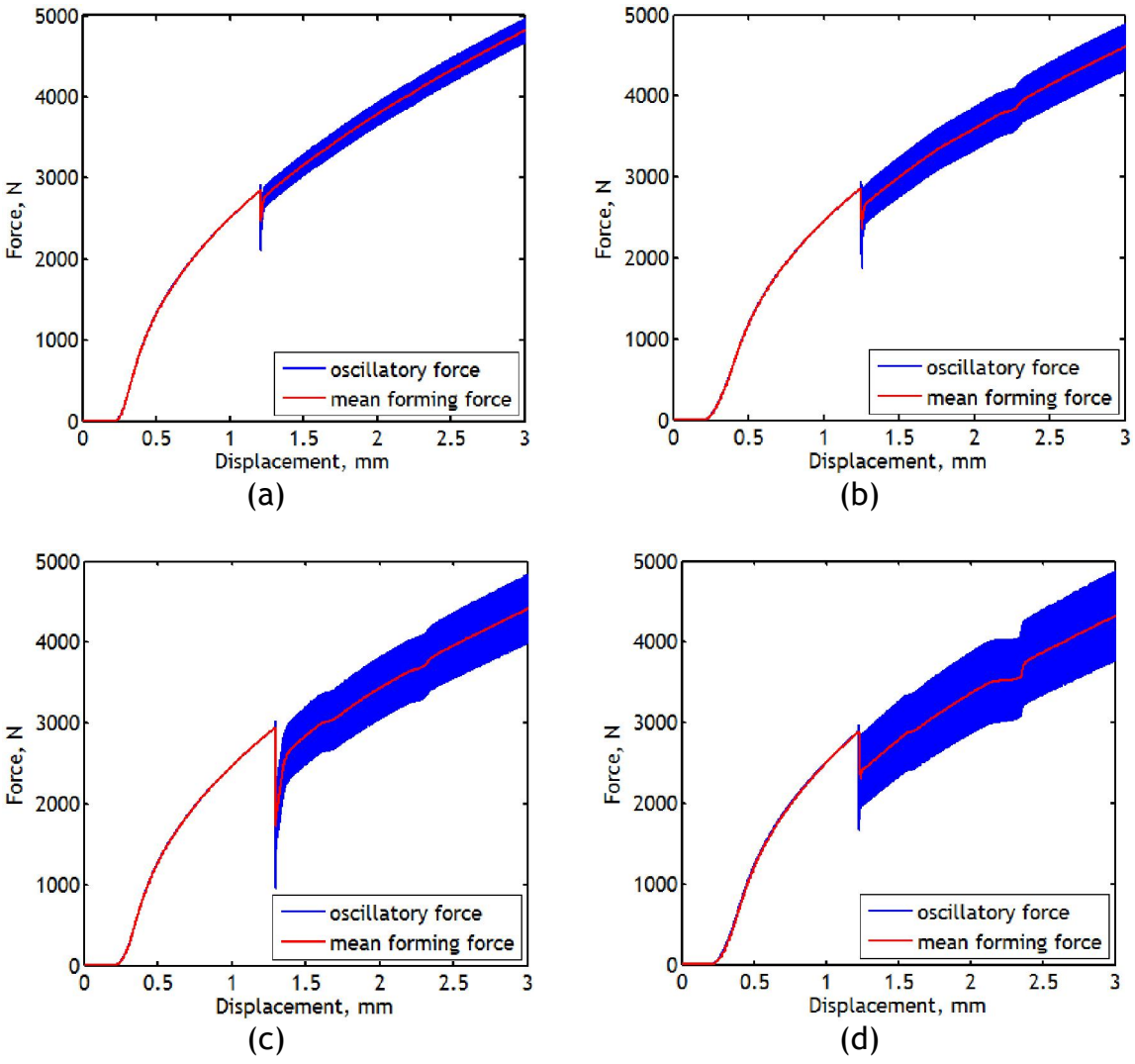

Figure 6-11 Round punch forming tests showing the measured mean forming force and oscillatory force on aluminium for (a) 5 μm, (b) 10 μm, (c) 15 μm and (d) 20 μm ultrasonic amplitude

As can be seen in Fig. 6-11 and Fig. 6-12, the measurement of mean forming force and oscillatory force did not produce a smooth force displacement curves during plastic deformation as observed in previous plots. A drop of force can be observed at between a displacement 2.0 mm and 2.5 mm in Fig. 6-11(b), (c) and (d). This can be accounted to drop in ultrasonic energy being applied to the via the transducer. This was also observed in Fig. 6-12 (b), (c) and (d) between a displacement of 1.5 mm and 2.0 mm, however, it can also be observed that in this behaviour continues above a displacement of 2.0 mm, while this was not seen above a displacement 2.5 mm in Fig. 6-11. This stems from the fact that the magnesium sample began to break at a displacement of 2 mm while the break point of aluminium sample was found to lie above the maximum displacement of 3 mm.

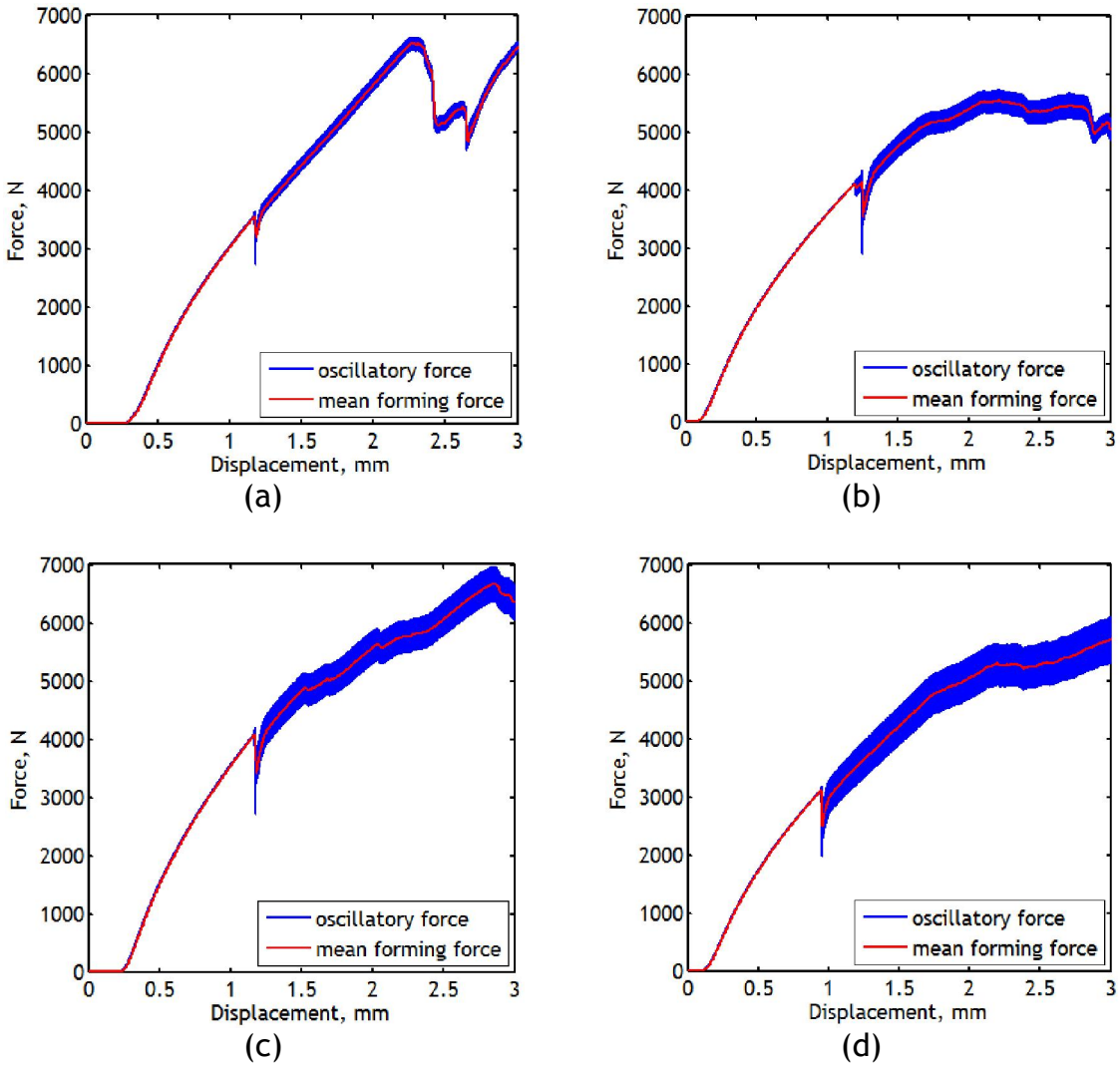

Figure 6-12 Round punch forming tests showing the measured mean forming force and oscillatory force on magnesium for (a) 5 µm, (b) 10 µm, (c) 15 µm and (d) 20 µm ultrasonic amplitude

Table 6-4 Amplitude of peak to peak oscillatory force on the round punch forming test

Material	Peak to peak oscillatory force for amplitude of			
	5 μm	10 μm	15 μm	20 μm
Aluminium	300 N	700 N	900 N	1200 N
Magnesium	200 N	350 N	500 N	800 N

6.2.4 Discussion of the effect of ultrasonic excitation on the static forming force and oscillatory force

A study of forming on single materials plates between a vibrated bowl shaped die and flat and round punches illustrated that superimposed ultrasonic excitation on a static forming test can produce beneficial effects on the material forming force. Two different commercial metals were used and four ultrasonic amplitudes were generated on the die to investigate the effect of ultrasonic excitation. The measurement results data recorded were plotted in force-displacement diagrams and it was found that the punch shape has significant influence on the static forming force which can be seen in Fig. 6-13.

In this study, the results were not measured in a true stress-strain diagram in order to explain the beneficial effect of ultrasonic excitation on the forming process. To create true stress-strain diagrams, a constant contact area, or if the contact area changes with respect to process duration, this change in area throughout the process is required. However in these experiments the change in contact could not be measured due to the shape of the die and punch.

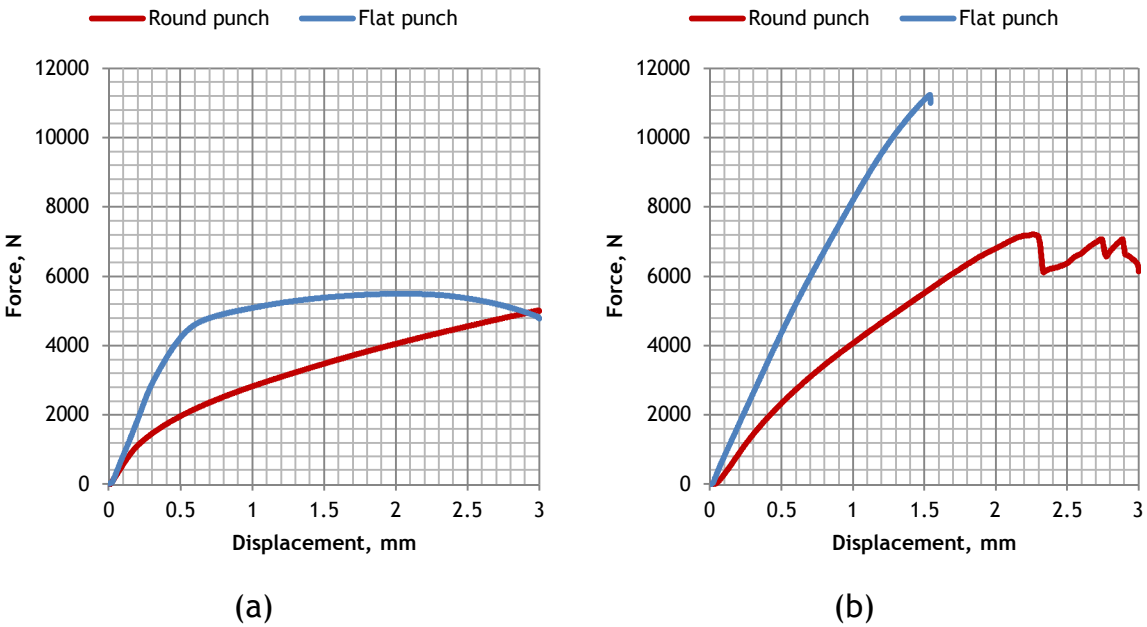

Figure 6-13 The influence of punch shape on static forming force for (a) aluminium and (b) magnesium during metal forming test

During ultrasonic excitation of the die, the mean forming force recorded by the machine load cell clearly exhibits a reduction in the material forming force in all tests, which was increased with the ultrasonic vibration amplitudes. These results demonstrate that the effect of ultrasonic excitation of the die in metal forming is highly dependent on the material and the amplitude of vibration [24, 65]. The force reduction measured is shown in Fig. 6-14 for flat punch and round punch forming tests. The reduction in material forming force is believed to occur because the vibration energy is absorbed by the material. This indicates an interaction between dislocations and the applied vibrations that enables deformation to proceed with a reduction in static forming force [75]. The movement of dislocation has been studied by Siu et al. [88] who investigated the microstructure of aluminium samples after they had undergone ultrasonic assisted indentation. It was found that samples exposed to ultrasonics during indentation exhibited enhanced subgrain formation in the microstructure after the deformation process. Siu et al. observed similar subgrain formation in samples which had undergone global heating, this suggested that subgrain formation in samples exposed to ultrasound experienced localised heating. It was also observed that dislocations could travel further in a given length of time in areas containing subgrain formation, providing evidence that ultrasonics could enhance dislocation motion.

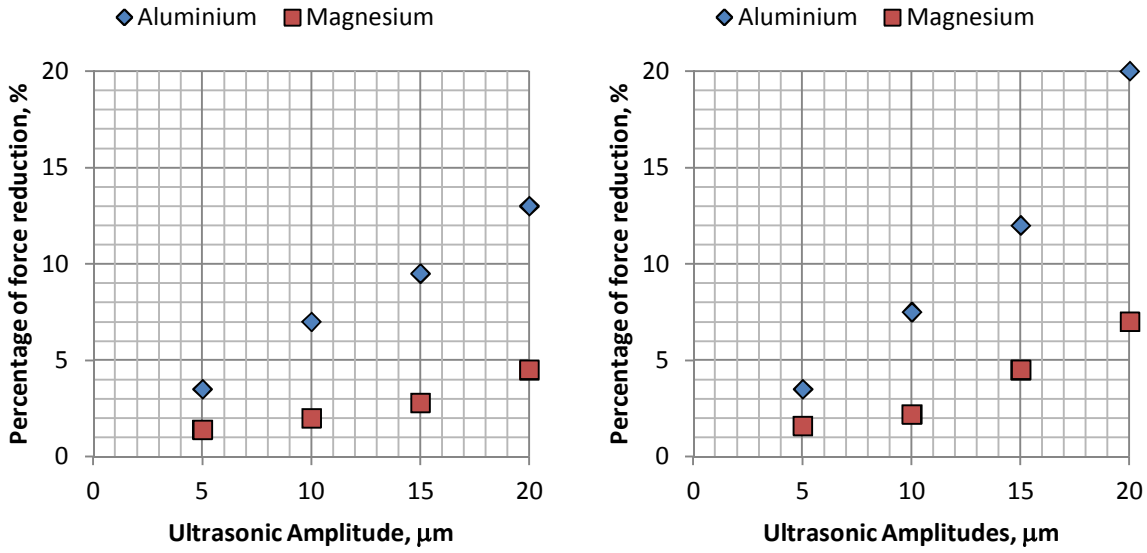

Figure 6-14 The percentage of force reduction in ultrasonic amplitudes measured in the experimental test for (a) flat punch and (b) round punch forming test

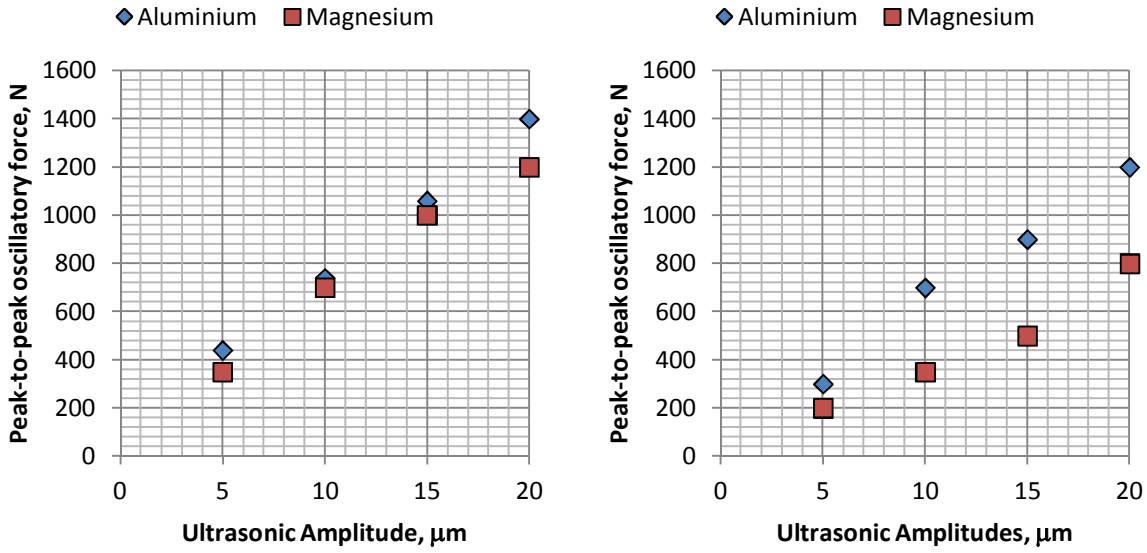

Figure 6-15 The peak-to-peak oscillatory force in ultrasonic amplitudes measured in the experimental test for (a) flat punch and (b) round punch forming test

The material softening can be explained by analyzing the oscillatory force measurements. The measurement of peak-to-peak oscillatory force is shown in Fig. 6-15 and it is seen to be proportional to ultrasonic vibration amplitudes for both the round and flat punch. It was found that the magnitude of oscillatory force is very similar for aluminium and magnesium in flat punch forming but significantly different in round punch forming.

The measured force-displacement relationship in the plate experiment followed the definition of oscillatory stress superposition as described earlier. For all experimental results shown in Fig. 6-9 to Fig. 6-11 illustrate the maximum path of oscillatory force and mean forming force are followed by the path of the static forming force curve and mean forming force which is lower than and parallel to the static force-displacement curve for aluminium, however, in magnesium the path of maximum oscillatory is observed slightly higher than static forming force but the mean forming force is recorded lower than and also parallel to the static force-displacement. Fig. 6-14 shows that the test using the round punch showed a high percentage force reduction compared to the flat punch.

On the other hand, this result also demonstrates that the effect of ultrasonic excitation of the die in metal forming is highly dependent on the material, where aluminium shows a higher percentage force reduction than die cast magnesium. It is shows that ultrasonic excitation could offer beneficial effects in terms of forming force, particularly for softer metals. For harder materials, it becomes more difficult to achieve significant forming force reduction benefits from ultrasonic energy of the forming tools because of the high forming loads required for metal forming processes. To progress these processes for harder metals, a more powerful ultrasonic transducer and generator system which can enable increased levels of ultrasonic energy into the material, should be utilised.

6.3 The static-ultrasonic metal forming test on excited die by modified ultrasonic generator system

6.3.1 Experimental setup

The same experimental setup was then performed for the second set of static-ultrasonic metal forming test as for the first set of static-ultrasonic metal forming test described in the previous section. A modification has been made to the ultrasonic generator which increases the electrical power supply to the transducer. Four more pieces of equipment were added to the experimental setup; a power amplifier, a voltage control and analyzer, transformers and a cooling fan. This new set-up of equipment can generate up to 1 kW electrical power supply to the ultrasonic transducer.

6.3.2 Experimental procedure

In this experiment, the die horn was excited by a piezoelectric transducer driven by the modified ultrasonic generator. The punch was connected to the cross-head of a Zwick-Roell test machine which provided a constant cross-head speed of 5 mm/min. After a 1 mm cross-head displacement, ultrasonic excitation was introduced. The ultrasonic amplitudes provided to the die horn were related to the range of electrical power from 100 Watts to 1000 Watts using the power amplifier. The static forming force and mean forming force were measured by the machine load cell. The tests were stopped at a cross-head displacement of 3 mm. Forming tests on two different metals were conducted to measure the effects of ultrasonic excitation of the forming die; aluminium and magnesium. In this study, the die amplitude could not be monitored due to a modification to the original 500W ultrasonic transducer system. Therefore, the amplitude of the ultrasonic die amplitude was controlled manually through a power amplifier.

In this system, the ultrasonic generator in Fig. 4-4(b) is used to supply an electrical power to the transducer was replaced to a power amplifier, voltage controller and analyser, transformers and cooling fan in order to develop a new ultrasonic system which could increase the ability to supply the electrical power up to 1kW to the transducer. Basically, the current ultrasonic generator used offers a facility of monitoring both amplitude and acoustic power and the transducer output generated at the end of transducer was controlled by the input voltage in the generator. The generator was set up to produced a limited input voltage in order to deliver at maximum amplitude of 10 μm. The new setup of ultrasonic system could increased the range of input voltage thus increased the ultrasonic amplitude. In this new ultrasonic system, the range of input voltage was monitored by changing the electrical power supply to the transducer. However, the new ultrasonic system has limit the maximum power supply at 1 kW in order to avoid damage the transducer and transformers. It was expected that the new system of generator could produce higher ultrasonic amplitudes by increased the electrical power supply to the transducer. However, in this study, the ultrasonic amplitudes were not measured due to lack of monitoring equipment and the amplitudes are difficult to control consistently throughout the ultrasonic loading.

6.3.3 Experimental results

Fig. 6-16 and Fig. 6-17 show the measured mean forming force from the round punch and flat punch forming tests for the range of power input to the transducer. These results clearly showed the static forming force reduction achievable with the modified ultrasonic generator. Fig. 6-16 and Fig. 6-17 show that the static forming force immediately drops when ultrasonic excitation is introduced at a displacement of 1mm, and can be observed for both metals. However, these results show that the path of the mean forming force was not parallel to the static forming force and it could be observed that this deviation from a parallel path was increased for increased power.

During superimposed ultrasonic excitation, it was noticed that specimen temperature was increased and it was also found that the material was softened around the outer circle of the deformation. This effect is due to thermal softening due to friction [90] where friction at the interface causes heat generation . In this study, it was found that the superimposed ultrasonic excitation reduces the material's yield force significantly. However, the force reduction effect was not only influenced by reduction in forming force but also by the surface effect of relative motion of surfaces, where there are significant temperature rises then softening due to frictional heating should also be incorporated as a material softening effects [90]. The high temperature is a feature of the higher input power and was not a feature of results using the lower power system. In this study, the temperature rise was not expected occurred during the experimental test therefore the heat generated on the material was not measured even it was a major concern during the superimposed ultrasonic excitation on metal forming.

Table 6-5 and Table 6-6 present the percentage force reduction for aluminium and magnesium samples during round punch and flat punch forming tests, while Fig. 6-18(a) and (b) show the force reduction against input power. It can be observed that the material forming force reduction increased in proportion with the electrical power, however, it was found that during superimposed ultrasonic excitation, it was difficult to retain consistent vibration ultrasonic energy to the material. It can also be seen that the modified system achieved a very significant reduction in static forming force for both metals tested. The inconsistency in ultrasonic energy can be seen in Fig. 6-16 and Fig. 6-17 for both aluminium and magnesium which as the force-displacement diagram does not provide smooth curve under superimposed ultrasonic excitation. This condition is obviously occurred with higher input power. However, Fig. 6-16(b) shows that when the magnesium specimen was compressed by the round punch it broke at a displacement of 2.5 mm and which can be seen as ripple lines in the trace. As there is a widening between the static and mean forming forces, the percentage drop of force was measured at the point at which ultrasonics was applied. This allowed comparisons to be made between the drop in force at each power level.

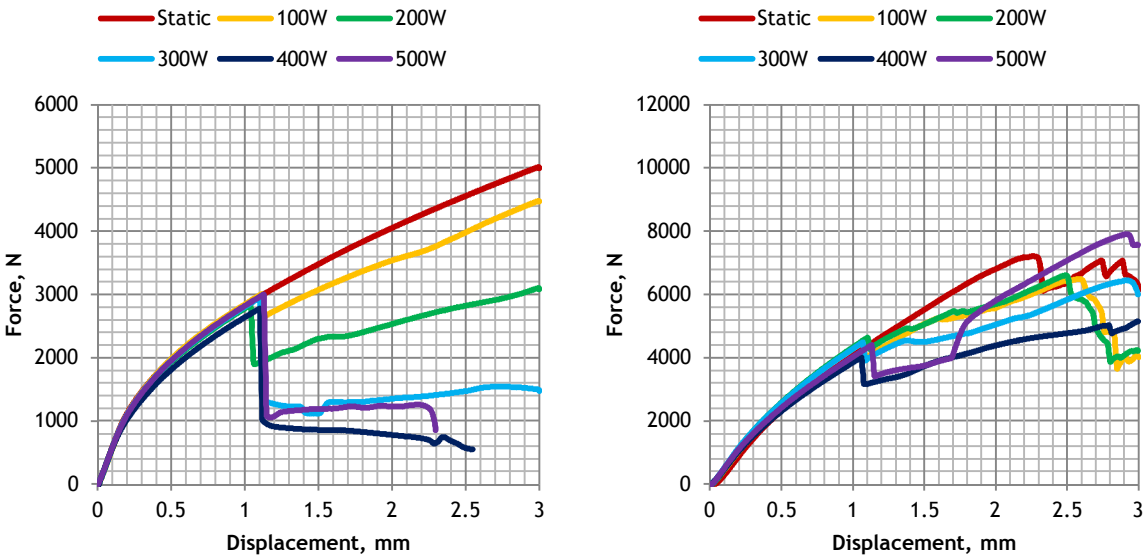

Figure 6-16 Measured mean forming force by electrical power supplied to ultrasonic generator for (a) aluminium and (b) magnesium on round forming punch

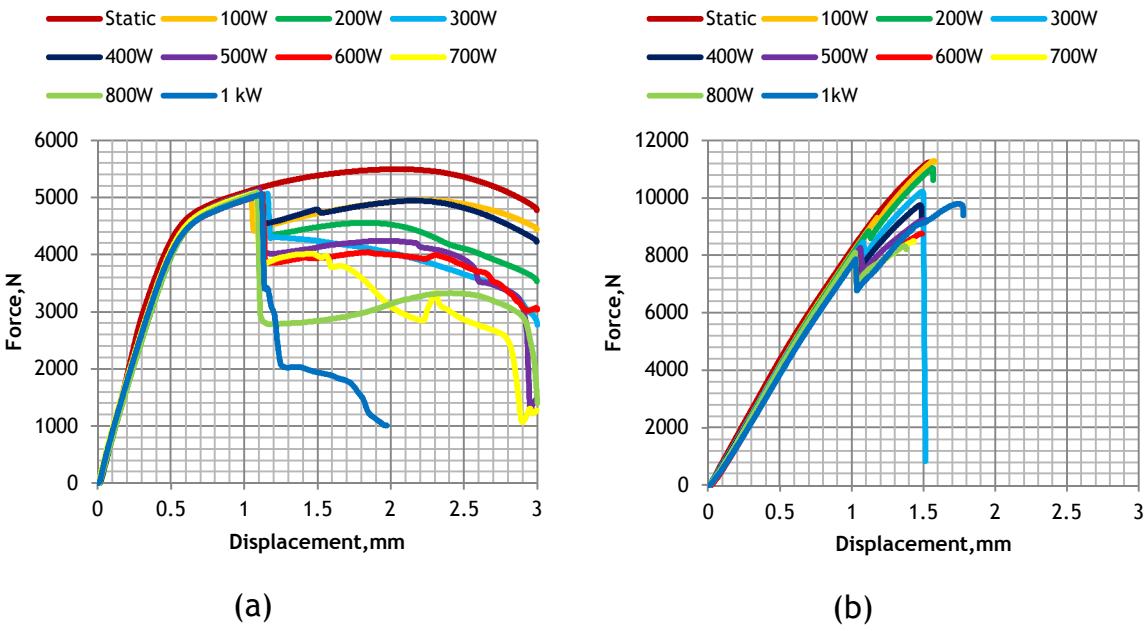

Figure 6-17 Measured mean forming force by electrical power supplied to ultrasonic generator for (a) aluminium and (b) magnesium on flat forming punch

Table 6-5 Reduction in mean forming force by electrical power supplied to ultrasonic generator on the round punch forming test

Power intensity of ultrasonic transducer	Reduction in mean forming force for material of	
	Aluminium	Magnesium
100 Watts	10 %	1 %
200 Watts	30 %	5 %
300 Watts	50 %	10 %
400 Watts	60 %	18 %
500 Watts	67 %	22 %

Table 6-6 Reduction in mean forming force by electrical power supplied to ultrasonic generator on the flat punch forming test

Power intensity of ultrasonic transducer	Reduction in mean forming force for material of	
	Aluminium	Magnesium
100 Watts	13 %	0.8 %
200 Watts	15 %	3 %
300 Watts	16 %	6.3 %
400 Watts	12 %	7.5 %
500 Watts	22 %	10.2 %
600 Watts	24 %	12.7 %
700 Watts	25 %	14.1 %
800 watts	45 %	14 %
1000 Watts	60 %	15 %

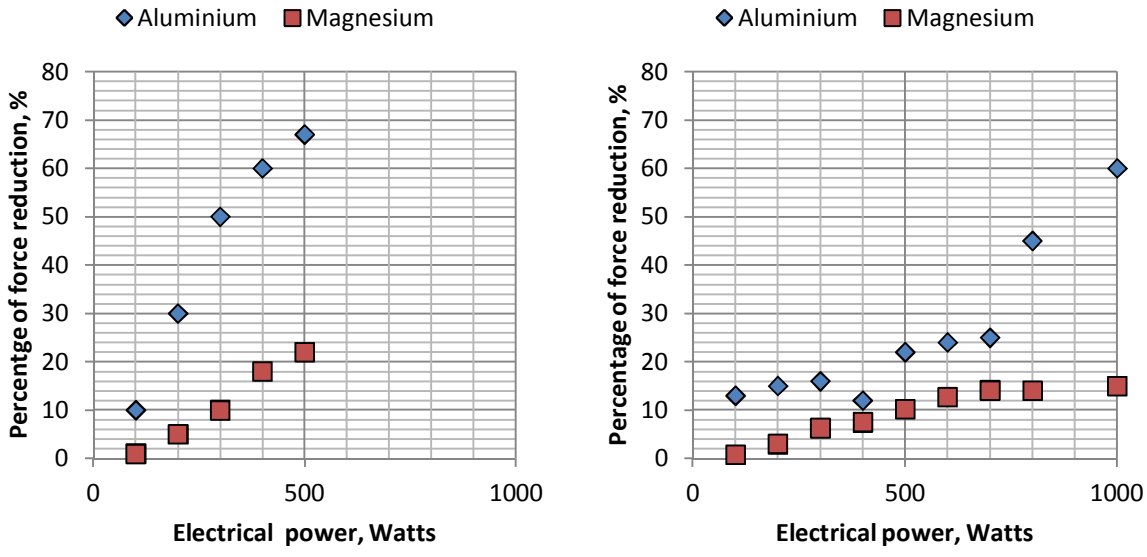

(a) (b)

Figure 6-18 Force reduction with electrical power supplied to ultrasonic transducer on (a) round punch and (b) flat punch forming test

6.4 The static-ultrasonic metal forming test on excited punch

6.4.1 Experimental setup

A similar set-up was used in the third set of static-ultrasonic metal forming test as the first set of static-ultrasonic metal forming test described in previous section of 6.2. The setup of the third ultrasonic forming test is shown in Fig. 6-19. In these experiments, the positions of the punch and die were inverted. The shaped punch consists of the tip of the ultrasonic horn which is tuned to a longitudinal mode at 20.8 kHz. The ultrasonic punch profile used is shown in Fig. 6-20. In this case a tuned punch is excited at 20.8 kHz during the forming test and the bowl shaped die is moved by the machine cross-head.

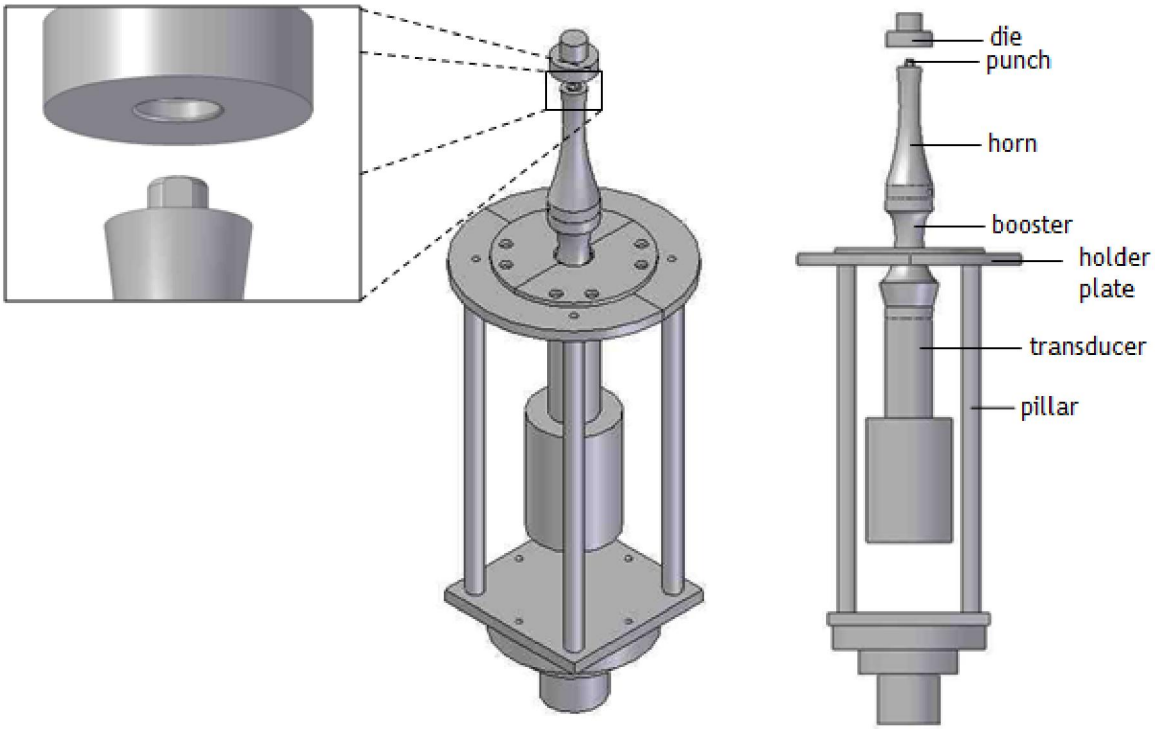

Figure 6-19 A schematic illustration of the apparatus for static and ultrasonic forming tests with insert zoom at bowl die and ultrasonic punch.

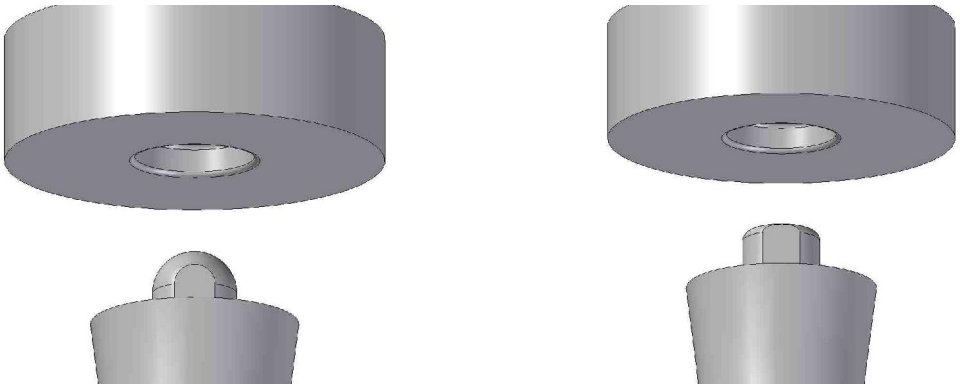

Figure 6-20 The profiles of the ultrasonic (a) round punch and (b) flat punch

6.4.2 Experimental procedure

The ultrasonic punch horn was excited by the 500W piezoelectric transducer. The die was connected to the cross-head of a Zwick-Roell test machine which provided a constant cross-head speed of 5 mm/min during measurements. Forming tests on flat 3mm thick plates manufactured from aluminium and magnesium were conducted to measure the effects of ultrasonic excitation of the forming punch. A series of static and ultrasonic forming tests were performed at ultrasonic vibration amplitudes of the punch horn between 5 μm and 20 μm. In these experiments, the specimen was compressed to approximately 1 mm displacement of die as measured by the machine cross-head, at which point ultrasonic excitation was introduced to the ultrasonic punch horn. The die was continuously loaded for 3 mm displacement. The static forming force and mean forming force were measured by the machine load cell.

6.4.3 Experimental results

Two sets of material forming force data were recorded from the machine load cell, and the force-displacement data can be seen in Fig. 6-21 and Fig. 6-22. The calculated force reduction is summarised in Table 6-7.

Fig. 6-21 and Fig. 6-22 show that the static forming force dropped immediately after the ultrasonic excitation was introduced for the flat and the round punch, while the force reduction was shown to almost linearly increase with the ultrasonic vibration amplitude, Fig. 6-23. This result illustrated that a vibrated round punch more effectively reduces material forming force during the superimposed ultrasonic excitation compared to the result achieved by the vibrated die as described in the previous section. It was believed that there are good coupling between the bowl die, specimen and vibration punch, where the ultrasonic energy was fully absorbed by the material, enabling the deformation to proceed at a lower forming force.

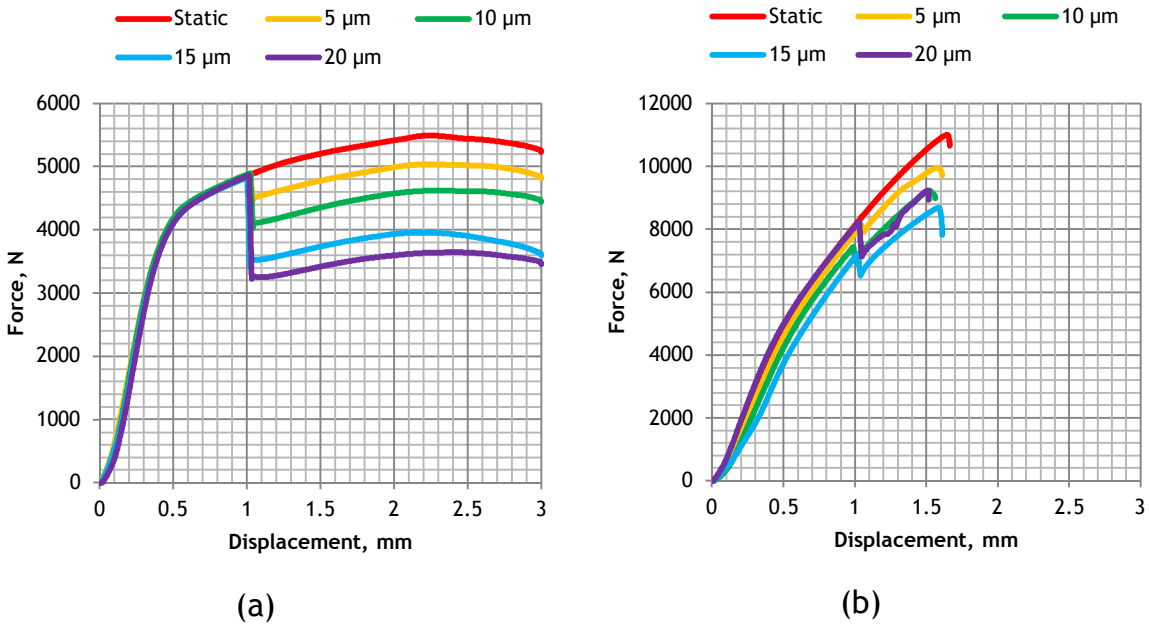

Figure 6-21 Forming tests with and without ultrasonic excitation of the flat punch on (a) aluminium and (b) magnesium

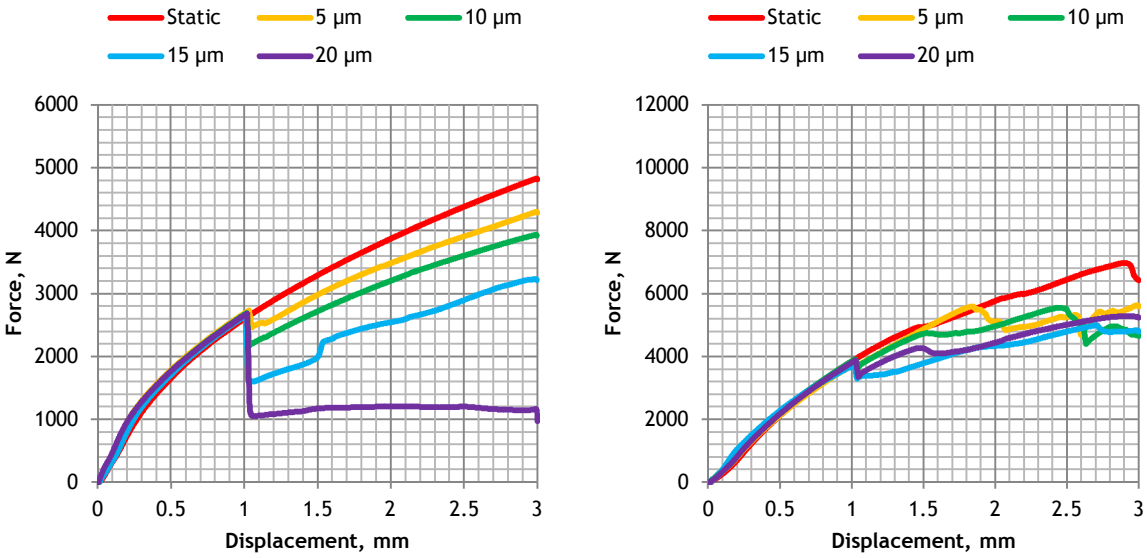

Figure 6-22 Forming tests with and without ultrasonic excitation of the round punch on (a) aluminium and (b) magnesium

Table 6-7 Force reduction on a vibratory punch forming test

Material	Ultrasonic amplitude	Reduction in mean forming force for a type punch of	
		Round	Flat
Aluminium	5 µm	9 %	7 %
	10 µm	18 %	16 %
	15 µm	40 %	27.4 %
	20 µm	60 %	33 %
Magnesium	5 µm	2.5 %	1 %
	10 µm	7 %	4 %
	15 µm	11 %	7 %
	20 µm	13.5 %	12 %

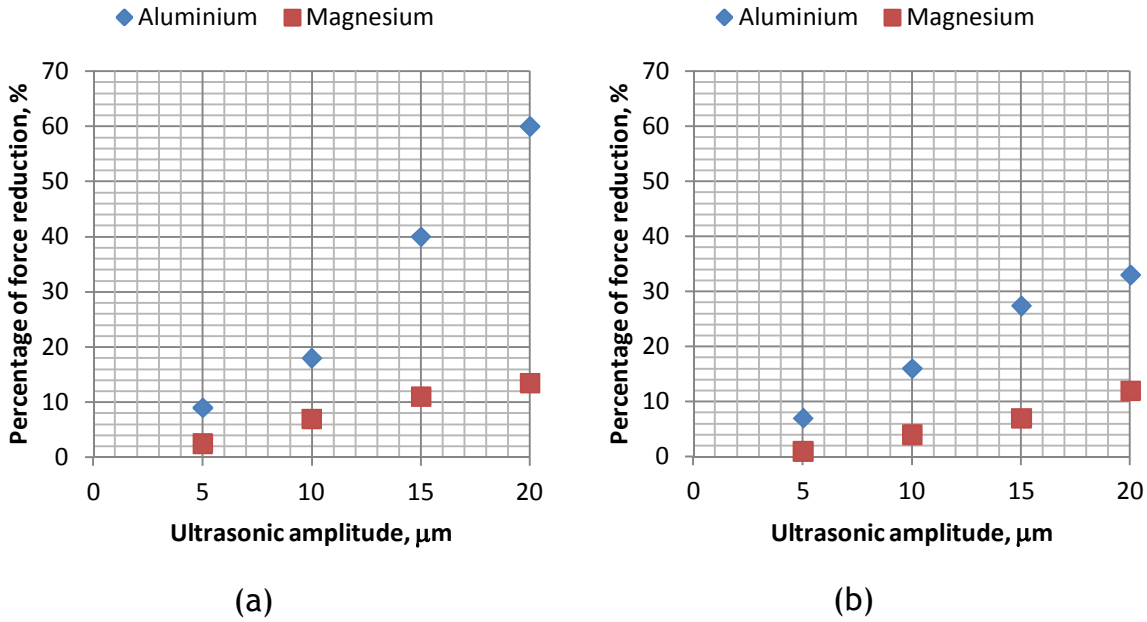

Figure 6-23 Force reduction to ultrasonic amplitudes on the static forming test for (a) round punch and (b) flat punch

6.5 The static-ultrasonic metal forming test on excited die in different loading speed

6.5.1 Experimental setup and procedure

The same experimental setup was then performed for the fourth set of static-ultrasonic metal forming test as for the first set of static-ultrasonic metal forming test described in the previous section. An investigation into the effect of force reduction during superimposed ultrasonic excitation during static forming tests with respect to forming speed was carried out. In this study, the specimen was pressed by into the die form using round punch. After a 1 mm punch displacement, the die was ultrasonically vibrated at 20 μm along the axial direction during the process until 3 mm punch displacement. The range of speed was taken as 10 mm/min, 20 mm/min and 30 mm/min of machine cross-head

speeds. The static forming force and mean forming force were measured by the machine load cell.

6.5.2 Experimental result and discussion

Force reduction in forming speed changes is shown in Fig. 6-24 for aluminium and magnesium specimen. The measurement of force reduction with forming speeds are summarised in Table 6-8.

Fig. 6-24 shows that static forming force reduced when a 20 μm ultrasonic amplitude was introduced on the die and the path of mean forming force was observed parallel to the path of static forming force for all the forming speeds applied to the aluminium and magnesium specimens. It was found that the force reduction on metal forming process does not change with the forming speeds applied. This result shows an agreement with previous studies [30, 37, 65, 67] where the effect of forming speed was independent to the effectiveness of the superimposed ultrasonic excitation during the forming test until the forming speed reached the critical maximum forming speed. The critical maximum forming speed was calculated as $V_{critical} = 2\pi af$ where a is the amplitude and f is the tuned frequency. However, in this experimental test, the forming speed could not exceed 30 mm/min because of constraints in adequately supplying the ultrasonic energy from the piezoelectric transducer during the forming test.

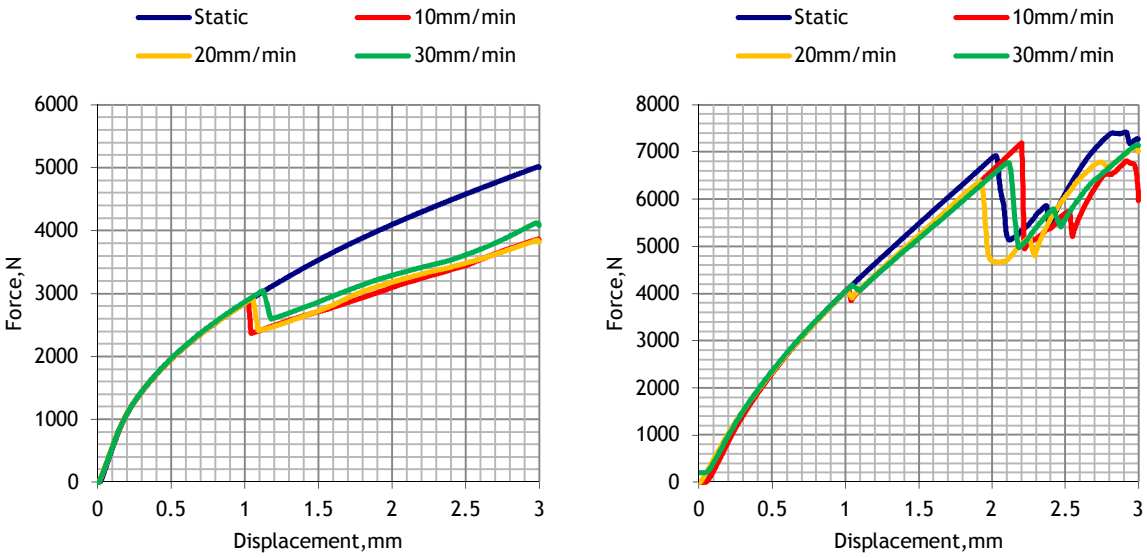

Figure 6-24 Force reduction in forming speed changed for (a) aluminium and (b) magnesium specimens at 20 μm

Table 6-8 Percentage of force reduction in forming speeds

Material	Machine cross-head speed	Percentage of force reduction measured by machine load cell
Aluminium	10 mm/min	18.5%
	20 mm/min	18.5%
	30 mm/min	15%
Magnesium	10 mm/min	5.5%
	20 mm/min	5%
	30 mm/min	5.5%

6.6 Conclusion

The effects of the application of ultrasonic excitation in forming test on single metal plate have been investigated. During plastic deformation, longitudinal mode ultrasonic oscillations were superimposed on both shaped die and punch where different type of shaped punch applied. Four sets of static-ultrasonic metal forming test were carried out. The material static forming force, mean forming force and oscillatory force were measured during the ultrasonically assisted forming test. It can be concluded that the material static forming force was reduced by the ultrasonic excitation which applied on shaped punch and die tool. This result agreed with previous studies of metal forming processes showing that the material forming force is reduced by ultrasonic vibration of the forming tool and it was shown from measurement of the oscillatory force that a reduction in the material forming force is directly indicate of a benefit of ultrasonic excitation which is the path of maximum oscillatory force was observed to be parallel or below the path of static forming force in most cases. Better ultrasonic excitation systems were carried out in order to require more effectively couple the ultrasonic energy into materials which shows that the material mean forming force are significantly reduced during superimposed ultrasonic excitation on either punch tool or die horn.

A study of the effect of ultrasonic excitation on the deformation behaviour of metal plates were investigated where forming force reduction was a major effect occurred during the superimposed ultrasonic excitation. Material softening effects were observed and it was found that the reduction in forming force is proportional to the applied ultrasonic vibration amplitudes. The material softening was generated by mechanisms of volume effect and surface effect which are influenced by the internal stresses during the plastic flow of metal and interfacial friction effect between the motion of tool and specimen. Further study on the mechanisms of volume effect and surface effect could provided a significant information since the constraints of changes of contact area, model of metal plate behaviours and monitoring measurement for ultrasonic amplitudes and material temperature can be solved.

CHAPTER 7

CONCLUSIONS

7.1 Conclusions

This thesis has presented experimental and finite element (FE) analyses of the static and ultrasonic forming of two metals; aluminium and magnesium. In this research, simple compression and forming tests were designed and the effects of superimposing ultrasonic vibrations on the tool and die, which is tuned to a longitudinal mode at 20.8 kHz, were studied via stress-strain measurements. Ultimately, a characterisation of superimposed ultrasonic excitation behaviour on static compression and forming tests was achieved. Findings on the effectiveness of ultrasonic excitation led the study to recognize that the lack of understanding of the effects of ultrasonic vibrations on the forming process has resulted in difficulties in maximising the benefits and applications of this technology. The results of this study illustrate how ultrasonically assisted metal forming can result in a lowering of the static flow stress, and the study shows how the benefits of ultrasonic excitation depend on the specimen material properties and the ultrasonic excitation parameters.

This thesis has concluded that evaluation of the benefits of ultrasonic excitation not only relies on measurements of the mean flow stress but also on measurement of the oscillatory stress during ultrasonic excitation. An analysis of the oscillatory stress measurements, especially of the paths of maximum oscillatory stress and mean flow stress in the stress-strain diagram, provided information to explain the contributions of material softening and friction effects. This study has investigated the use of ultrasonic vibrations in metal forming, which were characterised by an effective softening of the material properties during the intervals of superimposed ultrasonic excitation. The magnitude of the stress reduction in the metal specimens was shown to be

dependant on the relationship of elastic-plastic deformation and on the amplitude of the ultrasonic vibration.

The study began with the design of an ultrasonic excitation system, including ultrasonic booster and horn, all tuned to their first longitudinal mode of vibration at 20.8 kHz. The system was designed using analytical solutions and numerical finite element analysis, and was verified by experimental modal analysis.

Subsequently, the experiments and FE model of an ultrasonic compression test were setup and developed in order to investigate the material softening mechanisms during superimposed ultrasonic excitation. In the static and ultrasonic compression tests, the metal specimens were compressed between two flat platens under dry surface conditions in plastic deformation. Consequently, a significant stress reduction was exhibited under ultrasonic excitation. The characteristics of the material softening effects were then illustrated in the stress-strain diagram by plotting the mean flow stress path and oscillatory stress curve. Material model parameters were developed from the experimental results using stress-strain behaviour data which provided the value of the material dependent constant, K and coefficient of friction, μ.

An FE model was developed using these material model parameters which were identified from the experimental analysis. In this numerical study, the magnitude of the oscillatory stress, the maximum oscillatory stress and the mean flow stress were predicted during a simulation of superimposed ultrasonic excitation on the metal compression test. The FE model was used to investigate numerically the influence of the volume effect and surface effect on the resulting stress-strain relationship. This was achieved by adjusting the material property and contact condition parameters in the FE model to provide a match between experimental and numerical analysis data.

The FE model allowed the influence of the volume effect and surface effect to be studied separately. It was found that, in achieving a close match between experimental and numerical data, the volume effect significantly dominated the resulting oscillatory stress data during superimposed ultrasonic excitation in plastic deformation. Also, analysis of the oscillatory stress was shown to provide

a more meaningful interpretation of superimposed ultrasonic excitation on metal plastic deformation. In this case, the path of the mean oscillatory stress was demonstrated to be parallel to the static flow stress path, but the path of the maximum oscillatory stress was parallel but significantly lower than the static flow stress path. The FE models allowed it to be shown that this behaviour was a clear indication of an effective material softening, since a simple superimposition of ultrasonic excitation would result in a path of maximum oscillatory stress following the path of the static stress curve in the stress-strain diagram. A calculation of the ratio of percentage stress reduction to ultrasonic vibration amplitude provided a method for determining the beneficial effects obtainable for different materials.

Similarly, the influence of superimposed ultrasonic excitation was studied in the elastic deformation region of the metals. Similar experimental procedures and FE methods were adopted as for the study in the plastic deformation region to investigate the occurrence of stress reduction during elastic deformation. Adjustments to the material properties and contact conditions were again made in the FE model, but this time in the elastic region of the stress-strain diagram, to allow a match of experimental and numerical stress-strain data and to allow a study of the separate influences of the volume and surface effects during ultrasonic excitation. In this case, the surface effect mechanism dominated the resulting oscillatory stress-strain relationship. Again, in the elastic region, the softer metal exhibited a higher percentage of mean stress reduction than the harder metal. However, a significant difference observed in the elastic region for the oscillatory stress behaviour was that the path of the maximum oscillatory stress was parallel to but exceeded the static flow stress path, with this overshoot clearly observed for most of the tests.

The FE simulation in the elastic-plastic result on compression test was predicted the stress reduction in the elastic region is dominated by friction and causes overshoot and plastic region is dominated by material properties and results in undershoot. Furthermore, there were three significant mechanisms of material softening; oscillatory stress, stress reduction and friction reduction were clearly identified and analyzed. This phenomenon was explained by a mechanism of superimposition of steady and alternating stress where the oscillatory stress was significantly reduced the mean flow stress with softening effect resulted the

path of maximum oscillatory stress lowered than static flow stress in plastic region. However, the mechanism of stress superposition was not significant in elastic region caused the reduction in mean flow stress was very small compared to the amount of peak-to-peak oscillatory stress resulted the path of maximum oscillatory stress exceeded than static flow stress.

For both studies, in the elastic and plastic regions, the percentage reduction in mean stress was nearly proportional to the ultrasonic vibration amplitudes for both metals studied.

A force reduction in ultrasonic metal forming was further investigated by conducting a simple plate forming test with a shaped punch and die. It was found that the mean forming force was reduced under superimposed ultrasonic excitation. The oscillatory force behaviour showed the path of the maximum oscillatory force to be parallel to or lower than the static forming force, depending on the metal used. Further investigation of force reduction was studied by changing the experimental setup conditions, in one set of tests by using a higher power ultrasonic transducer and in another set of tests by tuning the punch rather than the die. For all test configurations, the mean forming force was reduced for increased ultrasonic vibration amplitude. It was also shown that good coupling between punch, specimen and die was optimal for coupling the ultrasonic energy effectively into the metal specimens during ultrasonic excitation, allowing very significant mean forming force reductions to be achieved.

7.2 Summary of findings and innovations

This study has provided detailed measurements and simulations of the effective influential characteristics of metal specimen deformation under ultrasonic excitation, such as static flow stress, oscillatory stress, mean flow stress and maximum oscillatory stress, in the elastic and plastic deformation regions. Such stress-strain behaviour data provide a meaningful interpretation of the

application of ultrasonic excitation in metal forming in terms of the volume and surface effects.

The present study has introduced the use of an ultrasonic booster, horn and high power ultrasonic transducer to generate high ultrasonic vibration amplitudes on the ultrasonic tool. The use of various different power intensities in this study using a higher power transducer was introduced for the first time. It was determined in this study that the higher ultrasonic vibration amplitude allows very significantly reductions in the mean flow stress to be achieved. This beneficial effect described in this thesis provides the foundation for ultrasonic tool and die design which could be utilised to enable much higher power ultrasonic forming to be achieved for more difficult to form metals.

7.3 Future works

Superimposed ultrasonic excitation on metal forming processes is believed to be capable of providing significant advantages in the areas of metal processing and manufacturing.

Further explanation is required on the specimen temperature rise during superimposed ultrasonic excitation on a simple forming test using a high power transducer, as discussed in Chapter 6, where a sample of flat sheet metal is forced into a shaped punch tool by an ultrasonic die on a test machine. A study on the characterisation of the temperature rise during the forming test may define the frictional heating mechanism and help to understand whether this aids or hinders application of this technology to more complex forming processes. In this work, the results are based on assumption that there are no temperature changes throughout all tests. Therefore the temperature changes could be further monitored and maintained in order to better explanation the effects of ultrasonic excitation on metal forming process.

In this study, all the findings throughout the thesis are focused on an appearance of material softening when superimposed ultrasonic excitation on metal forming process by measured the stress reduction, oscillatory stress and the path of maximum oscillatory stress in stress-strain diagram. There are no other evidence apart from the stress-strain data. Real time metallurgical or micro structure analysis could be studied to further prove the finding from this work.

Application of the high power ultrasonic technique in forming processes requires the use of specifically designed ultrasonic components to correctly transmit the energy from the transducer to the workpiece and die interface. Improvements in the design of the ultrasonic excitation system, especially amplitude control under high static loads, could provide a higher range of ultrasonic amplitudes.

Defining the material properties in FE modelling effectively defines the behaviour of the materials in the numerical analysis. The post-yield behaviour of the materials is specified using the classical metal plasticity model in Abaqus, the isotropic hardening model, the linear kinematic cyclic hardening model, the Johnson-Cook hardening model and the nonlinear isotropic/kinematic hardening model. Understanding and development of a more suitable plastic hardening model to correlate the measured and numerical data can provide for improved simulations of ultrasonic forming tests.

APPENDIX

LIST OF PUBLICATIONS

1. Abdul Aziz, S. and Lucas, M., *The effect of ultrasonic excitation in metal forming tests.* Applied Mechanics and Materials, 2010. **24-25**: p. 311-316.

2. Abdul Aziz, S. and Lucas, M., *A study of an ultrasonically assisted metal forming test.* AIP Conference Proceedings, 2011. **1315**: p. 733.

3. Abdul Aziz, S. and Lucas, M., *Characterising the acoustoplastic effect in an ultrasonically assisted metal forming process.* International Symposium On Ultrasound in the Control of Industrial Processes , 2012 (Spain).

REFERENCES

[1] *A dictionary of physics*. 2009, Oxford University Press: Oxford Reference Online.

[2] Mason, W.P., *Sonics and ultrasonics: Early history and applications*. IEEE Transactions on Sonics and Ultrasonics, 1976. SU-23(4).

[3] Galton, F., *Inquiries into human faculty and development* 1883, London: MacMillan.

[4] Lucas, M., Gachagan, A. and Cardoni, A., *Research applications and opportunities in power ultrasonics*. Proceedings of the Institution of Mechanical Engineers Part C-Journal of Mechanical Engineering Science, 2009. 223(12): p. 2949-2965.

[5] Siddiq, A. and Sayed, T.E., *Ultrasonic-assisted manufacturing processes: Variational model and numerical simulations*. Ultrasonics, 2012. 52: p. 521-529.

[6] Jüschke, M. and Koch, C., *Model processes and cavitation indicators for a quantitative description of an ultrasonic cleaning vessel: Part I: Experimental results*. Ultrasonics Sonochemistry, 2012. 19: p. 787–795.

[7] Albrecht, D.A., Schuler, A., Kratzer, W., Vogt, J.L., Haenle, M.M., Mason, R.A., Lorenz, R., and Klaus, J., *Benefit of early abdominal ultrasonography in non-surgical patients admitted to the emergency department: A pilot study*. Journal Medical Ultrasonics, 2011. 38: p. 203–208.

[8] Preedy, V.R. and Watson, R.R., *Handbook of disease burdens and quality of life measures*. Vol. Part 4. 2010: SpringerLink.

[9] Wade, G., *Human uses of ultrasound: ancient and modern*. Ultrasonics, 2000. 38: p. 1-5.

[10] Wood, R.W. and Loomis, A.L., *The physicial and biological effects of intense audible sound on living organisms and cells*. Phil. Mag., 1927. 4: p. 417.

[11] Firestone, F.A., *The supersonic reflectoscope for internal inspection*. Metal Progr., 1945. 48: p. 505.

[12] Desch, C.H., Sproule, D.O. and Dawson, W.J., *The detection of cracks in steel by means of supersonic waves*. J. Iron Steel Inst., 1946. 153: p. 319.

[13] Emslie, A.G. and McConnel, R.L., *Radar systems engineering*. Vol. 1. 1947, New York: McGraw-Hill.

[14] Mason, W.P. and Thurston, R.N. Physical Acoustics. Vol. I - IX. 1965: Academic Press.

[15] Graff, K.F. *Ultrasonics: Historical aspects*. in *Ultrasonics Symposium*. 1977.

[16] Mason, W.P., *Piezoelectric crystals and their application to ultrasonics*. 1950, New York: Van Nostrand.

[17] Albers, V.M., *Benchmark papers in acoustics: Underwater sound*. 1972, Stroudsburg: Dowden, Hutchinson & Ross.

[18] Shoh, A., *Industrial applications of ultrasound - A review 1. High power ultrasound*. IEEE Transactions on Sonics and Ultrasonics, 1975. SU-22(2): p. 60-71.

[19] Neppiras, E.A., *Macrosonics in industry 1. Introduction*. Ultrasonics, 1972. 10(1): p. 9-13.

[20] Willrich, H.O., *Applications of ultrasonic waves*. Welding, 1950. 18: p. 61.

[21] Graff , K.F., *Macrosonics in industry: Ultrasonic soldering*. Ultrasonics, 1977: p. 75.

[22] Kalpakjian, S. and Schmid, S., *Manufacturing engineering and technology 5th edition in SI units*. 2006, Singapore: Prentice Hall.

[23] Dallas, D.B., *The new look of ultrasonic machining*. Manufacturing Engineering and Management. 1970, University of Michigan: Society of Manufacturing Engineers.

[24] Blaha, F. and Langenecker, B., *Tensile deformation of zinc crystal under ultrasonic vibration*. Naturwissenschaften, 1955. 42(20): p. 556-556.

[25] Nevill, G.E. and Brotzen, F.R., *Effect of vibration on the yield strength of a low-carbon steel*, in *First Technical Report*. 1957, The Rice Institute, Solid Science Division, Air Force Office of Scientific Research, ARDC: Washington.

[26] Konovalov.E.G. and Skripnichenko.A.L., *Effect of ultrasonic vibrations on tensile properties of metals*. Russian Engineering Journal-Ussr, 1965. 4(8): p. 31-32.

[27] Eaves, A.E., Smith, A.W., Waterhouse, W.J. and Sansome, D.H., *Application of ultrasonic vibrations to deforming metals*. Ultrasonics, 1975. 13(4): p. 162-170.

[28] Tisza, M., *The use of superimposed ultrasonic vibrations in deep drawing*. Kohaszat, 1983. 116: p. 104-109.

[29] Nerubai, M.S., *Effect of ultrasonic vibrations on the mechanical-properties of difficult-to-deform materials*. Metal Science and Heat Treatment, 1987. 29(3-4): p. 254-258.

[30] Siegert, K. and Mock, A., *Wire drawing with ultrasonically oscillating dies*. Journal of Materials Processing Technology, 1996. 60(1-4): p. 657-660.

[31] Allen, K.R., *Ultrasonics - A practical approach*. Metal Finishing, 1999. 97(1): p. 165-173.

[32] Voelkner, W., *Present and future developments of metal forming: selected examples*. Journal of Materials Processing Technology, 2000. 106: p. 236-242.

[33] Babitsky, V.I., Astashev, V.K. and Meadows, A., *Vibration excitation and energy transfer during ultrasonically assisted drilling*. Journal of Sound and Vibration, 2007. 308: p. 805–814.

[34] Neppiras, E.A., *Ultrasonic machining and forming*. Ultrasonics, 1964: p. 167 - 173.

[35] Mitrofanov, A.V., Babitsky, V.I. and Silberschmidt, V.V., *Finite element simulations of ultrasonically assisted turning*. Computational Materials Science, 2003. 28(3-4): p. 645-653.

[36] Kirchner, H.O.K., Kromp, W.K., Prinz, F.B. and Trimmel, P., *Plastic-deformation under simultaneous cyclic and unidirectional loading at low and ultrasonic frequencies*. Materials Science and Engineering, 1985. 68(2): p. 197-206.

[37] Kristoffy.I, *Metal forming with vibrated tools*. Journal of Engineering for Industry, 1969. 91(4): p. 1168-1174.

[38] Perotti, G., *An experiment on the use of ultrasonic vibrations in cold upsetting*. Annals of the CIRP, 1978. 22: p. 195 - 197.

[39] Hung, J.C. and Hung, C.H., *The influence of ultrasonic-vibration on hot upsetting of aluminum alloy*. Ultrasonics, 2005. 43(8): p. 692-698.

[40] Susan, M. and Bujoreanu, L.G., *The metal-tool contact friction at the ultrasonic vibration drawing of ball-bearing steel wires*. Revista De Metalurgia, 1999. 35(6): p. 379-383.

[41] Rozner, A.G., *Effect of ultrasonic vibration on coefficient of friction during strip drawing*. Journal of the Acoustical Society of America, 1971. 49(5): p. 1368-1371.

[42] Abramov, O.V., *High intensity ultrasonics - Theory and industrial applications*. 1998, Singapore: Gordon and Breach Science Publisher.

[43] Winsper, C.E. and Sansome, D.H., *Fundamentals of ultrasonic wire drawing*. Journal of the Institute of Metals, 1969. 97: p. 274 - 280.

[44] Parrini, L., *New methodology for the design of advanced ultrasonic transducer for welding devices*. IEEE Ultrasonics Symposium, 2000: p. 699-703.

[45] Cracknell, M.F. and Cracknell, A.P., *Applications of ultrasonics*. Contemporary Physics, 1976. 17(1): p. 13-44.

[46] Giraud, J.Y., Villemin, S., Darmana, R., Cahuzac, J.P., Autefage, A., and Morucci, J.P., *Bone cutting*. Clinical Physics and Physiological Measurement, 1991. 12(1): p. 1-19.

[47] Vercellotti, T., *Piezoelectric bone surgery techniques in implantology : ridge expansion, sinus lift, bone harvesting and implant site preparation, Academy of Osseointegration*. 19th Annual Meeting (San Francisco, USA), 2004.

[48] Herrick, J.F. and Krusen, F.A., *Ultrasound and medicine*. IRE Trans. Ultrasonic Eng., 1954. 7: p. 4.

[49] Evans, K.D., Weiss, B. and Knopp, M., *High-intensity focused ultrasound (HIFU) for specific therapeutic treatments: A literature review*. Journal of Diagnostic Medical Sonography, 2007. 23(6): p. 319-327.

[50] Volkov, M.V. and Shepeleva, I.S., *The use of ultrasonics instrumentation for the transection and uniting of bone tissue in orthopaedic surgery*. Reconstr. Surg. Traum., 1974. 14: p. 177-152.

[51] Arabaci, T., Cicek, Y. and Canakci, C., *Sonic and ultrasonic scalers in periodontal treatment: A review*. International Journal Dental Hygiene, 2007. 5: p. 2-12.

[52] O'Daly, B., Morris, E., Gavin, G., O'Byrne, J. and McGuinness, G., *High-power low frequency ultrasound: A review of tissue dissection and ablation in medicine and surgery*. Journal of Materials Processing Technology, 2008. 200(1-3): p. 38-58.

[53] Suslick, K.S., *Sonochemistry*. Science, 1990. 247: p. 1439-1445.

[54] Henglein, A., *Sonochemistry: Historical developments and modern aspects*. Ultrasonics, 1987. 25: p. 6-16.

[55] Mason, T.J., *Sonochemistry and sonoprocessing: the link, the trend and (probably) the future*. Ultrasonics Sonochemistry, 2003. 10: p. 175-179.

[56] Prakash, M.N.K. and Ramana, K.V.R., *Ultrasound and its application in the food industry*. Journal Food Science Technology, 2003. 40(6): p. 563-570.

[57] Demirdove, A. and Baysal, T., *The use of ultrasound and combined technologies in food preservation*. Food Review International, 2009. 25(1): p. 1-11.

[58] Hunicke, R.L., *Industrial applications of high power ultrasound for chemical reactions*. Ultrasonics, 1990. 28: p. 291-294.

[59] Ashida, Y. and Aoyama, H., *Press forming using ultrasonic vibration*. Journal of Materials Processing Technology, 2007. 187: p. 118-122.

[60] Inoue, M., *Studies on ultrasonic metal tube drawing*. Memoira of Sagami Institute of Technology, 1984. 19: p. 1-7.

[61] Hayashi, M., Jin, M., Thipprakmas, S., Murakawa, M., Hung, J.C., Tsai, Y.C., and Hung, C.H., *Simulation of ultrasonic-vibration drawing using the finite element method (FEM)*. Journal of Materials Processing Technology, 2003. 140: p. 30-35.

[62] Jimma, T., Kasuga, Y., Iwaki, N., Miyazawa, O., Mori, E., Ito, K., and Hatano, H., *An application of ultrasonic vibration to the deep drawing process*. Journal of Materials Processing Technology, 1998. 80-81: p. 406-412.

[63] Murakawa, M. and Jin, M., *The utility of radially and ultrasonically vibrated dies in the wire drawing process*. Journal of Materials Processing Technology, 2001. 113(1-3): p. 81-86.

[64] Winsper, C.E. and Sansome, E., *A review of the application of oscillatory energy to metals deforming plasticity*. 8th International MTDR Conference, Manchester, 1967: p. 1359-1360.

[65] Izumi, O., Oyama, K. and Suzuki, Y., *Effects of superimposed ultrasonic vibration on compressive deformation of metals*. Transactions of the Japan Institute of Metals, 1966. 7(3): p. 162-167.

[66] Daud, Y., Lucas, M. and Huang, Z., *Modelling the effects of superimposed ultrasonic vibrations on tension and compression tests of aluminium*. Journal of Materials Processing Technology, 2007. 186: p. 179 - 190.

[67] Mousavi, S.A.A.A., Feizi, H. and Madoliat, R., *Investigations on the effects of ultrasonic vibrations in the extrusion process*. Journal of Materials Processing Technology, 2007. 187: p. 657-661.

[68] Huang, Z.H., Lucas, M. and Adams, M.J., *Influence of ultrasonics on upsetting of a model paste*. Ultrasonics, 2002. 40(1-8): p. 43-48.

[69] Hung, J.C., Tsai, Y.C. and Hung, C.H., *The effect of ultrasonic-vibration on upsetting*. Proceedings of the 8th Biennial Conference on Engineering Systems Design and Analysis, Vol 4, 2006: p. 791-797.

[70] Pandey, P.C. and Shan, H.S., *Modern machining processes*. 1980, New York: McGrawHill.

[71] Satyanarayana, A. and Krishna Reddy, B.G., *Design of velocity transformers for ultrasonic machining*. Electrical India, 1984. 24: p. 11 - 20.

[72] Amin, S.G., Ahmed, M.H.M. and Youssef, H.A., *Computer-aided design of acoustic horns for ultrasonic machining using finite-element analysis*. Journal of Materials Processing Technology, 1995. 55(3 - 4): p. 254 - 260.

[73] Blaha, F. and Langenecker, B., *Plastic behaviour of metals under ultrasonics*. Journal of Physical Metallurgy, 1960. 51: p. 636.

[74] Malygin, G.A., *Acoustoplastic effect and the stress superimposition mechanism*. Physical Solid State, 2000. 42: p. 72-78.

[75] Dawson, G.R., Winsper, C.E. and Sansome, D.H., *Application of high-frequency and low-frequency oscillations to plastic deformation of metals - a complete appraisal of development and potential*. Metal Forming, 1970. 37(8): p. 234-238.

[76] Mekaru, H., Goto, H. and Takahashi, M., *Development of ultrasonic micro hot embossing technology*. Microelectronic Engineering, 2007. 84: p. 1282 - 1287.

[77] Bunget, C. and Ngaile, G., *Influence of ultrasonic vibration on micro-extrusion*. Ultrasonics, 2011. 51: p. 606 - 616.

[78] Fridman, H.D. and Levesque, P., *Reduction of static friction by sonic vibrations*. Journal of Applied Physics, 1959. 30(10): p. 1572-1575.

[79] Blaha, F. and Langenecker, B., *Ultrasonic investigation of the plasticity of metal crystals*. Acta Metallurgica, 1959. 7(2): p. 93-100.

[80] Blaha, F. and Langenecker, B., *Investigations for processing recovery (deformation softening) of metal crystals* Journal of Physical Metallurgy, 1958. 49(7): p. 357-360.

[81] Izumi, O., Oyama, K. and Suzuki, Y., *On superimposing of ultrasonic vibration during compressive deformation of metals*. Transactions of the Japan Institute of Metals, 1966. 7(3): p. 158-162.

[82] Astashev, V.K., *Influence of high frequency vibration on plastic deformation under simultaneous and unidirectional loading at low and ultrasonic frequencies*. Soviet Machine Science (Mashinovedenie), 1983. 2: p. 1 - 9.

[83] Siegert, K. and Ulmer, J., *Influencing the friction in metal forming processes by superimposing ultrasonic waves*. Cirp Annals-Manufacturing Technology, 2001. 50(1): p. 195-200.

[84] Huang, Z.H., Lucas, M. and Adams, M.J., *Study of ultrasonic upsetting under radial and longitudinal die vibration*. Modern Practice in Stress and Vibration Analysis, 2003. 440-441: p. 389-396.

[85] Sansome, D.H., *Ultrasonic techniques*, in *Metal Forming*, Beadle, J.D., Editor. 1971, Macmillan Engineering Evaluations. p. 185 - 188.

[86] Mizuno, M. and Kuno, T., *Basic studies of plastic working with vibration (1st report, ultrasonic vibro-indentation hardness of carbon steels)*. Buletin of the JSME, 1973. 16(91): p. 40-48.

[87] Ahmed, N., Mitrofanov, A.V., Babitsky, V.I. and Silberschmidt, V.V., *Stresses in ultrasonically assisted turning*. Modern Practice in Stress and Vibration Analysis VI, Proceedings, 2006. 5-6: p. 351-357.

[88] Siu, K.W., Ngan, A.H.W. and Jones, I.P., *New insight on acoustoplasticity - Ultrasonic irradiation enhances subgrain formation during deformation.* International Journal of Plasticity, 2011. 27: p. 788-800.

[89] Merkulov, L.G., *Absorption and diffusive scattering of ultrasonic waves in metals.* Soviet Physics-Technical Physics, 1957. 2(5): p. 953-957.

[90] Siddiq, A. and Ghassemieh, E., *Thermomechanical analyses of ultrasonic welding process using thermal and acoustic softening effects.* Mechanics of Materials, 2008. 40: p. 982-1000.

[91] Winsper, C.E., Dawson, G.R. and Sansome, D.H., *An introduction to the mechanics of oscillatory metalworking.* Metal and Materials, 1970: p. 158 - 162.

[92] Pohlman, R. and Lehfeldt, E., *Influence of ultrasonic vibration on metallic friction.* Ultrasonics, 1966. 4(Oct): p. 178-185.

[93] Winsper, C.E. and Sansome, D.H., *The superposition of longitudinal sonic oscillations on the wire drawing process.* Proceedings Institution Mechanical Engineers Part I, 1968 - 1969. 183(25): p. 545 - 562.

[94] Astashev, V.K., *The influence of ultrasonic vibration on plastic deformation processes.* Machinovedenie (Machine science), 1983: p. 2.

[95] Williams, D.C., *Material science and engineering: An introduction.* 6th. ed. 2003, New Jersey: John Wiley & Sons.

[96] Reiner, M., *Reology*. 1958, Goettingen: Springer.

[97] Mase, G., *Theory and problems of continuum mechanics.* 1970, New York: McGraw-Hill.

[98] Astashev, V.K. and Babitsky, V.I., *Ultrasonic processes and machines - dynamics, control and applications*. 2007, New York: Springer.

[99] Kubota, M., Tamura, I. and Shimamura, N., *Ultrasonic machining with diamond impregnated tool.* Bulletin of Japanese Society of Precision Engineering, 1977: p. 11.

[100] Andronov, A., Vitt, A. and Khaikyn, S., *Theory of oscillations.* 1966, New York: Pergamon Press.

[101] Andronov, V., *Investigations of a hard intenders penetration into granular media when either static or subjected to vibration.* Mechanics of Solids, 1967: p. 3.

[102] Andronov, V., *A method of defining friction force and the corresponding coefficient of friction* Machine Science, 1970: p. 4.

[103] Andronov, V., *Forced vibration in systems with transformed dry friction.* Machine Science, 1975: p. 5.

[104] Storck, H., Littmann, W., Wallaschek, J. and Mracek, M., *The effect of friction reduction in presence of ultrasonic vibrations and its relevance to travelling wave ultrasonic motors.* Ultrasonics, 2002. 40: p. 379-383.

[105] Godfrey, D., *Vibration reduces metal to metal contact and causes an apparent reduction in friction.* Asle Transactions, 1967. 10(2): p. 183-192.

[106] Severdenko, V.P. and Petrenko, V.V., *Effect of ultrasonic vibrations on the effenciency of lubricants in the closed upsetting of carbon steel.* Fiz Khim Mat, 1970. 6(7): p. 1970.

[107] Yao, Z., Kim, G.Y., Faidley, L., Zou, Q., Mei, D., and Chen, Z., *Effects of superimposed high-frequency vibration on deformation of aluminum in micro/meso-scale upsetting.* Journal of Materials Processing Technology, 2012. 212: p. 640– 646.

[108] Hung, J.C. and Chiang, M.C., *The influence of ultrasonic-vibration on double backward-extrusion of aluminum alloy.* World Congress on Engineering 2009, Vols I and Ii, 2009: p. 1814-1819.

[109] Hung, J.C., Tsai, Y.C. and Hung, C.H., *Frictional effect of ultrasonic-vibration on upsetting.* Ultrasonics, 2007. 46(3): p. 277-284.

[110] Schmid, E., *Plasticity of insonated metals.* Transactions of the Japan Institute of Metals, 1968. S 9: p. 798-804.

[111] Petukhow, V.L., Abramov, O.V., Zubko, A.M., Manegin and Yu, V., *Extrusion of aluminium in an ultrasonic field.* Light Metal Age, 1973. 31: p. 6-8.

[112] Lucas, M., MacBeath, A., McCulloch, E. and Cardoni, A., *A finite element model for ultrasonic cutting.* Ultrasonics, 2006. 44: p. 503-509.

[113] Alam, K., Mitrofanov, A.V. and Silberschmidt, V.V., *Experimental investigations of forces and torque in conventional and ultrasonically-assisted drilling of cortical bone.* Medical Engineering & Physics, 2011. 33: p. 234-239.

[114] Murakawa, M., Kaewtatip, P. and Jin, M., *Improving ironing performance using dies subjected to ultrasonic radial vibration.* Technical Paper - Society of Manufacturing Engineers, 1999(MF99-153): p. 1-6.

[115] Cheers, C.F., *Ultrasonically assisted die necking*, in *Metal Box Technical Record*. 1985.

[116] Tsujino, J., Ueoka, T., Takiguchi, K., Satoh, H. and Takahashi, K., *Characteristics of bending parts of metal plates using ultrasonic bending systems with a vibration punch and a vibration die.* Japan Journal Application of Physics, 1993. 32: p. 2447 - 2451.

[117] Tawakoli, T. and Azarhoushang, B., *Influences of ultrasonic vibrations on dry grinding of soft steel.* International Journal of Machine Tool & Manufacture, 2008. 48: p. 1585-1591.

[118] Brehl, D.E. and Dow, T.A., *Review of vibration-assisted machining*. Precision Engineering, 2008. 32: p. 153–172.

[119] Heisel, U., Wallaschek, J., Eisseler, R. and Potthast, C., *Ultrasonic deep hole drilling in electrolytic copper ECu 57*. Cirp Annals-Manufacturing Technology, 2008. 57(1): p. 53-56.

[120] Kuhn, H. and Medlin, D., *ASM handbook volume 08: Mechanical testing and evaluation*. ASM Handbook. Vol. 8. 2000, Materials Park, Ohio: ASM International. 998.

[121] Suh, C.M., Song, G.H., Suh, M.S. and Pyoun, Y.S., *Fatigue and mechanical characteristics of nano-structured tool steel by ultrasonic cold forging technology*. Materials Science and Engineering a-Structural Materials Properties Microstructure and Processing, 2007. 443(1-2): p. 101-106.

[122] Shuyu, L., *Study on the multifrequency Langevin ultrasonic transducer*. Ultrasonics, 1995. 33: p. 445-448.

[123] Fish, J. and Belytschko, T., *A first course in finite elements*. 2007, West Sussex, England: Wiley.

[124] Hibbitt, K.S., *ABAQUS/Standard user's manual*. 2009, Hibbitt,Karlsson &Sorensen Inc.: United State of America.

[125] Lee, C.H. and Kobayash.S, *New solutions to rigid-plastic deformation problems using a matrix-method*. Journal of Engineering for Industry-Transactions of the ASME, 1973. 95(3): p. 865-873.

[126] Lucas, M. and Chapman, G., *Design of ultrasonically assisted radial dies by validated finite-element models*. Ultrasonics International 93 - Conference Proceedings, 1993: p. 707-710.

[127] Jin, M., Thipprakmas, S., Noguchi, H., Hayashi, M. and Murakawa, A., *Finite-element simulation of ultrasonic wire drawing process*. Simulation of Materials Processing: Theory, Methods and Applications, 2001: p. 475-479.

[128] Jin, M., Hayashi, M., Thipprakmas, S., Murakawa, M., Hung, J.C., Tsai, Y.C., and Hung, C.H., *Simulation of ultrasonic-vibration drawing using the finite element method (FEM)*. Journal of Materials Processing Technology, 2003. 140: p. 30-35.

[129] Ahmed, N., Mitrofanov, A.V., Babitsky, V.I. and Silberschmidt, V.V., *Analysis of material response to ultrasonic vibration loading in turning inconel 718*. Materials Science and Engineering a-Structural Materials Properties Microstructure and Processing, 2006. 424(1-2): p. 318-325.

[130] Lemaitre, J. and Chaboche, J.L., *Mechanics of solid materials*. 1990: Cambridge University Press.

[131] Chun, B.K., Kim, H.Y. and Lee, J.K., *Modelling the Bauschinger effect for sheet metals, Part II: Applications*. International Journal of Plasticity, 2002. 18: p. 597-616.

[132] Huber, N. and Tsakmakis, C., *Determination of constitutive properties from spherical indentation data using neural networks. Part II: Plasticity with nonlinear isotropic and kinematic hardening*. Journal of the Mechanics and Physics of Solids, 1999. 47(7): p. 1589-1607.

[133] Langenecker, B., *Effects of ultrasound on deformation characteristics of metals*. IEEE Transactions on Sonics and Ultrasonics, 1966. Su13(1): p. 1-8.

[134] Johnson, G.R. and Cook, W.H., *Fracture characteristic of three metals subjected to various strains, strain rates, temperatures and pressures*. International Journal of Engineering Fracture Mechanics, 1985. 21: p. 31-48.

[135] Cardoni, A. and Lucas, M., *Enhanced vibration performance of ultrasonic block horns*. Ultrasonics, 2002. 40(1-8): p. 365-369.

[136] Lucas, M., *Vibration sensitivity in the design of ultrasonic forming dies*. Ultrasonics, 1996. 34(1): p. 35-41.

[137] Peshkovsky, S.L. and Peshkovsky, A.S., *Matching a transducer to water at cavitation: Acoustic horn design principles*. Ultrasonics Sonochemistry, 2007. 14(3): p. 314-322.

[138] Cardoni, A. and Lucas, M., *Strategies for reducing stress in ultrasonic cutting systems*. Strain, 2005. 41: p. 11-18.

[139] Lin, S., *Study on the longitudinal-torsional composite mode exponential ultrasonic horns*. Ultrasonics, 1996. 34: p. 757 - 762.

[140] Merkulov, L.G., *Design of ultrasonic concentrations*. Soviet Physical Acoustics, 1957. 3: p. 230-238.

[141] McCulloch, E., *Experimental and finite element modelling of ultrasonic cutting of food*, in *PhD Thesis*. 2008, University of Glasgow: Glasgow.

[142] Reddy, J.N., *An introduction to the finite element method*. 3rd ed. 2006, New York: McGraw-Hill.

[143] Beer, F.P. and Johnston, E.R., *Mechanics of materials*. 1992: McGrawHill.

[144] Ewins, D.J., *Modal testing theory, practice and application*. 2000: Research Studies Press Ltd.

[145] Special, P.L.I., *Measurement solutions made possible by laser vibrometry*, Waldronn, P.G.D., Editor. 2003.

[146] http://www.polytec.com/uk/.

[147] Dieter, G.E., Kuhn, H.A. and Semiatin, S.L., *Handbook of workability and process design*. 2003, Material Park, USA: ASM International.

[148] Daud, Y., Lucas, M. and Huang, Z., *Superimposed ultrasonic oscillations in compression tests of aluminium*. Ultrasonics, 2006. 44: p. 511-515.

[149] http://www.matweb.com. *Online Materials Information Resource*. [cited 2012 17th October].

[150] Bronzino, J.D., *The Biomedical Engineering Handbook: Second Edition*. 2000, Florida: CRC Press.

[151] Langenecker, B., *Work-softening of metal crystal by alternating the rate of glide strain*. Acta Metallurgica, 1961. 9: p. 937-940.

[152] Green, R.E., *Non-linear effects of high-power ultrasonics in crystalline solids*. Ultrasonics, 1975. 13: p. 117-127.

[153] Mordyuk, N.S., *Influence of ultrasonic oscillations on the physical properties of metals and alloys*. 1975, Kiev: Naukova Dumka (in Russian).

[154] Fu, Z., Xian, X., Lin, S., Wanga, C., Hua, W., and Li, G., *Investigations of the barbell ultrasonic transducer operated in the full-wave vibrational mode*. Ultrasonics, 2012. 52(5): p. 578-586.

[155] Severdenko, V.P., Klubovich, V.V. and Stepanenko, A.V., *Metal working under pressure with ultrasound* 1973, Minsk: Nauka i Tkhnika (in Russian).

[156] Jones, J.B. *Ultrasonic metal deformation processing* in *In Proceedings of the International Conference on Manufacturing Technology*. 1967.